

PREPARATIONS, SOLUTION COMPOSITION,
AND REACTIONS OF COMPLEX METAL HYDRIDES
AND ATE COMPLEXES OF ZINC, ALUMINUM, AND COPPER

A THESIS

Presented to

The Faculty of the Division of Graduate Studies

By

John Joseph Watkins

In Partial Fulfillment

of the Requirements for the Degree

Doctor of Philosophy in the School of Chemistry

Georgia Institute of Technology

April, 1977

PREPARATIONS, SOLUTION COMPOSITION,
AND REACTIONS OF COMPLEX METAL HYDRIDES
AND ATE COMPLEXES OF ZINC, ALUMINUM, AND COPPER

Approved:

Erling Grovenstein, Jr., Chairman

H. O. House

E. C. Ashby

Date approved by Chairman 5/30/77

ACKNOWLEDGMENTS

Many individuals and organizations have contributed to the successful completion of this thesis. The following acknowledgments are not complete, but I hope I have expressed my gratitude to the people and organizations upon whom I depended the most.

The School of Chemistry supported my first three years of work by the award of an NSF fellowship. My last year of work was generously supported by the St. Regis Paper Company, who graciously gave me leave of absence with salary so that the requirements for this thesis could be completed. This stipend and tuition support of my work freed me to concentrate on research without the financial difficulties encountered by many graduate students.

All the faculty and staff of the School of Chemistry supported my research. I particularly would like to recognize Professor W. M. Spicer, Professor J. A. Bertrand, Professor C. L. Liotta, Mr. Gerald O'Brien, and Mr. D. E. Lillie. Post-doctoral assistants and fellow graduate students who contributed to my experience at the Georgia Institute of Technology include Dr. G. A. Marano, Dr. R. D. Schwartz, Dr. J. T. Leammle, Dr. J. H. Smith, Dr. G. E. Parris, and Mr. J. P. Oliver. I would especially like to recognize Mr. Roy L. Miller, Dr. Ivar H. Stockel, and Dr. R. D. Raymond of the St. Regis Paper Company. Without the special encouragement provided by these three people I may never have returned to finish this thesis.

Professor E. C. Ashby suggested the areas of study covered in this thesis and advised on the research as it progressed. Professor Ashby allowed me considerable freedom during the course of these studies to satisfy my curiosity regarding observations not directly linked to my thesis.

I thank Professor Erling Grovenstein, Jr. and Professor H. O. House for reading my thesis and making helpful comments.

My mother and father, Gladys C. and James L. Watkins, provided me with the opportunity and incentive to attend high school and college. Any success I have had or will have is based upon the foundation they laid.

My wife, Alice, and our three daughters, Lisa, Karen, and Susan, should be acknowledged for the patience, love, and understanding they provided during the preparation of this thesis.

TABLE OF CONTENTS

	Page
ACKNOWLEDGMENTS.	ii
LIST OF TABLES	viii
LIST OF ILLUSTRATIONS.	xi
SUMMARY.	xvi
Chapter	

PART I

The Synthesis and Characterization of Complex Metal Hydrides
Involving Zinc and the Alkali Metals (Li, Na, and K)

I. INTRODUCTION.	2
II. EXPERIMENTAL.	6
Apparatus	6
Analytical.	8
Materials	8
Procedure	10
Reactions Involving $(s\text{-C}_4\text{H}_9)_2\text{Zn}$	
Reactions Involving $(\text{CH}_3)_2\text{Zn}$ and LiH	
Reactions of KH with ZnCl_2 in THF	
Reaction of KCl with ZnCl_2 in 1:1 Molar Ratio in THF	
Reaction of AlH_3 with the Filtrate from the Reaction of KCl with ZnCl_2 in THF	
Reaction of NaH with ZnCl_2 in 1:1 Molar Ratio in THF	
Reaction of LiH with ZnBr_2 in 2:1 Molar Ratio in THF	
Reaction of NaH with ZnI_2 in 2:1 Molar Ratio in THF	
Reactions Involving $(\text{CH}_3)_2\text{Zn}$ with CH_3Li	
Reactions Involving $(\text{CH}_3)_2\text{Zn}$ with KH	
Reactions Involving $(\text{CH}_3)_2\text{Zn}$ with NaH	
III. RESULTS AND DISCUSSION.	35
Li_2ZnH_4	35

TABLE OF CONTENTS (Continued)

Chapter	Page
Li_3ZnH_5	40
LiZnH_3	41
LiZnH_5 and LiZn_3H_7	44
$\text{KZn}(\text{CH}_3)_2\text{H}$ and $\text{KZn}_2(\text{CH}_3)_4\text{H}$	44
KZn_2H_5	45
KZn_3H_7	51
KZnH_3	51
NaZnH_3	53
NaZn_2H_5	55
Reaction of Alkali Metal Hydrides with Zinc Halides in Tetrahydrofuran.	56
LITERATURE CITED	64

PART II

A Study Concerning the Existence of Complexes Between
 LiAlH_4 and AlH_3 in Ether Solvents and in the
Solid State

I. INTRODUCTION.	67
II. EXPERIMENTAL.	69
Apparatus	69
Analytical.	69
Materials	70
Procedure	70
Reaction of LiAlH_4 and AlH_3 in 1:1, 1:2, 1:3, and 1:4 Molar Ratio in Diethyl Ether	
Reaction of LiAlH_4 and AlH_3 in 1:1, 1:2, 1:3, and 1:4 Molar Ratio in THF	
Reaction of LiH and AlH_3 in 1:4 Molar Ratio in Diethyl Ether	
Reaction of LiAlH_4 with BeCl_2 in 4:1 Molar Ratio in Diethyl Ether. Formation of " LiAl_2H_7 "	
Reaction of LiAlH_4 with BeCl_2 in 2:1 Molar Ratio in Diethyl Ether	
Reaction of LiAlH_4 with BeCl_2 in 3:1 Molar Ratio. Formation of " $\text{LiAl}_3\text{H}_{10}$ "	
III. RESULTS AND DISCUSSION.	73
IV. CONCLUSIONS	98

TABLE OF CONTENTS (Continued)

Chapter	Page
LITERATURE CITED	100

PART III

A Study Concerning the Nature of Alkyl-Hydrido Group Exchange
Between Zinc and Aluminum in the Reactions
of $MZn_x(CH_3)_2H$ with Alane and AlH_4
with $(CH_3)_2Zn$ ($M = Li, Na, \text{ or } K$)

I. INTRODUCTION.	102
II. EXPERIMENTAL.	105
Apparatus	105
Analytical.	105
Materials	106
Procedure	107
Reaction of AlH_3 with $LiZn(CH_3)_2H$ in Tetrahydrofuran	
Reaction of AlH_3 with $LiZn_2(CH_3)_4H$ in THF	
Reaction of AlH_3 with $LiZn(CH_3)_2AlH_4$ in THF	
Reaction of AlH_3 with $LiZn_2(CH_3)_4AlH_4$ in THF	
Reaction of $LiAlH_4$ with $LiZn(CH_3)_2AlH_4$ in THF	
Reactions of $LiAlH_4$ with $LiZn_2(CH_3)_4AlH_4$ in THF	
Reactions of $LiAlH_4$ with $(CH_3)_2Zn$ in THF at Molar Ratios of 1:1, 2:3, and 1:2	
Reactions of $(CH_3)_2Zn$ with $LiAlH_4$ in THF at Molar Ratios of 1:1, 3:2, and 2:1	
Infrared Spectral Study of the Reaction of $LiAlH_4$ with $(CH_3)_2Zn$ in Diethyl Ether	
Redistribution of $LiAlH_4$ and $LiAl(CH_3)_4$	
Reactions where $(CH_3)_2Zn$ Is Added to $LiAlH_4$ in Diethyl Ether	
Reactions where $LiAlH_4$ Is Added to $(CH_3)_2Zn$ in Diethyl Ether	
Reaction of $LiZn(CH_3)_2AlH_4$ with $LiAlH_4$ in Diethyl Ether	
Reaction where $LiAlH_4$ Is Added to a Dilute Solution of $(CH_3)_2Zn$ in 1:1 Ratio	
Reaction of $NaZn(CH_3)_2H$ with AlH_3 in THF	
Reaction of $NaZn_2(CH_3)_4H$ with AlH_3 in Tetrahydrofuran	
Infrared Study of the Reaction of $NaAlH_4$ with $(CH_3)_2Zn$ in THF	
Reaction of $NaAlH_4$ with $(CH_3)_2Zn$ in a 1:1 Molar Ratio	
Reaction of AlH_3 with $(CH_3)_2Zn$ in THF	
Reaction of ZnH_2 with $NaAl(CH_3)_2H_2$ in THF	

TABLE OF CONTENTS (Concluded)

Chapter	Page
Preparation of KAlH_4	
Reaction of $\text{KZn}(\text{CH}_3)_2\text{H}$ with AlH_3 in THF	
Reaction of KAlH_4 with $(\text{CH}_3)_2\text{Zn}$ in THF in 1:1 Molar Ratio	
Reaction of KAlH_4 with $(\text{CH}_3)_2\text{Zn}$ in THF in a 1:2 Molar Ratio	
Reaction of $\text{KZn}_2(\text{CH}_3)_4\text{H}$ with AlH_3 in THF at Molar Ratios of 2:1, 1:1, and 1:2	
III. RESULTS AND DISCUSSION.	125
IV. CONCLUSIONS	186
LITERATURE CITED	219

PART IV

The Composition of Lithium Methylcuprates
in Etheral Solvents

I. INTRODUCTION.	222
II. EXPERIMENTAL.	224
Apparatus	224
Analytical.	224
Materials	225
Procedure	227
Preparation of Cuprates	
General Reactions with 4-tert-Butylcyclohexanone	
Molecular Weight Measurements	
Interpretation of Exchange Mechanisms for NMR Data	
III. RESULTS AND DISCUSSION.	232
IV. CONCLUSIONS	263
LITERATURE CITED	264
VITA	266

LIST OF TABLES

Table		Page
PART I		
1.	X-Ray Powder Patterns for Complex Metal Zinc Hydrides of Lithium	12
2.	X-Ray Powder Patterns of Solids from the Reaction of Alkali Metal Hydrides with ZnCl_2	17
3.	X-Ray Powder Patterns of Solids from the Reaction of Alkali Metal Hydrides with ZnBr_2 and ZnI_2	23
4.	X-Ray Powder Patterns for Complex Metal Zinc Hydrides of Potassium	27
5.	X-Ray Powder Patterns for Complex Metal Zinc Hydrides of Sodium.	32
PART II		
1.	Elemental Analysis of Mixtures of LiAlH_4 and AlH_3 in 1:1, 1:2, 1:3, and 1:4 Ratio in Diethyl Ether.	77
2.	X-Ray Powder Diffraction Patterns of the Solid Products Obtained in the Reactions of LiAlH_4 with AlH_3 in Diethyl Ether	78
3.	X-Ray Powder Diffraction Patterns of " LiAl_2H_7 " and " $\text{LiAl}_4\text{H}_{13}$ ".	93
PART III		
1.	Infrared Spectral Bands for $(\text{CH}_3)_2\text{Zn}$, AlH_3 , $\text{LiZn}-(\text{CH}_3)_2\text{H}$, $\text{LiZn}_2(\text{CH}_3)_4\text{H}$, $\text{LiZn}(\text{CH}_3)_2\text{AlH}_4$, and $\text{LiZn}_2(\text{CH}_3)_4\text{AlH}_4$ in THF.	127
2.	Chemical Shifts for Methyl Groups in $(\text{CH}_3)_2\text{Zn}$, $\text{LiZn}(\text{CH}_3)_2\text{H}$, $\text{LiZn}_2(\text{CH}_3)_4\text{H}$, $\text{LiZn}(\text{CH}_3)_2\text{AlH}_4$, and $\text{LiZn}_2(\text{CH}_3)_4\text{AlH}_4$ in THF.	134

LIST OF TABLES (Continued)

Table		Page
3.	Infrared Spectra of $(\text{CH}_3)_2\text{Zn}$, LiAlH_4 , $\text{LiZn}-(\text{CH}_3)_2\text{AlH}_4$, $\text{LiZn}_2(\text{CH}_3)_4\text{AlH}_4$, and the Products Obtained by Mixing LiAlH_4 and $(\text{CH}_3)_2\text{Zn}$ in THF	140
4.	Chemical Shifts for $\text{LiZn}(\text{CH}_3)_2\text{AlH}_4$ and $\text{LiZn}_2-(\text{CH}_3)_2\text{AlH}_4$ at Various Concentrations in THF	147
5.	Chemical Shifts for $\text{LiZn}(\text{CH}_3)_2\text{AlH}_4$ and $\text{LiZn}_2-(\text{CH}_3)_4\text{AlH}_4$ at Various Temperatures in THF	151
6.	Equilibrium Constants at Various Temperatures for the Reaction $\text{LiZr}(\text{CH}_3)_2\text{AlH}_4 \cdot \text{S} = \text{LiZr}(\text{CH}_3)_2\text{AlH}_4 + \text{S}$ in Tetrahydrofuran.	153
7.	Equilibrium Constants at Various Temperatures for the Reaction $\text{LiZn}_2(\text{CH}_3)_4\text{AlH}_4 \cdot \text{S} = \text{LiZn}_2(\text{CH}_3)_4\text{AlH}_4 + \text{S}$ in Tetrahydrofuran.	155
8.	Products Obtained from Various Reactions Between LiAlH_4 and $(\text{CH}_3)_2\text{Zn}$ in Diethyl Ether.	160

PART IV

1.	Chemical Shifts for the System $\text{CH}_3\text{Li}-\text{CH}_3\text{Cu}$ in Dimethyl Ether.	234
2.	Chemical Shifts for the System $\text{CH}_3\text{Li}-\text{CH}_3\text{Cu}$ in Tetrahydrofuran	236
3.	Chemical Shifts for the System $\text{CH}_3\text{Li}-\text{CH}_3\text{Cu}$ in Diethyl Ether	238
4.	Chemical Shifts for the System $\text{CH}_3\text{Li}-\text{CH}_3\text{Cu} \cdot \text{P}(\text{n-Bu})_3$ in Diethyl Ether.	240
5.	Cuprate Complexes That Exist in Various Ether Solvents.	242
6.	Equilibrium Constants and Thermodynamic Parameters for the Reaction $\frac{1}{4} (\text{CH}_3\text{Li})_4 + \frac{1}{2} (\text{LiCu}(\text{CH}_3)_2)_2 \xrightleftharpoons{\text{K}} \text{Li}_2\text{Cu}(\text{CH}_3)_3$	244
7.	Concentration Dependences of the Reciprocal Mean Exchange Times for ^1H Exchange in the $\text{CH}_3\text{Li}-\text{LiCu}(\text{CH}_3)_2$ System at -51° in Diethyl Ether.	257

LIST OF TABLES (Concluded)

Table	Page
8. Reactions of Organometallic Reagents with 4-tert-Butylcyclohexanone in Ether Solvents at -78°	260

LIST OF ILLUSTRATIONS

Figure		Page
PART I		
1.	Description of High Vacuum Portion of Mettler Thermoanalyzer II	7
2.	Vacuum DTA-TGA of Li_2ZnH_4	39
3.	Vacuum DTA-TGA of LiZnH_3	43
4.	Vacuum DTA-TGA of KZn_2H_5	47
5.	Vacuum DTA-TGA of K_2ZnH_4	49
6.	DTA-TGA of K_2ZnH_4 under Ar.	50
7.	Vacuum DTA-TGA of KZnH_3	52
8.	Vacuum DTA-TGA of NaZnH_3	54
9.	Vacuum DTA-TGA of NaZn_2H_5	57
PART II		
1.	Infrared Spectra of Mixtures of LiAlH_4 and AlH_3 in Diethyl Ether: (a) LiAlH_4 ; (b) AlH_3 ; (c) 1:1 $\text{LiAlH}_4 + \text{AlH}_3$; (d) 1:2 $\text{LiAlH}_4 + \text{AlH}_3$; (e) 1:3 $\text{LiAlH}_4 + \text{AlH}_3$; (f) 1:4 $\text{LiAlH}_4 + \text{AlH}_3$	74
2.	Infrared Spectra of Mixtures of LiAlH_4 and AlH_3 in THF: (a) LiAlH_4 ; (b) AlH_3 ; (c) 1:1 $\text{LiAlH}_4 + \text{AlH}_3$; (d) 1:2 $\text{LiAlH}_4 + \text{AlH}_3$; (e) 1:3 $\text{LiAlH}_4 + \text{AlH}_3$; (f) 1:4 $\text{LiAlH}_4 + \text{AlH}_3$	75
3.	Infrared Spectra in the 2000-1400 cm^{-1} Region for Diethyl Ether Solutions of (a) LiAlH_4 ; (b) AlH_3 ; (c) the Supernatant Remaining after the Reaction of LiAlH_4 with BeCl_2 in 4:1 Molar Ratio, " LiAl_2H_7 "; (d) the Supernatant Remaining after the Reaction of LiAlH_4 with BeCl_2 in 3:1 Molar Ratio, " $\text{LiAl}_3\text{H}_{10}$ "	79

LIST OF ILLUSTRATIONS (Continued)

Figure		Page
4.	Infrared Spectrum of the Solution Resulting on Admixture of LiH and AlH ₃ in 1:4 Molar Ratio in Diethyl Ether	80
5.	Vacuum DTA-TGA of Proposed "LiAl ₂ H ₇ ".	81
6.	Vacuum DTA-TGA of LiAl ₃ H ₁₀	82
7.	Vacuum DTA-TGA of LiAl ₄ H ₁₃	83
8.	Vacuum DTA-TGA of LiAl ₅ H ₁₆	84
9.	Vacuum DTA-TGA of LiAlH ₄	85
10.	Vacuum DTA-TGA of AlH ₃	86
11.	DTA-TGA of AlH ₃ under Static Argon Atmosphere	90
12.	DTA-TGA of LiAl ₄ H ₁₃ (LiAlH ₄ + 3 AlH ₃) under Static Argon Atmosphere	91
13.	DTA-TGA of LiAl ₄ H ₁₃ (LiH + 4 AlH ₃) under Static Argon Atmosphere.	92
14.	DTA-TGA of "LiAl ₂ H ₇ " (7 LiAlH ₄ + AlCl ₃ → 3 LiCl + 4 LiAl ₂ H ₇) under Static Argon Atmosphere	94

PART III

1.	Infrared Spectra of (a) (CH ₃) ₂ Zn in THF, (b) AlH ₃ in THF, (c) LiZn(CH ₃) ₂ H in THF, (d) LiZn(CH ₃) ₂ AlH ₄ in THF.	128
2.	Infrared Spectra of (a) (CH ₃) ₂ Zn in THF, (b) AlH ₃ in THF, (c) LiZn ₂ (CH ₃) ₄ H in THF, (d) LiZn ₂ (CH ₃) ₄ - AlH ₄ in THF	131
3.	The 1800-1200 cm ⁻¹ Region of the Infrared Spectrum for (a) AlH ₃ in THF, (b) LiZn(CH ₃) ₂ H in THF, (c) LiZn(CH ₃) ₂ AlH ₄ in THF, (d) LiZn ₂ (CH ₃) ₄ H in THF, (e) LiZn ₂ (CH ₃) ₄ AlH ₄ in THF.	132
4.	¹ H NMR Spectra in THF at 35°: (a) LiZn(CH ₃) ₂ AlH ₄ , (b) LiZn ₂ (CH ₃) ₄ AlH ₄	135

LIST OF ILLUSTRATIONS (Continued)

Figure	Page
5. Infrared Spectra of Solutions Obtained by Adding LiAlH_4 to $(\text{CH}_3)_2\text{Zn}$ in THF: (a) $(\text{CH}_3)_2\text{Zn}$; (b) LiAlH_4 ; (c) 1:1 $\text{LiAlH}_4 + (\text{CH}_3)_2\text{Zn}$; (d) 2:3 $\text{LiAlH}_4 + (\text{CH}_3)_2\text{Zn}$; (e) 1:2 $\text{LiAlH}_4 + (\text{CH}_3)_2\text{Zn}$; (f) $\text{LiZn}(\text{CH}_3)_2\text{AlH}_4$; (g) $\text{LiZn}_2(\text{CH}_3)_4\text{AlH}_4$	141
6. Infrared Spectra of Solutions Obtained by Adding $(\text{CH}_3)_2\text{Zn}$ to LiAlH_4 in THF: (a) 1:1 $(\text{CH}_3)_2\text{Zn} + \text{LiAlH}_4$; (b) 2:3 $(\text{CH}_3)_2\text{Zn} + \text{LiAlH}_4$; (c) 1:2 $(\text{CH}_3)_2\text{Zn} + \text{LiAlH}_4$	
7. Molecular Association Values for $\text{LiZn}(\text{CH}_3)_2\text{AlH}_4$	144
8. Molecular Association Values for $\text{LiZn}_2(\text{CH}_3)_4\text{AlH}_4$	145
9. ^1H NMR Spectra of $\text{LiZn}(\text{CH}_3)_2\text{AlH}_4$ in THF at Various Concentrations: (a) 0.48 M, (b) 0.39 M, (c) 0.19 M, (d) 0.10 M.	148
10. Plot of $\ln K$ vs $1/T$ for the Reactions: $\bigcirc \text{LiZn}(\text{CH}_3)_2\text{AlH}_4 \cdot \text{S} = \text{LiZn}(\text{CH}_3)_2\text{AlH}_4 + \text{S}$ $\square \text{LiZn}_2(\text{CH}_3)_4\text{AlH}_4 \cdot \text{S} = \text{LiZn}_2(\text{CH}_3)_4\text{AlH}_4 + \text{S}$	154
11. Infrared Spectra of Supernatant Solutions Obtained by Adding $(\text{CH}_3)_2\text{Zn}$ to LiAlH_4 in Diethyl Ether--Ratio $(\text{CH}_3)_2\text{Zn}:\text{LiAlH}_4$ (1) Pure LiAlH_4 , (2) 0.5:1.0, (3) 1.0:1.0, (4) 1.5:1.0, (5) 2.0:1.0	162
12. Infrared Spectra of Supernatant Solutions Obtained by Adding LiAlH_4 to $(\text{CH}_3)_2\text{Zn}$ in Diethyl Ether--Ratio $\text{LiAlH}_4:(\text{CH}_3)_2\text{Zn}$ (1) Pure $(\text{CH}_3)_2\text{Zn}$, (2) 0.5:1.0, (3) 0.75:1.0, (4) 1.0:1.0, (5) 2.0:1.0 -- Reaction Time of Five Minutes.	164
13. Infrared Spectra of Supernatant Solution Obtained by Adding LiAlH_4 to $(\text{CH}_3)_2\text{Zn}$ in Diethyl Ether--Ratio $\text{LiAlH}_4:(\text{CH}_3)_2\text{Zn}$ (1) 0.5:1.0, (2) 1.0:1.0, (3) 2.0:1.0 -- Reaction Time of One Hour.	167
14. Infrared Spectra of $\text{NaZn}(\text{CH}_3)_2\text{H}$ and THF Soluble Products from Its Reaction with AlH_3 --(a) $(\text{CH}_3)_2\text{Zn}$ in THF, (b) $\text{NaZn}(\text{CH}_3)_2\text{H}$ in THF, (c) $\text{NaZn}(\text{CH}_3)_2\text{H} + \text{AlH}_3$ in THF after Five Minutes, (d) $\text{NaZn}(\text{CH}_3)_2\text{H} + \text{AlH}_3$ in THF after 24 Hours-- $\text{NaAl}_2(\text{CH}_3)_4\text{H}_3$	171
15. Infrared Spectra of (a) $\text{NaZn}_2(\text{CH}_3)_4\text{H}$ and (b) $\text{NaZn}_2(\text{CH}_3)_4\text{AlH}_4$	172

LIST OF ILLUSTRATIONS (Continued)

Figure	Page
16. Infrared Spectra of Solutions Obtained When $(\text{CH}_3)_2\text{Zn}$ Was Added to NaAlH_4 in Tetrahydrofuran (a) NaAlH_4 to $(\text{CH}_3)_2\text{Zn}$, 1:1 (b) 1:2.	176
17. Infrared Spectra of Solutions Obtained by Adding NaAlH_4 to $(\text{CH}_3)_2\text{Zn}$ in Tetrahydrofuran - (a) 1:2 NaAlH_4 to $(\text{CH}_3)_2\text{Zn}$ (b) 2:3 NaAlH_4 to $(\text{CH}_3)_2\text{Zn}$, (c) 1:1 NaAlH_4 to $(\text{CH}_3)_2\text{Zn}$	177
18. Infrared Spectra of Solutions Obtained by Adding NaAlH_4 to $(\text{CH}_3)_2\text{Zn}$ in Tetrahydrofuran: (a) 1:1 NaAlH_4 to $(\text{CH}_3)_2\text{Zn}$ after Five Minutes, (b) 1:1 NaAlH_4 to $(\text{CH}_3)_2\text{Zn}$ after 2.5 Hours, (c) 1:1 NaAlH_4 to $(\text{CH}_3)_2\text{Zn}$ after 28 Hours, (d) 1:1 NaAlH_4 to $(\text{CH}_3)_2\text{Zn}$ after Four Days, (e) 1:1 NaAlH_4 to $(\text{CH}_3)_2\text{Zn}$ after Seven Days.	178
19. Infrared Spectra of $\text{KZn}(\text{CH}_3)_2\text{H}$, the Products from Its Reaction with AlH_3 , and the Products from the Reaction of KAlH_4 with $(\text{CH}_3)_2\text{Zn}$ in Tetrahydrofuran: (a) $\text{KZn}(\text{CH}_3)_2\text{H}$ in THF, (b) 1:1 $\text{KAlH}_4 + (\text{CH}_3)_2\text{Zn}$ after Three Minutes, (c) 1:1 $\text{KZn}(\text{CH}_3)_2\text{H}$ to AlH_3 after Three Hours, (d) 1:1 $\text{KAlH}_4 + (\text{CH}_3)_2\text{Zn}$ after Three Hours.	182
20. Infrared Spectra of $\text{KZn}_2(\text{CH}_3)_4\text{H}$, Products from the Reaction of KAlH_4 with $(\text{CH}_3)_2\text{Zn}$ in 1:2 Ratio, and Products from the Reaction of $\text{KZn}_2(\text{CH}_3)_4\text{H}$ with AlH_3 in Tetrahydrofuran: (a) 1:2 KAlH_4 to $(\text{CH}_3)_2\text{Zn}$ after Five Minutes, (b) 1:2 KAlH_4 to $(\text{CH}_3)_2\text{Zn}$ after 20 Minutes, (c) 1:2 KAlH_4 to $(\text{CH}_3)_2\text{Zn}$ after Four Hours, (d) 2:1 $\text{KZn}_2(\text{CH}_3)_4\text{H}$ to AlH_3 , (e) 1:1 $\text{KZn}_2(\text{CH}_3)_4\text{H}$ to AlH_3 after Five Minutes, (f) 1:1 $\text{KZn}_2(\text{CH}_3)_4\text{H}$ to AlH_3 after Four Hours, (g) 1:2 $\text{KZn}_2(\text{CH}_3)_4\text{H}$ to $\text{AlH}_3(\text{Al}(\text{CH}_3)_2\text{H})$, and (h) $\text{KZn}_2(\text{CH}_3)_4\text{H}$	184

PART IV

1. 60 MHz ^1H NMR at -136° in Dimethyl Ether for Solutions of $\text{CH}_3\text{Li}-\text{CH}_3\text{Cu}$	233
2. Plot of $\ln K$ versus $1/T$ for the Reaction $1/4(\text{CH}_3\text{Li})_4 + 1/2(\text{LiCu}(\text{CH}_3)_2)_2 \leftrightarrow \text{Li}_2\text{Cu}(\text{CH}_3)_3$ in the Systems: <div style="display: flex; align-items: center;"> <div style="border: 1px solid black; width: 15px; height: 15px; margin-right: 5px;"></div> $\text{CH}_3\text{Li}-\text{CH}_3\text{Cu}$ in Diethyl Ether, <div style="border: 1px solid black; border-radius: 50%; width: 15px; height: 15px; margin: 0 5px;"></div> $\text{CH}_3\text{Li}-\text{CH}_3\text{Cu} \cdot \text{P}(\text{n-Bu})_3$ in Diethyl Ether. </div>	245

LIST OF ILLUSTRATIONS (Concluded)

Figure	Page
3. Plot of $\ln K$ versus $1/T$ for the Reaction $1/4(\text{CH}_3\text{Li})_4 + 1/2(\text{LiCu}(\text{CH}_3)_2)_2 \leftrightarrow \text{Li}_2\text{Cu}(\text{CH}_3)_3$ in the Systems: \bigcirc $\text{CH}_3\text{Li}-\text{CH}_3\text{Cu}$ in THF, \square $\text{CH}_3\text{Li}-\text{CH}_3\text{Cu}$ in Dimethyl Ether	246
4. Molecular Association Data for the System $\text{CH}_3\text{Li}-\text{CH}_3\text{Cu}$ in THF -- Ratio $\text{CH}_3\text{Li}/\text{CH}_3\text{Cu}$: \square 2.89, \bigcirc 1.02, \triangle 0.52.	247
5. Molecular Association Data for the System $\text{CH}_3\text{Li}-\text{CH}_3\text{Cu}$ in Diethyl Ether -- Ratio $\text{CH}_3\text{Li}/\text{CH}_3\text{Cu}$: \square 2.91, \bigcirc 1.04, \triangle 0.68.	248
6. Molecular Association Data for the System $\text{CH}_3\text{Li}-\text{CH}_3\text{Cu}\cdot\text{P}(\text{n-Bu})_3$ in Diethyl Ether -- Ratio $\text{CH}_3\text{Li}/\text{CH}_3\text{Cu}$: \square 2.93, \bigcirc 1.02, \triangle 0.52.	249
7. Representative ^1H Spectra of the $\text{CH}_3\text{Li}-\text{LiCu}(\text{CH}_3)_2$ System in Diethyl Ether	253
8. $1/\tau_c$ for the ^1H Spectra of the System $\text{CH}_3\text{Li}-\text{CH}_3\text{Cu}\cdot\text{P}(\text{n-Bu})_3$ in Diethyl Ether at -51° as a Function of $[\text{CH}_3\text{Li}]_4/[(\text{LiCu}(\text{CH}_3)_2)_2]$	256

SUMMARY

Part I. The Synthesis and Characterization of Complex

Metal Hydrides Involving Zinc and the Alkali

Metals (Li, Na, and K)

A series of complex metal hydrides of zinc with composition $M_n Zn_m H_{2m+n}$, where $M = Li, Na, \text{ or } K$, has been synthesized by reacting an appropriate "ate" complex of zinc ($M_n Zn_m R_{2m+n}$) with either $LiAlH_4$, $NaAlH_4$, or AlH_3 . The 1:1, 2:1, and 3:1 complexes of methyllithium and dimethylzinc yielded $LiZnH_3$, Li_2ZnH_4 , and Li_3ZnH_5 when allowed to react with lithium aluminum hydride in diethyl ether. The reaction of potassium hydride with dimethylzinc in 1:1 and 1:2 ratios in tetrahydrofuran yielded potassium dimethylhydrido-zincate $[KZn(CH_3)_2H]$ and potassium tetramethylhydriododizincate $[KZn_2(CH_3)_4H]$. When either $KZn(CH_3)_2H$ or $KZn_2(CH_3)_4H$ was allowed to react with AlH_3 in tetrahydrofuran, KZn_2H_5 resulted; whereas, $KZnH_3$ was obtained from the reaction of $KZn(CH_3)_2H$ with lithium aluminum hydride in the same solvent. Both the 1:1 and 1:2 complexes of sodium hydride with dimethylzinc gave $NaZnH_3$ when allowed to react with sodium aluminum hydride in tetrahydrofuran. These reactions are presented as examples of a new and general route for the preparation of complex metal hydrides by the reaction of "ate" complexes with complex metal hydrides of aluminum or AlH_3 .

A convenient and economical preparation of ZnH_2 is reported. The reaction of KH with $ZnCl_2$ in 1:2, 1:1, 2:1, and 3:1 molar ratios has been

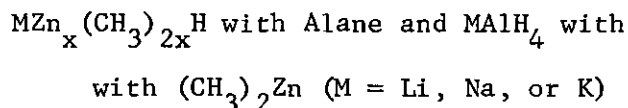
investigated. In these reactions zinc hydride and KCl are initially formed; however, the KCl reacts further with ZnCl_2 to form KZn_2Cl_5 and K_2ZnCl_4 . The reaction of NaH with ZnCl_2 in 1:1 molar ratio forms only ZnH_2 and NaCl. Likewise, the reaction of LiH with ZnBr_2 and NaH with ZnI_2 in 2:1 molar ratio produced only ZnH_2 and the corresponding alkali metal halide. A more thermally stable form of ZnH_2 , which is also more reactive than that prepared by any of the known methods, is produced in these reactions.

Part II. A Study Concerning the Existence of Complexes
Between LiAlH_4 and AlH_3 in Ethereal Solvents
and in the Solid State

The reaction between LiAlH_4 and AlH_3 in 1:1, 1:2, 1:3, and 1:4 molar ratios in both diethyl ether and THF has been investigated by infrared spectroscopy. Also solutions of LiAlH_4 and AlH_3 in diethyl ether were evaporated to dryness and the resulting solids examined by DTA-TGA and x-ray powder diffraction methods. Previous reports claiming the preparation of LiAl_2H_7 and $\text{LiAl}_3\text{H}_{10}$ by the reaction of LiAlH_4 with BeCl_2 and AlCl_3 in ether and also the reaction of LiH with AlH_3 and AlCl_3 were studied in detail and attempts made to prepare the complexes by exactly the same procedure reported. Contrary to previous reports, in no case was any evidence found to indicate the existence of LiAl_2H_7 , $\text{LiAl}_3\text{H}_{10}$, or any complex between LiAlH_4 and AlH_3 in ether or THF solution or in the solid state.

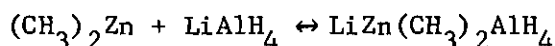
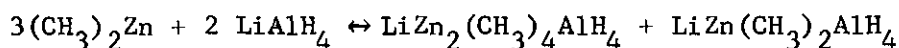
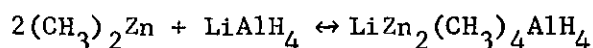
Part III. A Study Concerning the Nature of Alkyl-Hydrido Group

Exchange Between Zinc and Aluminum in the Reactions of



When AlH_3 is allowed to react with $\text{LiZn}(\text{CH}_3)_2\text{H}$ and $\text{LiZn}_2(\text{CH}_3)_4\text{H}$ in tetrahydrofuran in 1:1 molar ratio, $\text{LiZn}(\text{CH}_3)_2\text{AlH}_4$ and $\text{LiZn}_2(\text{CH}_3)_4\text{AlH}_4$ are formed as soluble complexes. These two compounds are the first reported triple metal hydride complexes involving lithium, aluminum, and zinc. Their solution composition is inferred from spectroscopic and colligative property studies. The mechanisms of formation of these compounds by the reaction of AlH_3 with $\text{LiZn}(\text{CH}_3)_2\text{H}$ and $\text{LiZn}(\text{CH}_3)_4\text{H}$ in THF are discussed in light of the spectroscopic results.

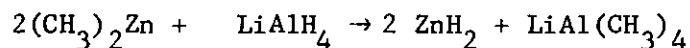
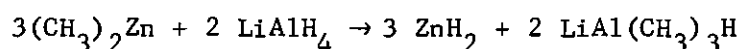
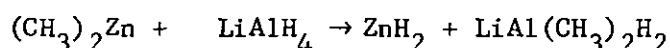
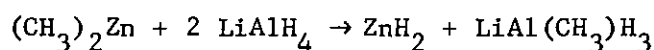
When $(\text{CH}_3)_2\text{Zn}$ was added to a THF solution of LiAlH_4 in 2:1, 3:2, and 1:1 molar ratios, $\text{LiZn}_2(\text{CH}_3)_4\text{AlH}_4$ and $\text{LiZn}(\text{CH}_3)_2\text{AlH}_4$ were formed according to the equations shown below. When the order of addition was reversed and LiAlH_4 was added to a THF solution of $(\text{CH}_3)_2\text{Zn}$ in 1:1, 2:3, and 1:2 molar ratios, $\text{LiZn}(\text{CH}_3)_2\text{AlH}_4$ and $\text{LiZn}_2(\text{CH}_3)_4\text{AlH}_4$ were again formed according to these equations:



Infrared and ^1H NMR spectroscopic studies, as well as ebullioscopic molecular weight measurements, were used to define the solution composi-

tion of the products obtained from these reactions. The role of $\text{LiZn}(\text{CH}_3)_2\text{AlH}_4$ as the intermediate involved in the formation of ZnH_2 from the reaction of LiAlH_4 with $(\text{CH}_3)_2\text{Zn}$ is discussed in light of the spectroscopic studies carried out on this reaction.

The reaction between lithium aluminum hydride and dimethylzinc in diethyl ether has been studied in detail. The course of the reaction was found to be dependent upon the mode of addition, the ratio, and concentration of the reactants. When $(\text{CH}_3)_2\text{Zn}$ was added to LiAlH_4 , the reaction was found to proceed according to the equations:



The identity of the aluminum containing products was established by spectral comparison with the products formed on redistribution of LiAlH_4 with $\text{LiAl}(\text{CH}_3)_4$. On the other hand, addition of LiAlH_4 to $(\text{CH}_3)_2\text{Zn}$ in 1:2 ratio produced the soluble complex $\text{LiZn}_2(\text{CH}_3)_4\text{AlH}_4$. The same addition in 1:1 ratio yielded a mixture of LiZnH_3 and ZnH_2 by way of the intermediate $\text{LiZn}(\text{CH}_3)_2\text{AlH}_4$. In 2:1 ratio the reaction gave ZnH_2 only. The mechanism of the reaction between LiAlH_4 and $(\text{CH}_3)_2\text{Zn}$ is discussed in light of these results.

When AlH_3 was allowed to react with $\text{NaZn}(\text{CH}_3)_2\text{H}$ in THF, the reaction products were found to be dependent on the initial concentration of

$\text{NaZn}(\text{CH}_3)_2\text{H}$. The reaction with dilute solutions of $\text{NaZn}(\text{CH}_3)_2\text{H}$ produced ZnH_2 ; whereas NaZn_2H_5 was produced from the more concentrated solutions. The reaction of AlH_3 with $\text{NaZn}_2(\text{CH}_3)_4\text{H}$ produced the soluble trimetal complex $\text{NaZn}_2(\text{CH}_3)_4\text{AlH}_4$. The reaction between NaAlH_4 and $(\text{CH}_3)_2\text{Zn}$ in 1:1 and 1:2 molar ratios produced $\text{NaZn}(\text{CH}_3)_2\text{AlH}_4$ and $\text{NaZn}_2(\text{CH}_3)_4\text{AlH}_4$. Concentrated solutions of $\text{NaZn}(\text{CH}_3)_2\text{AlH}_4$ were found to disproportionate giving NaZn_2H_5 ; whereas the more dilute solutions formed ZnH_2 . The mechanism for the formation of KZn_2H_5 or NaZn_2H_5 from the reaction of AlH_3 with $\text{KZn}(\text{CH}_3)_2\text{H}$ or $\text{NaZn}(\text{CH}_3)_2\text{H}$ is discussed in light of the results which are presented. The mechanism by which KZn_2H_5 is formed in the reaction of $\text{KZn}_2(\text{CH}_3)_4\text{H}$ with AlH_3 is discussed.

Part IV. The Composition of Lithium Methylcuprates in Etheral Solvents

Variable temperature ^1H NMR of the system $\text{CH}_3\text{Li}-\text{CH}_3\text{Cu}$ in various stoichiometric ratios has been studied in Me_2O , Et_2O , and THF. In Me_2O and THF, $\text{LiCu}_2(\text{CH}_3)_3$ and $\text{LiCu}(\text{CH}_3)_2$ have been found to exist as pure stoichiometric compounds when the $\text{CH}_3\text{Li}:\text{CH}_3\text{Cu}$ ratio is 1:2 and 1:1, respectively. When the $\text{CH}_3\text{Li}:\text{CH}_3\text{Cu}$ ratio is 2:1, $\text{Li}_2\text{Cu}(\text{CH}_3)_3$ is formed in an equilibrium mixture containing $\text{LiCu}(\text{CH}_3)_2$ and CH_3Li . In Et_2O , evidence is presented to indicate the existence of $\text{Li}_2\text{Cu}_3(\text{CH}_3)_5$, $\text{LiCu}(\text{CH}_3)_2$, and $\text{Li}_2\text{Cu}(\text{CH}_3)_3$. The first two compounds can be prepared stoichiometrically pure. However, the latter compound is part of an equilibrium mixture. The solution composition of these cuprates will be presented based on variable temperature NMR and molecular association data.

Previously reported unusual stereochemistry in the reaction of 4-tert-butylcyclohexanone with $\text{CH}_3\text{Li-LiCu}(\text{CH}_3)_2$ is attributed to complexation of the ketone by $\text{LiCu}(\text{CH}_3)_2$ followed by addition of CH_3Li to the carbonyl group rather than by addition of a $\text{CH}_3\text{Li-LiCu}(\text{CH}_3)_2$ complex, e.g., $\text{Li}_2\text{Cu}(\text{CH}_3)_3$ directly to the uncomplexed ketone.

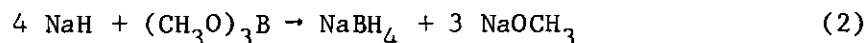
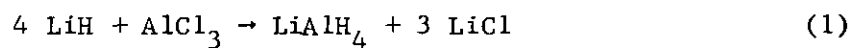
PART I

The Synthesis and Characterization of Complex Metal Hydrides Involving Zinc and the Alkali Metals (Li, Na, and K)

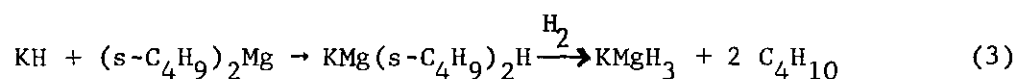
CHAPTER I

INTRODUCTION

Complex metal hydrides of aluminum and boron (e.g., LiAlH_4 and NaBH_4) have proven to be invaluable reagents in organic synthesis. These compounds are prepared by the reaction of a Group IA metal hydride with a Group IIIA metal derivative.^{1,2}



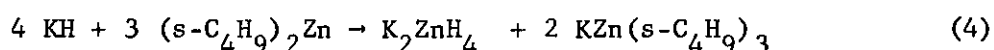
Recently we reported the preparation of the first complex metal hydride of magnesium (KMgH_3) by the hydrogenolysis of an "ate" complex of magnesium.³



The necessity for this synthetic scheme is due to the fact that the reaction of KH directly with MgCl_2 (analogous to the preparation of LiAlH_4) produces MgH_2 and not KMgH_3 .⁴ The particular R_2Mg compound used [$(\text{s-Bu})_2\text{Mg}$] is difficult to prepare but its use is necessitated by the fact that it is the only known R_2Mg compound soluble in benzene and

benzene solvent is necessitated due to the fact that MMgR_2H compounds (where $\text{M} = \text{Li}, \text{Na}$ or K) cleave ether solvents.^{5,6} In addition it is known that R-Mg compounds can be hydrogenolyzed to H-Mg compounds most easily when the R group is branched in the α position, such as in *s*-butyl-compounds.⁷

For this reason the synthesis of K_2ZnH_4 and Na_2ZnH_4 ,⁸ reported recently, was carried out by hydrogenolysis of an "ate" complex of zinc. In view of this success we wished to expand our synthetic studies to

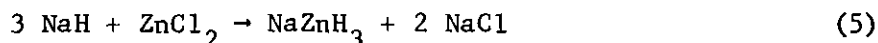


include other complex metal hydrides of zinc. Our initial plan was to investigate the reaction of LiH with di-*s*-butylzinc in both hydrocarbon and ether solvents in an attempt to prepare a spectrum of lithium dialkylzinc hydrides ranging from $\text{Li}_3\text{ZnR}_2\text{H}_3$ to $\text{LiZn}_3\text{R}_6\text{H}$, where $\text{R} = \text{s-butyl}$. The lithium dialkylzinc hydrides were to be converted to the corresponding complex metal hydrides by high pressure hydrogenation, since the carbon-zinc bond of the *s*-butyl-zinc group should be easily converted to an H-Zn bond by hydrogenation (see Eq. 3).

Our initial plan proved to be unfeasible when the intermediate lithium *s*-butylzinc hydrides were found to cleave ether solvents too rapidly for hydrogenation to be an effective tool for R-Zn to H-Zn conversion. Unfortunately, the above reaction did not take place at all in benzene.

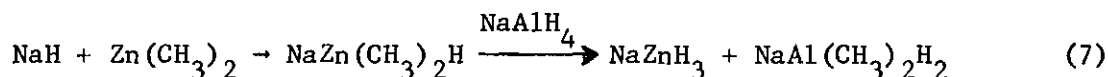
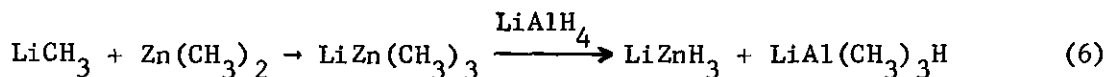
It is clear that a more convenient and economical method for the

preparation of these compounds would involve the reaction of an alkali metal hydride with the Group II metal halide (e.g., Eq. 5). This scheme is reasonable since both NaBH_4 and LiAlH_4 can be prepared in this manner.^{1,2}



Therefore, an attempt was made to prepare complex metal hydrides of zinc (e.g., KZnH_3 , K_2ZnH_4 , K_3ZnH_5 , etc.) by the reaction of an alkali metal hydride with zinc chloride, bromide, or iodide. However, analogous to the reaction of KH with MgCl_2 , the reaction of KH with ZnCl_2 , NaH with ZnI_2 , or LiH with ZnBr_2 all yield ZnH_2 instead of complex metal hydrides of zinc.

The plan was, then, modified in two ways. First, conversion of R-Zn to H-Zn was carried out by reaction of the "ate" complex with LiAlH_4 since alkyl exchange from zinc to aluminum and hydrogen exchange from aluminum to zinc might be expected at temperatures lower than zero degrees. At these temperatures MZnR_2H and MZnR_3 compounds should not cleave ether solvents. Second, dimethylzinc could be used as a starting material rather than di-s-butylzinc since methyl group exchange should be more rapid than s-butyl group exchange. In addition, Shriver and co-workers,⁹ in their



report on the preparation and properties of $MZnR_2H$ compounds, showed that $LiZn(CH_3)_2H$ and $NaZn(CH_3)_2H$ are better defined species in solution than the higher alkyl analogues.

The advantages of using this method for preparation of complex metal hydrides of zinc are as follows: (1) the reactions are instantaneous and quantitative, (2) no ether cleavage products are formed, (3) high pressure hydrogenation is not required, and (4) methyl-metal compounds in ether are much easier to prepare than the secondary butyl compounds in hydrocarbon solvent.

CHAPTER II

EXPERIMENTAL

Apparatus

Reactions were performed under nitrogen at the bench using Schlenk tube techniques. Filtrations and other manipulations were carried out in a glove box equipped with a recirculating system using manganese oxide columns to remove oxygen and dry ice-acetone to remove solvent vapors.¹⁰

Infrared spectra were obtained using a Perkin Elmer 621 Spectrophotometer. Solids were run as Nujol mulls between CsI plates. Solutions were run in matched 0.10 mm pathlength NaCl cells. X-ray powder data were obtained on a Philips-Norelco X-ray unit using a 114.6 mm camera with nickel filtered CuK_α radiation. Samples were sealed in 0.5 mm capillaries and exposed to x-rays for six hours. D-spacings were read on a precalibrated scale equipped with viewing apparatus. Intensities were estimated visually. A 300 ml Magne-Drive autoclave (Autoclave Engineers, Inc.) was used for high pressure hydrogenation. Differential thermal and thermal gravimetric (DTA-TGA) data were obtained under vacuum with a modified Mettler Thermoanalyzer II. A diagram of the vacuum line attached to the balance chamber is shown in Figure 1. Operation of the DTA-TGA under vacuum with the U-trap between R_1 and the pump cooled to liquid nitrogen temperature permits one to distinguish between condensable and non-condensable evolved gases by use of the gauges J_1 and J_2 . The U-shaped

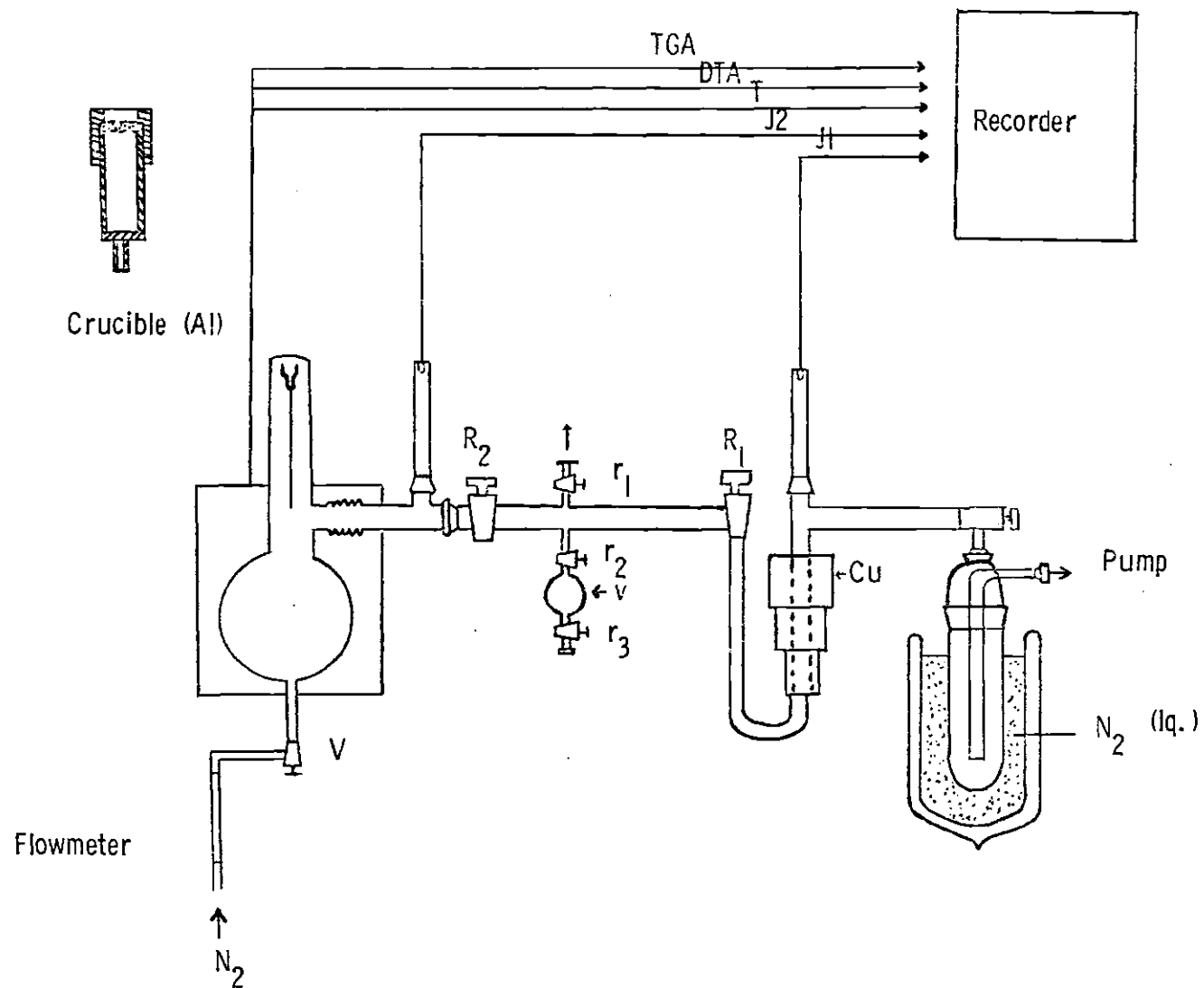


Figure 1. Description of High Vacuum Portion of Mettler Thermoanalyzer II

tube can also be used as an analytical device to separate the condensed gases after the desired temperature limit has been reached. After the liquid nitrogen has been removed, slow warming of the copper branch produces a vertical thermal gradient which assures a good separation of the trapped products, the more volatile ones escaping first. The vacuum was constructed to allow the use of the DTA-TGA under various conditions: vacuum, static pressure, or gas flow. In the latter case, the gas enters the chamber by V and leaves through r_1 or r_2 and r_3 ; R_2 open, R_1 closed.¹¹

Analytical

Gas analyses were carried out by hydrolyzing samples with hydrochloric acid on a standard vacuum line equipped with a Toepler pump.¹⁰ Methane in the presence of hydrogen was determined in a tensimeter of calibrated volume. Alkali metals were determined by flame photometry. Aluminum was determined by EDTA titration. Zinc in the presence of aluminum was determined by masking the aluminum with triethanolamine and titrating the zinc with EDTA. Zinc alone was determined by EDTA titration. Halogens were determined by the Volhard procedure.

Materials

Potassium and sodium hydride were obtained from Alfa Inorganics as a slurry in mineral oil. Lithium hydride was prepared by hydrogenolysis of t-butyllithium at 4000 psig for 24 hours. Solutions of lithium and sodium aluminum hydride (Ventron, Metal Hydride Division) were prepared in both diethyl ether and tetrahydrofuran in the usual manner. Dimethyl- and di-s-butylzinc were prepared by the procedure of Noller.¹² Methyl

and s-butyl iodides were obtained from Fisher Scientific. The iodides were dried over anhydrous MgSO_4 and distilled prior to use. Zinc-copper couple was obtained from Alfa Inorganics. The reactions of zinc-copper couple with methyl iodide were allowed to proceed overnight. The dimethylzinc was distilled from the reaction mixture at atmospheric pressure under nitrogen while di-s-butylzinc was distilled at reduced pressure. Methyl lithium (made from CH_3Cl) was obtained as a 5% solution in ether from Matheson, Coleman, and Bell and stored at -20° until ready to use. Tetrahydrofuran and benzene (Fisher Certified Reagent Grade) were distilled under nitrogen over NaAlH_4 and diethyl ether (Fisher Reagent) over lithium aluminum hydride. Ultra-pure hydrogen (99.9995%) obtained from the Matheson Corporation was used for hydrogenation experiments. Alane was prepared by the reaction of 100% H_2SO_4 with LiAlH_4 in THF. Li_2SO_4 was removed by filtration and a lithium free solution of AlH_3 in THF was obtained.¹³

Potassium, sodium, and lithium hydride were used as a slurry in THF. Each slurry was prepared by washing the respective hydride several times with generous portions of benzene, then several times with THF to remove soluble impurities. The resulting solid, while still under THF, was transferred to a round bottom flask and more THF was added.

Anhydrous zinc chloride, bromide, and iodide were obtained from Fisher Scientific. Zinc chloride was fused under vacuum in order to make it anhydrous prior to dissolving in THF. Zinc bromide and iodide were sublimed under vacuum prior to dissolving in THF. The final zinc halide

solutions were prepared by stirring the dried zinc halide with THF overnight and filtering the next morning. The zinc iodide solution was stored in the dark.

Procedure

Reactions Involving $(s-C_4H_9)_2Zn$

Reaction of LiH and $(s-C_4H_9)_2Zn$ in Benzene. Di-s-butylzinc (66 mmoles) in benzene was added to a slurry of LiH (66 mmoles) in benzene. After stirring for one week, the mixture was filtered. The filtrate showed a Zn:s-butyl ratio of 1:1.98, but no lithium or hydridic hydrogen was found. Analysis of the solid showed a Li:Zn:H ratio of 10:1:7.

Reaction of LiH and $(s-C_4H_9)_2Zn$ in THF. Di-butylzinc (27.9 mmoles) in THF was added to 27.9 mmoles of a LiH slurry in THF. The mixture was stirred at room temperature overnight. A clear solution resulted which exhibited a Li:Zn:s- C_4H_9 :H ratio of 1.00:0.96:1.88:0.32. Gas chromatography of the hydrolysate showed a large butanol peak due to extensive THF cleavage. A similar reaction was carried out in such a way that all of the THF was removed under vacuum immediately after the lithium hydride dissolved. But the lithium di-s-butylhydrido-zincate complex decomposed to lithium hydride and di-s-butylzinc under vacuum. Thus, it was not possible to remove all the THF and dissolve the residue in a non-cleaving solvent, such as benzene.

Reaction of LiH and $(s-C_4H_9)_2Zn$ in Diethyl Ether. Di-s-butylzinc (28 mmoles) in diethyl ether was added to a slurry of 28 mmoles of LiH in diethyl ether. The mixture was stirred for one week and filtered. The filtrate showed a Li:Zn ratio of 0.20:1.00. The solid exhibited a Li:Zn:H

ratio of 1.00:0.06:0.97. The reaction was repeated under reflux conditions for two weeks. Still little reaction occurred.

Reaction of $\text{LiZn}(\text{s-C}_4\text{H}_9)_2\text{H}$ with LiAlH_4 in THF. Preparation of Li_2ZnH_4 . Lithium hydride slurry (5.49 mmol) in THF was added to 5.49 mmol of di-s-butylzinc in THF. This mixture was stirred until all the lithium hydride dissolved (about 21 hours); the 8.11 mmol of LiAlH_4 in THF was added rapidly. After five minutes a white solid began to appear; after 30 minutes the mixture had a slightly gray, thick, milky appearance. The mixture was stirred overnight at room temperature. The solid, now having a gray appearance, was separated by filtration and dried at room temperature in vacuo. Anal. Calcd. for Li_2ZnH_4 : Li, 16.7; Zn, 78.5; H, 4.85. Found: Li, 16.3; Zn, 79.5; H, 4.11. The molar ratio of Li:Zn:H is 1.93:1.00:3.36. The filtrate contained 8.50 mmol of aluminum, 3.40 mmol of zinc, and 10.31 mmol of lithium. The amount of Li_2ZnH_4 recovered was 2.09 mmol of a theoretical 2.75 mmol. The x-ray powder diffraction data are given in Table 1. The infrared spectrum of the solid product (Nujol mull) showed two strong broad bands at 400-1000 cm^{-1} centered at 650 cm^{-1} and 1200-1650 cm^{-1} centered at 1450 cm^{-1} . This spectrum was very similar to that found for K_2ZnH_4 .⁸

Reactions Involving $(\text{CH}_3)_2\text{Zn}$ and LiH

Reaction of $\text{LiZn}(\text{CH}_3)_2\text{H}$ with LiAlH_4 in THF. Attempted Preparation of LiZnH_3 . Ten mmol of dimethylzinc in THF was added to 10 mmol of LiH slurry in THF. After five hours stirring the solution was clear. Ten mmol of LiAlH_4 in THF was added quickly. After one minute the solution became faintly cloudy; after 30 minutes a thick white mixture was present.

Table 1. X-Ray Powder Patterns for Complex Metal Zinc Hydrides of Lithium

Li_2ZnH_4 d, Å	+ Zn ^a I/I ₀	Li_2ZnH_4 d, Å	+ Zn ^b I/I ₀	Li_2ZnH_4 d, Å	+ Zn ^c I/I ₀	Li_2ZnH_4 ^d d, Å	I/I ₀
4.25	m	4.25	m	4.22	mw	5.02	m
3.83	m	3.85	m	3.85	w	4.69	w
3.67	w	3.69	mw	3.69	w	4.25	s
3.44	m	3.44	m	3.42	w	3.84	vs
2.95	m	2.95	m	3.25	vw	3.65	m
2.70	w	2.68	mw	2.95	mw	3.42	ms
2.47	m	2.46	ms	2.73	w	2.95	ms
2.43	m	2.29	ms	2.46	ms	2.71	mw
2.29	w	2.09	vs	2.29	ms	2.46	s
2.12	w	1.90	vw	2.09	s	2.42	s
2.08	m	1.83	vw	1.68	m	2.32	m
1.95	w	1.68	m	1.34	m	2.26	mw
1.84	w	1.33	m	1.33	m	2.24	mw
1.68	w	1.23	w	1.23	w	2.12	m
1.60	w	1.17	m	1.17	m	2.07	w
1.17	w	1.15	w	1.15	w	1.99	m
0.90	w	1.12	m	1.12	m	1.91	m
0.865	w	1.09	w	1.09	w	1.84	m
		1.04	w	1.04	w	1.79	m
		0.941	w	0.941	w	1.70	w
		0.907	w	0.907	w	1.67	w
		0.904	w	0.905	w	1.64	w
		0.903	w	0.870	w	1.60	m
		0.870	w	0.856	w	1.57	w
		0.856	w	0.855	w	1.54	w
		0.854	w	0.821	w	1.52	w
		0.821	w	0.819	w	1.50	w
		0.818	w			1.48	m
						1.47	M
						1.456	w
						1.44	w
						1.397	w
						1.36	w
						1.34	w
						1.32	w
						1.29	w
						1.21	w

^a $\text{LiZn(s-C}_4\text{H}_9)_2\text{H} + \text{LiAlH}_4$ in THF. ^b $\text{LiZn(CH}_3)_2\text{H} + \text{LiAlH}_4$ in THF.

^c $\text{LiZn}_2(\text{CH}_3)_4\text{H} + \text{LiAlH}_4$ in THF. ^d $\text{Li}_2\text{Zn(CH}_3)_4 + \text{LiAlH}_4$ in diethyl ether.

^e $\text{Li}_3\text{Zn(CH}_3)_5 + \text{LiAlH}_4$ in diethyl ether.

Table 1. Continued

$\text{Li}_3\text{ZnH}_5^e$		LiZnH_3^f		$^g\text{LiZn}_2\text{H}_5$		$^h\text{LiZn}_3\text{H}_7 + \text{Zn}$	
d, Å	I/I ₀	d, Å	I/I ₀	d, Å	I/I ₀	d, Å	I/I ₀
4.45	w	6.25	m	6.24	m	6.24	m
2.84	s	5.02	w	4.45	s	4.45	s
2.78	w	4.45	vs	4.30	m	3.24	m
2.64	m	4.30	m	3.26	s	3.10	m
2.50	m	4.19	m	3.10	m	2.91	mw
1.91	w	3.81	ms	2.94	m	2.81	m
1.79	w	3.65	w	2.81	m	2.45	m
1.63	ms	3.42	mw	2.50	m	2.31	mw
1.50	m	3.24	vs	2.41	m	2.16	mw
1.385	w	3.10	m	2.24	w	2.09	s
		2.94	s	2.17	mw	1.98	w
		2.81	s	2.07	w	1.96	w
		2.50	mw	1.98	w	1.75	w
		2.45	m	1.95	w	1.68	w
		2.41	m	1.75	w	1.33	w
		2.31	w	1.60	w	1.17	w
		2.24	mw	1.495	w	1.12	w
		2.16	mw	1.25	vw		
		2.12	w				
		2.06	w				
		1.98	mw				
		1.94	mw				
		1.90	mw				
		1.84	w				
		1.75	mw				
		1.64	w				
		1.60	m				
		1.52	w				
		1.495	w				
		1.44	w				
		1.244	w				

$^f\text{LiZn}(\text{CH}_3)_3 + \text{LiAlH}_4$ in diethyl ether. $^g\text{LiZn}_2(\text{CH}_3)_5 + \text{LiAlH}_4$ in diethyl ether. $^h\text{LiZn}_3(\text{CH}_3)_7 + \text{LiAlH}_4$ in diethyl ether.

Table 1. Continued

Zn^i		LiH^j		ZnH_2^k	
d, Å	I/I ₀	d, Å	I/I ₀	d, Å	I/I ₀
				4.51	vw
				4.23	s
				3.80	vw
				3.40	m
				2.97	vw
				2.828	vw
2.473	m			2.608	w
		2.357	m	2.468	vw
2.308	m			2.387	m
				2.290	m
2.091	s			2.225	m
		2.041	s	2.135	w
				2.085	w
				2.017	vw
1.687	m			1.905	w
				1.764	w
		1.444	m	1.688	vw
1.342	m			1.603	vw
1.332	m			1.562	vw
1.237	w	1.231	mw	1.486	vw
1.173	m	1.178	w	1.464	vw
1.154	w			1.416	vw
1.124	w			1.336	vw
1.091	w			1.305	vw
1.046	w			1.295	vw
		1.020	vw	1.259	vw
		0.9374	w	1.219	vw
		0.9130	w	1.172	vw
		0.8335	w	1.157	vw
		0.7859	vw	1.123	vw

ⁱASTM file. ^jASTM file. ^k $\text{LiAlH}_4 - (\text{C}_2\text{H}_5)_2\text{Zn}$, see reference 5.

w, weak; m, medium; s, strong; v, very

The mixture was stirred overnight at room temperature and filtered the next day. The precipitate, which had now become very gray due to decomposition to zinc metal, was dried at room temperature in vacuo. Anal. Calcd. for LiZnH_3 : Li, 9.2; Zn, 86.8; H, 4.0. Found: Li, 9.4; Zn, 87.2; H, 3.35. The molar ratio of Li:Zn:H was 1.00:1.00:2.51. The filtrate contained 10.78 mmoles of aluminum, 1.41 mmoles of zinc, and 11.20 mmoles of lithium. The amount of solid recovered was 8.59 mmoles of a theoretical 10 mmoles. The x-ray powder diffraction data which are given in Table 1 showed lines for Li_2ZnH_4 and zinc metal only.

Reaction of LiH and $(\text{CH}_3)_2\text{Zn}$ in 2:1 Ratio in THF. Attempted Preparation of $\text{Li}_2\text{Zn}(\text{CH}_3)_2\text{H}_2$. Twenty mmoles of lithium hydride slurry in THF was added to 10 mmoles of dimethylzinc in THF. The resulting mixture was stirred for two weeks at room temperature. A solid was always present. The solid was separated by filtration and dried at room temperature in vacuo. The solid had a molar ratio of Li:Zn of 15.22:1.00. The x-ray powder diffraction pattern of the solid product contained lines due to lithium hydride and zinc metal only. The Li:Zn ratio of the filtrate was 1.28:1.00.

Reaction of $\text{LiZn}_2(\text{CH}_3)_4\text{H}$ with LiAlH_4 in THF. Attempted Preparation of LiZn_2H_5 . Five mmoles of a lithium hydride slurry in THF was added to 10 mmoles of dimethylzinc in THF. Within five minutes a clear solution resulted. After addition of 20 mmoles of LiAlH_4 an infrared spectrum of the solution showed only bands due to LiAlH_4 . After 30 minutes some gray solids began to appear. The mixture was stirred overnight at room temperature. The next day, very gray, almost black solids were present.

The precipitate was separated by filtration and dried at room temperature in vacuo. The molar ratio of Li:Zn:H in the solid was 1.00:2.06:2.96.

The filtrate contained 20.20 mmol of aluminum, 1.02 mmol of zinc, and 19.60 mmol of lithium. The gas evolved on hydrolysis of the filtrate was found to contain hydrogen to methane in the molar ratio 4.28:1.00.

The infrared spectrum of the filtrate corresponded to a mixture of $\text{LiAl}(\text{CH}_3)_2\text{H}_2$ and LiAlH_4 . X-ray powder diffraction data for the solid, which are given in Table 1, showed lines for Li_2ZnH_4 and zinc metal only. Infrared analysis (Nujol mull) of the solid showed three broad bands ($400\text{--}700\text{ cm}^{-1}$, $950\text{--}1150\text{ cm}^{-1}$, $1350\text{--}2000\text{ cm}^{-1}$).

Reactions of KH with ZnCl_2 in THF

Reaction of KH with ZnCl_2 in 1:1 Molar Ratio. Potassium hydride slurry (5 mmol) in THF was added to 5 mmol of ZnCl_2 in THF. A solid remained during the entire reaction period. After two days stirring the mixture was separated by filtration. The resulting white solid was dried under vacuum at room temperature. An analysis of the filtrate revealed that it contained K, Zn, Cl, and H in molar ratios of 1.01:2.00:4.91:0.00. The filtrate contained 1.71 mmol of the starting zinc. An analysis of the solid revealed that it contained K, Zn, Cl, and H in molar ratios of 1.28:1.00:1.71:1.51. The solid contained 3.33 mmol of the starting zinc. The x-ray powder diffraction pattern of the solid is given in Table 2.

Reaction of KH with ZnCl_2 in 1:2 Molar Ratio. Potassium hydride slurry (5 mmol) in THF was added to 10 mmol of ZnCl_2 in THF. A solid remained during the entire reaction period. After 24 hours stirring the

Table 2. X-Ray Powder Patterns of Solids from the Reaction of Alkali Metal Hydrides with ZnCl_2

Solid from 1:1 Reaction of KH with ZnCl_2		Solid from 1:2 Reaction of KH with ZnCl_2		Solid from 2:1 Reaction of KH with ZnCl_2		Solid from 3:1 Reaction of KH with ZnCl_2	
d, Å	I/I ₀ ^f	d, Å	I/I ₀	d, Å	I/I ₀	d, Å	I/I ₀
5.06	m	6.10	w	3.12	vs	3.28	m
3.59	m	5.08	m	2.82	m	3.12	s
3.45	vw	4.44	w	2.60	m	2.84	m
3.28	vw	3.58	m	2.46	m	2.80	m
3.12	s	3.10	vw	2.20	s	2.60	m
2.80	ms	2.89	w	2.08	m	2.46	m
2.65	w	2.82	ms	1.90	w	2.20	s
2.59	ms	2.67	w	1.80	m	2.09	m
2.44	ms	2.60	ms	1.68	w	2.00	m
2.21	s	2.53	w	1.62	vw	1.90	w
2.01	w	2.46	ms	1.56	mw	1.80	m
1.90	mw	2.33	w	1.46	m	1.71	m
1.80	m	2.29	w	1.395	m	1.68	w
1.71	w	2.25	w	1.360	w	1.64	w
1.62	mw	2.08	ms	1.33	w	1.56	mw
1.56	mw	1.90	m	1.329	w	1.48	m
1.47	m	1.86	w	1.169	w	1.40	m
1.40	m	1.81	vw	1.119	w	1.30	w
1.378	vw	1.68	w	1.09	w	1.276	m
1.280	m	1.62	mw			1.170	w
1.109	w	1.475	ms			1.109	w
1.091	vw	1.370	m			1.043	mw
1.045	w	1.335	w			0.991	mw
1.011	vw	1.329	w				
0.946	w	1.169	w				
0.939	vw	1.119	w				
0.905	w	1.09	w				
0.871	w						
0.840	w						

Table 2. Continued

Solid from 1:1 Reaction of KCl with ZnCl_2		Solid from Reaction of KCl + ZnCl_2 Filtrate with AlH_3		Solid from 1:1 Reaction of NaH with ZnCl_2	
d, Å	I/I ₀	d, Å	I/I ₀	d, Å	I/I ₀
6.10	m	3.12	s	3.22	w
5.08	s	2.20	s	2.80	s
4.44	m	1.80	m	2.45	ms
3.93	w	1.56	mw	2.31	ms
3.57	s	1.395	mw	2.08	vs
3.40	w	1.273	w	1.98	ms
3.10	mw	1.101	vw	1.72	w
2.98	w	1.041	w	1.68	m
2.87	m	0.987	w	1.62	m
2.67	ms	0.942	w	1.401	w
2.53	m	0.866	vw	1.333	m
2.40	w	0.837	vw	1.321	m
2.33	mw			1.256	mw
2.25	mw			1.230	w
2.14	mw			1.169	m
2.07	mw			1.148	mw
1.94	w			1.119	m
1.87	m			1.086	w
1.83	mw			1.040	w
1.78	w			0.941	w
1.70	w				
1.65	w				
1.57	w				
1.54	w				
1.50	w				
1.47	w				
1.44	vw				

Table 2. Continued

ZnCl_2^a		KCl^b		KH^c		Zn^d		NaCl^e	
d, Å	I/I ₀	d, Å	I/I ₀	d, Å	I/I ₀	d, Å	I/I ₀	d, Å	I/I ₀
7.6	vs	3.146	s	3.30	vs	2.473	m	3.22	w
6.85	vs	2.224	ms	2.86	s	2.308	m	2.80	s
6.31	mw	1.816	m	2.02	s	2.091	s	1.98	s
5.61	w	1.573	w	1.72	s	1.687	m	1.72	w
5.10	vs	1.407	m	1.65	m	1.342	m	1.62	m
4.75	vw	1.284	m	1.43	m	1.332	m	1.401	w
4.20	m	1.1126	w	1.31	m	1.237	w	1.256	mw
4.04	s	1.049	w	1.28	m	1.173	m		
3.77	mw	0.9951	w	1.17	m	1.154	w		
3.61	s	0.9486	w	1.10	m	1.124	w		
3.31	m	0.9083	vw	1.01	w	1.091	w		
3.22	mw	0.8727	w			1.046	w		
3.12	s	0.8410	w						
2.99	w								
2.95	m								
2.84	w								
2.76	mw								
2.58	w								
2.52	w								
2.49	w								
2.45	mw								
2.36	s								
2.25	vw								
2.18	vw								
2.03	s								
1.96	w								
1.88	mw								
1.82	ms								
1.77	ms								
1.73	ms								

^aSample obtained by stripping a THF solution of ZnCl_2 to dryness.

^bASTM file. ^cASTM file. ^dASTM file. ^eASTM file.

^fw, weak; m, medium; s, strong; v, very; d, diffused.

mixture was separated by filtration. The resulting white solid was dried under vacuum at room temperature. Analysis of the filtrate revealed that it contained K, Zn, Cl, and H in molar ratios of 0.29:1.00:2.27:0.00. The filtrate contained 5.86 mmols of the starting zinc. Analysis of the solid revealed that it contained K, Zn, Cl, and H in molar ratios of 0.82:1.00:1.62:1.19. The solid contained 4.20 mmols of the starting zinc. The x-ray powder diffraction pattern of the solid is given in Table 2.

Reaction of KH with ZnCl_2 in 2:1 Molar Ratio. Potassium hydride slurry (10 mmols) in THF was added to 5 mmols of ZnCl_2 in THF. A solid remained during the entire reaction period. After two days stirring the mixture was separated by filtration. The resulting white solid was dried under vacuum at room temperature. Analysis of the filtrate showed that it contained none of the starting zinc. Analysis of the solid showed that it contained K, Zn, Cl, and H in molar ratios of 3.08:1.00:1.94:2.97. The solid contained all the starting zinc. Its x-ray powder diffraction pattern is shown in Table 2.

Reaction of KCl with ZnCl_2 in 1:1 Molar Ratio in THF

Dry KCl (1.1250 gm or 15.09 mmols) was placed in a 250 ml round bottom flask and 80 ml of THF added. Then ZnCl_2 (15.09 mmols) in THF was added. The mixture was stirred for four days, during which time a white solid was always present. The mixture was separated by filtration. The resulting white solid was dried under vacuum at room temperature. An analysis of the filtrate showed that it contained K, Zn, and Cl in molar ratios of 1.06:2.00:4.94. The filtrate contained 10.06 mmols of

the starting zinc. Analysis of the solid showed that it contained K, Zn, and Cl in molar ratios of 1.96:1.00:3.94. The solid contained 5.05 mmoles of the starting zinc. The x-ray powder pattern of the solid is shown in Table 2.

Reaction of AlH_3 with the Filtrate from the Reaction of KCl with ZnCl_2 in THF

Alane in THF (20 mmoles) was added to the filtrate from the reaction of KCl with ZnCl_2 (analysis indicated KZn_2Cl_5). A white precipitate appeared immediately. This slurry was stirred for one hour, then the solid separated by filtration. The solid was dried under vacuum at room temperature. Analysis of the filtrate showed it to contain K, Zn, Al, Cl, and H in molar ratios of 0.00:0.00:1.00:1.08:2.07. The filtrate contained all of the aluminum. An analysis of the solid showed that it contained K, Zn, Cl, H, and Al in molar ratios of 0.46:1.00:0.52:2.00:0.00. The solid contained all the potassium and zinc. The x-ray powder pattern of the solid is shown in Table 2.

Reaction of NaH with ZnCl_2 in 1:1 Molar Ratio in THF

Sodium hydride slurry (10 mmoles) in THF was added to 10 mmoles of ZnCl_2 in THF. A solid remained during the entire reaction period. After one day stirring the mixture was separated by filtration. The solid had turned black while stirring overnight. The solid was dried under vacuum at room temperature. Analysis of the filtrate showed that it contained Na, Zn, Cl, and H in molar ratios of 0.00:1.00:1.96:0.00. The filtrate contained 5.12 mmoles of the starting zinc. Analysis of the solid showed that it contained Na, Zn, Cl, and H in molar ratios of 1.94:1.00:1.97:1.27.

The solid contained 4.98 mmols of the starting zinc. The x-ray powder pattern of the solid is shown in Table 2.

Reaction of LiH with ZnBr_2 in 2:1 Molar Ratio in THF

Lithium hydride slurry (5 mmols) in THF was added to 2.5 mmols of ZnBr_2 in THF. A solid remained during the entire reaction period. After two days stirring the mixture was separated by filtration. The resulting white solid was dried under vacuum at room temperature. Analysis of the filtrate showed it to contain Li, Zn, Br, and H in molar ratios of 1.00:0.02:0.98:0.00. The filtrate contained 0.20 mmole of the starting zinc. Analysis of the solid showed it to contain Li, Zn, Br, and H in molar ratios of 0.03:1.00:0.04:1.89. The solid contained 2.41 mmols of the starting zinc. An x-ray powder diffraction pattern of the solid is shown in Table 3.

Reaction of NaH with ZnI_2 in 2:1 Molar Ratio in THF

Sodium hydride slurry (20 mmols) in THF was added to 10 mmols of ZnI_2 in THF. A solid remained during the entire reaction period. After two days stirring the mixture was separated by filtration. The resulting white solid was dried under vacuum at room temperature. An analysis of the filtrate showed it to contain Na, Zn, I, and H in molar ratios of 1.06:0.01:1.00:0.00. The filtrate contained 0.21 mmole of the starting zinc. Analysis of the solid showed it to contain Na, Zn, I, and H in molar ratios of 0.06:1.00:0.05:1.97. The solid contained 9.89 mmols of the starting zinc. The x-ray powder diffraction pattern of the solid is shown in Table 3.

Table 3. X-Ray Powder Patterns of Solids from the Reaction of Alkali Metal Hydrides with ZnBr_2 and ZnI_2

ZnH ₂ from 2:1 Reaction of LiH with ZnBr ₂		ZnH ₂ from 2:1 Reaction of NaH with ZnI ₂		ZnH ₂ ^a from Reaction of LiAlH ₄ with (C ₂ H ₅) ₂ Zn in Diethyl Ether		ZnH ₂ ^b from Reaction of LiAlH ₄ with (CH ₃) ₂ Zn in Diethyl Ether	
d, Å	I/I ₀	d, Å	I/I ₀	d, Å	I/I ₀	d, Å	I/I ₀
4.90	w	4.90	w	4.51	vw	6.27	w
3.79	w	3.79	w	4.23	s	4.50	m
2.82	s	2.82	s	3.80	vw	4.16	m
2.60	s	2.60	s	3.40	m	3.79	m
2.46	s	2.46	s	2.97	vw	3.27	w
2.29	m	2.29	m	2.828	vw	3.12	m
2.08	s	2.08	s	2.608	w	2.94	w
1.90	ms	1.90	ms	2.468	vw	2.83	w
1.68	m	1.68	m	2.387	m	2.61	vw
1.62	ms	1.62	ms	2.290	m	2.50	w
1.475	s	1.475	s	2.225	m	2.40	w
1.370	ms	1.370	ms	2.135	w	2.29	w
1.335	m	1.335	m	2.085	w	2.23	m
1.329	m	1.329	m	2.017	vw	2.18	m
1.300	w	1.300	w	1.905	w	2.14	vvw
1.234	w	1.234	w	1.764	w	2.08	m
1.169	m	1.169	m	1.688	vw	2.02	vw
1.150	w	1.150	w	1.630	vw	1.98	vw
1.119	m	1.119	m	1.562	vw	1.90	vw
1.09	m	1.09	m	1.486	vw	1.77	w
1.04	mw	1.04	mw	1.464	vw	1.63	vvw
1.013	mw	1.013	mw	1.416	vw	1.61	vvw
0.974	mw	0.974	mw	1.336	vw	1.57	vvw
				1.305	vw	1.51	w
				1.295	vw	1.42	vw
				1.259	vw	1.35	w
				1.219	vw		
				1.172	vw		
				1.157	vw		
				1.123	vw		

^aSee reference 5. ^bSee reference 8. ^cw, weak; m, medium; s, strong, v, very; d, diffused.

Reactions Involving $(\text{CH}_3)_2\text{Zn}$ with CH_3Li

Reaction of LiAlH_4 with $\text{LiZn}(\text{CH}_3)_3$ in Diethyl Ether. Preparation of LiZnH_3 . Five mmoles of methyllithium in diethyl ether was added to 5 mmoles of dimethylzinc in diethyl ether. The resulting solution was stirred at room temperature for one hour, then 7.5 mmoles of LiAlH_4 in diethyl ether was added. A white precipitate appeared immediately. This mixture was stirred at room temperature for another hour and filtered. The white solid was dried at room temperature in vacuo and analyzed. Anal. Calcd. for LiZnH_3 : Li, 9.2; Zn, 86.8; H, 4.0. Found: Li, 9.2; Zn, 86.5; H, 4.30. The molar ratio of Li:Zn:H was 1.00:1.00:3.21. The filtrate contained 7.53 mmoles of aluminum, no zinc, and 7.34 mmoles of lithium. The amount of LiZnH_3 recovered was 5 mmoles of a theoretical 5 mmoles. The x-ray powder diffraction data are given in Table 1.

Reaction of LiAlH_4 with $\text{Li}_2\text{Zn}(\text{CH}_3)_4$ in Diethyl Ether. Preparation of Li_2ZnH_4 . Ten mmoles of dimethylzinc in diethyl ether was added to 20 mmoles of methyllithium in diethyl ether. The resulting solution was stirred for one hour at room temperature followed by addition of 20 mmoles of LiAlH_4 in diethyl ether. White solids appeared immediately; however, the mixture was stirred for an additional one hour at room temperature in vacuo. Anal. Calcd. for Li_2ZnH_4 : Li, 16.7; Zn, 78.5; H, 4.85. Found: Li, 14.8; Zn, 80.4; H, 4.85. The molar ratio of Li:Zn:H was 1.73:1.00:3.94. The filtrate contained 19.30 mmoles of aluminum, no zinc, and 20.01 mmoles of lithium. The amount of Li_2ZnH_4 recovered was 10 mmoles of a theoretical 10 mmoles. The x-ray powder diffraction data are given in Table 1. Infrared analysis (Nujol mull) showed three broad bands (400-

900 cm^{-1} , 1200-1400 cm^{-1} centered at 1290 cm^{-1} , and 1400-1900 cm^{-1} centered at 1580 cm^{-1}). Infrared analysis of the filtrate (KBr cell, 0.10 mm path length) showed a strong peak in the Al-H stretching region centered at 1700 cm^{-1} and a moderate peak in the Al-H deformation region centered at 760 cm^{-1} . This spectrum is characteristic of the species $\text{LiAl}(\text{CH}_3)_2\text{H}_2$.

Reaction of LiAlH_4 with $\text{Li}_3\text{Zn}(\text{CH}_3)_5$ in Diethyl Ether. Preparation of Li_3ZnH_5 . Fifteen mmoles of methyllithium in diethyl ether was added to 5 mmoles of dimethylzinc in diethyl ether. The resulting solution was stirred for one hour at room temperature followed by addition of 12.5 mmoles of LiAlH_4 in diethyl ether. A white precipitate appeared immediately. The mixture was stirred for an additional hour at room temperature and then filtered. The resulting white solid was dried at room temperature in vacuo and analyzed. Anal. Calcd. for Li_3ZnH_5 : Li, 4.86; Zn, 91.6; H, 3.54. Found: Li, 5.08; Zn, 91.6; H, 3.45. The molar ratio of Li:Zn:H was 1.00:1.92:4.66. The filtrate contained 12.55 mmoles of aluminum, 0.04 mmole of zinc, and 12.59 mmoles of lithium. The amount of solid recovered was 5 mmoles of a theoretical 5 mmoles. The x-ray powder diffraction data are given in Table 1.

Reaction of LiAlH_4 with $\text{LiZn}_3(\text{CH}_3)_7$ in Diethyl Ether. Attempted Preparation of LiZn_3H_7 . Fifteen mmoles of dimethylzinc in diethyl ether was added to 5 mmoles of methyllithium in diethyl ether. The resulting solution was stirred for one hour at room temperature followed by addition of 17.5 mmoles of LiAlH_4 in diethyl ether. A white precipitate appeared immediately. This mixture was stirred for an hour and filtered. The solid, which had turned slightly gray, was dried under vacuum at room

temperature. Anal. Calcd. for LiZn_3H_7 : Li, 3.30; Zn, 93.4; H, 3.36. Found: Li, 3.11; Zn, 93.6; H, 3.34. The molar ratio of Li:Zn:H was 1.00:3.20:7.37. The filtrate contained 18.02 mmols of aluminum, no zinc, and 18.20 mmols of lithium. The yield of solid was 100%. The x-ray powder diffraction data are given in Table 1.

Reactions Involving $(\text{CH}_3)_2\text{Zn}$ with KH

Reaction of KH (excess) and $(\text{CH}_3)_2\text{Zn}$ in Diethyl Ether. Dimethylzinc (26.73 mmols) in diethyl ether was added to a slurry of 60.4 mmols of potassium hydride in diethyl ether. The slurry became hot immediately and solvent came to reflux. A solid was always present during the reaction. The mixture was stirred overnight at room temperature and filtered the next day. The resulting white solid was dried under vacuum at room temperature. The x-ray powder diffraction data are given in Table 4. The filtrate showed a molar ratio of K:Zn of 0.92:1.00, but it contained only 0.59 mmole of zinc; i.e., only 2.22% of the starting zinc was found in the filtrate. The solid was slurried for three hours in THF, then filtered. The residual solid was shown to be KH by x-ray powder diffraction and the filtrate had a molar ratio of K:Zn: CH_3 :H of 0.98:1.00:2.14:0.39. The $\text{KZn}(\text{CH}_3)_2\text{H}$ formed cleaved THF at room temperature producing a soluble product.

Reaction of AlH_3 with $\text{KZn}(\text{CH}_3)_2\text{H}$ in THF. Preparation of KZn_2H_5 . Ten mmols of dimethylzinc in THF was added to 10 mmols of a slurry of KH in THF at room temperature. The mixture was clear within one minute. The mixture was quickly cooled to -80° to prevent ether cleavage, and stirred for two additional hours. Next, 10 mmols of AlH_3 in THF was

Table 4. X-Ray Powder Patterns for Complex Metal Zinc Hydrides of Potassium

$\text{KZn}(\text{CH}_3)_2\text{H} + \text{KH}^a$		KH^b		K_2ZnH_4^c		ZnH_2^d		KZn_2H_5^e	
d, Å	I/I ₀	d, Å	I/I ₀	d, Å	I/I ₀	d, Å	I/I ₀	d, Å	I/I ₀
6.10	mw			5.10	w	4.51	vw	6.03	s
5.30	mw			4.26	m	4.23	s	4.10	mw
4.05	mw, d			3.89	w	3.80	vw	3.72	mw
3.89	mw, d			3.62	vw	3.40	m	3.36	vs
3.59	ms, d			3.47	m	2.97	vw	3.01	m
3.40	ms, d			3.24	w	2.828	vw	2.67	vw
3.27	s	3.30	vs	3.09	s	2.608	w	2.59	vw
2.83	s	2.86	s	2.940	s	2.468	vw	2.42	s
2.75	w			2.744	w	2.387	m	2.35	s
2.45	m			2.568	vw	2.290	m	2.18	m
2.10	w			2.354	w	2.225	m	2.14	vw
2.00	ms	2.02	s	2.128	w	2.135	w	2.00	vw
1.71	ms	1.72	s	1.946	w	2.085	w	1.93	ms
1.64	w	1.65	m	1.814	w	2.017	vw	1.85	m
1.57	vw			1.734	w	1.905	w	1.80	m
1.43	w	1.43	m	1.648	vw	1.764	w	1.68	m
1.30	w	1.31	m	1.624	vw	1.688	vw	1.54	w
1.27	w	1.28	m	1.571	w	1.630	vw	1.49	m
1.16	w	1.17	m	1.488	w	1.562	vw	1.431	w
1.09	w	1.10	m	1.470	w	1.486	vw	1.414	w
0.96	w	1.01	w	1.384	vw	1.464	vw	1.371	mw
				1.213	w	1.416	vw	1.355	mw
						1.336	vw	1.328	w
						1.305	vw	1.269	vw
						1.295	vw	1.238	vw
						1.219	vw	1.222	w
						1.172	vw	1.176	w
						1.157	vw	1.151	vw
						1.123	vw	1.111	w
						1.042	vw	1.076	vw
								1.060	vw
								1.005	vw
								0.983	vw
								0.922	vw
								0.888	vw

^aExcess KH + $(\text{CH}_3)_2\text{Zn}$ in diethyl ether. ^bASTM files. ^cKH + $(s\text{-C}_4\text{H}_9)_2\text{Zn}$ in benzene, see ref. 5. ^d $\text{LiAlH}_4 + (\text{C}_2\text{H}_5)_2\text{Zn}$, see ref. ^e $\text{KZn}(\text{CH}_3)_2\text{H} + \text{AlH}_3$ in tetrahydrofuran. ^f $\text{KZn}_2(\text{CH}_3)_4\text{H} + \text{AlH}_3$ in tetrahydrofuran.

Table 4. Continued

KZn_2H_5^f		$^g\text{KZn}_3\text{H}_7$		KZnH_3^h	
d, Å	I/I ₀	d, Å	I/I ₀	d, Å	I/I ₀
6.03	s	6.02	ms	6.25	ms
4.08	mw	4.06	mw	5.60	vw
3.72	w	3.72	w	5.10	s
3.36	vs	3.36	vw	4.40	vw
3.02	mw	3.02	mw	3.71	vw
2.69	w	2.79	vw	3.59	m
2.61	w	2.69	vw	3.43	vs
2.43	s	2.60	vw	3.31	m
2.34	s	2.43	s	3.11	ms
2.18	m	2.35	s	2.80	s
2.02	w	2.28	vw	2.71	vs
1.93	ms	2.19	m	2.58	s
1.85	m	2.09	m	2.33	s
1.68	m	2.01	vw	2.18	w
1.53	w	1.93	ms	2.15	vw
1.490	m	1.86	m	2.12	vw
1.432	w	1.81	m	2.07	m
1.415	w	1.69	m	2.03	w
1.371	w	1.65	vw	1.94	vw
1.351	w	1.53	vw	1.90	ms
1.322	w	1.49	m	1.86	w
1.270	w	1.435	mw	1.85	vw
1.234	vw	1.419	w	1.79	m
1.222	w	1.361	mw	1.77	m
1.191	vw	1.355	mw	1.73	m
1.175	w	1.321	vw	1.72	w
1.154	vw	1.300	vw	1.69	m
1.111	w	1.271	vvw	1.66	w
1.078	w	1.239	vvw	1.64	w
1.057	w	1.223	w	1.595	m
1.003	vw	1.221	vw	1.57	w
0.986	vw	1.175	vw	1.55	w
0.022	vw	1.152	vw	1.455	mw
0.906	vw	1.111	w	1.370	mw
		1.079	w	1.325	mw
		1.059	w		

$^g\text{KZn}_3(\text{CH}_3)_6 + \text{AlH}_3$ in tetrahydrofuran. $^h\text{KZn}(\text{CH}_3)_2\text{H} + \text{LiAlH}_4$ in tetrahydrofuran.

w, weak; m, medium; s, strong; v, very; d, diffused.

added at -80° . The bath was removed and the reaction mixture allowed to warm to room temperature. After 15 minutes a white precipitate began to form. The mixture was stirred an additional hour and filtered. The solid was dried under vacuum at room temperature. Anal. Calcd. for KZn_2H_5 : K, 22.4; Zn, 74.8; H, 2.88. Found: K, 23.2; Zn, 74.0; H, 2.79. The molar ratio of K:Zn:CH₃:H was 1.05:2.00:0.00:4.92. The filtrate contained 10.21 mmoles of aluminum, no zinc, and 5.26 mmoles of potassium. The molar ratio of K:Al in the filtrate was 1.03:2.00. The x-ray powder diffraction pattern of the solid is given in Table 4.

Reaction of LiAlH_4 with $\text{KZn}(\text{CH}_3)_2\text{H}$ in THF. Preparation of KZnH_3 .
 Ten mmoles of dimethylzinc in THF was added to 10 mmoles of KH slurried in THF. The clear solution which resulted was cooled to -80° and stirred for one hour. Next 10 mmoles of lithium aluminum hydride in THF was added to the solution. The solution was warmed to room temperature and a white precipitate resulted. This mixture was stirred for one hour and filtered. The resulting white solid was dried under vacuum at room temperature. Anal. Calcd. for KZnH_3 : K, 36.4; Zn, 60.8; H, 2.81. Found: K, 36.6; Zn, 60.5; H, 2.86. The molar ratio of Li:K:Zn:H was 0.00:1.01:1.00:2.96. The filtrate contained 9.64 mmoles of aluminum, no zinc, no potassium, and 9.75 mmoles of lithium. The molar ratio of K:Li:Al in the filtrate was 0.00:1.01:1.00. The x-ray powder diffraction pattern of the solid is given in Table 4.

Reaction of AlH_3 with $\text{KZn}_2(\text{CH}_3)_4\text{H}$ in THF. Preparation of KZn_2H_5 .
 Twenty mmoles of dimethylzinc in THF was added to 10 mmoles of KH slurried in THF. A clear solution resulted even before all the dimethylzinc could

be introduced. The solution was quickly cooled to -80° and stirred for an additional hour at this temperature. Next, 14.82 mmol of AlH_3 in THF was added to the solution, at -80° . A faint white precipitate appeared immediately. The bath was removed and the mixture stirred for one hour, then filtered. The solid was dried under vacuum at room temperature. Anal. Calcd. for KZn_2H_5 : K, 22.4; Zn, 74.8; H, 2.88. Found: K, 21.5; Zn, 75.8; H, 2.79. The molar ratio of K:Zn:H was 1.00:2.10:5.04. The filtrate contained 16.96 mmol of aluminum, no zinc, and 0.83 mmol of potassium. The molar ratio of K:Al in the filtrate was 0.098:2.00. The x-ray powder diffraction pattern of the solid is given in Table 4.

Reaction of AlH_3 with $\text{KZn}_3(\text{CH}_3)_6\text{H}$ in THF. Attempted Preparation of KZn_3H_7 . Fifteen mmol of dimethylzinc in THF was added to 5 mmol of KH slurried in THF. The clear solution which resulted was cooled to -80° and stirred for one hour. Next, 15 mmol of AlH_3 in THF was added to the solution, at -80° . The mixture was allowed to warm to room temperature (a white precipitate formed in the process), stirred for one hour, then filtered. The solid was dried under vacuum at room temperature. Anal. Calcd. for KZn_3H_7 : K, 16.1; Zn, 80.9; H, 2.92. Found: K, 15.0; Zn, 82.1; H, 2.92. The molar ratio of K:Zn:H was 1.00:3.29:7.56. The filtrate contained 16.09 mmol of aluminum, no zinc, and 0.44 mmol of potassium. The molar ratio of K:Al in the filtrate was 0.055:2.00. The x-ray diffraction pattern of the solid, which is given in Table 4, showed lines due to KZn_2H_5 only.

Reactions Involving $(\text{CH}_3)_2\text{Zn}$ with NaH

Reaction of NaAlH_4 with $\text{NaZn}(\text{CH}_3)_2\text{H}$ in THF. Preparation of NaZnH_3 .

Ten mmoles of dimethylzinc in THF was added to 10 mmoles of NaH slurried in THF. The mixture was quickly cooled to -80° and stirred at that temperature until the Na:Zn ratio in the supernatant was 1:1. At this point, 5 mmoles of the supernatant $[\text{NaZn}(\text{CH}_3)_2\text{H}]$ solution was allowed to react with 5 mmoles of sodium aluminum hydride in THF. A white precipitate appeared within minutes. The mixture was stirred 20 minutes and filtered. The resulting white solid was dried under vacuum at room temperature.

Anal. Calcd. for NaZnH_3 : Na, 25.2; Zn, 71.5; H, 3.30. Found: Na, 25.2; Zn, 71.6; H, 3.24. The molar ratio of Na:Zn:H was 1.00:1.00:2.94. The x-ray powder diffraction pattern is given in Table 5. The filtrate contained 4.62 mmoles of aluminum, 0.47 mmole of zinc, and 5.06 mmoles of sodium.

Reaction of AlH_3 and $\text{NaZn}(\text{CH}_3)_2\text{H}$ in THF. Preparation of NaZn_2H_5 .

Five mmoles of dimethylzinc in THF was added to 5 mmoles of a slurry of NaH in THF at room temperature. Quickly, 5 mmoles of AlH_3 in THF was added at room temperature. An off white precipitate appeared. The mixture was stirred for a couple of hours and filtered. The solid was dried under vacuum at room temperature. Anal. Calcd. for NaZn_2H_5 : Na, 14.5; Zn, 82.4; H, 3.15. Found: Na, 15.2; Zn, 81.7; H, 3.01. The molar ratio of Na:Zn:H was 1.06:2.00:4.83. The molar ratio of Na:Al:Zn in the filtrate was 1.03:2.00:0.061. The x-ray powder diffraction pattern of the solid is given in Table 5.

Table 5. X-Ray Powder Patterns for Complex Metal Zinc Hydrides of Sodium

NaZnH_3^a		NaZnH_3^b		NaZnH_3^c		NaH^d		$\text{NaZn}_2\text{H}_5^e$	
d, Å	I/I ₀	d, Å	I/I ₀	d, Å	I/I ₀	d, Å	I/I ₀	d, Å	I/I ₀
8.70	vw	8.70	vw						
5.99	w	5.99	w	5.87	vw			5.84	m
4.90	vw	4.90	vs	4.90	s			4.89	s
4.39	w	4.40	w						
3.98	w	3.91	w						
3.30	m	3.52	w						
3.11	vs	3.27	ms	3.26	m			3.29	vs
2.91	m	3.11	vs	3.11	vs			3.09	m
2.81	w	2.92	m						
2.63	mw	2.81	m	2.84	w	2.83	s	2.83	s
2.56	m	2.62	w					2.50	w
2.49	ms	2.56	ms						
2.43	m	2.49	s	2.51	m	2.44	ms	2.44	m
2.38	vw	2.44	m	2.45	w				
2.26	w	2.25	w	2.38	vw			2.36	m
2.22	w	2.20	w	2.28	vw			2.26	m
2.15	w	2.15	vw	2.23	vw			2.15	w
2.07	w	2.07	w	2.16	vvw			2.09	w
1.96	mw	2.02	vw	2.09	vw			2.09	w
1.83	mw	1.97	mw	2.02	vvw			2.01	mw
1.78	w	1.84	w	1.98	w				
1.72	vw	1.78	w	1.79	vvw	1.73	ms	1.70	m
1.66	mw	1.70	w	1.70	vvw	1.47	ms	1.62	w
1.61	mw	1.66	w	1.67	vw	1.41	m	1.55	w
1.58	vw	1.61	mw	1.62	w	1.22	mw	1.50	w
1.53	mw	1.58	w	1.55	w	1.12	m	1.465	w
1.49	vw	1.53	mw	1.47	vvw	1.09	m		
1.38	vw	1.49	vw	1.35	vw	0.996	m	1.375	w
1.34	w	1.47	vw			0.939	m	1.351	w
1.22	vw	1.37	vw			0.863	mw	1.301	vw
1.06	vw	1.34	vw			0.825	m		
1.00	vw	1.22	vw			0.813	m		
		1.00	vvw						

^a $\text{NaZn}(\text{CH}_3)_2\text{H} + \text{NaAlH}_4$ in tetrahydrofuran. ^b $\text{NaZn}(\text{CH}_3)_4\text{H} + \text{NaAlH}_4$ in tetrahydrofuran. ^cSee ref. 11, made by thermally decomposing $\text{NaZn}_2(\text{CH}_3)_2\text{H}_3$.

^dASTM file. ^e $\text{NaZn}(\text{CH}_3)_2\text{H} + \text{AlH}_3$ in tetrahydrofuran. w, weak; m, medium; s, strong; v, very.

Reaction of $\text{NaZn}(\text{CH}_3)_2\text{H}$ with LiAlH_4 in THF. Preparation of NaZnH_3 .

Six mmols of $\text{NaZn}(\text{CH}_3)_2\text{H}$ in THF at -80° was added to 6 mmols of LiAlH_4 in THF. This mixture was allowed to warm to room temperature during which time a white precipitate resulted. The resulting white solid was filtered and dried at room temperature under vacuum. The molar ratio of Na:Zn:H in the solid was 1.00:1.00:2.75. The x-ray powder diffraction pattern, given in Table 5, was identical to that of NaZnH_3 . The filtrate contained 5.82 mmols of aluminum and 3.04 mmols of zinc.

Reaction of NaAlH_4 with $\text{NaZn}_2(\text{CH}_3)_4\text{H}$ in THF. Attempted Preparation of NaZn_2H_5 . Twenty mmols of dimethylzinc in THF was added to 10 mmols of NaH slurried in THF. The mixture was quickly cooled to -80° and stirred until the Na:Zn ratio in the supernatant was 0.50:1.00. At this point, 5 mmols of the supernatant [$\text{NaZn}_2(\text{CH}_3)_4\text{H}$ solution] was allowed to react with 10 mmols of sodium aluminum hydride in THF. A white precipitate appeared within minutes. The mixture was stirred for an hour and filtered. The resulting white solid was dried at room temperature under vacuum. The molar ratio of Na:Zn:H in the solid was 1.00:1.00:2.90. The x-ray powder diffraction pattern, given in Table 5, was identical to that for NaZnH_3 . The filtrate contained 10.00 mmols of aluminum, 3.06 mmols of zinc, and 9.50 mmols of sodium.

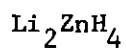
Reaction of NaH with $(s\text{-Bu})_2\text{Zn}$ in THF. Attempted Preparation of $\text{Na}_2\text{Zn}(\text{CH}_3)_2\text{H}_2$ and Na_2ZnH_4 . Ten mmols of NaH slurried in THF was added to 5 mmols of $(s\text{-Bu})_2\text{Zn}$ in THF. The mixture was stirred at room temperature for one day. A solid remained throughout this period and then filtered. The solid was dried under vacuum at room temperature. The molar

ratio of Na:H:Zn in the solid was found to be 1.00:1.03:0.070. The x-ray powder diffraction pattern and vacuum DTA-TGA showed that the solid was mostly NaH. The filtrate, which contained sodium and zinc in a molar ratio of 1.11:1.00, when allowed to react with NaAlH_4 , yielded NaZnH_3 only.

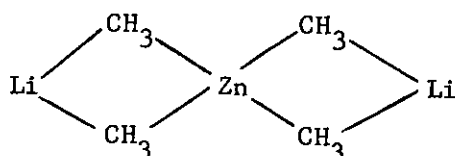
CHAPTER III

RESULTS AND DISCUSSION

While it is known that metal hydrides of the main group elements can be prepared by the reduction of a metal alkyl with lithium aluminum hydride,¹⁴ there have been no reports of the application of this simple reaction to the synthesis of new complex metal hydrides. When we found that the "ate" complexes of zinc (i.e., $\text{LiZn}(\text{s-C}_4\text{H}_9)_2\text{H}$) are cleaved by ether solvents, at the temperatures necessary to carry out hydrogenolysis ($75\text{-}150^\circ$) to the corresponding hydride, it was necessary to develop another method of reduction that could be carried out at lower temperature. It was found that LiAlH_4 , NaAlH_4 , or AlH_3 will reduce the "ate" complex to the corresponding hydride rapidly at room temperature

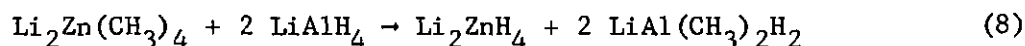


The "ate" complex $\text{Li}_2\text{Zn}(\text{CH}_3)_4$, lithium tetramethylzincate, first prepared by Hurd¹⁵ in 1948, has been characterized both by NMR,¹⁶ and x-ray crystallography.¹⁷ Its structure is shown below.



When $\text{Li}_2\text{Zn}(\text{CH}_3)_4$ and LiAlH_4 were allowed to react, Li_2ZnH_4 was obtained in 100% yield according to Eq. 8. The x-ray powder diffraction

pattern of Li_2ZnH_4 (Table 1) contains no lines due to LiH or ZnH_2 ; therefore, the product is not a physical mixture of the two simple hydrides.

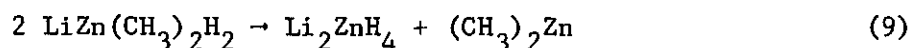


On the other hand, both the powder diffraction pattern and infrared spectrum of Li_2ZnH_4 were similar to that found for K_2ZnH_4 (Table 4). The infrared spectrum of the solution that remained after filtration of Li_2ZnH_4 showed that the aluminum containing species was $\text{LiAl}(\text{CH}_3)_2\text{H}_2$. Therefore, complete exchange of the methyl groups from zinc to aluminum had occurred. The structure of Li_2ZnH_4 might be similar to that of $\text{Li}_2\text{Zn}(\text{CH}_3)_4$, however, due to the insolubility of the hydride; association, ir, and nmr data are not available to establish this point.

Oddly enough, the reaction of either $\text{LiZn}(\text{s-C}_4\text{H}_9)_2\text{H}$, $\text{LiZn}(\text{CH}_3)_2\text{H}$, or $\text{LiZn}_2(\text{CH}_3)_4\text{H}$ with LiAlH_4 in tetrahydrofuran also yields Li_2ZnH_4 . The x-ray powder diffraction patterns of Li_2ZnH_4 from each of these reactions (Table 1) show weak to moderate lines for Li_2ZnH_4 and strong lines for zinc metal. It was found that the presence of a large excess of tetrahydrofuran with any of the complex metal hydrides discussed here always greatly increased the rate of decomposition to zinc metal at room temperature. After this trend had been noticed, all solid products were filtered as quickly as possible. Lithium tetrahydrido-zincate prepared from $\text{Li}_2\text{Zn}(\text{CH}_3)_4$ showed no zinc metal lines when it was stirred in the reaction mixture for only one hour before filtration.

The route by which Li_2ZnH_4 is formed from $\text{LiZn}(\text{s-C}_4\text{H}_9)_2\text{H}$,

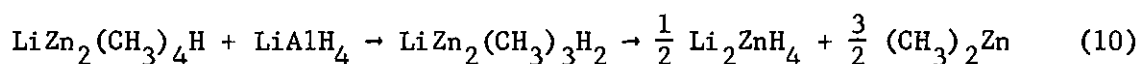
$\text{LiZn}(\text{CH}_3)_2\text{H}$ and $\text{LiZn}_2(\text{CH}_3)_4\text{H}$ is not clear, especially in the case of $\text{LiZn}_2(\text{CH}_3)_4\text{H}$. A reasonable explanation for the formation of Li_2ZnH_4 from $\text{LiZn}(\text{s-C}_4\text{H}_9)_2\text{H}$ or $\text{LiZn}(\text{CH}_3)_2\text{H}$ is that LiAlH_4 undergoes hydrogen-alkyl group exchange with the LiZnR_2H compound in a stepwise fashion. After the first alkyl exchange step, it is suggested that LiZnRH_2 (where $\text{R} = \text{CH}_3$ or $\text{s-C}_4\text{H}_9$) forms which could then disproportionate to Li_2ZnH_4 and ZnR_2 faster than it reacts with LiAlRH_3 (Eq. 9).



This explanation is supported by elemental analysis of the reaction mixtures from reduction of $\text{LiZn}(\text{s-C}_4\text{H}_9)_2\text{H}$ and $\text{LiZn}(\text{CH}_3)_2\text{H}$ with LiAlH_4 . The solid product from the reaction of $\text{LiZn}(\text{s-C}_4\text{H}_9)_2\text{H}$ with LiAlH_4 had a molar ratio of $\text{Li}:\text{Zn}:\text{H}$ of 2:1:4. The filtrate contained one-half of the initial amount of zinc. Thus, the solid (Li_2ZnH_4) contained the other half. This is consistent with the disproportionation of an intermediate complex to equimolar amounts of di-s-butylzinc and Li_2ZnH_4 . Evidently, di-s-butylzinc was not reduced to zinc hydride by the intermediate aluminum hydride species, $\text{LiAl}(\text{s-C}_4\text{H}_9)_3\text{H}$. The solid from the reaction of $\text{LiZn}(\text{CH}_3)_2\text{H}$ with LiAlH_4 had a molar ratio of $\text{Li}:\text{Zn}:\text{H}$ of 1:1:3. The filtrate contained very little of the starting zinc compound and the x-ray powder diffraction pattern showed only lines for Li_2ZnH_4 and zinc metal. Thus, the solid product must be a mixture of Li_2ZnH_4 and ZnH_2 , where the ZnH_2 comes from reduction of $(\text{CH}_3)_2\text{Zn}$ with $\text{LiAl}(\text{CH}_3)_3\text{H}$. A situation similar to this was encountered by Coates¹⁸ in the preparation of LiBeH_3 .

The x-ray powder diffraction pattern of the compound contained lines due to Li_2BeH_4 only, but the analysis showed a molar ratio of Li:Be:H of 1:1:3. Coates concluded that the product was an equimolar mixture of Li_2BeH_4 and BeH_2 .

The mechanism of formation of Li_2ZnH_4 by reaction of $\text{LiZn}_2(\text{CH}_3)_4\text{H}$ with LiAlH_4 is not as well understood. Even less understandable is the reason why $\text{LiZn}_2(\text{CH}_3)_4\text{H}$ reacts so slowly with LiAlH_4 . It took five days for essentially all the zinc to appear in the solid whereas most of the "ate" complexes used in this work react with LiAlH_4 instantaneously to yield solid products containing all of the original zinc. The solid did contain Li:Zn in a ratio of 1:2, but the active hydrogen was very low indicating considerable decomposition. It is possible that the initial reduction product was LiZn_2H_5 , which decomposed to Li_2ZnH_4 and ZnH_2 . A more reasonable reaction path consists of a slow stepwise exchange of a methyl group of $\text{LiZn}_2(\text{CH}_3)_4\text{H}$ to the intermediate complex, $\text{LiZn}_2(\text{CH}_3)_3\text{H}_2$, which could then disproportionate to Li_2ZnH_4 and $(\text{CH}_3)_2\text{Zn}$ according to Eq. 10.



The $(\text{CH}_3)_2\text{Zn}$ would then presumably be reduced rapidly in the presence of LiAlH_4 to ZnH_2 . The major part of the decomposition is probably due to decomposition of ZnH_2 .

The vacuum DTA-TGA of Li_2ZnH_4 , as shown in Figure 2, decomposes evolving noncondensable gases at 136° and 310° . The thermal effect

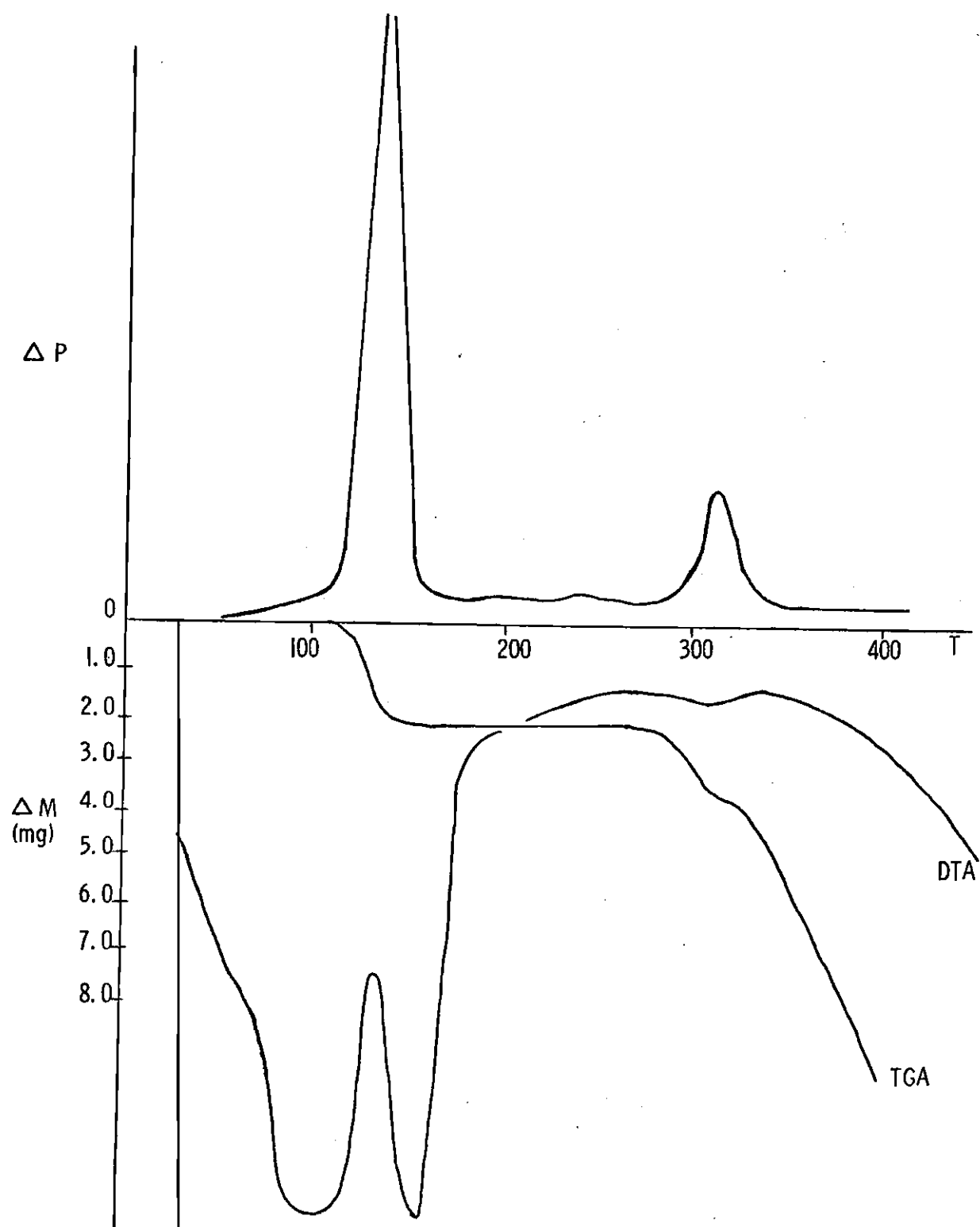
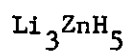
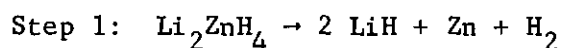
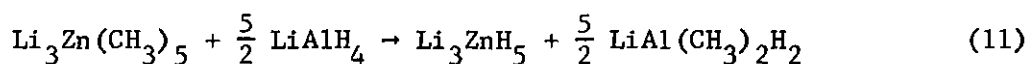


Figure 2. Vacuum DTA-TGA of Li_2ZnH_4

for the first gas evolution contains a sharp exotherm superimposed on a broad deep endotherm. The thermal effect for the next gas evolution is a small endotherm. The ratio of weight loss for the two gas evolutions is 1:1. The first gas evolution is attributed to decomposition of Li_2ZnH_4 to LiH and ZnH_2 with simultaneous decomposition of ZnH_2 . The last endotherm is due to the decomposition of LiH . An x-ray powder diffraction pattern taken after the first step showed the presence of LiH and Zn metal. The steps involved in the decomposition are shown below.



In their low temperature NMR work on the system $\text{CH}_3\text{Li}-(\text{CH}_3)_2\text{Zn}$, Seitz and Brown¹⁶ reported the existence of two complexes, $\text{Li}_2\text{Zn}(\text{CH}_3)_4$ and $\text{Li}_3\text{Zn}(\text{CH}_3)_5$. Since reduction of $\text{Li}_2\text{Zn}(\text{CH}_3)_4$ with LiAlH_4 yields Li_2ZnH_4 , reduction of $\text{Li}_3\text{Zn}(\text{CH}_3)_5$ with LiAlH_4 should provide a convenient route to Li_3ZnH_5 (Eq. 11).



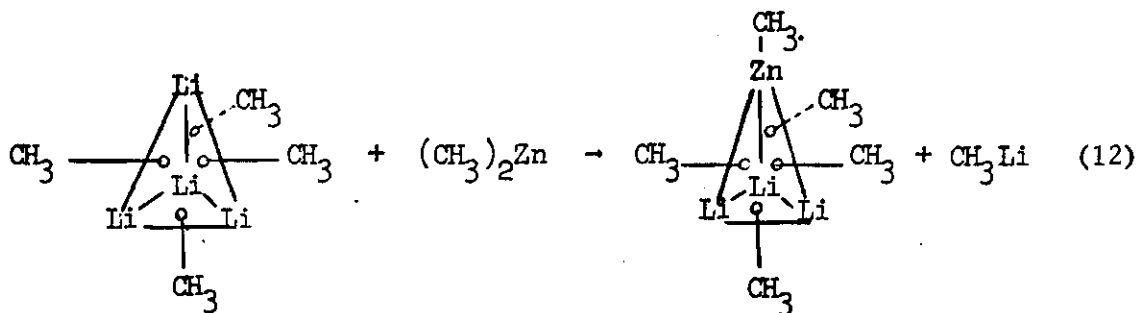
The reaction of $\text{Li}_3\text{Zn}(\text{CH}_3)_5$ with LiAlH_4 in diethyl ether at room temperature gave Li_3ZnH_5 , in 100% yield. The product contained a small amount of LiAlH_4 which precipitated with the product. The x-ray powder diffraction pattern (Table 1) did not contain any lines due to Li_2ZnH_4 ,

ZnH_2 or LiH ; therefore, the product of the reaction is not a physical mixture. The infrared spectrum contained two strong and two moderate bands. The two strong bands are centered at 680 cm^{-1} and 1550 cm^{-1} . The two moderate bands are centered at 990 cm^{-1} and 1280 cm^{-1} . Although the structure of Li_3ZnH_5 might be similar to that proposed by Brown¹⁶ for $\text{Li}_3\text{Zn}(\text{CH}_3)_5$, because of the insolubility of the hydride; molecular association, ir and nmr data could not be obtained to establish this point.

The vacuum DTA-TGA of this compound, run several months after it was originally prepared, was similar to that observed for Li_2ZnH_4 . At this point it was thought that Li_3ZnH_5 decomposed slowly over a period of months to Li_2ZnH_4 and LiH ; however, subsequent attempts to reprepare Li_3ZnH_5 have failed. In each case the product was a mixture of Li_2ZnH_4 and LiH . This is the only complex metal hydride reported in this work, the preparation of which could not be reproduced. In spite of this result, the original data indicated the unequivocal formation of Li_3ZnH_5 .

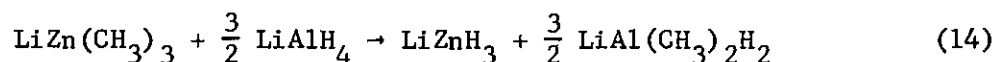
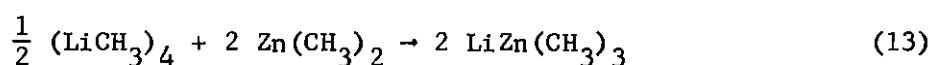
LiZnH_3

Trilithium pentamethylzincate has been reported¹⁶ to be formed in diethyl ether by substitution of one dimethylzinc molecule for one methyl lithium unit in the methyl lithium tetramer (Eq. 12).



Lithium trimethylzincate could then be formed by substitution of two methyl lithium units in the methyl lithium tetramer by two molecules of dimethylzinc. Lithium trimethylzincate formed in this way should provide an excellent precursor to LiZnH_3 .

The reaction of a 1:1 mixture of methyllithium and dimethylzinc with LiAlH_4 in diethyl ether did produce LiZnH_3 (Eq. 13 and 14).



The x-ray powder diffraction pattern of LiZnH_3 (Table 1) was very different from that of Li_2ZnH_4 or Li_3ZnH_5 and did not contain any lines in common with LiH or ZnH_2 . Little information concerning the structure of LiZnH_3 is available since the compound is not soluble enough to obtain molecular association and nmr data.

The vacuum DTA-TGA of LiZnH_3 is shown in Figure 3. It contained noncondensable gas evolutions at 97° , 136° , and 290° . The gas evolution at 97° was accompanied by a strong exothermal effect and is probably due to disproportionation of LiZnH_3 to Li_2ZnH_4 and ZnH_2 , with simultaneous decomposition of ZnH_2 . The decomposition of ZnH_2 normally occurs between 90° and 100° . The fact that the next two gas evolutions correspond to those accompanying decomposition of Li_2ZnH_4 supports this proposal.

The thermal decomposition of LiZnH_3 is believed to occur in essentially three steps, as follows.

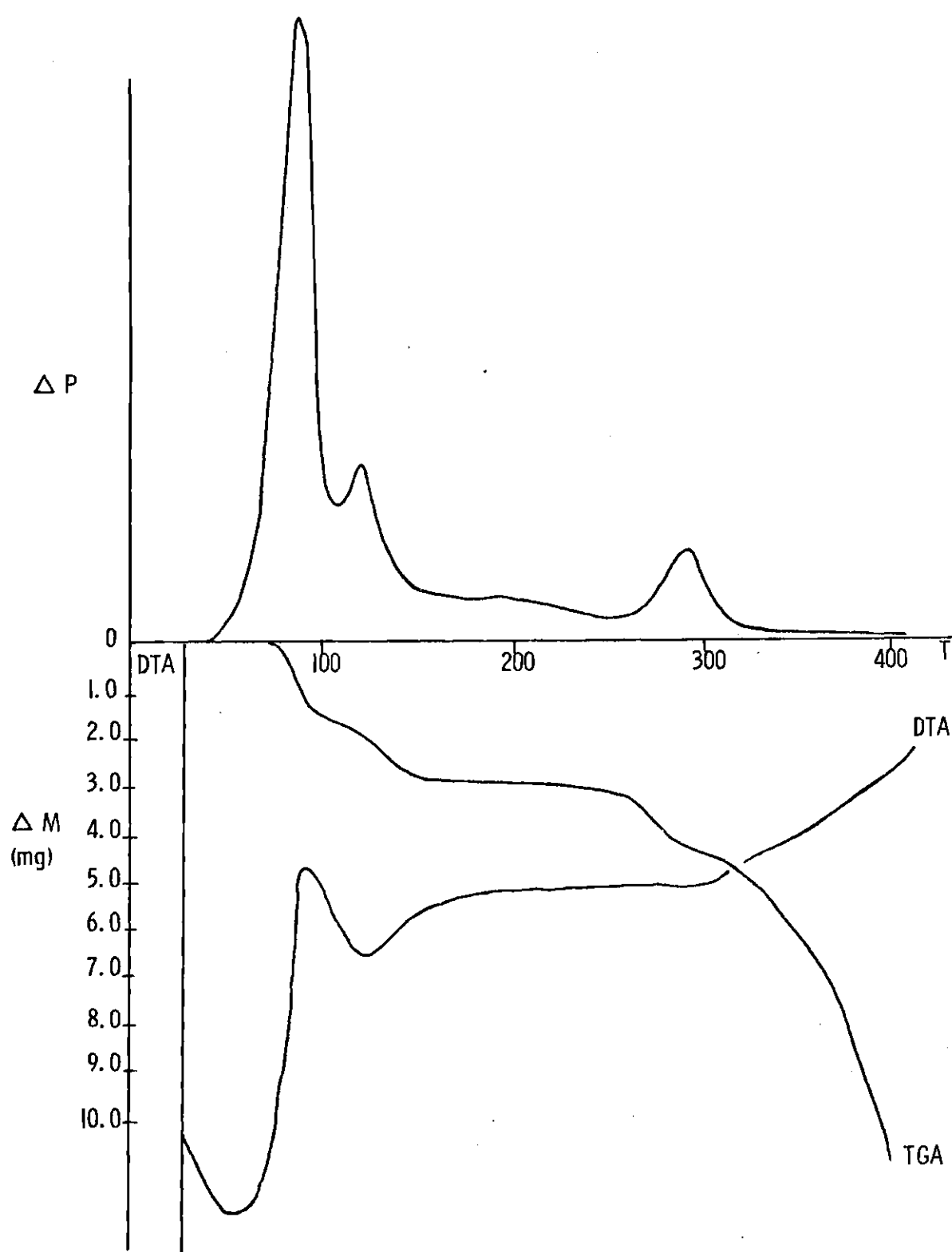
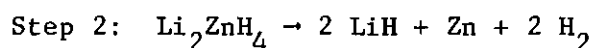
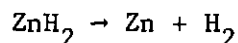
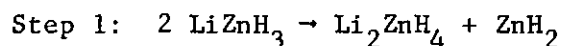


Figure 3. Vacuum DTA-TGA of LiZnH_3



The first step is slow compared to the second which has ZnH_2 decomposing very rapidly once formed. The decomposition of Li_2ZnH_4 occurs at higher temperatures.

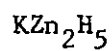
LiZnH_5 and LiZn_3H_7

Mixtures of methyllithium and dimethylzinc in ratios of 1:2 and 1:3, respectively, were allowed to react with LiAlH_4 in diethyl ether. The solid compounds obtained had Li:Zn:H ratios of 1:2:5 and 1:3:7. However, the x-ray powder diffraction patterns of the solids (Table 1) contained lines due only to LiZnH_3 . Thus, the solid compounds are 1:1 and 1:2 mixtures of LiZnH_3 and ZnH_2 .

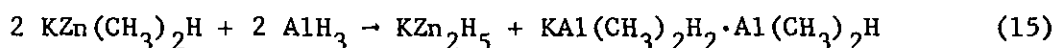
$\text{KZn}(\text{CH}_3)_2\text{H}$ and $\text{KZn}_2(\text{CH}_3)_4\text{H}$

In contrast to the reaction of di-s-butylzinc with KH which yields K_2ZnH_4 directly, KH and dimethylzinc react in 1:1 ratio in either diethyl ether or tetrahydrofuran to form $\text{KZn}(\text{CH}_3)_2\text{H}$ in quantitative yield. This complex had not been prepared previously; however, its properties were found to be analogous to those of $\text{LiZn}(\text{CH}_3)_2\text{H}$ and $\text{NaZn}(\text{CH}_3)_2\text{H}$ which had been prepared earlier by Shriver.⁹ Like the lithium and sodium complexes, $\text{KZn}(\text{CH}_3)_2\text{H}$ was insoluble in diethyl ether, soluble in tetrahydrofuran,

and was found to react with another molecule of $(\text{CH}_3)_2\text{Zn}$. This gave $\text{KZn}_2(\text{CH}_3)_4\text{H}$, which like the lithium and sodium complexes decomposed to $\text{KZn}(\text{CH}_3)_2\text{H}$ and $(\text{CH}_3)_2\text{Zn}$ when an attempt was made to isolate it as a solid.

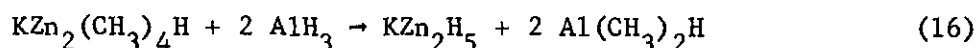


The reaction of $\text{KZn}(\text{CH}_3)_2\text{H}$ with AlH_3 in tetrahydrofuran (AlH_3 was chosen as reducing agent because of the possibility of alkali metal exchange if LiAlH_4 were used) was selected as a convenient route to KZnH_3 . However, the reaction readily proceeds to give KZn_2H_5 (Eq. 15) in quantitative yield.



The x-ray powder diffraction pattern for KZn_2H_5 (Table 4) contains no lines due to KH , ZnH_2 , or K_2ZnH_4 . The infrared spectrum of the filtrate containing the $\text{KAl}(\text{CH}_3)_2\text{H}_2 \cdot \text{Al}(\text{CH}_3)_2\text{H}$ showed a broad band in the Al-H stretching region centered at 1618 cm^{-1} . Dimethylalane absorbs at 1750 cm^{-1} in THF, thus the species is not a mixture of $\text{Al}(\text{CH}_3)_2\text{H}$ and $\text{KAl}(\text{CH}_3)_2\text{H}_2$ in solution.

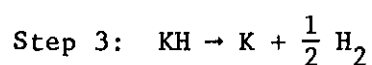
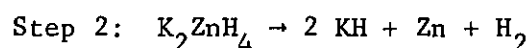
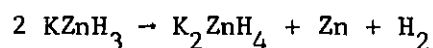
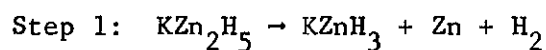
Potassium pentahydridodizincate was also formed by reduction of $\text{KZn}_2(\text{CH}_3)_4\text{H}$ with AlH_3 in tetrahydrofuran (Eq. 16).



In this reaction very little potassium was found in the filtrate. The x-ray powder diffraction pattern of KZn_2H_5 obtained from this reaction is

shown in Table 4.

The vacuum DTA-TGA of KZn_2H_5 is shown in Figure 4. Large noncondensable gas evolutions occurred at 125° , 223° , and 267° . The ratio of the weight loss during the first gas evolution to that during the second was 3:1. The thermal effect for the first gas evolution showed a sharp endotherm superimposed on a broad exotherm. The exotherm is believed to be due to decomposition of KZn_2H_5 to KZnH_3 and ZnH_2 with simultaneous decomposition of ZnH_2 to Zn and H_2 . The endotherm is believed to be due to disproportionation of KZnH_3 to K_2ZnH_4 and ZnH_2 with simultaneous decomposition of the ZnH_2 . The thermal effects for the second and third gas evolutions were endothermal. The second gas evolution is due to the decomposition of K_2ZnH_4 to KH and ZnH_2 with simultaneous decomposition of ZnH_2 . The third gas evolution is due to decomposition of KH . The mechanism of decomposition, shown in the three steps below, is supported by x-ray powder diffraction data, taken after the first two stages of gas evolution. The x-ray powder pattern taken after the first step showed lines for K_2ZnH_4 and Zn metal only. The x-ray powder pattern taken after the second step showed lines for KH and Zn metal. More evidence is provided by the fact that the ratio of the weight loss in Step 1 to that in Step 2 should be 3, which is what was found.



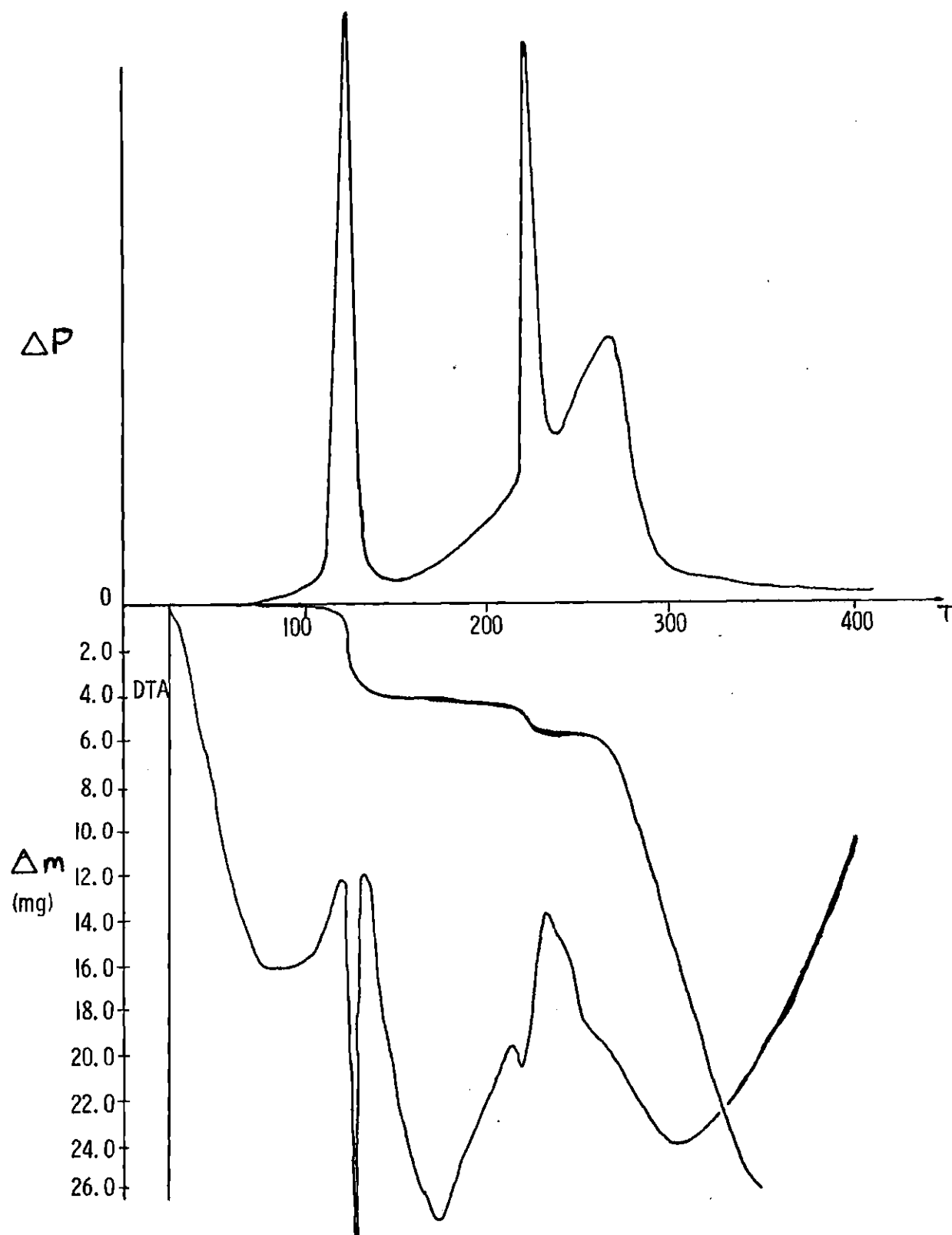


Figure 4. Vacuum DTA-TGA of KZn_2H_5

In order to substantiate that Steps 2 and 3 are the only steps involved in the decomposition of K_2ZnH_4 , the DTA-TGA of K_2ZnH_4 was investigated. The vacuum DTA-TGA shown in Figure 5 contained one very broad noncondensable gas evolution which peaked at 285° and had shoulders at 200° and 237° . Further information concerning the decomposition of K_2ZnH_4 by observing the DTA-TGA under argon flush is shown in Figure 6. The DTA-TGA contained three well separated weight losses with corresponding endotherms at 150° , 266° , and 355° . This differs somewhat with the DTA-TGA for K_2ZnH_4 obtained, under argon, in our earlier report.⁸ In the earlier work, K_2ZnH_4 was reported to have lost all solvent before 80° and to have endothermal decomposition steps at 242° , 292° , and 336° . No attempt was made to study the precise reactions involved in the decomposition steps. In the present work, the endothermal weight loss at 150° was found to be due to loss of solvent, since an x-ray powder diffraction pattern of a sample heated to 200° contained lines due only to K_2ZnH_4 . The endothermal weight loss at 266° can be represented by the following reaction (Eq. 17)



since an x-ray powder pattern of a sample heated to 300° showed lines due only to KH and zinc metal. Thus, the last endotherm can be represented by the reaction (Eq. 18)



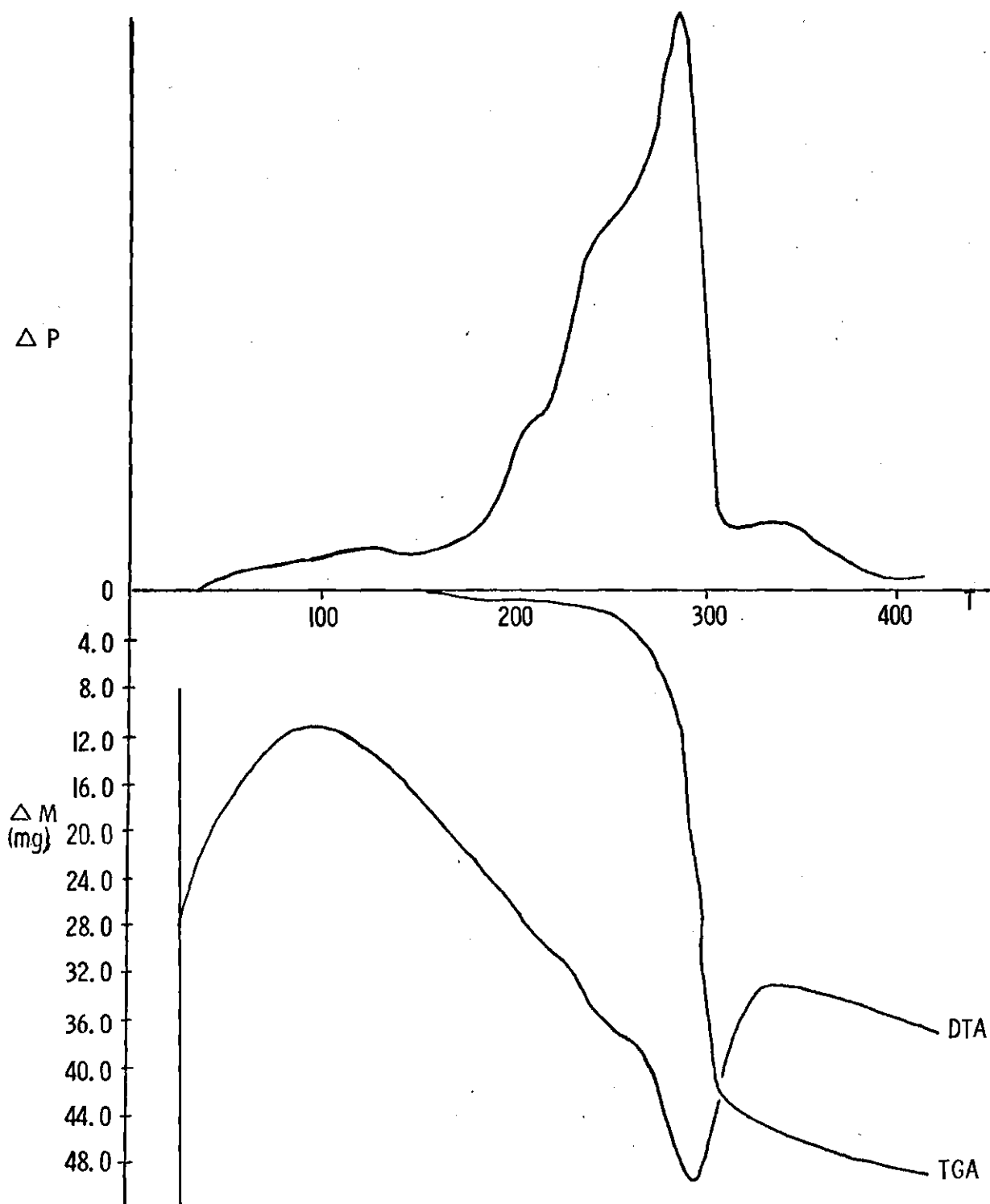


Figure 5. Vacuum DTA-TGA of K_2ZnH_4

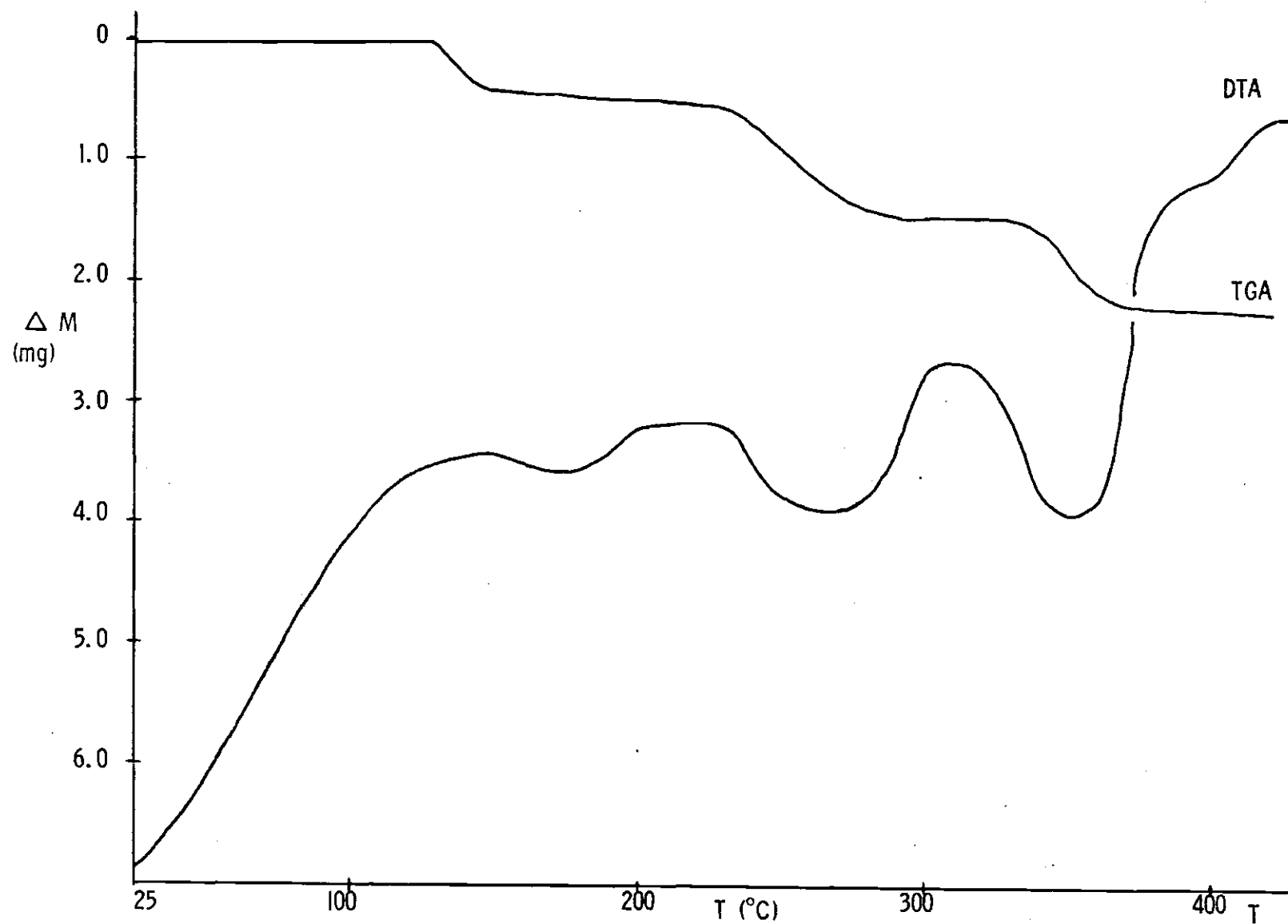
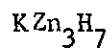


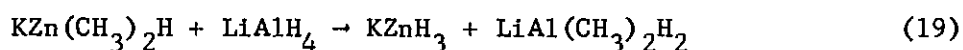
Figure 6. DTA-TGA of K_2ZnH_4 under Ar



Reaction of a 1:3 mixture of KH and $(\text{CH}_3)_2\text{Zn}$ with AlH_3 in tetrahydrofuran gave a white solid with K:Zn:H ratio of 1:3:7; however, the x-ray powder diffraction pattern showed only lines for KZn_2H_5 . Thus, the compound must be a 1:1 mixture of KZn_2H_5 and ZnH_2 .

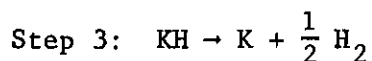
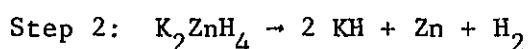
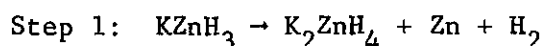


The reaction of $\text{KZn}(\text{CH}_3)_2\text{H}$ with LiAlH_4 in tetrahydrofuran gave KZnH_3 (no alkali metal exchange) in quantitative yield (Eq. 19).



The x-ray powder diffraction pattern of KZnH_3 (Table 4) did not contain any lines due to KZn_2H_5 , K_2ZnH_4 , ZnH_2 , or KH.

The vacuum DTA-TGA of KZnH_3 is shown in Figure 7. Three stages of noncondensable gas evolution were observed at 125° , 213° , and 280° . The thermal effect of the first gas evolution was exothermic, while that of the latter two was endothermic. The weight losses accompanying the first and second stages of gas evolution were equivalent. The x-ray powder diffraction pattern of the solid left after the first gas evolution showed lines for K_2ZnH_4 and Zn only. The x-ray powder pattern of the solid left after the second gas evolution showed lines due to KH and Zn. These data lead to the following suggested decomposition pattern of KZnH_3 .



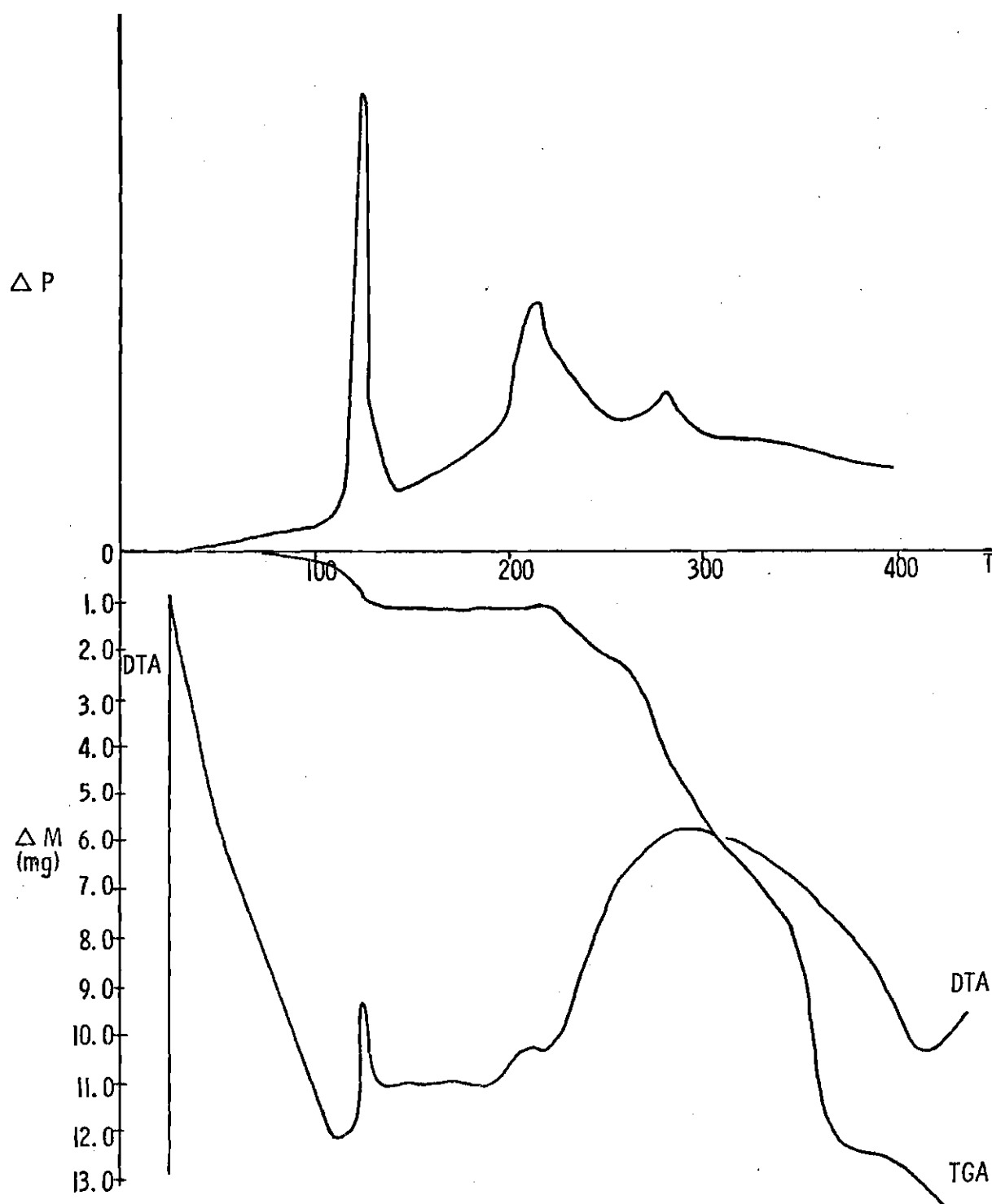
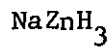
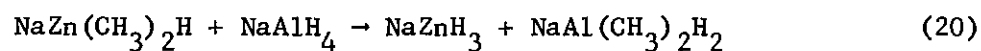


Figure 7. Vacuum DTA-TGA of KZnH_3

The weight losses during Steps 1 and 2 should be equivalent. This is what was observed.



The reaction of $\text{NaZn}(\text{CH}_3)_2\text{H}$ with NaAlH_4 in tetrahydrofuran gave NaZnH_3 (Eq. 20).



The x-ray powder diffraction pattern (Table 5) was identical to that reported by Shriver¹⁰ in his preparation of NaZnH_3 . [Shriver's preparation involved thermal decomposition of $\text{NaZn}_2(\text{CH}_3)_2\text{H}_3$ under vacuum to give NaZnH_3 and $(\text{CH}_3)_2\text{Zn}$.] Vacuum DTA-TGA analysis of NaZnH_3 , shown in Figure 8, showed a strong exotherm at 72° and moderate endotherms at 104° , 183° , and 250° . The simultaneous weight loss curve showed inflections that corresponded to equivalent weight losses at each of the endotherms and no weight loss at the exotherm. The first endotherm (104°) corresponds to the thermal decomposition of ZnH_2 ; therefore, the exotherm at 72° can be attributed to disproportionation of NaZnH_3 to Na_2ZnH_4 and ZnH_2 . This observation explains why NaZnH_3 turns black on standing at room temperature (a phenomenon reported by Shriver⁹ and observed by the author). The endotherm at 183° corresponds to the decomposition of Na_2ZnH_4 and the endotherm at 250° corresponds to the decomposition of NaH . The DTA-TGA reported previously by us is different from the one reported here; however, the difference is probably due to the fact that the earlier DTA-TGA was run under argon at one atmosphere pressure whereas the DTA-TGA reported

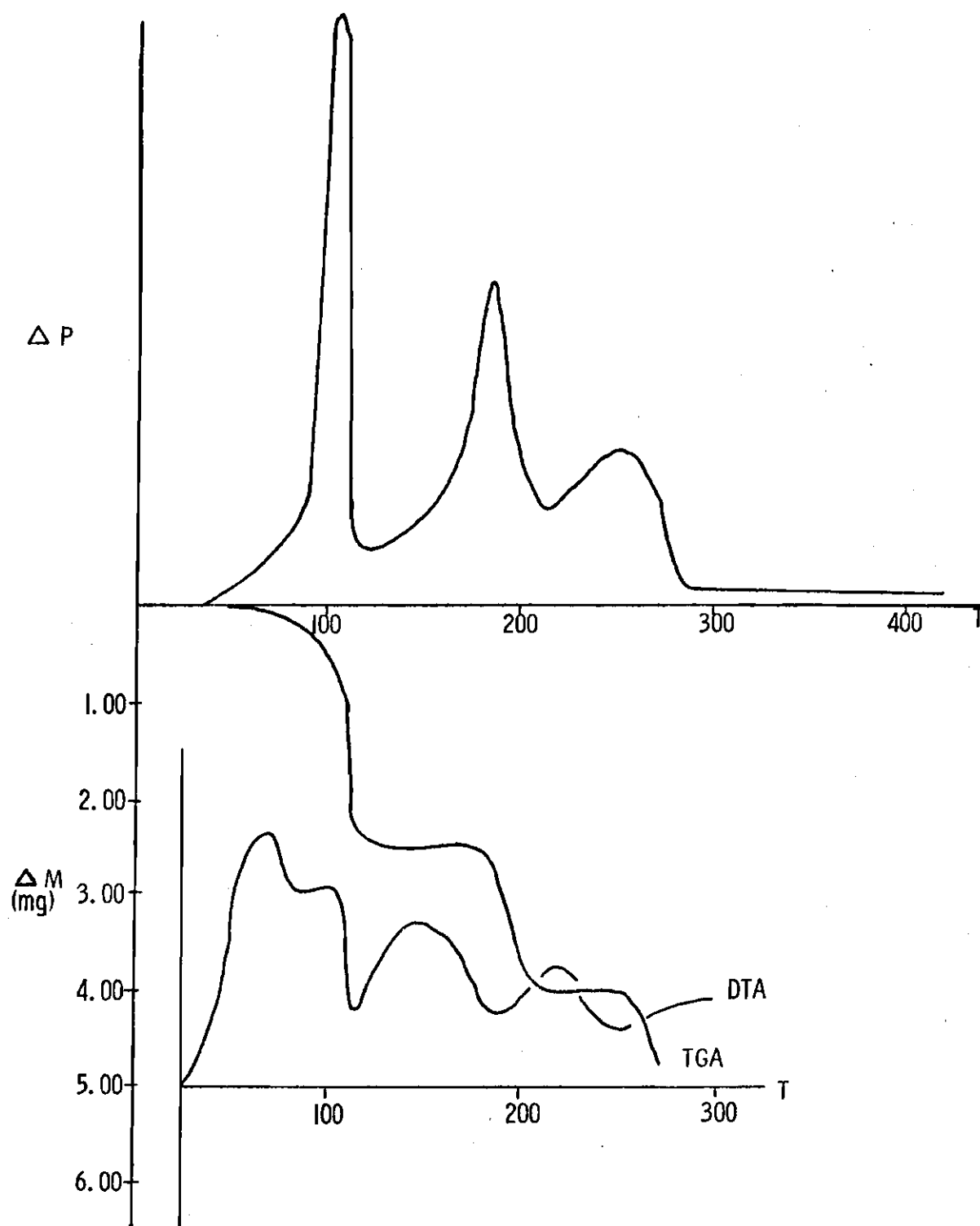
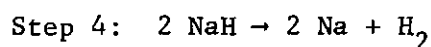
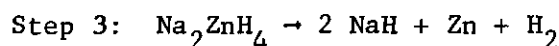
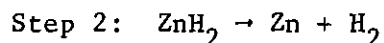
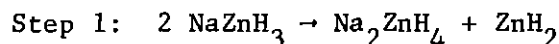
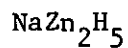


Figure 8. Vacuum DTA-TGA of NaZnH_3

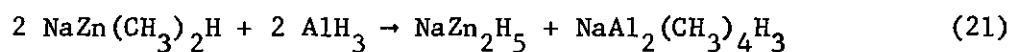
here was carried out under vacuum. Thermal decomposition of NaZnH_3 is envisioned as proceeding by the following series of steps.



The reaction of $\text{NaZn}_2(\text{CH}_3)_4\text{H}$ with NaAlH_4 also yielded NaZnH_3 . The x-ray powder diffraction pattern of NaZnH_3 prepared by this route is given in Table 5. The mechanism by which NaZnH_3 was formed in this reaction is not understood at present.



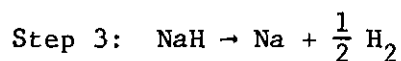
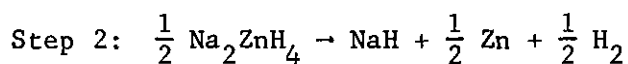
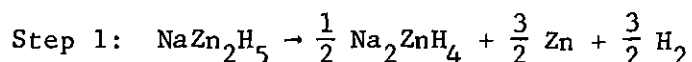
In a manner similar to the reaction of $\text{KZn}(\text{CH}_3)_2\text{H}$ with AlH_3 which formed KZn_2H_5 , AlH_3 was also found to react with $\text{NaZn}(\text{CH}_3)_2\text{H}$ to form NaZn_2H_5 (Eq. 21).



The x-ray powder pattern of NaZn_2H_5 (Table 5) contained no lines due to NaH , ZnH_2 , Na_2ZnH_4 , or NaZnH_3 . The infrared spectrum of the filtrate remaining after filtration of the solid NaZn_2H_5 showed a very broad band in the Al-H stretching region centered at 1610 cm^{-1} . In view of this spectrum and elemental analysis of the filtrate, the product in solution is

believed to be a complex between Me_2AlH and $\text{NaAlMe}_2\text{H}_2$.

The vacuum DTA-TGA of NaZn_2H_5 is shown in Figure 9. Large noncondensable gas evolutions occurred at 123° , 210° , and 315° . The ratio of the weight loss during the first gas evolution to that during the second and third ones was 3:1:1. The thermal effect for the first gas evolution was endothermic. This endotherm is believed to be due to disproportionation of NaZn_2H_5 to Na_2ZnH_4 and ZnH_2 with simultaneous decomposition of the ZnH_2 . The thermal effects for the second and third gas evolutions were also endothermic. The second gas evolution is due to decomposition of Na_2ZnH_4 to NaH and ZnH_2 with simultaneous decomposition of ZnH_2 . The third gas evolution is due to decomposition of NaH . The mechanism of decomposition, shown in the three steps below, is supported by x-ray powder diffraction data, taken after the first two stages of gas evolution. The x-ray powder pattern taken after the first step showed lines for Na_2ZnH_4 and Zn metal only. The x-ray powder pattern taken after the second step showed lines for NaH and Zn metal. More evidence is provided by the fact that the ratio of the weight losses in the three steps should be 3:1:1, which is what was observed.



Reaction of Alkali Metal Hydrides with Zinc Halides in Tetrahydrofuran

The reaction of LiH with ZnBr_2 and NaH with ZnI_2 in 2:1 molar ratio

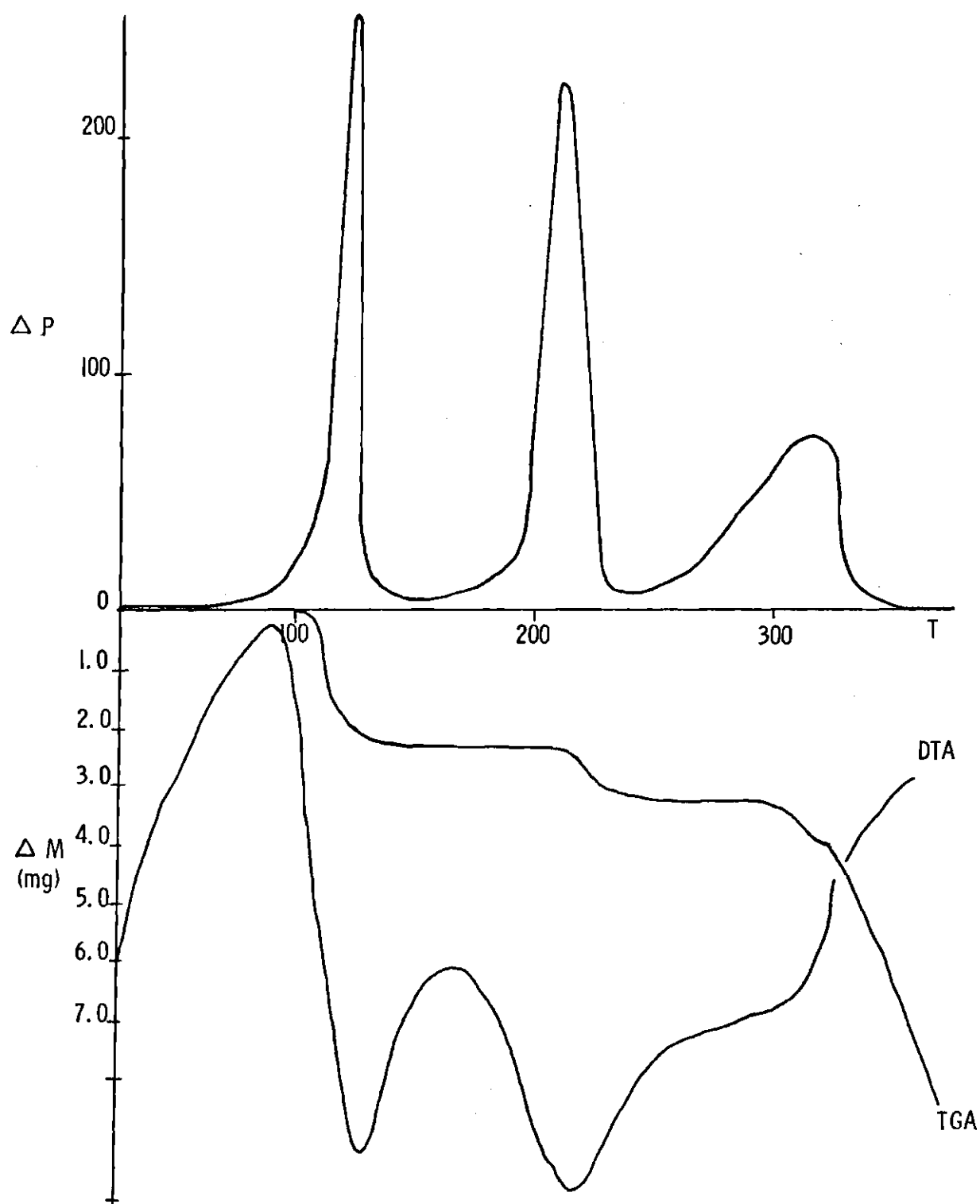
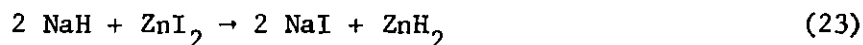
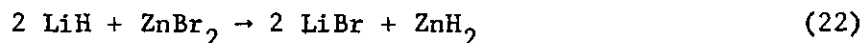


Figure 9. Vacuum DTA-TGA of NaZn_2H_5

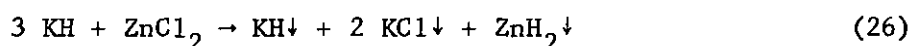
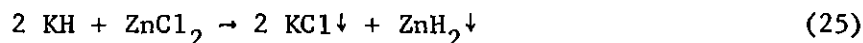
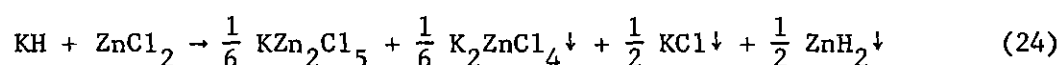
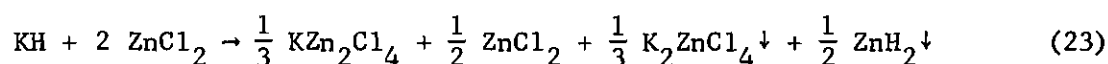
in THF proceeds according to Eq. 22 and 23. In both cases the alkali metal halide remains in solution while the ZnH_2 precipitates.



In both cases all of the alkali metal and halide are found in solution, while all of the zinc and active hydride precipitate from solution. The x-ray powder patterns of the ZnH_2 obtained from these two reactions are shown in Table 2. Also given in Table 2 are the x-ray powder patterns of ZnH_2 prepared by the reaction of LiAlH_4 with $(\text{C}_2\text{H}_5)_2\text{Zn}$ ⁸ and $(\text{CH}_3)_2\text{Zn}$.¹⁹ The latter two patterns differ from one another, as well as from the pattern of ZnH_2 prepared in this study. However, the x-ray powder patterns of ZnH_2 prepared by the reaction of LiH with ZnBr_2 and NaH with ZnI_2 are identical. It has been our experience that ZnH_2 prepared by the reaction of LiAlH_4 with a dialkylzinc compound is usually amorphous, yielding an x-ray powder pattern with only two broad, diffuse lines, one at a d-spacing of about 4.0 and the other at 2.5. Indeed, two reports in the recent literature^{8,19} claim different x-ray powder patterns for ZnH_2 prepared by the latter method. In addition, ZnH_2 prepared by the Schlesinger method ($\text{LiAlH}_4 + \text{R}_2\text{Zn}$) turns black after a few days at room temperature and hydrolyzes slowly with water. The ZnH_2 prepared in the present study remains white for several weeks and hydrolyzes rapidly with water at room temperature, in addition to giving a distinct, reproducible powder pattern.

However, it does decompose thermally at 90° to produce zinc metal and hydrogen.

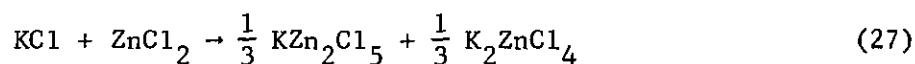
The reactions of KH with ZnCl in 1:2, 1:1, 2:1, and 3:1 molar ratios proceed according to Eq. 23-26.



In the reaction of KH with ZnCl₂ in a 1:2 molar ratio, KZn₂Cl₅ remains in solution, while K₂ZnCl₄ and ZnH₂ precipitate from solution. This statement is supported by the fact that the filtrate from this reaction mixture contained K:Zn:Cl:H in molar ratios of 0.29:1.00:2.27:0.00 and 58.6% of the starting zinc. A mixture of $\frac{1}{3} \text{KZn}_2\text{Cl}_5 + \frac{1}{2} \text{ZnCl}_2$ will have K:Zn:Cl in molar ratios of 0.282:1.00:2.28 and contain $((3/2 + 1/2)/2)100 = 58.5\%$ of the starting zinc. The solid from the reaction mixture contained K:Zn:Cl:H in molar ratios of 0.82:1.00:1.62:1.19. A mixture of $\frac{1}{3} \text{K}_2\text{ZnCl}_4 + \frac{1}{2} \text{ZnH}_2$ will have K:Zn:Cl:H in molar ratios of 0.80:1.00:1.60:1.21. The x-ray powder diffraction pattern of the solid (shown in Table 2) corresponds to a mixture of K₂ZnCl₄ and ZnH₂. The pattern for ZnH₂ in the mixture is the same as that for ZnH₂ produced by the reactions of LiH with ZnBr₂ and NaH

with ZnI_2 .

At this stage it might be interesting to consider the origin of the KZn_2Cl_5 found in the filtrate and the K_2ZnCl_4 found in the precipitate. The reaction between KCl and ZnCl_2 in a 1:1 molar ratio is shown in Eq. 27.

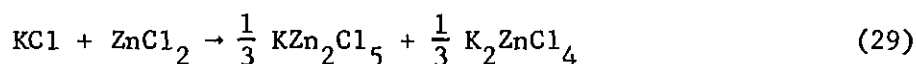
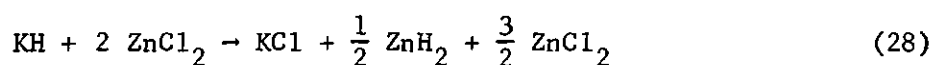


The filtrate from this reaction mixture contains K:Zn:Cl in molar ratios of 0.06:2.00:4.94 and 2/3 of the starting zinc. The solid contains K:Zn:Cl in molar ratios of 1.96:1.00:3.94 and 1/3 of the starting zinc. The analytical data are consistent with the proposed reaction products. The solid product is not a physical mixture of KCl and ZnCl_2 in 2:1 ratio since the x-ray powder diffraction pattern (shown in Table 2) of the product contains no lines common to either KCl or ZnCl_2 . Thus, the solid product is presumed to be a true coordination compound (K_2ZnCl_4). The compound in the filtrate is represented as KZn_2Cl_5 for two reasons. First, KCl is not soluble in THF; therefore, if it is in solution, it should be present as a complex. Second, if the remaining KCl is not complexed to ZnCl_2 as KZn_2Cl_5 , one would expect to see all of the KCl react with one half of the ZnCl_2 to give one half an equivalent of K_2ZnCl_4 , instead of one third. In the latter case, one would expect to find half the starting zinc in the filtrate and half in the solid. This is not what is observed and therefore KZn_2Cl_5 must be a true coordination complex.*

*It has been suggested that K_2ZnCl_4 and KZn_2Cl_5 might be co-crystallates of KCl and ZnCl_2 . In order to be able to establish the authenticity of Zn_2Cl_5^- and ZnCl_4^- anions, one would need the corresponding

An opportunity was given for KZn_2Cl_5 to react with AlH_3 to form KZn_2H_5 . The reaction of KZn_2Cl_5 with AlH_3 yielded a white solid containing K:Zn:Cl:H in molar ratios of 0.46:1.00:0.52:2.00. The x-ray powder pattern of the solid (shown in Table 2) contains lines for KCl, and therefore it must be a mixture of KCl and ZnH_2 . The ZnH_2 formed in this reaction did not show any distinct lines; therefore, it must be amorphous, as is the ZnH_2 that sometimes is produced from the reaction of LiAlH_4 with a dialkylzinc compound. The complex KZn_2Cl_5 evidently is not completely reduced to KZn_2H_5 , but instead KCl and ZnH_2 are formed.

With this information, one can write a reasonable sequence for the reaction of KH with ZnCl_2 in 1:2 molar ratio. The sequence is shown below.

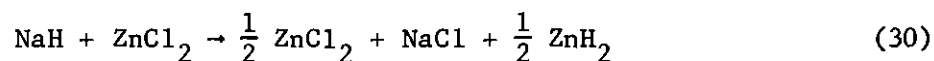


First, KH reacts with two equivalents of ZnCl_2 to give one equivalent of KCl, one half equivalent of ZnH_2 , and three halves equivalent of ZnCl_2 . After this, the KCl reacts with an equivalent of ZnCl_2 to give one third equivalent each of KZn_2Cl_5 and K_2ZnCl_4 .

interatomic distances to support such a claim. These interatomic distances are not available at the present time. However, x-ray powder diffraction patterns are available and these powder patterns do show that the above compounds are not simple, physical mixtures of KCl and ZnCl_2 . Thus, if these compounds are co-crystallates of KCl and ZnCl_2 , it does seem more than just fortuitous that the analytical data would turn out as it did. For KZn_2Cl_5 , the molar ratios of K:Zn:Cl were 1.06:2.00:4.94. For K_2ZnCl_4 , the molar ratios of K:Zn:Cl were 1.96:1.00:3.94.

The reactions of KH with ZnCl_2 in 1:1, 2:1, and 3:1 molar ratios are similar to the reaction just discussed. The first step is the maximum conversion of KH into KCl with the simultaneous formation of ZnH_2 . Then, if any ZnCl_2 remains, KCl reacts with it to give KZn_2Cl_5 and K_2ZnCl_4 . The total reactions as written in Eq. 24-26 are supported by analytical and x-ray powder diffraction data (Table 2). It is important to note that the ZnH_2 formed in all these reactions of KH with ZnCl_2 gives the same powder pattern as the ZnH_2 prepared by the reaction of LiH with ZnBr_2 and NaH with ZnI_2 .

The reaction of NaH with ZnCl_2 in 1:1 molar ratio proceeds according to Eq. 30. The filtrate from this reaction contained Na:Zn:Cl:H in molar ratios of 0.00:1.00:1.96:0.00 and one half the starting zinc.



The solid contained Na:Zn:Cl:H in molar ratios of 1.94:1.00:1.97:1.27. The analytical data support the reaction as written and the x-ray powder pattern of the solid (Table 3) contained lines only for NaCl and zinc metal. The powder pattern for ZnH_2 seen in the other cases was not observed. Also, this was the only reaction between an alkali metal hydride and zinc halide where the ZnH_2 produced turned black after just a few days. Why the ZnH_2 from this reaction behaved thus is unknown at present.

Several salient points about ZnH_2 are worth noting at this point. First, ZnH_2 is an isolable species which has moderate stability at or below room temperature. Second, ZnH_2 is the most thermally stable of the

Group II B hydrides. Cadmium hydride^{14,20} and mercury hydride¹⁴ decompose rapidly even below 0°. Third, ZnH_2 exhibits ready reactivity in situations where the produce is soluble. The ZnH_2 prepared in this study remains stable longer and is more reactive than ZnH_2 prepared by the Schlesinger method.

LITERATURE CITED^{*}

1. A. E. Finholt, A. C. Bond, and H. F. Schlesinger, J. Amer. Chem. Soc., 69, 1199 (1947).
2. H. I. Schlesinger, H. C. Brown, H. R. Hoekstra, and L. R. Rapp, J. Amer. Chem. Soc., 75, 199 (1953).
3. E. C. Ashby, R. Kovar, and R. Arnott, J. Amer. Chem. Soc., 92, 2182 (1970).
4. E. C. Ashby and R. D. Schwartz, Inorg. Chem., 10, 355 (1971).
5. E. C. Ashby, R. Kovar, and R. Arnott, J. Amer. Chem. Soc., 92 (1970).
6. G. E. Coates and J. A. Heslop, J. Chem. Soc. (A), 514 (1968).
7. W. E. Becker and E. C. Ashby, J. Org. Chem., 20, 954 (1964).
8. E. C. Ashby and R. G. Beach, Inorg. Chem., 10, 2486 (1971).
9. G. J. Kubas and D. F. Shriver, J. Amer. Chem. Soc., 92, 1949 (1970).
10. D. F. Shriver, "The Manipulations of Air-Sensitive Compounds," McGraw Hill, New York, N. Y., 1969.
11. E. C. Ashby, P. Claudy and Bousquet, J. Chem. Ed. (in press).
12. C. R. Noller, Org. Syn., 12, 86 (1932).
13. H. C. Brown and H. M. Yoon, J. Amer. Chem. Soc., 88, 1464 (1966).
14. G. D. Barbaras, C. Dillard, A. E. Finholt, T. Wartick, K. E. Wilzbach, and H. I. Schlesinger, J. Amer. Chem. Soc., 73, 4585 (1951).
15. D. J. Hurd, J. Org. Chem., 13, 711 (1948).
16. L. M. Seitz and T. L. Brown, J. Amer. Chem. Soc., 88, 4140 (1966).
17. E. Weiss and R. Wolfrum, Chem. Ber., 101, 35 (1968).

^{*}Journal title abbreviations used are listed in "List of Periodicals," Chemical Abstracts (1961).

18. N. A. Bell and G. E. Coates, J. Chem. Soc., A, 628 (1968).
19. D. J. Shriver, G. J. Kubas, and J. A. Marshall, J. Amer. Chem. Soc., 93, 5067 (1971).
20. E. Wiberg and W. Henle, Z. Naturf., 6b, 461 (1951).

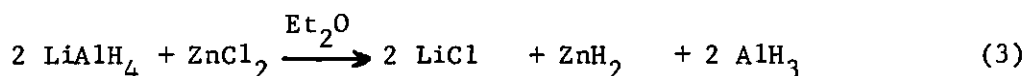
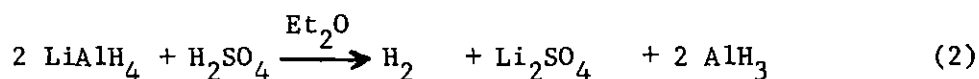
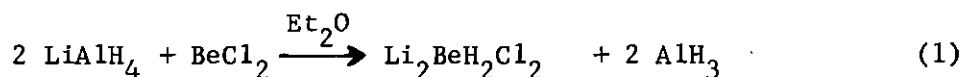
PART II

A Study Concerning the Existence of Complexes Between
 LiAlH_4 and AlH_3 in Ether Solvents and in the
Solid State

CHAPTER I

INTRODUCTION

Recently we found that diethyl ether soluble aluminum hydride can be prepared by a number of different methods.^{1,2,3} This finding allows a



convenient study of the interaction between LiAlH_4 and AlH_3 in diethyl ether which has been reported by a number of laboratories to be strong enough so as to produce stable complexes ($\text{LiAlH}_4 \cdot n\text{AlH}_3$, where $n = 1, 2, 3$, and 4). Although aluminum hydride can be prepared in tetrahydrofuran, complexes between LiAlH_4 and AlH_3 would not be expected to be stable due to the strong aluminum-oxygen bond in $\text{H}_3\text{Al-OC}_4\text{H}_8$. Recent Russian work⁴ claims the preparation of LiAl_2H_7 ($\text{LiAlH}_4 \cdot \text{AlH}_3$) and $\text{LiAl}_3\text{H}_{10}$ ($\text{LiAlH}_4 \cdot 2\text{AlH}_3$) in diethyl ether; however, the compounds were reported to be more stable in the solid state than in ether solution. Also a recent study concerning the structure and properties of LiAl_2H_7 has appeared in the French literature.⁵ These workers reported LiAl_2H_7

to be stable in the solid state, but unstable in diethyl ether solution. In addition, other French workers⁶ have reported the preparation of the compound $\text{LiAl}_4\text{H}_{13}$ ($\text{LiAlH}_4 \cdot 3\text{AlH}_3$) by the reaction of LiH with AlH_3 in ether solvent. In each case the reports claim solid state stability of the complexes, but report diethyl ether solutions as being unstable.

On the other hand, several reports have appeared that claim the formation of complexes of the type $\text{LiAlH}_4 \cdot n\text{AlH}_3$ in ether solvent. It has been reported that the electrical conductivity of solutions of LiAlH_4 and AlH_3 in diethyl ether indicates the formation of alternate ions to those arising from LiAlH_4 and AlH_3 separately.^{7,8} Because of these reports and because of the analogy to the $\text{MAlH}_4 \cdot n\text{AlR}_3$ systems,⁹ further claims for the existence of $\text{MAlH}_4 \cdot n\text{AlR}_3$ complexes have been made; in particular, LiAl_2H_7 .¹⁰

We have been evaluating new hydrides as stereoselective reducing agents and felt that $\text{LiAlH}_4 \cdot \text{AlH}_3$ compounds would behave differently than either LiAlH_4 or AlH_3 . Reduction studies in this laboratory have shown that a mixture of LiAlH_4 and AlH_3 in ether solvent give the same stereochemistry of reduction of 4-t-butylcyclohexanone and 3,3,5-trimethylcyclohexanone as would be expected for a simple physical mixture of LiAlH_4 and AlH_3 . At this point we decided to take a closer look at the so called complexes " $\text{LiAlH}_4 \cdot n\text{AlH}_3$ " both in ether solution by infrared spectroscopy and in the solid state by DTA-TGA and powder diffraction.

CHAPTER II

EXPERIMENTAL

Apparatus

Reactions were performed under nitrogen at the bench using Schlenk tube techniques.¹¹ Filtrations and other manipulations were carried out in a glove box equipped with a recirculating system using manganese oxide columns to remove oxygen and dry ice-acetone traps to remove solvent vapors.¹²

Infrared spectra were obtained using a Perkin-Elmer 621 spectrophotometer. Solids were run as nujol mulls between CsI plates. Solutions were run in matched 0.10 mm path length NaCl cells. X-ray powder data were obtained on a Philips-Norelco x-ray unit using a 114.6 mm camera with nickel filtered CuK_{α} radiation. Samples were sealed in 0.5 mm capillaries and exposed to x-rays for six hours. d-Spacings were read on a precalibrated scale equipped with viewing apparatus. Intensities were estimated visually. DTA-TGA data were obtained under vacuum with a modified Mettler thermoanalyzer II. A more detailed description of this apparatus has been given elsewhere.^{13,14}

Analytical

Gas analyses were carried out by hydrolyzing samples with hydrochloric acid on a standard vacuum line equipped with a Toepler pump.¹¹ Alkali metals were determined by flame photometry. Aluminum

was determined by EDTA titration.

Materials

Lithium tetrahydridoaluminate was obtained as gray, lumpy solids from Ventron, Metal Hydrides Division. Solutions of LiAlH_4 in diethyl ether and THF were prepared by stirring the solid hydride for 24 hours with freshly distilled solvent, followed by filtration, to yield a clear, colorless solution. Lithium hydride was prepared by the hydrogenation of t-butyl lithium at room temperature at 3000 psi for 24 hours. A slurry of LiH in diethyl ether was used. Aluminum hydride in diethyl ether was prepared by the reaction of LiAlH_4 with BeCl_2 in a 2:1 molar ratio.^{1,2} The white solid was removed by filtration leaving a nearly lithium free clear solution of aluminum hydride. The molar ratios of Al, H, and Li in this solution were 1.00:3.13:0.043. Aluminum hydride in THF was prepared by the reaction of 100% H_2SO_4 with LiAlH_4 in THF according to the procedure of Brown.³ The Li_2SO_4 was removed by filtration and a nearly lithium free solution of AlH_3 in THF was obtained. The molar ratios of Al, H, and Li in this solution were 1.00:3.06:0.016. These reactant solutions were standardized by aluminum analysis and transferred volumetrically. All solvents were distilled at atmospheric pressure from LiAlH_4 (diethyl ether) or NaAlH_4 (THF) immediately before use.

Procedure

Reaction of LiAlH_4 and AlH_3 in 1:1, 1:2, 1:3, and 1:4 Molar Ratio in Diethyl Ether

In four separate experiments, 2.5 mmoles of LiAlH_4 in diethyl

ether was added to 2.5, 5.0, 7.5, and 10 mmols of AlH_3 in diethyl ether. The resulting clear solutions were stirred for one hour and the infrared spectra recorded (Figure 1). The solvent was then removed from the solution under vacuum until a dry white solid resulted. Elemental analysis of the solid products are given in Table 1, the x-ray powder diffraction patterns are recorded in Table 2 and the vacuum DTA-TGA of the resulting solids are recorded in Figures 5, 6, 7, and 8. In all cases the infrared spectrum of the solids (Nujol mulls) yielded broad, non-distinct bands.

Reaction of LiAlH_4 and AlH_3 in 1:1, 1:2, 1:3, and 1:4 Molar Ratio in THF

Five mmols of LiAlH_4 in THF were added to each of the following quantities of AlH_3 in THF: (1) 5 mmols, (2) 10 mmols, (3) 15 mmols, and (4) 20 mmols. In each case the resulting solutions were stirred for one hour, then the infrared spectrum recorded. The infrared spectra for these solutions are shown in Figure 2.

Reaction of LiH and AlH_3 in 1:4 Molar Ratio in Diethyl Ether

A slurry of 5 mmols of LiH in ether was added to 20 mmols of AlH_3 in ether. The resulting clear solution was stirred for one hour and the infrared spectrum recorded (Figure 4). The solvent was then removed from the solution under vacuum producing a dry white solid. Elemental analysis of the solid showed Li, Al, H, and ether in molar ratio of 1.00:4.02:13.22:1.16. The x-ray powder diffraction patterns are recorded in Table 2 and the DTA-TGA of the resulting solid under argon atmosphere are recorded in Figure 12.

Reaction of LiAlH_4 with BeCl_2 in 4:1 Molar Ratio in Diethyl Ether.

Formation of " LiAl_2H_7 "

Twenty mmoles of LiAlH_4 in diethyl ether was added to 5 mmoles of BeCl_2 in diethyl ether. A white precipitate appeared immediately. After 30 minutes stirring the precipitate was allowed to settle. An infrared spectrum was then run on the clear solution. The spectrum is shown in Figure 3.

Reaction of LiAlH_4 with BeCl_2 in 2:1 Molar Ratio in Diethyl Ether

Ten mmoles of BeCl_2 in diethyl ether was added slowly with stirring to 20 mmoles of LiAlH_4 in diethyl ether cooled at -5° . A white precipitate appeared immediately. The mixture was stirred for one hour and the precipitate was allowed to settle. The infrared spectrum of the clear solution was identical with the infrared spectrum of AlH_3 .

Reaction of LiAlH_4 with BeCl_2 in 3:1 Molar Ratio. Formation of " $\text{LiAl}_3\text{H}_{10}$ "

Fifteen mmoles of LiAlH_4 in diethyl ether was added to 5 mmoles of BeCl_2 in diethyl ether. A white precipitate appeared immediately. After 30 minutes stirring, the precipitate was allowed to settle. An infrared spectrum was then run on the clear solution. The spectrum is shown in Figure 3.

CHAPTER III

RESULTS AND DISCUSSIONS

The infrared spectra of LiAlH_4 and AlH_3 in diethyl ether and tetrahydrofuran as well as mixtures of these compounds in 1:1, 1:2, 1:3, and 1:4 ratio are shown in Figures 1 and 2. In each case the infrared spectrum of a mixture of LiAlH_4 and AlH_3 corresponds to a superposition of the same bands for LiAlH_4 and AlH_3 in the same solvent. If an actual complex between LiAlH_4 and AlH_3 were formed in any of the four cases studied, the infrared spectrum of the resulting solution would be expected to be different from the individual components. For example, a complex between LiAlH_4 and AlH_3 in solution would be expected to exhibit an Al-H-Al bridge bond. The asymmetric Al-H stretching vibration for such a bond in diethyl ether or tetrahydrofuran would be expected to occur between 1600 and 1400 cm^{-1} .⁹ No such band was observed for any of the mixtures mentioned above; therefore, in diethyl ether or THF solution there is no evidence that LiAlH_4 and AlH_3 form complexes of the type $\text{LiAlH}_4 \cdot n(\text{AlH}_3)$ where $n = 1, 2, 3$, or 4 .

Other workers⁴⁻⁶ have reported that complexes of the type $\text{LiAlH}_4 \cdot n(\text{AlH}_3)$ are not stable in diethyl ether or tetrahydrofuran, but are stable in the solid state. In order to investigate this possibility, the same 1:1, 1:2, 1:3, and 1:4 mixtures of LiAlH_4 and AlH_3 in diethyl ether on which the infrared spectra were taken, were evaporated to dryness. Analysis of the resulting white solids indicated the appropriate

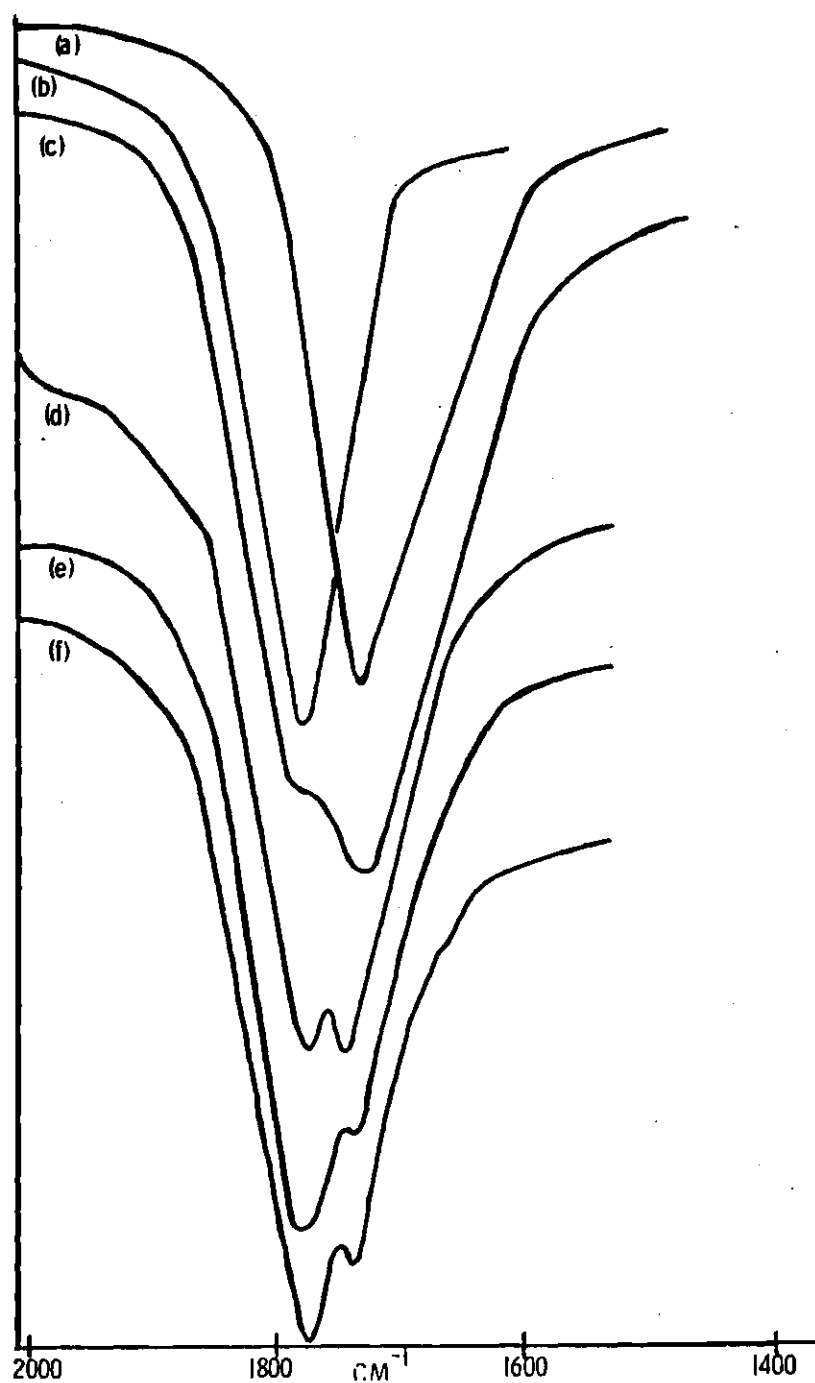


Figure 1. Infrared Spectra of Mixtures of LiAlH_4 and AlH_3 in Diethyl Ether: (a) LiAlH_4 ; (b) AlH_3 ; (c) 1:1 $\text{LiAlH}_4 + \text{AlH}_3$; (d) 1:2 $\text{LiAlH}_4 + \text{AlH}_3$; (e) 1:3 $\text{LiAlH}_4 + \text{AlH}_3$; (f) 1:4 $\text{LiAlH}_4 + \text{AlH}_3$

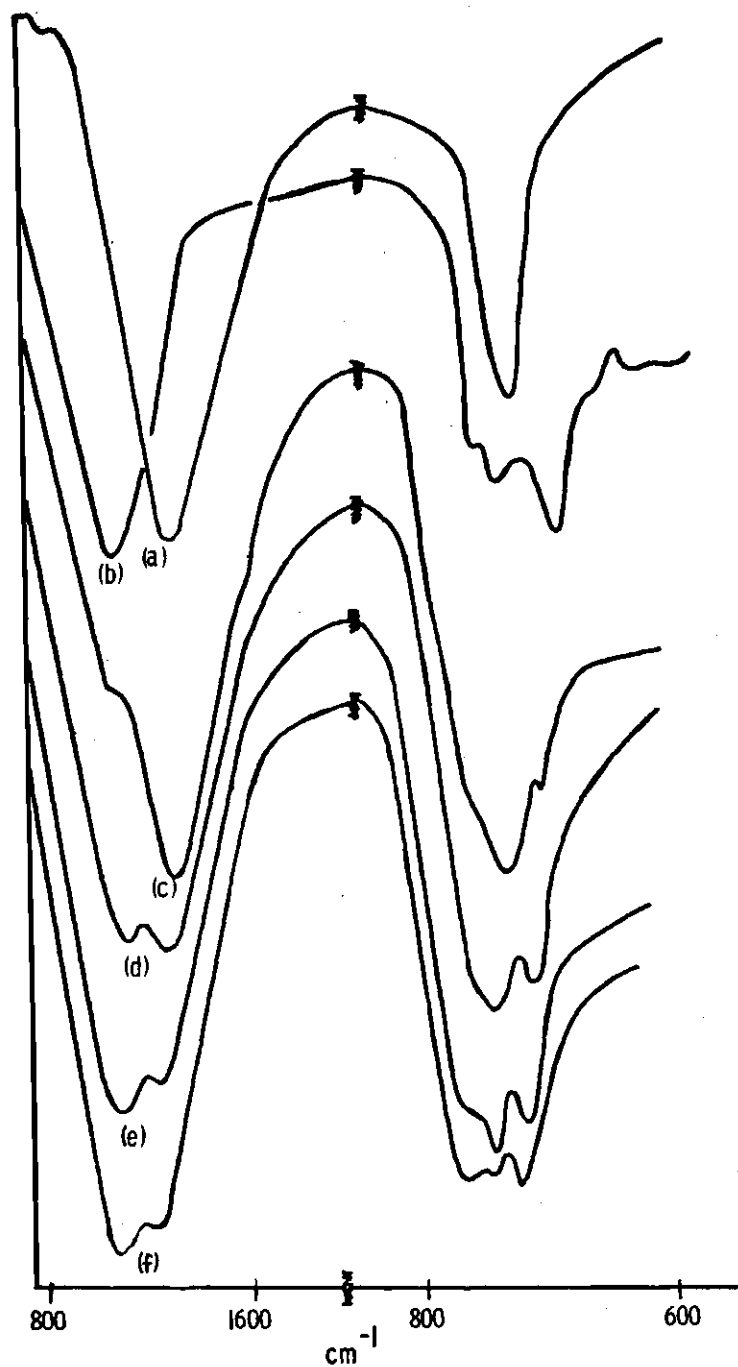


Figure 2. Infrared Spectra of Mixtures of LiAlH_4 and AlH_3 in THF: (a) LiAlH_4 ; (b) AlH_3 ; (c) 1:1 $\text{LiAlH}_4 + \text{AlH}_3$; (d) 1:2 $\text{LiAlH}_4 + \text{AlH}_3$; (e) 1:3 $\text{LiAlH}_4 + \text{AlH}_3$; (f) 1:4 $\text{LiAlH}_4 + \text{AlH}_3$

empirical formula (Table 1) (LiAl_2H_7 , $\text{LiAl}_3\text{H}_{10}$, $\text{LiAl}_4\text{H}_{13}$, and $\text{LiAl}_5\text{H}_{16}$) which indicated the proper stoichiometric ratios and the absence of hydrolysis or ether cleavage. In each case these white solids were subjected to DTA-TGA and x-ray powder diffraction analysis.

The x-ray powder diffraction pattern for " LiAl_2H_7 " is shown in Table 2. It is readily seen that the so called complex corresponds to a mixture of LiAlH_4 and AlH_3 . The vacuum DTA-TGA of " LiAl_2H_7 " is shown in Figure 5. The thermogram shows gas evolution at 110, 163, 221, and 355° with simultaneous weight losses of 14.75, 1.00, 0.50, and 0.50 mg. The vacuum DTA-TGA of separate samples of LiAlH_4 and AlH_3 are shown in Figures 9 and 10. Aluminum hydride (Figure 10) is seen to decompose at 110° with almost simultaneous loss of both solvent and hydrogen. The first gas evolution in Figure 5 for " LiAl_2H_7 " also occurs at 110° and its corresponding large weight loss is undoubtedly due to loss of both solvent and hydrogen. Due to large amounts of solvent loss, only the lower portion of the TGA



is shown in Figures 5-8 so that the weight losses for the last three gas evolutions could be seen more easily. LiAlH_4 (Figure 9) is seen to decompose with gas evolution at 165, 224, and 410° with simultaneous weight loss in the ratio of 2:1:1. The last three gas evolutions in Figure 5 correspond

Table 1. Elemental Analysis of Mixtures of LiAlH_4 and AlH_3 in 1:1, 1:2, 1:3, and 1:4 Ratio in Diethyl Ether

Ratio $\text{LiAlH}_4:\text{AlH}_3$	Elemental Analysis				Mole Ratio			
	Li	Al	H	Et_2O	Li	: Al	: H	: Et_2O
1:1	7.45	56.79	7.45	28.31	1.02	:2.00	: 7.08	:0.35
1:2	4.91	55.58	6.97	32.54	1.03	:3.00	:10.13	:0.64
1:3	3.58	53.20	6.52	36.70	1.05	:4.00	:13.22	:1.01
1:4	2.65	51.08	6.17	40.10	1.01	:5.00	:16.31	:1.43

Table 2. X-Ray Powder Diffraction Patterns of the Solid Products Obtained in the Reactions of LiAlH_4 with AlH_3 in Diethyl Ether

$^a\text{LiAl}_2\text{H}_7$		$^b\text{LiAl}_3\text{H}_{10}$		$^c\text{LiAl}_4\text{H}_{13}$		$^d\text{LiAl}_5\text{H}_{16}$		$^e\text{LiAlH}_4$		$^f\text{AlH}_3$		$^h\text{LiAl}_2\text{H}_7$		$^i\text{LiAl}_4\text{H}_{13}$		$^j\text{LiAl}_4\text{H}_{13}$	
d, Å	I/I ₀	d, Å	I/I ₀	d, Å	I/I ₀	d, Å	I/I ₀	d, Å	I/I ₀	d, Å	I/I ₀	d, Å	I/I ₀	d, Å	I/I ₀	d, Å	I/I ₀
11.4	m	11.6	m	11.6	s	11.6	s	5.36	w	11.6	vs	4.43	ms	9.450	ms	11.6	s
5.31	w	5.30	w	5.33	w	4.61	ms	4.48	m	4.59	s	4.20	w	5.586	w	6.7	w
4.61	mw	4.65	m	4.62	m	4.47	vw	4.00	vw	3.24	ms	3.89	s	5.265	vw	4.55	s
4.45	m	4.41	m	4.44	w	3.87	ms	3.89	s	2.89	ms	3.68	vw	4.548	s	4.30	s
3.85	s	3.85	s	3.85	s	3.65	vw	3.68	m			3.55	mw	4.439	vs	3.85	s
3.67	m	3.63	m	3.66	w	3.31	w	3.53	vw			3.30	mw	3.045	ms	3.66	m
3.41	m	3.47	m	3.45	w	3.25	s	3.43	w			2.90	vww	3.888	s	3.45	m
3.31	m	3.30	m	3.33	m	3.00	vw	3.32	m			2.65	mw	3.666	vs	3.33	w
3.22	mw	3.24	m	3.24	s	2.87	ms	3.24	m			2.588	w	3.527	w	3.02	w
3.00	w	3.01	w	3.01	w	2.66	vw	3.03	m			2.504	m	3.456	m	2.95	m
2.92	w	2.96	w	2.95	w	2.40	vw	3.00	w			2.376	w	3.324	w	2.85	s
2.85	mw	2.85	m	2.85	m			2.95	m			2.337	vw	3.229	vs	2.65	vw
2.67	w	2.65	w	2.65	w			2.68	m			2.295	vw	3.035	ms	2.54	m
2.45	w	2.45	vw	2.45	vw			2.54	vw			2.093	mw	2.952	vw	2.39	w
2.16	w	2.40	w	2.39	vw			2.45	w			1.992	mw	2.882	vs	2.29	m
2.01	w	2.02	vw	2.12	vw			2.42	m			1.949	mw	2.799	vw	2.25	w
1.78	w							2.24	w			1.929	vww	2.680	w	2.075	w
								2.15	w			1.883	vww	2.566	vw	1.98	vww
								2.05	w			1.782	vww	2.506	vww	1.80	w
								2.01	vw			1.765	w	2.424	w	1.69	vw
								1.98	w			1.655	w	2.405	w	1.65	vww
								1.92	vw			1.604	vww	2.342	s	1.54	vw
								1.89	vw			1.572	vw	2.316	s	1.52	vw
								1.80	vw			1.558	vww	2.271	ms	1.34	vww
								1.78	w			1.517	w	2.220	ms		
								1.76	w			1.480	w	2.038	ms		
								1.74	w			1.375	vww	1.530	ms		
												1.352	vww	1.473	w		
												1.301	vww	1.442	w		
												1.281	vww	1.415	w		
												1.194	vww	1.344	w		

^aSolid from $\text{LiAlH}_4 + \text{AlH}_3$ in 1:1 molar ratio; ^bSolid from $\text{LiAlH}_4 + \text{AlH}_3$ in 1:2 molar ratio;

^cSolid from $\text{LiAlH}_4 + \text{AlH}_3$ in 1:3 molar ratio; ^dSolid from $\text{LiAlH}_4 + \text{AlH}_3$ in 1:4 molar ratio; ^eSolid from evaporating ethereal LiAlH_4 ; ^fSolid from evaporating ethereal $\text{AlH}_3 \cdot \text{AlH}_3$ prepared from 2:1

$\text{BeCl}_2 + \text{LiAlH}_4$; ^gs, strong; m, moderate; w, weak; v, very; ^hSee reference 5; ⁱSee reference 6;

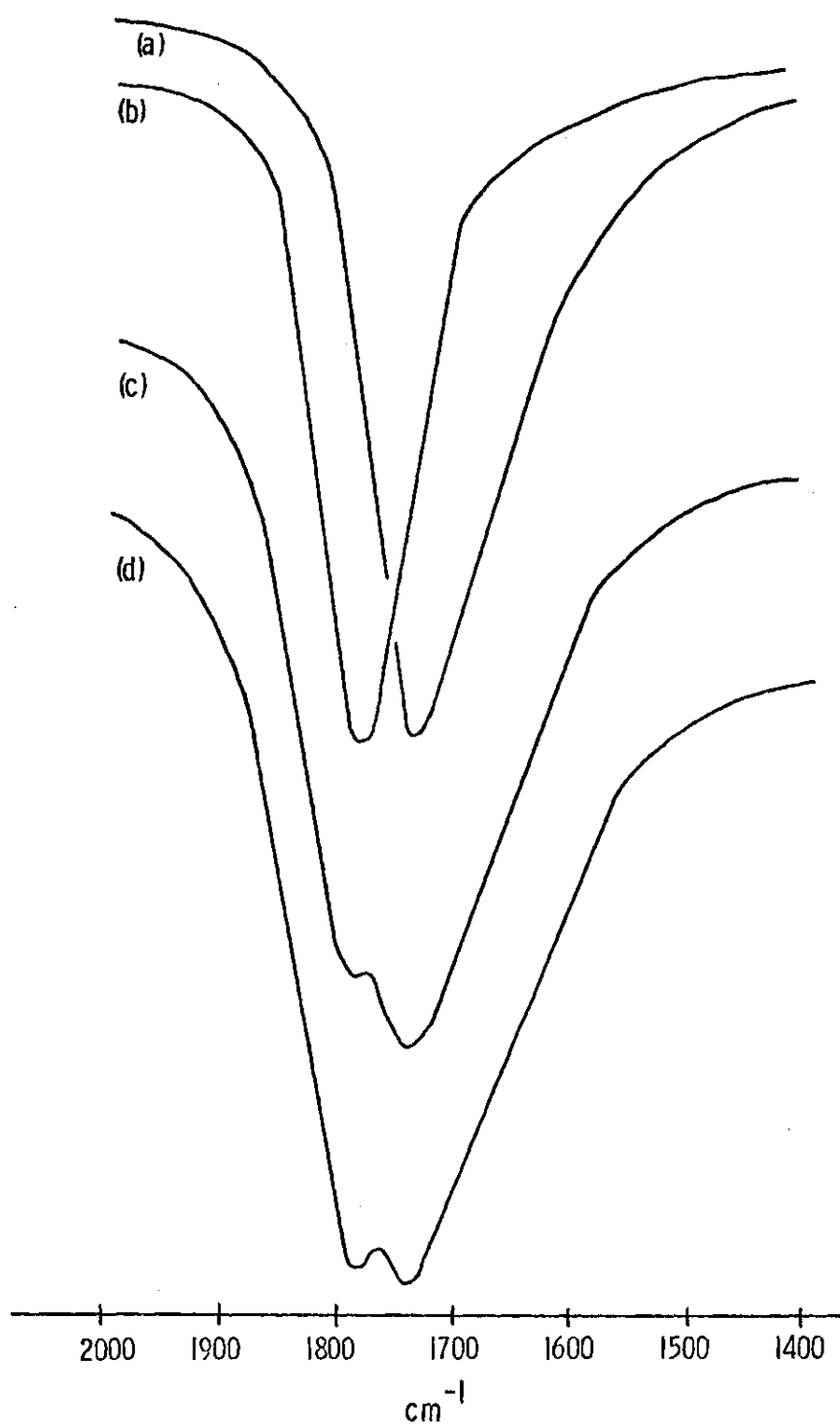


Figure 3. Infrared Spectra in the 2000-1400 cm^{-1} Region for Diethyl Ether Solutions of (a) LiAlH_4 ; (b) AlH_3 ; (c) the Supernatant Remaining after the Reaction of LiAlH_4 with BeCl_2 in 4:1 Molar Ratio, " LiAl_2H_7 "; (d) the Supernatant Remaining after the Reaction of LiAlH_4 with BeCl_2 in 3:1 Molar Ratio, " $\text{LiAl}_3\text{H}_{10}$ "

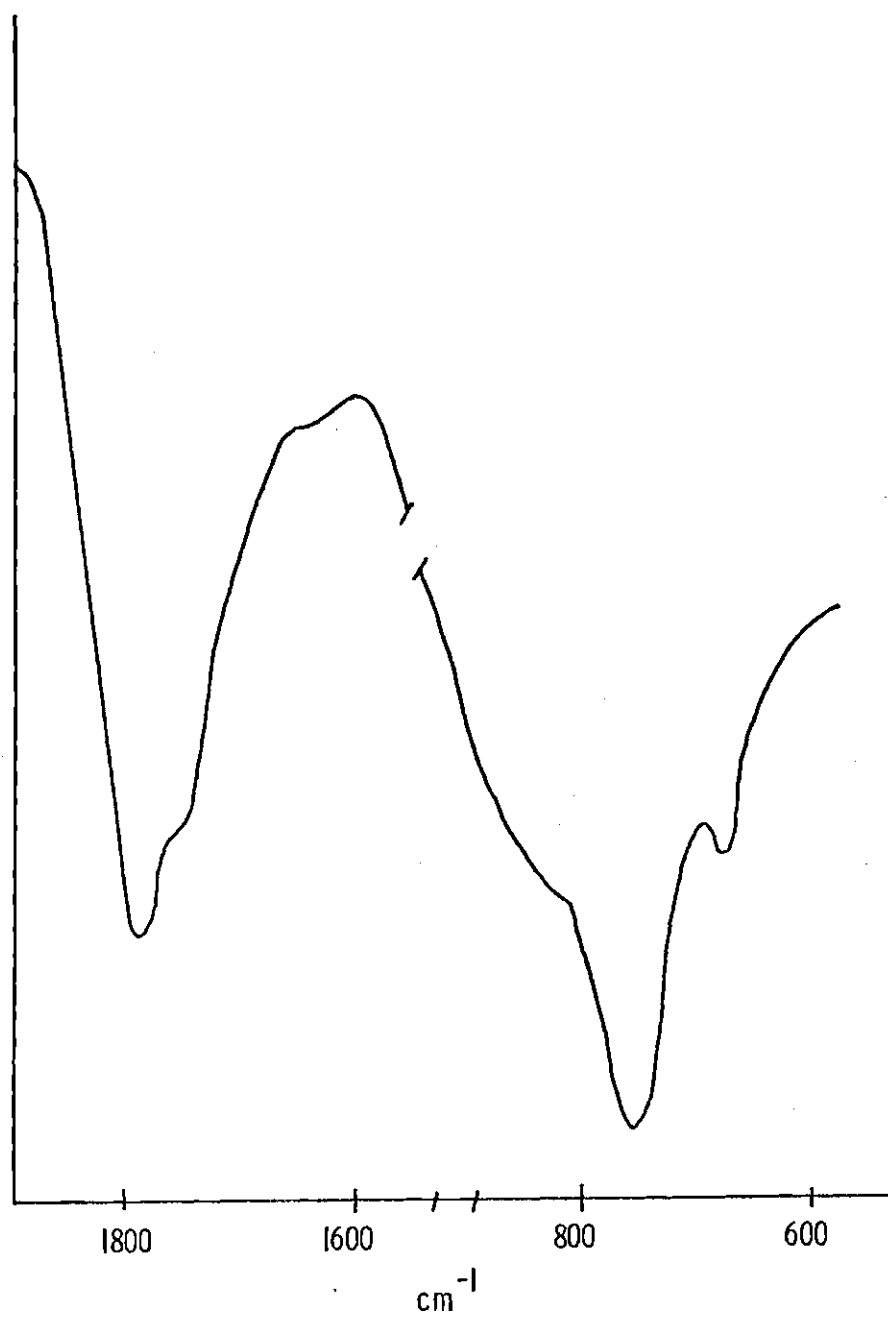


Figure 4. Infrared Spectrum of the Solution Resulting on Admixture of LiH and AlH₃ in 1:4 Molar Ratio in Diethyl Ether

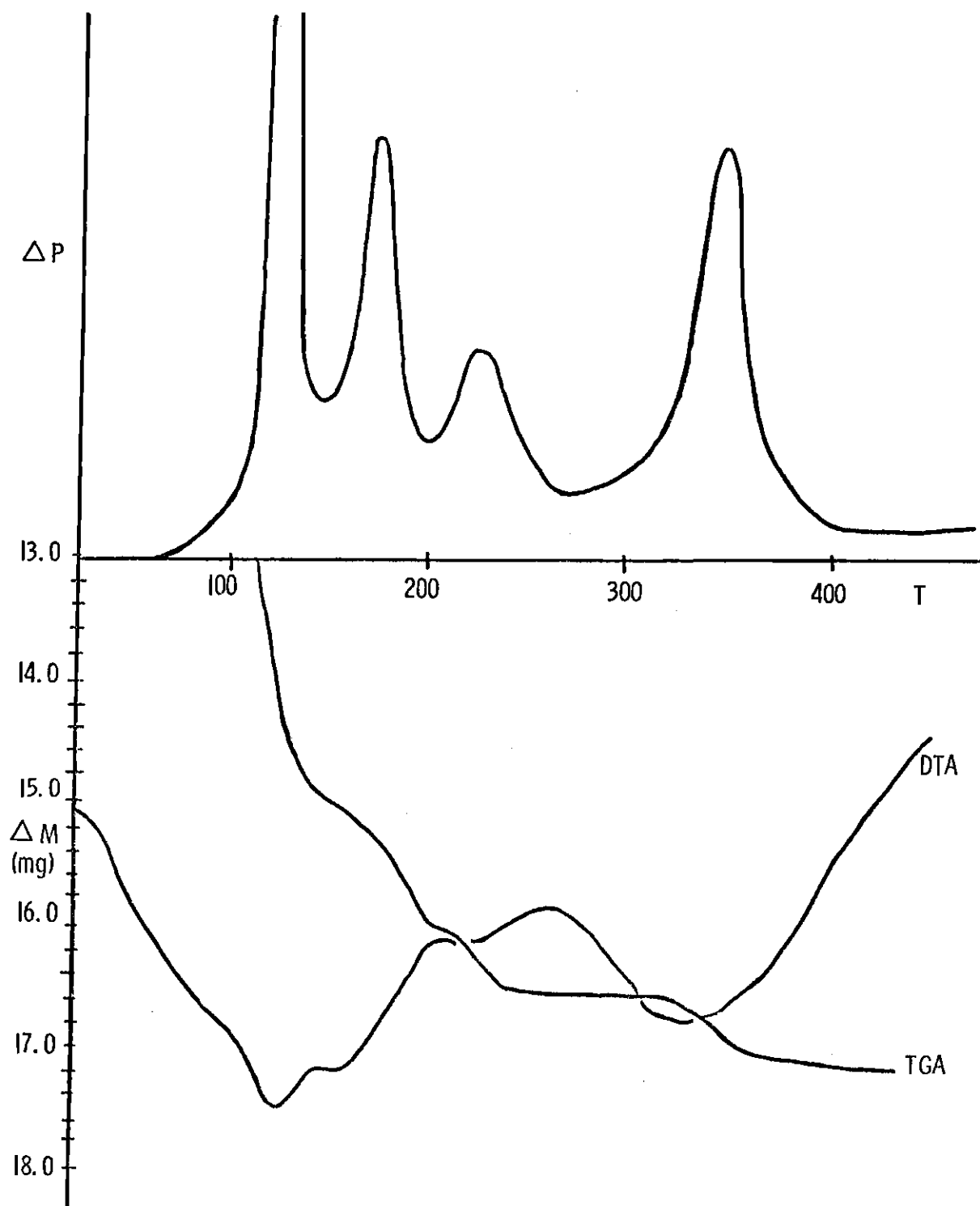


Figure 5. Vacuum DTA-TGA of Proposed " LiAl_2H_7 "

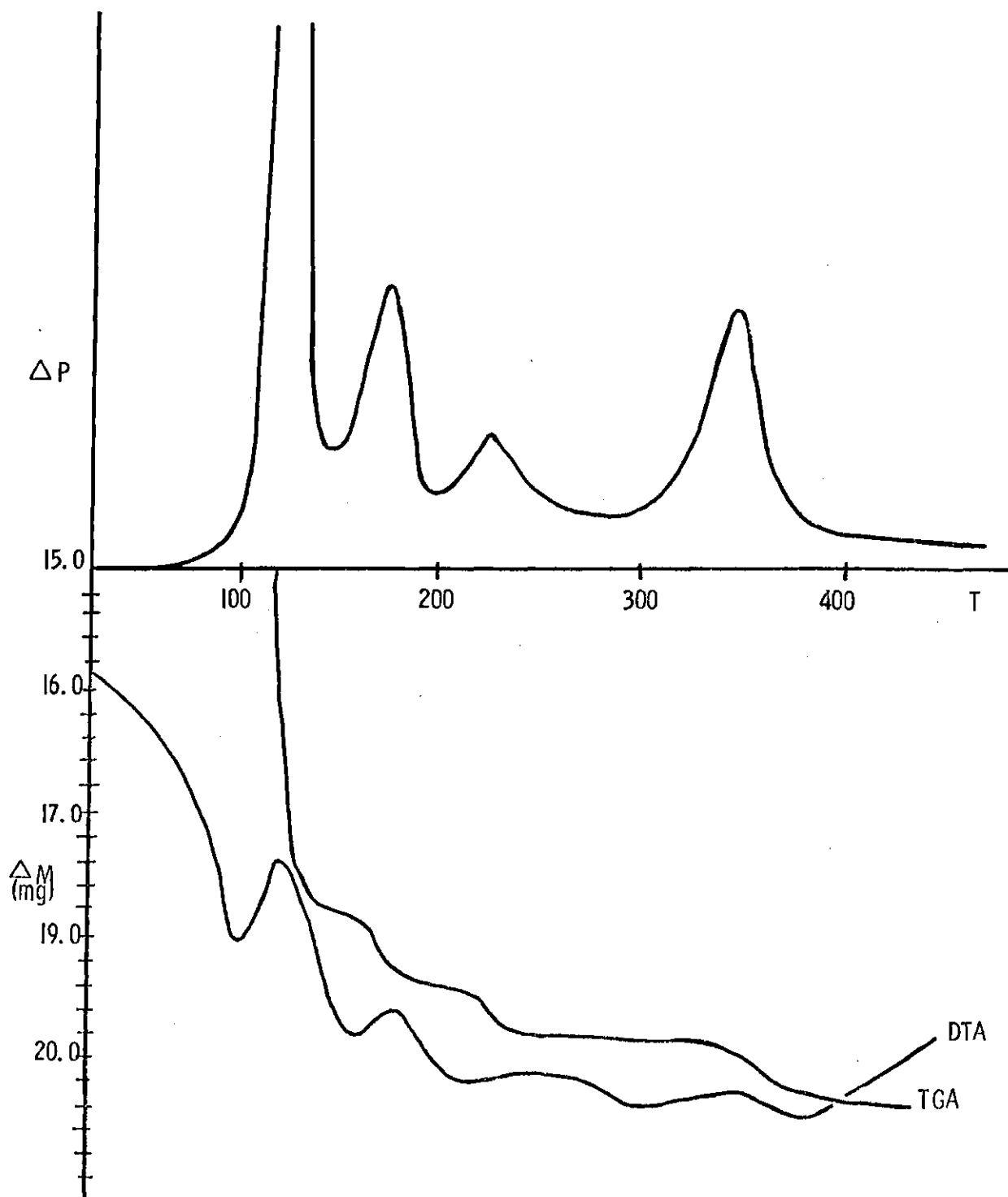


Figure 6. Vacuum DTA-TGA of LiAlH_4

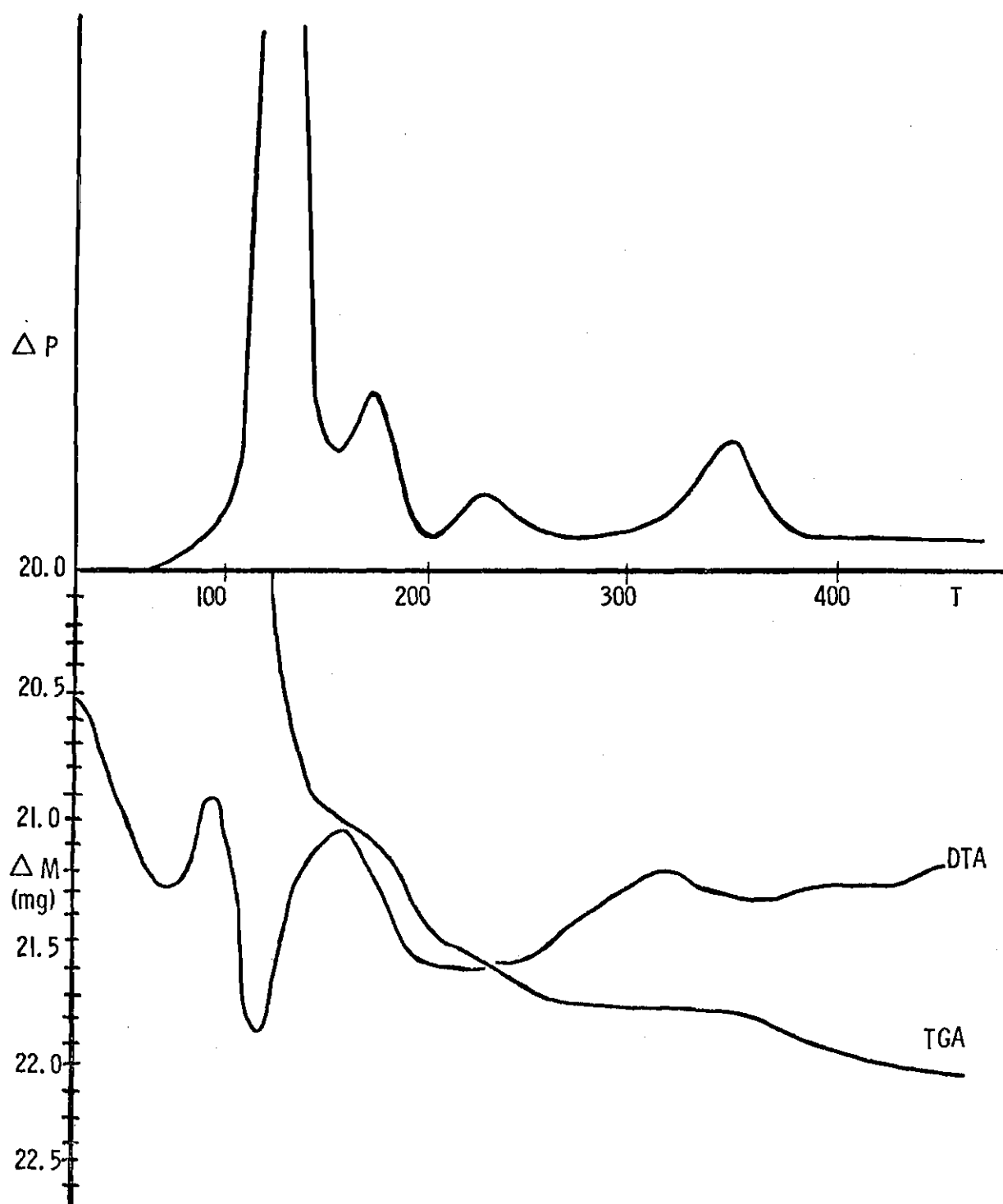


Figure 7. Vacuum DTA-TGA of $\text{LiAl}_4\text{H}_{13}$

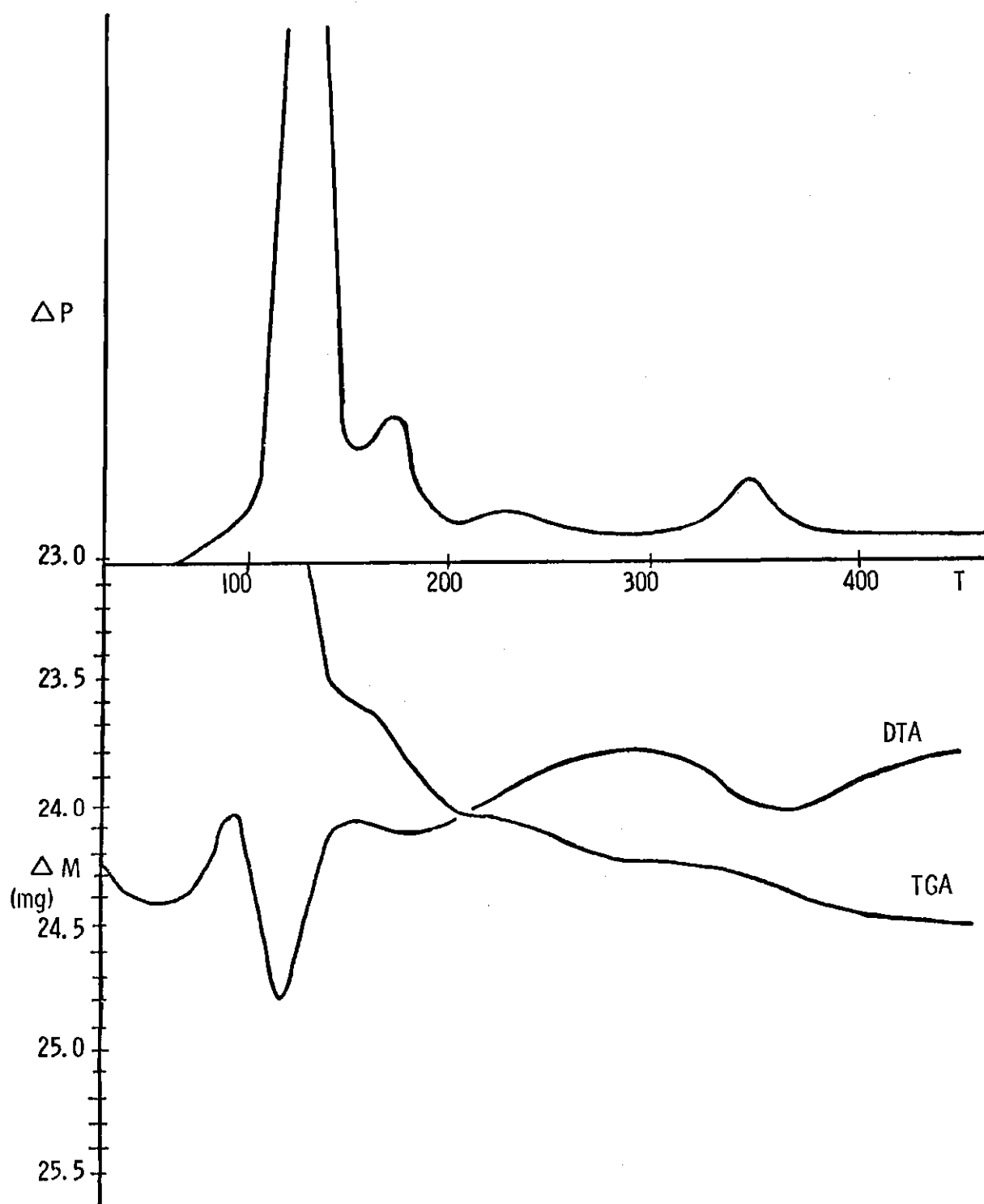


Figure 8. Vacuum DTA-TGA of $\text{LiAl}_5\text{H}_{16}$

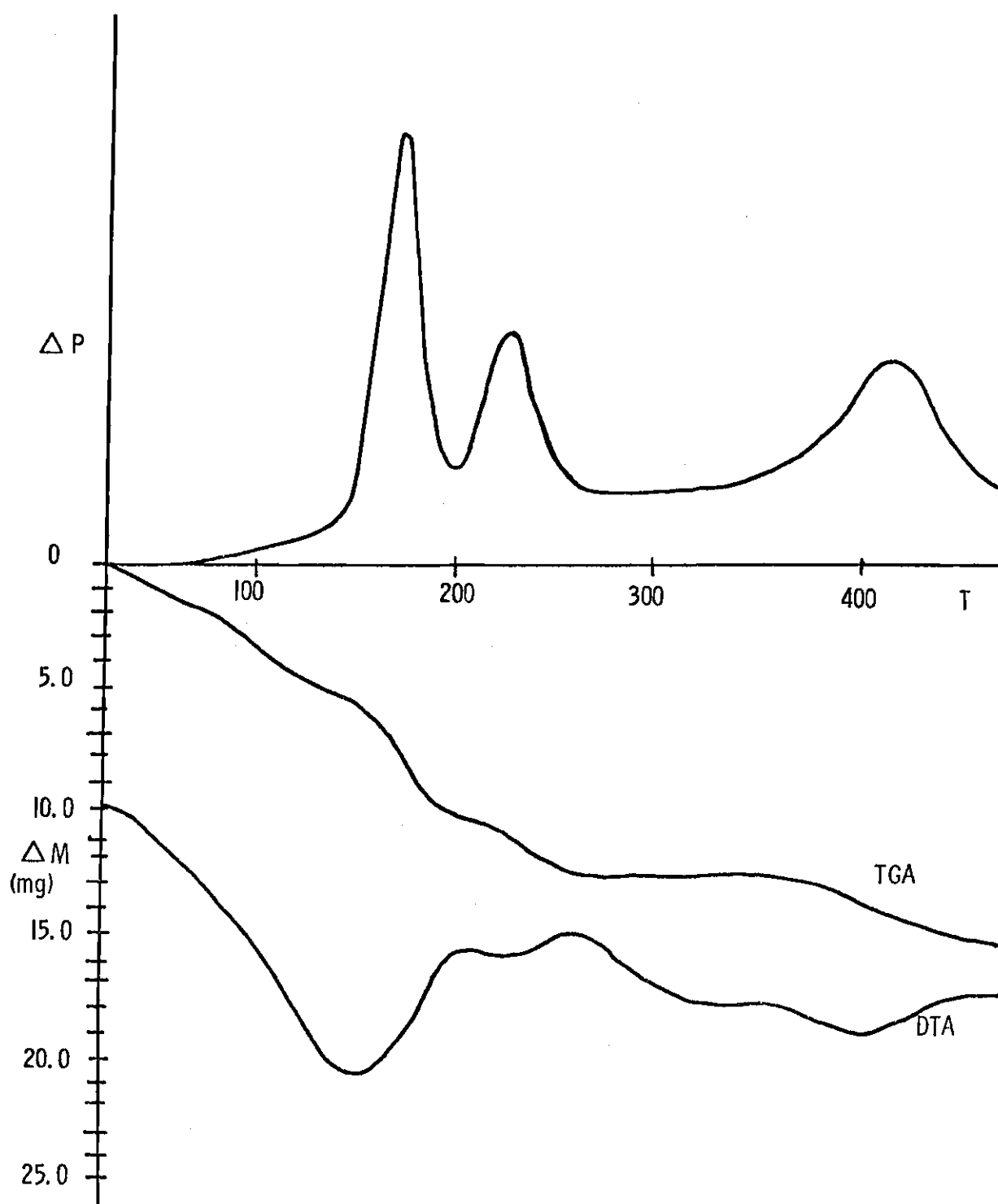


Figure 9. Vacuum DTA-TGA of LiAlH_4

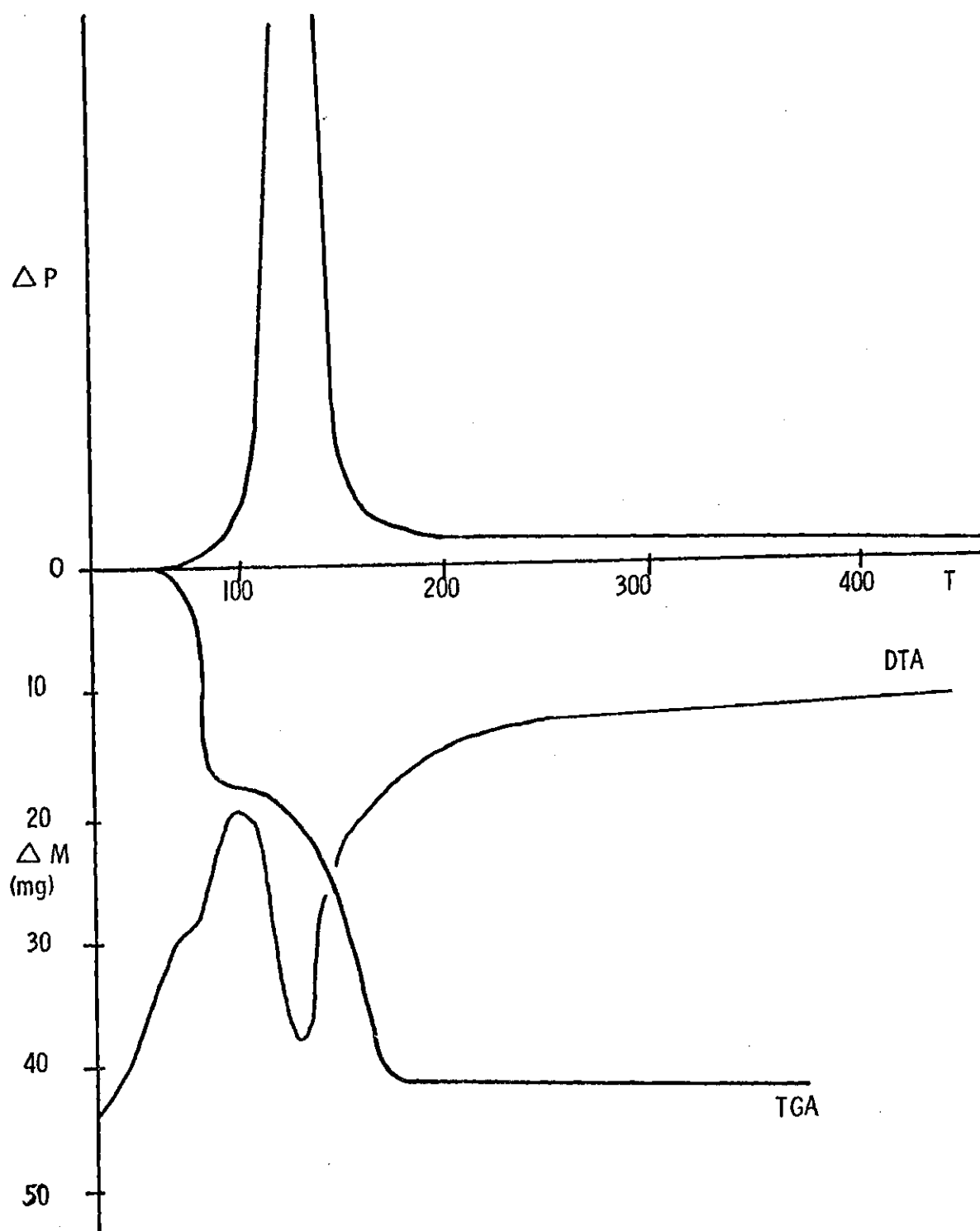
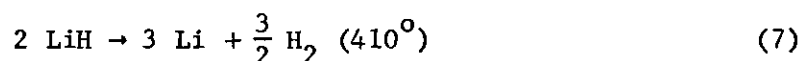
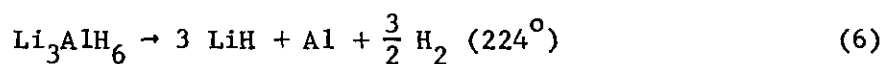
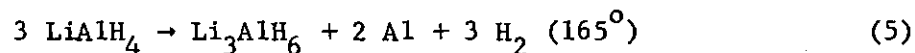


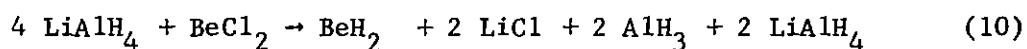
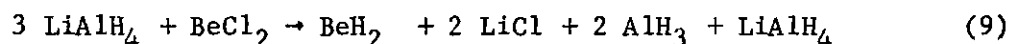
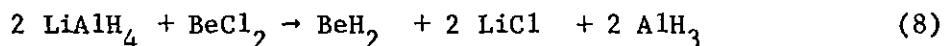
Figure 10. Vacuum DTA-TGA of AlH_3



exactly with the gas evolutions in Figure 9, except for the last one; however, the ratio of the weight loss for the last three gas evolutions in Figure 5 is 2:1:1, the same as for LiAlH_4 . When " LiAl_2H_7 " was heated to 130° under vacuum and stopped, the x-ray powder pattern of the resulting solid showed only lines for LiAlH_4 and Al . The DTA-TGA for " LiAl_2H_7 ", shown in Figure 5, is readily interpreted to be due to a 1:1 mixture of LiAlH_4 and AlH_3 . Thus, the product of solution of LiAlH_4 and AlH_3 is not a complex but a physical mixture.

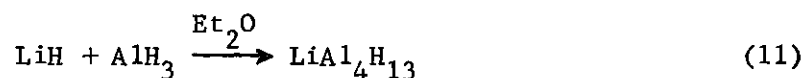
The data indicating the composition of " LiAl_2H_7 " as a physical mixture of AlH_3 and LiAlH_4 could be explained by assuming the existence of the complex LiAl_2H_7 which then dissociates at 110° to LiAlH_4 and AlH_3 . However, the powder diffraction data were obtained at room temperature which shows the product " LiAl_2H_7 " to be actually a physical mixture of LiAlH_4 and AlH_3 . Although the preparation of LiAl_2H_7 and $\text{LiAl}_3\text{H}_{10}$ have been reported⁴ by the reaction of LiAlH_4 and BeCl_2 , the infrared spectra (Figure 3) of the solutions obtained by reacting LiAlH_4 and BeCl_2 in diethyl ether in 4:1 and 3:1 mole ratios clearly shows the presence of LiAlH_4 and AlH_3 in the solution. The infrared spectrum of the solution obtained by the reaction of LiAlH_4 and BeCl_2 in diethyl ether at -5°

in 2:1 mole ratio indicates the presence of only AlH_3 in solution.



The x-ray powder diffraction patterns for the proposed compounds: " $\text{LiAl}_3\text{H}_{10}$ ", " $\text{LiAl}_4\text{H}_{13}$ ", and " $\text{LiAl}_5\text{H}_{16}$ " are shown in Table 2. The DTA-TGA thermograms for these compounds are shown in Figures 6-8. Analogous to the reasoning used for " LiAl_2H_7 ", these compounds are also shown to be mixtures of LiAlH_4 and AlH_3 .

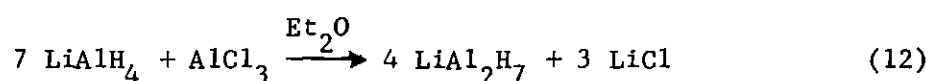
We have repeated the work of Bosquet and co-workers⁶ in an attempt to prepare $\text{LiAl}_4\text{H}_{13}$ by the method used in their laboratory. The infrared spectrum of the solution obtained by reaction of an ether solution of LiAlH_4 with an ether solution of AlH_3 is shown in Figure 4. The infrared



spectrum of the solution clearly shows the presence of LiAlH_4 and AlH_3 in the solution. The x-ray powder pattern of the solid obtained on complete removal of solvent is shown in Table 2. It is readily seen that the proposed complex closely corresponds to a mixture of LiAlH_4 and AlH_3 . The DTA-TGA thermograms for the solids obtained by either

evaporation of the solutions formed on mixing LiAlH_4 and AlH_3 in diethyl ether in 1:3 mole ratio and by the reaction shown above (Eq. 11) are shown in Figures 12 and 13. The DTA-TGA of both solids are identical. Also there is a striking similarity between these thermograms and the DTA-TGA of a physical mixture of one mole of LiAlH_4 and three moles of LiAlH_4 .

The reaction of LiAlH_4 and AlCl_3 in 7:1 molar ratio in diethyl ether at 0° (Eq. 12) yields a white precipitate of lithium chloride and a clear solution containing LiAlH_4 and AlH_3 in equal molar portions. The presence of LiAlH_4 and AlH_3 in solution is confirmed by the occurrence



of characteristic strong bands at 1785 cm^{-1} (Al-H st. vibration in AlH_3) and 1760 cm^{-1} (Al-H st. vibration in LiAlH_4). The elemental analysis of the white solid isolated after complete removal of ether solvent showed a Li:Al:H ratio of 0.571:1.00:3.33. Anal. Calcd. for " LiAl_2H_7 ". 0.29 Et_2O : Li, 7.75; Al, 60.32; H, 7.88. Found: Li, 7.90; Al, 60.32; H, 7.42. The x-ray powder diffraction pattern for " LiAl_2H_7 " is shown in Table 3. It is readily seen that the so-called complex corresponds to a mixture of LiAlH_4 and AlH_3 . However, the weak line at 11.6 \AA is not as well defined as in the physical mixture of LiAlH_4 and AlH_3 (1:1 molar ratio). The DTA-TGA of " LiAl_2H_7 " under static argon atmosphere is shown in Figure 14. The thermogram shows gas evolution at 95 and 170° .

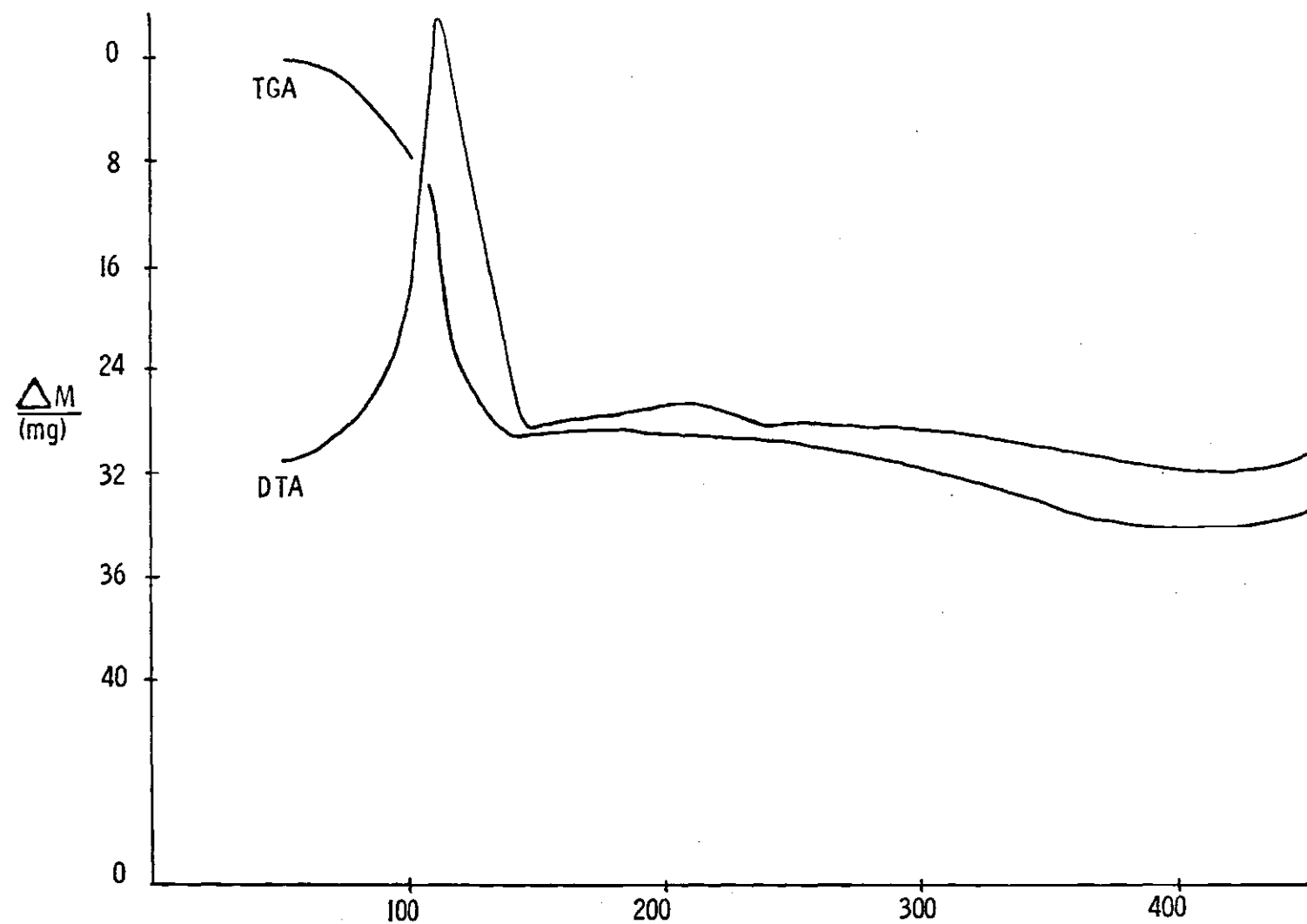


Figure 11. DTA-TGA of AlH_3 under Static Argon Atmosphere

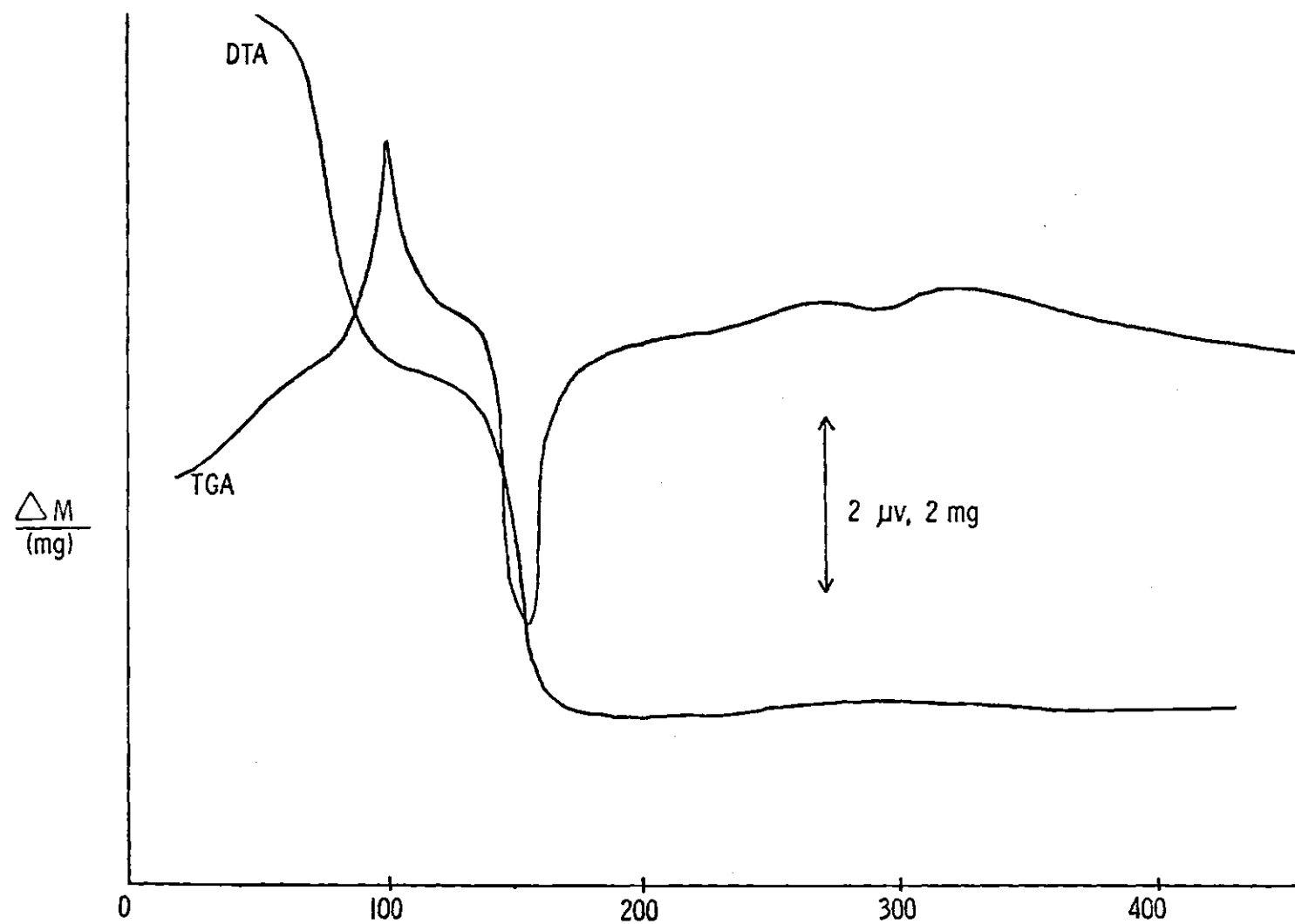


Figure 12. DTA-TGA of $\text{LiAl}_4\text{H}_{13}$ ($\text{LiAlH}_4 + 3 \text{ AlH}_3$) under Static Argon Atmosphere

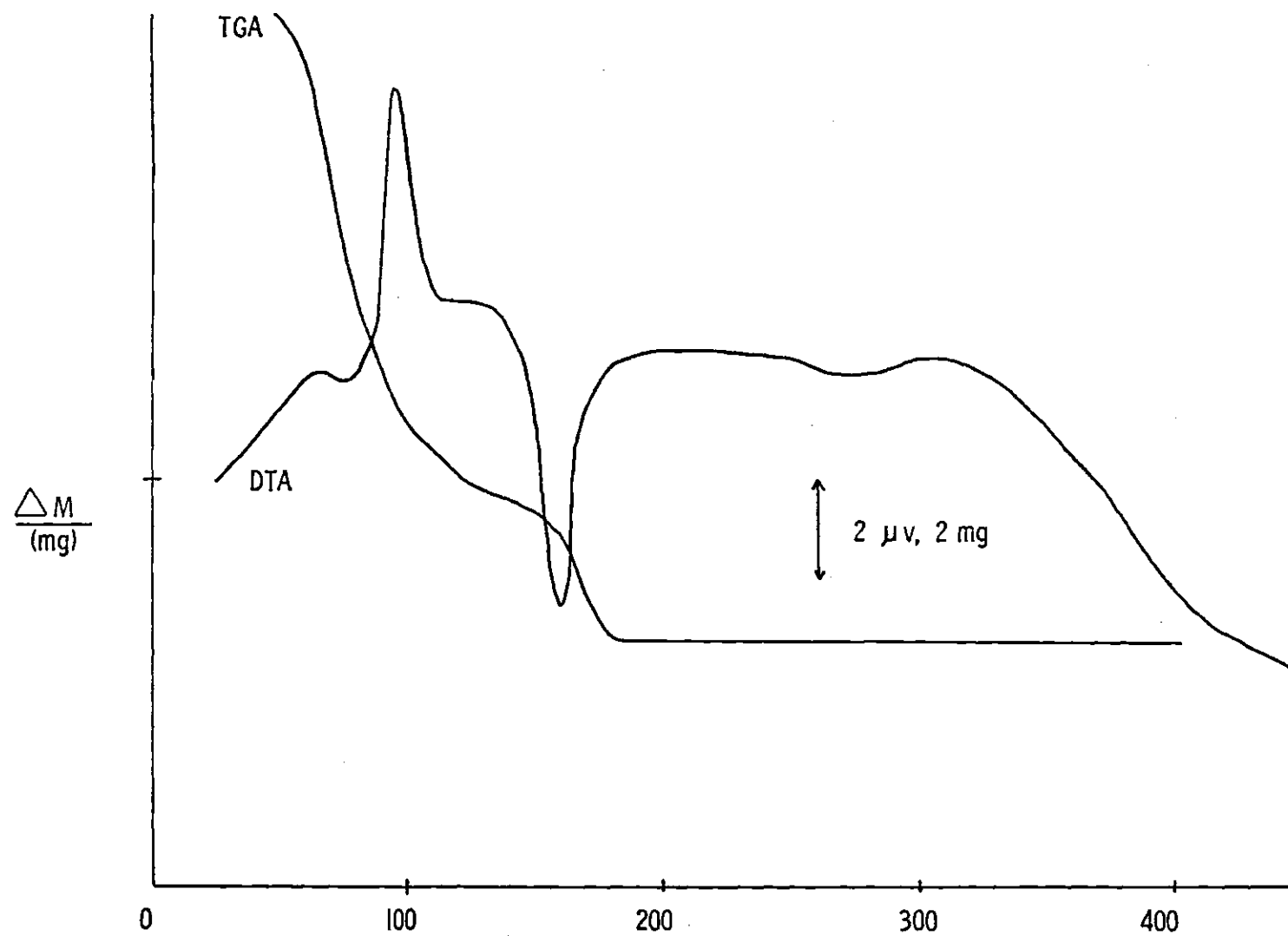


Figure 13. DTA-TGA of $\text{LiAl}_4\text{H}_{13}$ ($\text{LiH} + 4 \text{AlH}_3$) under Static Argon Atmosphere

Table 3. X-Ray Powder Diffraction Patterns of "LiAl₂H₇" and "LiAl₄H₁₃"

"LiAl ₂ H ₇ " ^a	"LiAl ₂ H ₇ " ^b	"LiAl ₂ H ₇ " ^c	"LiAl ₄ H ₁₃ " ^d	"LiAl ₄ H ₁₃ " ^e	LiAlH ₄	AlH ₃	"LiAl ₃ H ₁₀ " ^f
d, Å I/I ₀	d, Å I/I ₀	d, Å I/I ₀	d, Å I/I ₀	d, Å I/I ₀	d, Å I/I ₀	d, Å I/I ₀	d, Å I/I ₀
	11.6 mw	11.6 mw				11.6 vs	11.5 s
11.4 m	5.15 m	6.70 vvw	11.6 s	11.6 s	5.36 w		6.8 vvw
5.31 w	4.45 ms	5.15 mw	5.33 w	6.6 vw	4.48 m	4.59 s	5.4 vvw
4.61 mw	3.85 s	4.45 ms	4.62 m	5.58 w	4.00 vw		4.6 s
4.45 m	3.65 ms	3.85 s	4.44 w	4.6 ms	3.89 s		3.85 s
3.85 s	3.32 s	3.65 ms	3.85 s	3.85 s	3.68 m		3.65 m
3.67 m	3.25 s	3.32 s	3.66 w	3.65 m	3.53 vw		3.52 m
3.41 m	2.98 m	3.25 s	3.45 w	3.50 ms	3.43 w		
3.31 m	2.92 m	2.98 ms	3.33 m	3.24 s	3.32 m		
3.22 mw	2.67 m	2.92 m	3.24 s	2.85 w	3.24 m	3.24 m	3.25 s
3.00 w	2.57 w	2.67 m	3.01 w	2.78 w	3.03 m		
2.92 w	2.45 mw	2.58 w	2.95 w	2.65 vvw	3.00 w		
2.85 mw	2.325mw	2.45 mw	2.85 m	2.55 vvw	2.95 m		2.96 s
2.67 w	2.18 m	2.30 w	2.65 w	2.30 w		2.89 ms	
2.45 w	2.10 w	2.18 w	2.45 vw	2.12 vvw	2.68 m		2.65 w
2.16 w	2.05 mw	2.10 w	2.39 vw	1.96 vw	2.54 vw		2.56 w
2.01 w	1.970vvw	2.08 mw	2.12 vw		2.45 w		
1.78 w	1.78 vw	1.97 vvw			2.42 m		2.35 vvw
	1.62 w	1.78 vw			2.24 w		
	1.52 w	1.64 w			2.15 w		2.15 w
	1.48 vvw				2.05 w		2.08 w
					2.01 vw		2.025 w
					1.98 w		
					1.92 vw		
					1.89 vw		
					1.80 vw		
					1.78 w		
					1.76 w		
					1.74 w		

^aSolid from LiAlH₄ + AlH₃ in 1:1 molar ratio; ^bSolid from LiAlH₄ + AlCl₃ in 7:1 molar ratio;

^cSolid from LiH + AlCl₃ in 7:2 molar ratio; ^dSolid from LiAlH₄ + AlH₃ in 1:3 molar ratio; ^eSolid from LiAlH₄ + AlCl₃ in 13:3 molar ratio; ^fSolid from LiAlH₄ + AlCl₃ in 5:1 molar ratio.

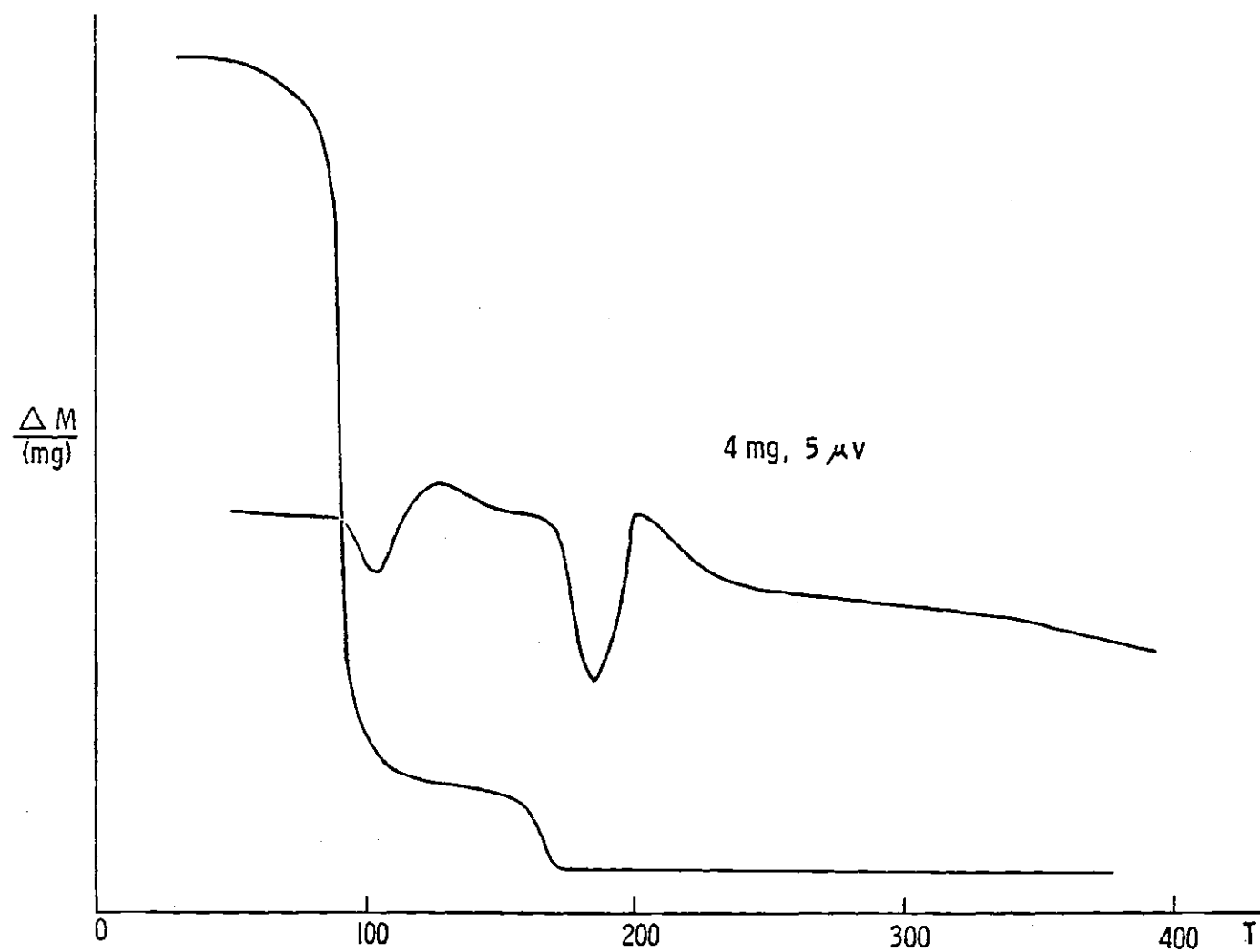
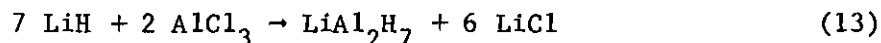


Figure 14. DTA-TGA of " LiAl_2H_7 " ($7 \text{ LiAlH}_4 + \text{AlCl}_3 \rightarrow 3 \text{ LiCl} + 4 \text{ LiAl}_2\text{H}_7$) under Static Argon Atmosphere

with simultaneous weight losses of 11.0 mg (13.2%) and 3.7 mg (4.4%) respectively. The first gas evolution corresponds to a large weight loss and is undoubtedly due to loss of both solvent and decomposition of AlH_3 . The second gas evolution is probably due to decomposition of LiAlH_4 . It is important to note that the thermogram (Figure 14) is quite similar to the thermogram of the solid obtained after mixing ether solutions of AlH_3 and LiAlH_4 in 1:1 molar ratio followed by removal of solvent under vacuum (Figure 8).

As we noted earlier, the solid obtained by this method is indeed a physical mixture of LiAlH_4 and AlH_3 and not the complex " LiAl_2H_7 ". We have also shown that the thermogram (Figure 14) is almost identical to the thermogram obtained for a physical mixture of solid LiAlH_4 and solid AlH_3 mixed in 1:1 ratio. Thus, the reaction of LiAlH_4 and AlCl_3 in 7:1 molar ratio in diethyl ether yields a mixture of LiAlH_4 and AlH_3 .

The x-ray powder pattern for " LiAl_2H_7 " reported by Mayet and co-workers⁵ is shown in Table 2. This powder pattern resembles that of LiAlH_4 , although no lines for AlH_3 can be detected. The " LiAl_2H_7 " was prepared by the reaction shown in Equation 13. Unfortunately, these



workers did not report any DTA-TGA or infrared spectra in their studies. We have now studied the reaction of LiH with AlCl_3 in detail. The reaction of LiH and AlCl_3 in 7:2 molar ratio in diethyl ether at 0° also yields a mixture of LiAlH_4 and AlH_3 in solution as determined by

infrared spectroscopy. The x-ray powder diffraction data (Table 3) of the solid obtained after complete removal of solvent shows it to be a physical mixture of LiAlH_4 and AlH_3 . The DTA-TGA of the solid is similar to the thermogram (Figure 14) of the solid obtained by the reaction of LiAlH_4 and AlCl_3 in 7:1 molar ratio.

We decided to attempt to prepare $\text{LiAl}_4\text{H}_{13}$ by the reaction of LiAlH_4 and AlCl_3 in 13:3 mole ratio in an attempt to determine if AlCl_3 plays any role in the formation of the so-called complexes of LiAlH_4 and AlH_3 .⁶ The reaction of LiAlH_4 and AlCl_3 in 13:3 molar ratio in diethyl ether at 0° yields a mixture of LiAlH_4 and AlH_3 in solution confirmed by infrared spectroscopy. The elemental analysis of the white solid obtained after complete removal of solvent corresponds to an empirical formula $\text{LiAl}_4\text{H}_{13} \cdot 0.96 \text{Et}_2\text{O}$. The x-ray powder diffraction data are given in Table 3. The DTA-TGA of the solid is similar to that shown in Figure 14.

The x-ray powder diffraction data as well as DTA-TGA of the solid shows it to be a physical mixture of LiAlH_4 and AlH_3 rather than a complex.

Similarly, in an attempt to prepare $\text{LiAl}_3\text{H}_{10}$ by the reaction of LiAlH_4 and AlCl_3 in 5:1 molar ratio in diethyl ether at 0° , no evidence was found to indicate the presence of $\text{LiAl}_3\text{H}_{10}$ complex. The infrared spectrum of the clear solution obtained after the complete reaction of LiAlH_4 and AlCl_3 showed the presence of LiAlH_4 and AlH_3 in solution. Elemental analysis of the white solid obtained after complete removal of the solvent corresponds to an empirical formula $\text{LiAl}_3\text{H}_{10} \cdot 0.81 \text{Et}_2\text{O}$.

The x-ray powder diffraction data (Table 3) as well as the DTA-TGA of the solid under static argon atmosphere (Figure 14) indicate that actually it is a physical mixture of LiAlH_4 and AlH_3 and not a complex.

CHAPTER IV

CONCLUSIONS

In this study, evidence has been presented to show that LiAlH_4 and AlH_3 do not react, under the conditions studied, to form complexes of the type $\text{LiAlH}_4 \cdot n(\text{AlH}_3)$ in either diethyl ether or THF solution. Also, evidence has been presented showing that the solids left after evaporation of the solvent from 1:1, 1:2, 1:3, and 1:4 mixtures of LiAlH_4 and AlH_3 in diethyl ether failed to produce complexes of the type LiAlH_4 and $\text{LiAlH}_4 \cdot n(\text{AlH}_3)$. The equivalence of solutions formed by (1) addition of LiAlH_4 and AlH_3 in diethyl ether, (2) reaction of LiAlH_4 and BeCl_2 in diethyl ether, and (3) reaction of LiH and AlH_3 has been demonstrated and the solids resulting from these solutions have been shown by x-ray powder diffraction and DTA-TGA to be physical mixtures of LiAlH_4 and AlH_3 .

We have repeated the work of previous workers⁴⁻¹⁰ in exactly the same manner described in the literature. However, we do not find convincing evidence to indicate the existence of LiAl_2H_7 , $\text{LiAl}_3\text{H}_{10}$, and $\text{LiAl}_4\text{H}_{13}$. The difference in x-ray powder diffraction data and DTA-TGA of the so-called " LiAlH_4 - AlH_3 " complexes reported by previous workers may be due to the isolation of solids with different degrees of solvation than the LiAlH_4 and AlH_3 to which it was compared. In addition we now know that ether cleavage of $\text{AlH}_3 \cdot \text{Et}_2\text{O}$ occurs during the DTA-TGA heating process resulting in the formation of hydridoaluminum alkoxides.

These alkoxides decompose at temperatures different from LiAlH_4 and AlH_3 , possibly giving misleading information that complexes are present.

LITERATURE CITED*

1. E. C. Ashby, J. P. Sanders, P. Claudy, and R. D. Schwartz, Inorg. Chem., **12**, 2860 (1973).
2. E. C. Ashby, J. R. Sanders, P. Claudy, and R. D. Schwartz, J. Amer. Chem. Soc., **95**, 6485 (1973).
3. H. C. Brown and H. M. Yoon, J. Amer. Chem. Soc., **88**, 1464 (1966).
4. J. N. Dymova, et al., Dokl. Akad. Nauk. SSSR, **184**, 1338 (1969).
5. J. Mayet, S. Kovacevic, and J. Tranchant, Bull. Soc., Chim. France, 506 (1973).
6. J. Bousquet, J. Choury, and P. Claudy, Bull. Soc. Chim. France, 3852 (1967).
7. Yu M. Kessler, N. M. Alpatova, and O. R. Osipov, Uspekhi Khim., **33**, 261 (1964).
8. H. Noth, British Patent 820, 513 (1959).
9. P. Kobetz, W. E. Becker, R. Pinkerton, and J. B. Honeycutt, Inorg. Chem., **2**, 859 (1963).
10. N. M. Alpatova, T. N. Dymova, Yu M. Kessler, and O. R. Osipov, Russ. Chem. Rev., **37**, 99 (1968).
11. D. F. Shriver, "The Manipulation of Air Sensitive Compounds," McGraw-Hill, New York, N. Y., 1969.
12. E. C. Ashby and R. D. Schwartz, J. Chem. Ed., **51**, 65 (1974).
13. E. C. Ashby and John J. Watkins, Inorg. Chem., **12**, 2493 (1973).
14. E. C. Ashby and P. Claudy, J. Chem. Ed., in press.

*Journal title abbreviations used are listed in "List of Periodicals," Chemical Abstracts (1961).

PART III

A Study Concerning the Nature of Alkyl-Hydrido Group Exchange

Between Zinc and Aluminum in the Reactions

of $MZn_x(CH_3)_{2x}H$ with Alane and $MAIH_4$

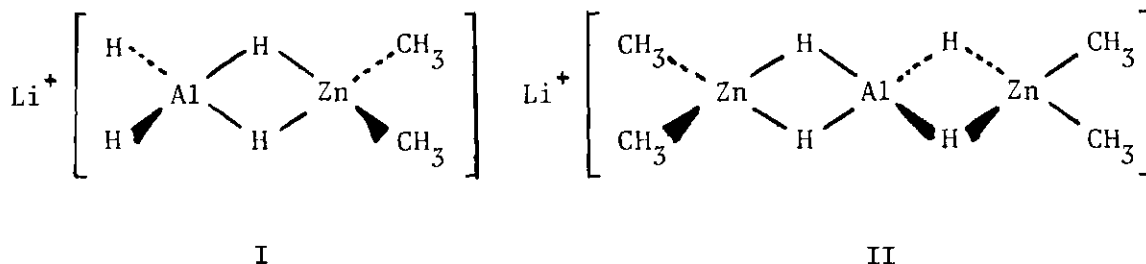
with $(CH_3)_2Zn$ ($M = Li, Na, \text{ or } K$)

CHAPTER I

INTRODUCTION

Recently Ashby and co-workers reported the synthesis of several complex metal hydrides of zinc¹⁻³: Li_3ZnH_5 , Li_2ZnH_4 , LiZnH_3 , Na_2ZnH_4 , NaZnH_3 ,⁴ NaZn_2H_5 , K_2ZnH_4 , KZnH_3 , and KZn_2H_5 . All but two of these complex metal hydrides were prepared by alkyl-hydrido exchange reactions between either LiAlH_4 , NaAlH_4 , or AlH_3 and an ate complex of zinc. Li_3ZnH_5 , Li_2ZnH_4 , and LiZnH_3 were prepared by reacting the ate complexes: $\text{Li}_3\text{Zn}(\text{CH}_3)_5$, $\text{Li}_2\text{Zn}(\text{CH}_3)_4$, and $\text{LiZn}(\text{CH}_3)_3$ with LiAlH_4 in diethyl ether. NaZnH_3 was obtained by the reaction of $\text{NaZn}(\text{CH}_3)_2\text{H}$ with NaAlH_4 in THF, and KZnH_3 was prepared by the analogous reaction of $\text{KZn}(\text{CH}_3)_2\text{H}$ with LiAlH_4 . The reactions of AlH_3 with $\text{NaZn}(\text{CH}_3)_2\text{H}$ and $\text{KZn}(\text{CH}_3)_2\text{H}$ in THF produced NaZn_2H_5 and KZn_2H_5 .

Since the discovery of the use of aluminohydrides in the synthesis of main group complex metal hydrides, this laboratory has been very interested in the nature of exchange reactions between Al-H species and main group alkyl-metal species. The reaction of $\text{LiZn}(\text{CH}_3)_2\text{H}$ with AlH_3 , while it would have been expected to give LiZnH_3 in a manner similar to the above reactions, resulted instead in the formation of the THF soluble complex $\text{LiZn}(\text{CH}_3)_2\text{AlH}_4$. The similar complex $\text{LiZn}_2(\text{CH}_3)_4\text{AlH}_4$ was then prepared by reacting $\text{LiZn}_2(\text{CH}_3)_4\text{H}$ with AlH_3 in THF. These compounds are believed to have the structures represented by I and II, shown on the next page.



In addition to providing a possible route to triple metal hydrides, an indepth study of the formation of these complexes could provide insight into the nature of exchange reactions between aluminohydride compounds and ate complexes of zinc.

The compounds $\text{LiZn}(\text{CH}_3)_2\text{AlH}_4$ and $\text{LiZn}_2(\text{CH}_3)_4\text{AlH}_4$ can also be formed by the reaction of $(\text{CH}_3)_2\text{Zn}$ with LiAlH_4 in THF under a variety of conditions. The fact that the triple metal complex, $\text{LiZn}(\text{CH}_3)_2\text{AlH}_4$, can be prepared by allowing LiAlH_4 to react with $(\text{CH}_3)_2\text{Zn}$ offers the first indication of what could be the intermediate involved in the formation of ZnH_2 from these two reagents in diethyl ether.¹⁶ An infrared spectral study of the reaction between $(\text{CH}_3)_2\text{Zn}$ and LiAlH_4 in THF and diethyl ether does indeed provide evidence that $\text{LiZn}(\text{CH}_3)_2\text{AlH}_4$ is involved.

The soluble complex $\text{LiZn}(\text{CH}_3)_2\text{AlH}_4$ was found to decompose slowly at room temperature to give a black solid with contained Li and Zn in a molar ratio of 1:2. The black solid was identified as a mixture of LiZnH_3 and partially decomposed ZnH_2 . This information would lead one to propose that the complex $\text{LiZn}(\text{CH}_3)_2\text{AlH}_4$ was not actually decomposing, but undergoing a disproportionation reaction to yield LiZn_2H_5 , which then decomposed to LiZnH_3 and ZnH_2 . If this were the case, the $\text{LiZn}(\text{CH}_3)_2\text{AlH}_4$ would be the primary intermediate in the reaction of $\text{LiZn}(\text{CH}_3)_2\text{H}$ with AlH_3 to

give LiZn_2H_5 . Also, then, the reactions of $\text{NaZn}(\text{CH}_3)_2\text{H}$ and $\text{KZn}(\text{CH}_3)_2\text{H}$ with AlH_3 , which yield NaZn_2H_5 and KZn_2H_5 , should proceed via an intermediate similar to $\text{LiZn}(\text{CH}_3)_2\text{AlH}_4$, e.g., $\text{NaZn}(\text{CH}_3)_2\text{AlH}_4$ and $\text{KZn}(\text{CH}_3)_2\text{AlH}_4$. In this connection, an infrared spectral study of these two reactions has been carried out in an effort to provide evidence concerning the existence of these intermediates.

CHAPTER II

EXPERIMENTAL

Apparatus

Reactions were performed under nitrogen using Schlenk tube techniques.⁵ Filtrations and other manipulations were carried out in a glove box equipped with a recirculating system.⁶

Infrared spectra were obtained using a Perkin Elmer 621 Spectrophotometer. Solutions were studied in matched 0.10 mm pathlength NaCl or KBr cells. X-ray powder data were obtained on a Phillips-Norelco x-ray unit with a 114.6 mm camera with nickel filtered CuK_α radiation. Samples were sealed in 0.5 mm capillaries and exposed to x-rays for six hours. d-Spacings were read on a precalibrated scale equipped with viewing apparatus. Intensities were estimated visually. Proton magnetic resonance spectra were obtained on a Varian A-60 spectrometer equipped with a standard variable temperature unit. Ebullioscopic molecular association studies were carried out in THF under vacuum (240 mm Hg abs) using the technique developed by Walker and Ashby.⁷

Analytical

Gas analyses were carried out by hydrolyzing samples with hydrochloric acid on a standard vacuum line equipped with a Toepler pump.⁵ Methane in the presence of hydrogen was determined in a previously described tensimeter.⁵ Alkali metals were determined by flame photometry.

Aluminum was determined by EDTA titration. Zinc in the presence of aluminum was determined by masking the aluminum with triethanolamine and titrating the zinc with EDTA. Zinc in the absence of other metals was determined by EDTA titration.

Materials

Lithium hydride was prepared by hydrogenolysis of *t*-butyllithium at 4000 psi for 24 hours. Dimethylzinc was prepared by the procedure of Noller.⁸ Methyl iodide was obtained from Fisher Scientific. The iodide was dried over anhydrous MgSO_4 and distilled prior to use. Zinc-copper couple was obtained from Alfa Inorganics. The reaction of zinc-copper with methyl iodide was allowed to proceed overnight. The dimethylzinc was distilled from the reaction mixture under nitrogen. Tetrahydrofuran (Fisher Certified Reagent Grade) was distilled under nitrogen over NaAlH_4 . Ultra-pure hydrogen (99.9995%) obtained from the Matheson Corporation was used for hydrogenation experiments. Aluminum hydride was prepared by the reaction of 100% H_2SO_4 with LiAlH_4 in THF. Li_2SO_4 was removed by filtration resulting in a clear and colorless solution of AlH_3 in THF.⁹

Potassium and sodium hydride were obtained from Alfa Inorganics as a slurry in mineral oil. Solutions of lithium and sodium aluminum hydride (Ventron, Metal Hydride Division) were prepared in THF and diethyl ether in the following manner.

LiAlH_4 was obtained as gray, lumpy solids from Ventron, Metal Hydrides Division. Solutions of LiAlH_4 in diethyl ether were prepared by stirring the solid hydride for 24 hours with freshly distilled solvent, followed by filtration, to yield a clear, colorless solution. The solution

of LiAlH_4 in diethyl ether was standardized by aluminum analysis and transferred volumetrically. Diethyl ether was distilled under nitrogen over LiAlH_4 .

Lithium tetramethylaluminate ($\text{LiAl}(\text{CH}_3)_4$) was prepared by the reaction of CH_3Li with $(\text{CH}_3)_3\text{Al}$. Trimethylaluminum was obtained from Texas Alkyls, Inc. and distilled through a 12 inch glass helix packed column at reduced pressure. Methyl lithium was prepared by the reaction of excess lithium metal with $(\text{CH}_3)_2\text{Hg}$ in diethyl ether at -20° . Dimethylmercury was obtained from Org-Met and used without any further purification. Lithium metal was obtained as a 30% dispersion in petrolatum from Alfa-Ventron. The diethyl ether solution of $\text{LiAl}(\text{CH}_3)_4$ was standardized by aluminum analysis.

Procedure

Reaction of AlH_3 with $\text{LiZn}(\text{CH}_3)_2\text{H}$ in Tetrahydrofuran

Five mmoles of dimethylzinc in THF was added to 5 mmoles of lithium hydride slurry in THF. This mixture was stirred until all the lithium hydride dissolved, then 5 mmoles of AlH_3 in THF was added. After one hour of stirring, an infrared spectrum, NMR spectrum and ebullioscopic molecular weight were obtained on the clear solution. The infrared spectrum is shown in Figure 1(d) in addition to the spectrum of $(\text{CH}_3)_2\text{Zn}$, AlH_3 , and $\text{LiZn}(\text{CH}_3)_2\text{H}$ in THF. The infrared spectrum of the solution does not correspond to a mixture of AlH_3 and $\text{LiZn}(\text{CH}_3)_2\text{H}$. The NMR spectrum in the region upfield from TMS is shown in Figure 4. The molecular weight measurement gave an i -value of one in the concentration range 0.06-0.18 M when based on aluminum concentration.

Infrared spectra were run on a 0.18 M solution obtained from the reaction of $\text{LiZn}(\text{CH}_3)_2\text{H}$ with AlH_3 at time periods of 1 hour, 5 hours, 24 hours, 2 days, 4 days, 7 days, 2 weeks, and 3 weeks after the initial mixing of the reactants. In every case the infrared spectrum of the supernatant solution was the same as that shown in Figure 1(d), except the spectra became less intense with time. After the first four hours a black solid began to precipitate and continued to do so during the remainder of the three week period. At the end of this time period, the supernatant solution contained a little less than one half of the starting zinc (2.47 mmoles of the starting 5 mmoles of zinc). The black solid was separated by filtration, washed with THF, and dried under vacuum overnight at room temperature. Analysis revealed that it contained Li, Zn, H, and Al in the molar ratio of 1.06:2.00:1.93:0.07. An x-ray powder diffraction pattern of the solid contained lines due to LiZnH_3 and Zn metal only.

In a separate experiment, $\text{LiZn}(\text{CH}_3)_2\text{H}$ and AlH_3 were allowed to react at room temperature for one week and at a concentration of 0.18 M. At the end of this time, a black solid had formed and was separated by filtration, washed with THF, and dried under vacuum. Analysis of the black solid indicated a Li:Zn:H:Al molar ratio of 1.04:2.00:3.28:0.04. An x-ray powder diffraction pattern of the solid contained lines due to LiZnH_3 and Zn metal only.

In another experiment, $\text{LiZn}(\text{CH}_3)_2\text{H}$ and AlH_3 were allowed to react at a concentration of 0.02 M. This reaction produced instead of a clear solution a white solid. The solid was separated by filtration, washed with THF, and dried under vacuum. Analysis of the solid indicated Li:Zn:H:Al molar ratios of 0.01:1.00:1.98:0.03. An x-ray powder diffraction

pattern showed the solid to be ZnH_2 .

Attempts were made to obtain the compound formed by reacting $\text{LiZn}(\text{CH}_3)_2\text{H}$ with AlH_3 as a solid by stripping off the THF solvent at room temperature because of our interest in obtaining x-ray powder diffraction and DTA-TGA analysis on this material. However, these attempts always gave a black, gummy material which was unsuitable for use. An attempt was made to separate the compound as a solid by crystallization at reduced temperature but no crystals formed. The solution of this compound in THF stayed clear and did not precipitate any black solid for indefinite periods of time when cooled to Dry Ice-acetone temperature. An attempt to obtain the solid compound by stripping THF from solution at reduced temperatures resulted in a gum which turned black on warming to room temperature.

Reaction of AlH_3 with $\text{LiZn}_2(\text{CH}_3)_4\text{H}$ in THF

Dimethylzinc in THF (8.35 mmol) was added to 4.17 mmol of LiH slurried in THF. A clear solution resulted to which was added 4.17 mmol of AlH_3 in THF. The mixture remained clear even after one hour stirring. An infrared spectrum, NMR spectrum, and ebullioscopic molecular weight were obtained on the solution. The infrared spectrum is shown in Figure 2(d) along with the infrared spectrum of $(\text{CH}_3)_2\text{Zn}$, AlH_3 , and $\text{LiZn}_2(\text{CH}_3)_4\text{H}$ in THF. The infrared spectrum of the solution does not correspond to a mixture of AlH_3 and $\text{LiZn}_2(\text{CH}_3)_4\text{H}$. The NMR spectrum is shown in Figure 4. The molecular weight measurement gave an i -value of one in the concentration range 0.04-0.12 M when based on aluminum concentration.

The solution obtained from the reaction of $\text{LiZn}_2(\text{CH}_3)_4\text{H}$ with AlH_3 stood overnight before any black solid was observed. Attempts to obtain

a solid sample of soluble product from this reaction failed.

Reaction of AlH_3 with $\text{LiZn}(\text{CH}_3)_2\text{AlH}_4$ in THF

Dimethylzinc in THF (5 mmol) was added to 5 mmol of LiH slurried in THF. A clear solution resulted to which was added 5 mmol of AlH_3 in THF. The resulting solution, which was 0.18 M in $\text{LiZn}(\text{CH}_3)_2\text{AlH}_4$, was stirred for one hour, then 5 mmol more of AlH_3 was added. A white precipitate appeared immediately. The solid was slurried for one hour then separated by filtration, washed with THF, and dried under vacuum. Analysis of the solid indicated Li:Zn:H:Al molar ratios of 0.03:1.00:2.04:0.00. An x-ray powder diffraction pattern and vacuum DTA-TGA showed the solid to be ZnH_2 . The filtrate contained 4% of the starting zinc and Li, Al, Zn, CH_3 , and H in the molar ratio of 1.00:1.91:0.03:1.96:4.89. An infrared spectrum of the filtrate (bands in the metal-hydrogen stretching region at 1745 and 1693 cm^{-1}) indicated the presence of $(\text{CH}_3)_2\text{AlH}$ and LiAlH_4 .

Reaction of AlH_3 with $\text{LiZn}_2(\text{CH}_3)_4\text{AlH}_4$ in THF

Dimethylzinc in THF (8.35 mmol) was added to 4.18 mmol of LiH slurried in THF. A clear solution resulted to which was added 4.17 mmol of AlH_3 in THF. The resulting solution which was 0.12 M in $\text{LiZn}_2(\text{CH}_3)_4\text{AlH}_4$, was stirred for one hour, then 4.17 mmol more of AlH_3 was added. A white precipitate appeared immediately. The solid was slurried for one hour, then separated by filtration, washed with THF, and dried under vacuum. Analysis of the solid indicated a Li:Zn:H:Al molar ratio of 0.02:1.00:2.08:0.06. An x-ray powder diffraction pattern showed the solid to be ZnH_2 . The filtrate contained 5% of the starting zinc and Li, Al, Zn,

CH_3 , and H in the molar ratio of 1.00:1.93:0.10:3.93:1.99. An infrared spectrum of the filtrate (bands in the terminal Al-H stretching region at 1747 and 1660 cm^{-1}) indicated the presence of $(\text{CH}_3)_2\text{AlH}$ and $\text{LiAl}(\text{CH}_3)_2\text{H}_2$.

Reaction of LiAlH_4 with $\text{LiZn}(\text{CH}_3)_2\text{AlH}_4$ in THF

Dimethylzinc in THF (5 mmoles) was added to 5 mmoles of LiH slurried in THF. A clear solution resulted to which was added 5 mmoles of AlH_3 in THF. The resulting solution was stirred for one hour, then 5 mmoles of LiAlH_4 in THF was added. The solution still remained clear. It was stirred for two hours and an infrared spectrum run on the solution. The spectrum corresponded to a mixture of LiAlH_4 and $\text{LiZn}(\text{CH}_3)_2\text{AlH}_4$.

Reactions of LiAlH_4 with $\text{LiZn}_2(\text{CH}_3)_4\text{AlH}_4$ in THF

A solution of $\text{LiZn}_2(\text{CH}_3)_4\text{AlH}_4$ (2.5 mmoles) was prepared as described above, then 5 mmoles of LiAlH_4 in THF was added. The solution which remained clear, was stirred for two hours and the infrared spectrum recorded. The spectrum corresponded to a mixture of LiAlH_4 and $\text{LiZn}_2(\text{CH}_3)_4\text{AlH}_4$.

Reactions of LiAlH_4 with $(\text{CH}_3)_2\text{Zn}$ in THF at Molar Ratios of 1:1, 2:3, and 1:2

In three separate reactions, 10 mmoles, 7.5 mmoles, and 5 mmoles of a 0.386 M solution of LiAlH_4 in THF were added to 10 mmoles of a 0.820 M solution of $(\text{CH}_3)_2\text{Zn}$ in THF. In each case, the resulting clear solution was stirred for about 15 minutes, then a small sample was subjected to infrared analysis. The resulting infrared spectra, in addition to the spectra of $(\text{CH}_3)_2\text{Zn}$, LiAlH_4 , $\text{LiZn}(\text{CH}_3)_2\text{AlH}_4$, and $\text{LiZn}_2(\text{CH}_3)_4\text{AlH}_4$, are shown in Figure 5. Table 3 contains a listing of the infrared bands observed for the spectra given in this figure. NMR spectra and ebullio-

scopic molecular association studies were run on the 1:1 and 1:2 mixtures of LiAlH_4 and $(\text{CH}_3)_2\text{Zn}$. Analysis of these solutions indicated the presence of Li, Al, CH_3 , H, and Zn in 1.03:1.00:1.91:3.96:0.98 ratio for the 1:1 mixture and 0.98:1.00:4.02:3.91:2.02 ratio for the 1:2 mixture.

In a separate experiment, 10 mmoles of 0.386 M LiAlH_4 in THF was added to 10 mmoles of 0.820 M $\text{Zn}(\text{CH}_3)_2$ in THF. The resulting clear solution was divided into two portions. One was set aside to stand for one week at room temperature. The other was diluted twentyfold immediately with THF. Within five minutes a white precipitate began to form in the diluted solution (ca. 0.01 M). The initial concentrated solutions remained clear for almost three hours before any black solid began to precipitate. Infrared spectra of both the concentrated and diluted solutions (or supernatants if a solid is present) were recorded after 15 minutes, 30 minutes, 2 hours, 4 hours, 1 day, 3 days, and 1 week. In each case the infrared spectra corresponded to the spectrum of $\text{LiZn}(\text{CH}_3)_2\text{AlH}_4$. The white solid that formed after the 0.253 M solution of $\text{LiZn}(\text{CH}_3)_2\text{AlH}_4$ had been diluted was found to be ZnH_2 . The solids in both the concentrated and dilute samples had turned black after sitting a week at room temperature under THF. In each case the solids were separated by filtration, washed with THF, and dried under vacuum at room temperature. The solid from the more concentrated solution of $\text{LiZn}(\text{CH}_3)_2\text{AlH}_4$ exhibited Li:Zn:H:Al in molar ratios of 1.06:2.00:3.20:0.05 and contained 22.4% of the starting zinc. (The remainder of the zinc was in the supernatant.) An x-ray powder pattern of this solid revealed that it contained LiZnH_3 and Zn metal only. The solid from the more dilute solution of $\text{LiZn}(\text{CH}_3)_2\text{AlH}_4$ was found to exhibit Li:Zn:H:Al in molar ratios of 0.04:1.00:1.42:0.05

and contained 48.2% of the starting zinc. An x-ray powder pattern of this solid revealed that it contained ZnH_2 and Zn metal.

In another, separate experiment, 10 mmoles of 0.820 M $(\text{CH}_3)_2\text{Zn}$ in THF was added to 724 ml of freshly distilled THF, then 10 mmoles of 0.386 M LiAlH_4 in THF was added. The mixture was stirred for 30 seconds, then an infrared spectrum was obtained on the solution while it was still clear. This infrared spectrum was the same as that of $\text{LiZn}(\text{CH}_3)_2\text{AlH}_4$. Within five minutes after the LiAlH_4 had been added to the $(\text{CH}_3)_2\text{Zn}$, a white solid began to form. This white solid was found to be ZnH_2 . When the reaction mixture was allowed to stand at room temperature for one week, the white solid turned black. An infrared spectrum of the supernatant remaining at this point showed that $\text{LiZn}(\text{CH}_3)_2\text{AlH}_4$ was still present. An analysis of the black solid revealed that it contained Li:Zn:H:Al in molar ratios of 0.06:1.00:1.31:0.05. A little less than half of the initial zinc added (46.4%) was found in the black solid. An x-ray powder pattern of the solid revealed that it contained ZnH_2 and Zn metal.

Reactions of $(\text{CH}_3)_2\text{Zn}$ with LiAlH_4 in THF at Molar Ratios of 1:1, 3:2, and 2:1

In three separate reactions, 10 mmoles, 15 mmoles, and 20 mmoles of 0.820 M solution of $(\text{CH}_3)_2\text{Zn}$ in THF were added to 10 mmoles of a 0.386 M solution of LiAlH_4 in THF. In each case, the resulting clear solution was stirred for about 15 minutes, followed by infrared analysis (Figure 6). Table 3 contains a listing of the infrared bands observed for the spectra given in this figure. On standing in THF at room temperature and on dilution with THF, the mixture obtained on adding $(\text{CH}_3)_2\text{Zn}$ to LiAlH_4 in 1:1

ratio behaved in the same way as described earlier for the mixture obtained on adding LiAlH_4 to $(\text{CH}_3)_2\text{Zn}$.

Infrared Spectral Study of the Reaction of LiAlH_4 with $(\text{CH}_3)_2\text{Zn}$ in Diethyl Ether

A 1.16 M solution of LiAlH_4 in diethyl ether was placed in a two-neck round-bottom flask fitted with a condenser and a three-way stopcock. Increments of 0.83 M solution of $(\text{CH}_3)_2\text{Zn}$ in diethyl ether were added via syringe under nitrogen to the magnetically stirred LiAlH_4 solution. After each addition, the solution was stirred for five minutes at room temperature, then the stirring was stopped in order to allow the precipitate to settle. Infrared spectra were obtained by withdrawing samples of the supernatant solution by syringe under nitrogen. The additions were continued until the ratio of $(\text{CH}_3)_2\text{Zn}$ to the original LiAlH_4 was 2:1. The infrared spectra obtained in this way are shown in Figure 11.

In a similar manner a 1.16 M solution of LiAlH_4 in diethyl ether was added in increments to a 0.83 M solution of $(\text{CH}_3)_2\text{Zn}$. The infrared spectra obtained from this study are shown in Figure 12.

Redistribution of LiAlH_4 and $\text{LiAl}(\text{CH}_3)_4$

Reactions between LiAlH_4 and $\text{LiAl}(\text{CH}_3)_4$ were performed by mixing standard solutions of the reagents in ratios appropriate to produce $\text{LiAl}(\text{CH}_3)_3\text{H}$, $\text{LiAl}(\text{CH}_3)_2\text{H}_2$, and $\text{LiAl}(\text{CH}_3)\text{H}_3$. After stirring for one hour at room temperature, infrared spectra were obtained on the resulting solution.

Reactions where $(\text{CH}_3)_2\text{Zn}$ Is Added to LiAlH_4 in Diethyl Ether

2.0 LiAlH_4 - 1.0 $(\text{CH}_3)_2\text{Zn}$. A diethyl ether solution of $(\text{CH}_3)_2\text{Zn}$

(0.83 M) was added dropwise by syringe (under nitrogen flush) to a magnetically stirred 1.16 M solution of LiAlH_4 in diethyl ether until the ratio of reactants was 1.0:2.0 ($(\text{CH}_3)_2\text{Zn}:\text{LiAlH}_4$). A white precipitate formed immediately. After stirring for one hour at room temperature, the mixture was filtered. The resulting solid was washed with diethyl ether and dried under vacuum at room temperature. Analysis of the solid showed it to contain Li, Zn, H, and Al in molar ratios of 0.02:1.00:2.04:0.03 and all the starting zinc. An x-ray powder diffraction pattern of the solid showed it to be zinc hydride. Analysis of the filtrate showed it to contain Li, Al, CH_3 , H, and Zn in molar ratios of 1.04:1.00:0.98:3.11:0.00.

1.0 LiAlH_4 - 1.0 $(\text{CH}_3)_2\text{Zn}$. This reaction was performed in a manner identical with that above. The precipitate, after isolating and drying, was found to contain Li, Zn, H, and Al in molar ratios of 0.04:1.00:2.03:0.03 and 98.2% of the starting zinc. An x-ray powder diffraction pattern showed the solid to be ZnH_2 . The filtrate contained Li, Al, CH_3 , H, and Zn in molar ratios of 1.01:1.00:2.01:1.99:0.02.

0.67 LiAlH_4 - 1.0 $(\text{CH}_3)_2\text{Zn}$. In this reaction 95.7% of the starting zinc was recovered in the precipitate which contained Li, Zn, H, and Al in molar ratios of 0.01:1.00:2.08:0.02. An x-ray powder diffraction pattern showed the solid to be ZnH_2 . The filtrate contained Li, Al, CH_3 , H, and Zn in molar ratios of 1.03:1.00:2.97:0.96:0.04.

0.50 LiAlH_4 - 1.0 $(\text{CH}_3)_2\text{Zn}$. In this reaction 97.4% of the starting zinc was recovered in the precipitate which contained Li, Zn, H, and Al in molar ratios of 0.03:1.00:2.05:0.02. An x-ray powder diffraction pattern showed the solid to be ZnH_2 . The filtrate contained Li, Al, CH_3 ,

H, and Zn in molar ratios of 1.04:1.00:3.98:0.00:0.03.

Reactions where LiAlH_4 Is Added to $(\text{CH}_3)_2\text{Zn}$ in Diethyl Ether

0.50 LiAlH_4 - 1.0 $(\text{CH}_3)_2\text{Zn}$. A diethyl ether solution of LiAlH_4 (1.16 M) was added dropwise by syringe (under nitrogen flush) to a magnetically stirred solution of 0.83 M $(\text{CH}_3)_2\text{Zn}$ in diethyl ether until the ratio of reactants was 1.0:2.0 ($\text{LiAlH}_4:(\text{CH}_3)_2\text{Zn}$). The clear solution was stirred for one hour, but still no precipitate was visible. An analysis of the solution showed it to contain Li, Zn, Al, CH_3 , and H in molar ratios of 1.02:2.00:0.99:3.98:4.02. The infrared spectrum of the solution (Figure 13-1 was the same as that shown in Figure 12-2 taken after five minutes stirring).

1.0 LiAlH_4 - 1.0 $(\text{CH}_3)_2\text{Zn}$. This reaction was performed in a manner identical with that above. This time a white precipitate formed. After stirring for one hour at room temperature, the mixture was filtered. The resulting solid was washed with diethyl ether and dried under vacuum at room temperature. An analysis of the solid showed it to contain Li, Zn, H, and Al in molar ratios of 0.62:2.00:4.63:0.00 and 97.1% of the starting zinc. An x-ray powder diffraction pattern of the solid showed it to be a mixture of LiZnH_3 and ZnH_2 . An analysis of the filtrate showed it to contain Li, Al, CH_3 , H, and Zn in molar ratios of 0.69:1.00:1.98:1.70:0.03. The infrared spectrum of this solution is shown in Figure 13-2.

2.0 LiAlH_4 - 1.0 $(\text{CH}_3)_2\text{Zn}$. In this reaction all of the starting zinc was recovered in the precipitate which contained Li, Zn, H, and Al in molar ratios of 0.01:1.00:2.02:0.00. An x-ray powder diffraction pattern showed the solid to be ZnH_2 . An analysis of the filtrate showed it to contain Li, Al, CH_3 , H, and Zn in molar ratios of 1.01:1.00:1.03:3.04:

0.00. The infrared spectrum of this solution is shown in Figure 13-3.

Reaction of $\text{LiZn}(\text{CH}_3)_2\text{AlH}_4$ with LiAlH_4 in Diethyl Ether

A 1.16 M solution of LiAlH_4 (10 mmoles) was added with stirring to a 0.83 M solution of $(\text{CH}_3)_2\text{Zn}$ (10 mmoles) in diethyl ether. A clear solution resulted, but after 30 seconds of stirring a white precipitate began to form. The mixture was stirred for five minutes, then the stirring was stopped, and the small amount of solid that was present was allowed to settle for one minute. A sample of the supernatant solution gave an infrared spectrum similar to that shown in Figure 12-4. Analysis of this sample showed that Zn and Al were present in a 0.91:1.00 ratio.

As soon as the sample had been taken, 10 mmoles of 1.16 M LiAlH_4 was added to the mixture with stirring. There was an immediate formation of more solid. After stirring for five minutes at room temperature, the mixture was filtered. The resulting solid was washed with diethyl ether and dried under vacuum at room temperature. An analysis of the solid showed that it contained Li, Zn, H, and Al in molar ratios of 0.03:1.00:2.01:0.00 and all of the starting zinc. An x-ray powder diffraction pattern of the solid showed it to be essentially ZnH_2 . The filtrate contained Li, Al, CH_3 , H, and Zn in molar ratios of 1.02:1.00:1.03:3.05:0.00. The infrared spectrum showed $\text{LiAl}(\text{CH}_3)\text{H}_3$ to be present.

Reaction where LiAlH_4 Is Added to a Dilute Solution of $(\text{CH}_3)_2\text{Zn}$ in 1:1 Ratio

A 0.83 M solution of $(\text{CH}_3)_2\text{Zn}$ (5 mmoles) in diethyl ether was added to 100 ml of diethyl ether. A 1.16 M solution of LiAlH_4 (5 mmoles) was added dropwise by syringe (under nitrogen flush) to the above solution

while stirring. A white precipitate formed. After stirring for one hour at room temperature, the mixture was filtered. The resulting solid was washed with diethyl ether and dried under vacuum at room temperature. An analysis of the solid showed that it contained Li, Zn, H, and Al in molar ratios of 0.03:1.00:2.03:0.00 and 98.3% of the starting zinc. An x-ray powder diffraction pattern showed the solid to be ZnH_2 . An analysis of the filtrate showed it to contain Li, Al, CH_3 , H, and Zn in molar ratios of 1.01:1.00:1.93:2.01:0.02. An infrared spectrum of the concentrated solution showed $\text{LiAl}(\text{CH}_3)_2\text{H}_2$ to be present.

Reaction of $\text{NaZn}(\text{CH}_3)_2\text{H}$ with AlH_3 in THF

AlH_3 Added to 0.45 M $\text{NaZn}(\text{CH}_3)_2\text{H}$. Five mmoles of 0.820 M solution of $(\text{CH}_3)_2\text{Zn}$ in THF was added to 5 mmoles of a 1.00 M slurry of NaH in THF. A clear solution of $\text{NaZn}(\text{CH}_3)_2\text{H}$ formed. Next 5 mmoles of a 0.332 M solution of AlH_3 was added. An off white precipitate appeared immediately. Infrared spectra were obtained on the $(\text{CH}_3)_2\text{Zn}$ solution, the $\text{NaZn}(\text{CH}_3)_2\text{H}$ solution, and the supernatant left after five minutes and 24 hours. The infrared spectra are shown in Figure 14. After sitting one day the precipitate was filtered, washed with THF, and dried at room temperature under vacuum. The ratio of Na:Zn:H in the solid was 1.02:2.00:4.86 and it contained all the starting zinc. An x-ray powder diffraction pattern showed the solid to be NaZn_2H_5 . The filtrate contained Na, Al, CH_3 , H, and Zn in molar ratios of 1.03:2.00:3.89:3.08:0.061. An infrared spectrum of the filtrate showed a broad band in the Al-H stretching region centered at 1625 cm^{-1} . Dimethylalane absorbs at 1720 cm^{-1} in THF; thus the filtrate was not a mixture of $\text{NaAl}(\text{CH}_3)_2\text{H}_2$ and $(\text{CH}_3)_2\text{AlH}$.

AlH₃ Added to 0.01 M NaZn(CH₃)₂H. The reaction was performed in a manner identical with that above except the NaZn(CH₃)₂H solution was diluted to 0.01 M before the addition of AlH₃. After this addition the clear solution remained for about three hours, then a white precipitate began to form. The mixture was stirred overnight, then the precipitate was filtered, washed, and dried. The solid which was gray at this point contained Na, Zn, H, and Al in molar ratios of 0.02:1.00:1.86:0.01 and 51.8% of the starting zinc. (Repeating the reaction for longer periods of time did not produce any more solid.) An x-ray powder diffraction pattern of the solid showed it to be essentially ZnH₂.

Reaction of NaZn₂(CH₃)₄H with AlH₃ in Tetrahydrofuran

Ten mmoles of a 0.820 M solution of (CH₃)₂Zn in THF was added to 5 mmoles of NaH slurried in THF, followed by 5 mmoles of a 0.557 M solution of AlH₃ in THF. A clear solution resulted which was believed to be NaZn₂(CH₃)₄AlH₄. An analysis of the solution indicated that Na, Al, CH₃, H, and Zn were present in ratios of 1.00:1.00:3.84:3.91:0.98. Infrared spectra were obtained on the NaZn₂(CH₃)₄H solution and the adduct between NaZn₂(CH₃)₄H and AlH₃. These spectra are shown in Figure 15. Five mmoles of AlH₃ was then added to the NaZn₂(CH₃)₄AlH₄ solution. A white precipitate formed immediately. This mixture was stirred about one hour, then filtered, and the precipitate washed and dried. The solid contained Na, Zn, H, and Al in a ratio of 0.00:1.00:2.01:0.00 and all the starting zinc. An x-ray powder diffraction pattern of the solid showed it to be ZnH₂. The filtrate corresponded to NaAl₂(CH₃)₄H₃ by infrared spectra and analysis (ratio Na:Al:CH₃:H:Zn was 1.01:2.00:3.88:3.11:0.00).

Infrared Study of the Reaction of NaAlH_4 with $(\text{CH}_3)_2\text{Zn}$ in THF

A 0.82 M solution of $(\text{CH}_3)_2\text{Zn}$ in THF was placed in a round-bottom flask fitted with a three-way stopcock. A 0.813 M solution of NaAlH_4 was added in increments by syringe under nitrogen flush to the magnetically stirred $(\text{CH}_3)_2\text{Zn}$ solution. After each addition, the solution was stirred for 15 minutes at room temperature; the infrared spectrum was obtained on the resulting solution. The addition of NaAlH_4 was made in three increments such that after each addition the ratio of total zinc to aluminum was 2:1, 4:3, and 1:1. The resulting infrared spectra are shown in Figure 16. Clear solutions were present after the first two additions, but the third addition caused the formation of a precipitate.

In like manner, a 0.82 M solution of $(\text{CH}_3)_2\text{Zn}$ in THF was added in two increments to a solution of 0.813 M NaAlH_4 . The resulting infrared spectra are shown in Figure 17. The two increments were made such that the ratio of total zinc to aluminum would be 1:1 and 2:1. After the first addition, a precipitate formed, but upon the second addition, the entire precipitate redissolved and a clear solution resulted.

Reaction of NaAlH_4 with $(\text{CH}_3)_2\text{Zn}$ in a 1:1 Molar Ratio

Ten mmols of a 0.921 M solution of $(\text{CH}_3)_2\text{Zn}$ in THF was added to 10 mmols of a 0.813 M solution of NaAlH_4 in THF. Initially a white precipitate appeared, but it quickly disappeared and an off-white precipitate formed. Infrared spectra were obtained on the supernatant solution 5 minutes, 2.5 hours, 28 hours, 4 days, and 7 days after the initial addition. The infrared spectra are shown in Figure 18.

In a separate experiment, 10 mmols of $(\text{CH}_3)_2\text{Zn}$ was added to 10 mmols of NaAlH_4 in THF. The resulting solution was stirred for about

three hours and filtered. The solid contained Na, Zn, and H in a molar ratio of 1.00:2.00:4.87 and about 31.0% of the starting zinc. An x-ray powder diffraction pattern showed the solid to be NaZn_2H_5 . The molar ratio of Na:Al:Zn in the filtrate was 1.75:2.00:1.38.

In another separate experiment, $(\text{CH}_3)_2\text{Zn}$ and NaAlH_4 were allowed to react in a 1:1 molar ratio. After stirring for nine days, the mixture was filtered. An x-ray powder diffraction pattern of the resulting solid showed NaZn_2H_5 and zinc metal to be present. An analysis of the filtrate showed the presence of Na, Al, CH_3 , H, and Zn in ratios of 1.01:2.00:3.99:2.82:0.00. An infrared spectrum showed bands corresponding to $\text{NaAl}_2(\text{CH}_3)_4\text{H}_3$.

Reaction of AlH_3 with $(\text{CH}_3)_2\text{Zn}$ in THF

Five mmols of a 0.820 M solution of $(\text{CH}_3)_2\text{Zn}$ in THF was added to 5 mmols of a 0.555 M solution of AlH_3 in THF. A white precipitate formed immediately. The mixture was stirred about one hour and filtered. The ratio of Zn:H in the solid was 1.00:2.03 and an x-ray powder pattern showed it to be ZnH_2 . No zinc remained in the filtrate. An infrared spectrum of the filtrate showed it to be $\text{Al}(\text{CH}_3)_2\text{H}$.

Reaction of ZnH_2 with $\text{NaAl}(\text{CH}_3)_2\text{H}_2$ in THF

Zinc hydride (2.5 mmols) slurried in THF was added to 2.5 mmols of $\text{NaAl}(\text{CH}_3)_2\text{H}_2$ in THF. All the ZnH_2 dissolved in less than a minute and a clear solution formed. An infrared spectrum was obtained on this clear solution and it corresponded to $\text{NaZn}(\text{CH}_3)_2\text{AlH}_4$. After about 20 minutes an off-white precipitate began to appear. This mixture was stirred for a day and filtered. The solid contained Na:Zn:H in a molar ratio of 1.06:2.00:4.81 and an x-ray powder pattern showed it to be NaZn_2H_5 . The fil-

trate was allowed to stand another week. After this time more solid appeared. The mixture was refiltered. The molar ratio of Na:Zn in the solid was 1.05:2.00. The molar ratio of Na:Al:Zn in the filtrate was now 1.03:2.00:0.17. An infrared spectrum of the filtrate corresponded to $\text{NaAl}_2(\text{CH}_3)_4\text{H}_3$.

Preparation of KAlH_4

Ten mmoles of KH slurried in THF were added to 10 mmoles of a 0.1025 M solution of AlH_3 in THF. The mixture was stirred for a few days, then a sample of the solid isolated and analyzed. The molar ratio of K:Al:H in the solid was 1.03:1.00:3.91. The KAlH_4 was stored under THF and used as a slurry.

Reaction of $\text{KZn}(\text{CH}_3)_2\text{H}$ with AlH_3 in THF

Five mmoles of KH slurried in THF was added to 5 mmoles of $(\text{CH}_3)_2\text{Zn}$ in THF. An infrared spectrum was obtained on the solution formed. Next 5 mmoles of a 0.1025 M solution of AlH_3 in THF was added to the solution of $\text{KZn}(\text{CH}_3)_2\text{H}$. As quickly as possible an infrared spectrum was obtained on the supernatant hoping to see the spectrum of the intermediate which leads to the products KZn_2H_5 and $\text{KAl}_2(\text{CH}_3)_4\text{H}_3$. The spectra are shown in Figure 19.

Reaction of KAlH_4 with $(\text{CH}_3)_2\text{Zn}$ in THF in 1:1 Molar Ratio

A 0.921 M solution of $(\text{CH}_3)_2\text{Zn}$ (2.5 mmoles) in THF was added to 2.5 mmoles of KAlH_4 slurried in THF. The mixture was stirred for 30 minutes during which time a solid remained throughout. After this period of time, an infrared spectrum was obtained on the supernatant solution. The spectrum is shown in Figure 19. After two additional hours the mixture was filtered and the solid was found to contain K:Zn:H in a molar

ratio of 0.99:2.00:4.92. The x-ray powder diffraction pattern of the solid showed it to be KZn_2H_5 . The ratio of K:Al:Zn in the filtrate was 1.01:2.00:0.00.

Reaction of KAlH_4 with $(\text{CH}_3)_2\text{Zn}$ in THF in a 1:2 Molar Ratio

Five mmoles of a 0.921 M solution of $(\text{CH}_3)_2\text{Zn}$ in THF was added to 2.5 mmoles of KAlH_4 slurried in THF. A clear solution formed within seconds. As quickly as possible an infrared spectrum was obtained on this solution. After 10 minutes a white solid began to appear. The mixture was stirred for four hours and then filtered. The solid contained K:Zn:H in a molar ratio of 1.02:2.00:4.87. An x-ray powder diffraction pattern of the solid showed it to be KZn_2H_5 . The molar ratio of K:Zn:Al in the filtrate was 1.01:2.00:5.09. An infrared spectrum obtained on the filtrate is shown in Figure 20.

Reaction of $\text{KZn}_2(\text{CH}_3)_4\text{H}$ with AlH_3 in THF at Molar Ratios of 2:1, 1:1, and 1:2

Potassium hydride (2.5 mmoles) slurried in THF was added to 5 mmoles of a 0.921 M solution of $(\text{CH}_3)_2\text{Zn}$ in THF. After the solution turned clear, marking the formation of $\text{KZn}_2(\text{CH}_3)_4\text{H}$, 1.25 mmoles of 0.1025 M solution of AlH_3 in THF was added. The resulting clear solution was stirred 15 minutes then an infrared spectrum was obtained. Another 1.25 mmoles of 0.1025 M solution of AlH_3 in THF was then added to this solution which still was clear. A white precipitate began forming immediately. An infrared spectrum was obtained on the supernatant solution. Next, another 2.5 mmoles of AlH_3 was added. The mixture was stirred 15 minutes, then another infrared spectrum obtained, and finally the mixture was filtered. The solid contained K:Zn:H in a molar ratio of 1.02:2.00:4.85, and

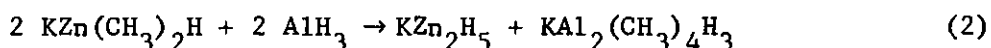
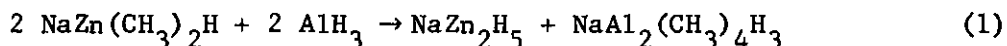
an x-ray powder diffraction pattern showed it to be KZn_2H_5 . The infrared spectrum showed the filtrate to be $(\text{CH}_3)_2\text{AlH}$. All spectra are shown in Figure 20.

In a separate experiment, 2.5 mmoles of AlH_3 in THF was added to 2.5 mmoles of $\text{KZn}_2(\text{CH}_3)_4\text{H}$ in THF. The resulting slurry was stirred for four hours then filtered. The solid contained K:Zn:H in a molar ratio of 1.06:2.00:4.91. An x-ray powder diffraction pattern showed the solid to be KZn_2H_5 . The molar ratio of K:Zn:Al in the filtrate was 1.02:2.00:5.05.

CHAPTER III

RESULTS AND DISCUSSION

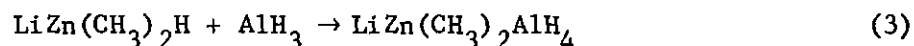
When AlH_3 was allowed to react with $\text{NaZn}(\text{CH}_3)_2\text{H}$ and $\text{KZn}(\text{CH}_3)_2\text{H}$ in THF, the insoluble complex metal hydrides, NaZn_2H_5 and KZn_2H_5 , were formed according to Eq. 1 and 2. On the other hand, the reaction of AlH_3 with



$\text{LiZn}(\text{CH}_3)_2\text{H}$ did not yield a precipitate but only a clear solution. This behavior indicates that LiZn_2H_5 was not formed since this compound would be expected to be insoluble in THF. (The compounds KZn_2H_5 and NaZn_2H_5 as well as Li_2ZnH_4 and LiZnH_3 were all found to be insoluble in THF.^{1,3}) Information concerning the nature of the species present in solution can be obtained by examining the infrared spectrum, NMR spectrum, and colligative properties of the reaction solution.

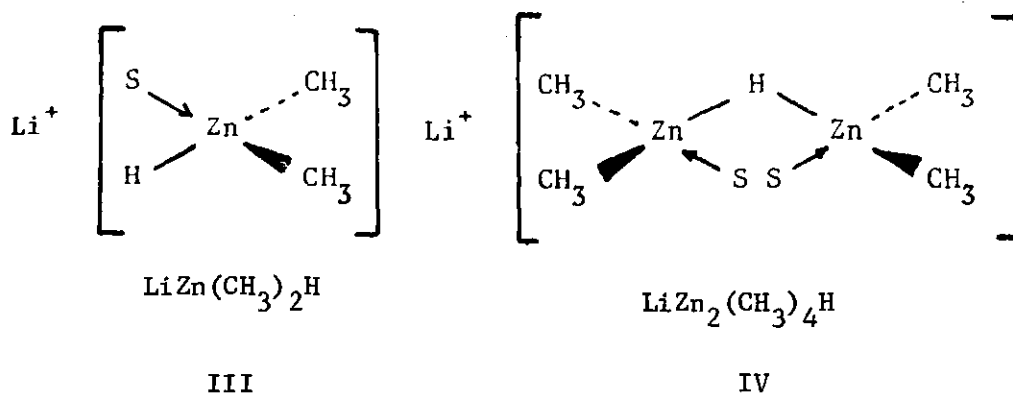
Ebullioscopic molecular weight measurements on the solution from the reaction of $\text{LiZn}(\text{CH}_3)_2\text{H}$ with AlH_3 over a concentration range of 0.06-0.18 M (based on aluminum) yielded *i*-values ranging from 1.01-1.08. Glpc analysis of hydrolyzed samples both before and after the molecular weight experiment showed the absence of any THF cleavage products. An analysis of the reaction mixture showed Li, Zn, Al, CH_3 , and H to be present in

1.05:1.00:0.98:2.11:3.99 molar ratios. Since the i-value is based on the concentration of aluminum in the solution, a singular compound of the stoichiometry $\text{LiZn}(\text{CH}_3)_2\text{AlH}_4$ is indicated.



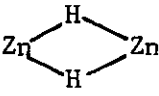
The infrared spectrum of the reaction mixture (Table 1 and Figure 1(d)) contains two strong broad bands in the metal hydrogen stretching region, one at 1660 cm^{-1} and the other at 1400 cm^{-1} . The fact that these bands are shifted to 1180 cm^{-1} and 1015 cm^{-1} in the infrared spectrum of $\text{LiZn}(\text{CH}_3)_2\text{AlD}_4$ (prepared from $\text{LiZn}(\text{CH}_3)_2\text{D}$ and AlD_3) shows that they actually are due to metal hydrogen stretching modes.

Shriver and co-workers¹⁰ have suggested structures III and IV for



$\text{LiZn}(\text{CH}_3)_2\text{H}$ and $\text{LiZn}_2(\text{CH}_3)_4\text{H}$. Referring to the data generated in this study (Table 1), one can see that the Zn-H stretching frequency for $\text{LiZn}_2(\text{CH}_3)_4\text{H}$ (1290 cm^{-1}) is lower than that for $\text{LiZn}(\text{CH}_3)_2\text{H}$ (1450 cm^{-1}). These data are consistent with the suggested structures since one would expect

Table 1. Infrared Spectral Bands for $(\text{CH}_3)_2\text{Zn}$, AlH_3 , $\text{LiZn}(\text{CH}_3)_2\text{H}$, $\text{LiZn}_2(\text{CH}_3)_4\text{H}$, $\text{LiZn}(\text{CH}_3)_2\text{AlH}_4$, and $\text{LiZn}_2(\text{CH}_3)_4\text{AlH}_4$ in THF^a

$(\text{CH}_3)_2\text{Zn}$	AlH_3	$\text{LiZn}(\text{CH}_3)_2\text{H}$	$\text{LiZn}_2(\text{CH}_3)_4\text{H}$	$\text{LiZn}(\text{CH}_3)_2\text{AlH}_4^{\text{d}}$	$\text{LiZn}_2(\text{CH}_3)_4\text{AlH}_4^{\text{e}}$	Approximate Assignment
550 s		498 s	521 s	475 s	479 s	Zn-C stretch
674 vs		680 vs	668 vs	690 vs	700 vs	CH_3 rock
	728 vs			720 sh, s		Al-H deformation
	755 w			775 s		
	795 s					
840 m		795 w				Solvent O-C stretch
1,153 m		1,118 m	1,120 m	1,118 m	1,140 m	CH_3 deformation
				1,162 m	1,170 w	
		1,450 br, ^c s	1,290 br, ^c s			Zn-H stretch
				1,400 br, ^c s	1,400 br, ^c s	 stretch
	1,740 vs			1,660 br, ^c vs		Terminal Al-H stretch

^aAll spectra were run with THF as reference. Typical errors in the measurements were $\pm 5 \text{ cm}^{-1}$.

^bAbbreviations: w, weak; m, medium; s, strong; sh, shoulder; v, very; br, broad. ^cThese bands were broad. The frequency given is approximately the center of the band. ^dConcentration = 0.15 M.

^eConcentration = 0.10 M.

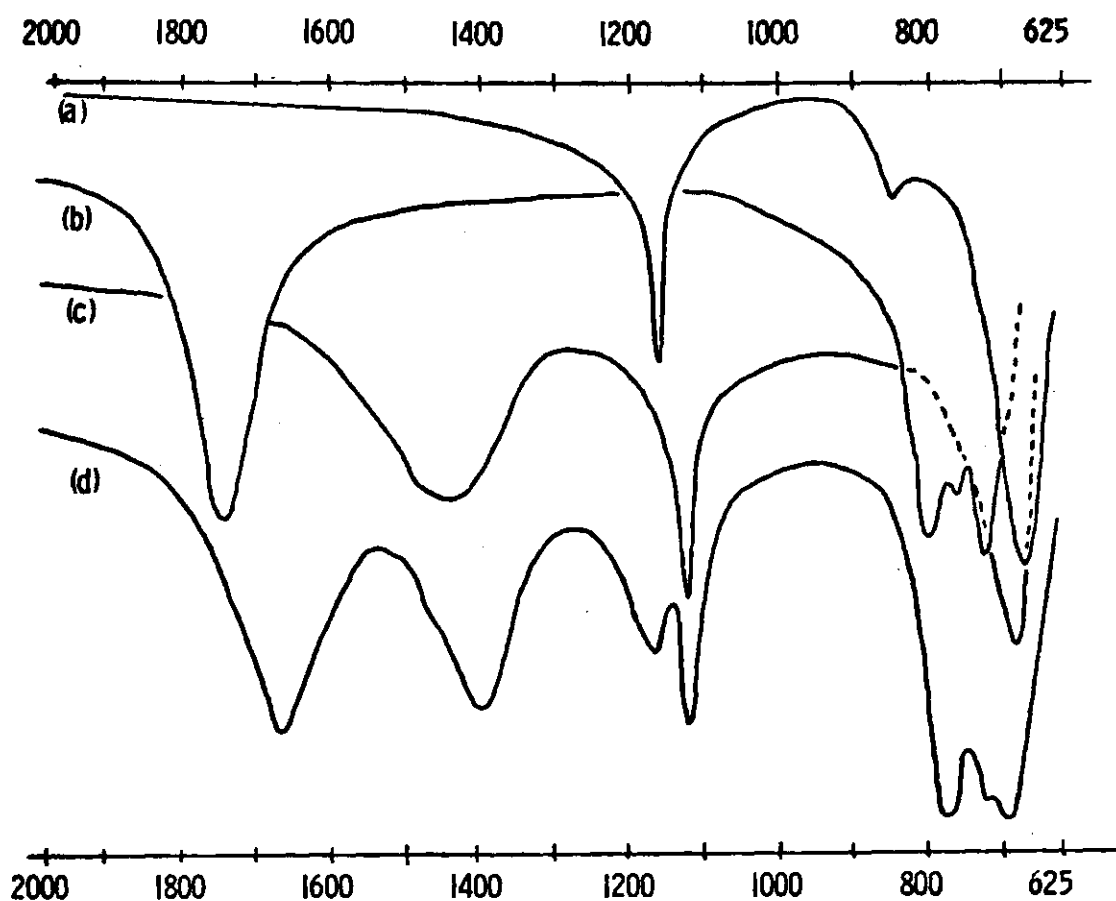
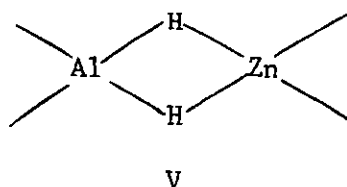


Figure 1. Infrared Spectra of (a) $(\text{CH}_3)_2\text{Zn}$ in THF, (b) AlH_3 in THF, (c) $\text{LiZn}(\text{CH}_3)_2\text{H}$ in THF, (d) $\text{LiZn}(\text{CH}_3)_2\text{AlH}_4$ in THF

the bridging Zn-H-Zn band in the $\text{LiZn}_2(\text{CH}_3)_4\text{H}$ to have a lower stretching frequency than the nonbridging Zn-H in $\text{LiZn}(\text{CH}_3)_2\text{H}$.^{*} The infrared spectra of the deuterated compounds, $\text{LiZn}(\text{CH}_3)_2\text{D}$ and $\text{LiZn}_2(\text{CH}_3)_4\text{D}$, show that the bands at 1450 and 1290 cm^{-1} for the hydride complexes are shifted to 1041 and 896 cm^{-1} , establishing that these bands are indeed due to metal-hydrogen bonds.

The band at 1400 cm^{-1} for $\text{LiZn}(\text{CH}_3)_2\text{AlH}_4$ is close to the terminal Zn-H stretching band for $\text{LiZn}(\text{CH}_3)_2\text{H}$, but at a lower frequency. The data in Table 1 suggest that stretching bands due to Al-H absorb at somewhat higher frequencies than those due to Zn-H. Therefore, the structural unit Al-H-Zn should have a stretching band at higher frequency than the band due to Zn-H-Zn in $\text{LiZn}_2(\text{CH}_3)_4\text{H}$ although it might be expected to be roughly equivalent to the terminal Zn-H band for $\text{LiZn}(\text{CH}_3)_2\text{H}$. With this in mind, the band at 1400 cm^{-1} in $\text{LiZn}(\text{CH}_3)_2\text{AlH}_4$ could be assigned to the double hydrogen bridge structure V. These conclusions, together with the fact



that the band at 1660 cm^{-1} corresponds to a terminal Al-H stretching vibration, lead to the conclusion that $\text{LiZn}(\text{CH}_3)_2\text{AlH}_4$ has the structure I, where the zinc and aluminum atoms are tetrahedrally coordinated. The po-

^{*}It is interesting to note that the Zn-H stretching band reported by Shriver and co-workers for desolvated $\text{LiZn}(\text{C}_6\text{H}_5)_2\text{H}$ in Nujol mull occurred as a broad peak extending from 1250-1650 cm^{-1} . The band reported in this work for the Zn-H stretching modes of $\text{LiZn}(\text{CH}_3)_2\text{H}$ in THF (Figure 1) also extends from 1250-1650 cm^{-1} with the center at 1450 cm^{-1} .

sition of the CH_3 groups in this structure is consistent with the infrared spectrum in the metal-carbon stretching region. There are no bands in the Al-C stretching region, $700\text{-}550\text{ cm}^{-1}$.¹¹ The observed band at 475 cm^{-1} is consistent with terminal Zn-C stretching modes. For $(\text{CH}_3)_2\text{Zn}$ in THF, this band is at 547 cm^{-1} , but it shifts to lower frequency ($500\text{-}400\text{ cm}^{-1}$) upon complex formation.^{10,12}

The reaction of $\text{LiZn}_2(\text{CH}_3)_4\text{H}$ with AlH_3 , like the reaction of $\text{LiZn}(\text{CH}_3)_2\text{H}$ with AlH_3 , yielded a clear solution. Ebullioscopic molecular weight measurements on the reaction mixture over a concentration range of $0.04\text{-}0.12\text{ M}$ (based on aluminum) yielded i -values ranging from $0.98\text{-}1.07$. Again, glpc analysis of hydrolyzed samples both before and after the molecular weight experiment showed the absence of THF cleavage products. An analysis of the reaction mixture showed Li, Zn, Al, Me, and H to be present in the molar ratio $0.97\text{:}2.00\text{:}1.02\text{:}3.97\text{:}3.99$. Since the i -value is based on the aluminum concentration, these data indicate the presence of a compound of stoichiometry $\text{LiZn}_2(\text{CH}_3)_4\text{AlH}_4$. The infrared spectrum of the reaction mixture (Figure 2d) did not contain any bands in the terminal Al-H stretching region ($1900\text{-}1600\text{ cm}^{-1}$), but only a broad peak centered at 1400 cm^{-1} . Also there is no terminal Al-H deformation band in its characteristic region ($800\text{-}700\text{ cm}^{-1}$); but there is a Zn- CH_3 stretching band at 479 cm^{-1} . With the exception of the band at 1660 cm^{-1} and the bands in the terminal Al-H deformation region, the spectrum of $\text{LiZn}_2(\text{CH}_3)_4\text{AlH}_4$ exactly matched the spectrum of $\text{LiZn}(\text{CH}_3)_2\text{AlH}_4$. Based on the arguments used above for $\text{LiZn}(\text{CH}_3)_2\text{AlH}_4$, $\text{LiZn}_2(\text{CH}_3)_4\text{AlH}_4$ would be expected to have structure II, where the zinc and aluminum atoms are tetrahedrally coordinated. In view of the fact that there are no terminal aluminum hydrogen

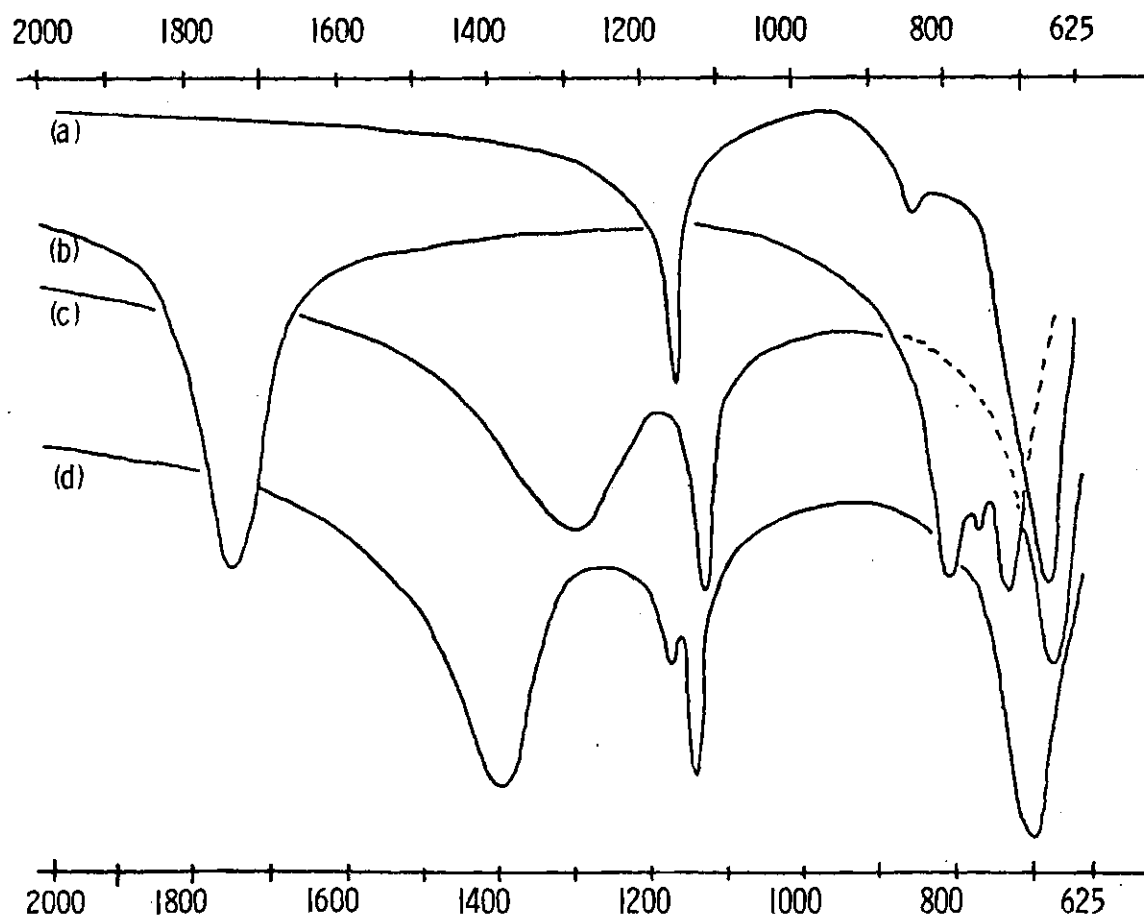


Figure 2. Infrared Spectra of (a) $(\text{CH}_3)_2\text{Zn}$ in THF, (b) AlH_3 in THF, (c) $\text{LiZn}_2(\text{CH}_3)_4\text{H}$ in THF, (d) $\text{LiZn}_2(\text{CH}_3)_4\text{AlH}_4$ in THF

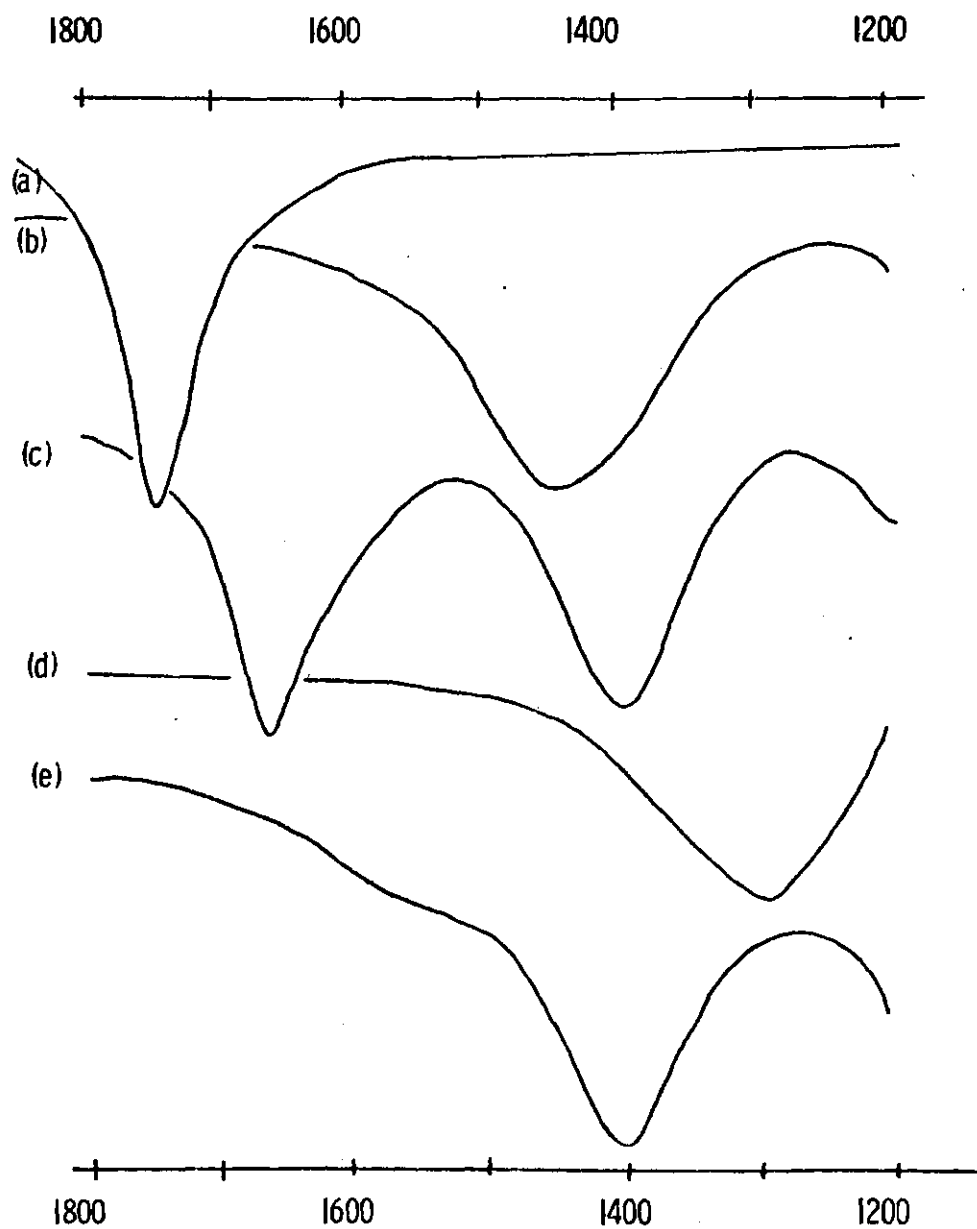


Figure 3. The 1800-1200 cm^{-1} Region of the Infrared Spectrum for (a) AlH_3 in THF, (b) $\text{LiZn}(\text{CH}_3)_2\text{H}$ in THF, (c) $\text{LiZn}(\text{CH}_3)_2\text{-AlH}_4$ in THF, (d) $\text{LiZn}_2(\text{CH}_3)_4\text{H}$ in THF, (e) $\text{LiZn}_2(\text{CH}_3)_4\text{AlH}_4$ in THF

bands in the infrared spectrum of the complex, and that the molecular weight measurements indicate the presence of a single species, the above structure seems to be the only reasonable one which can be drawn. Thus, the assignment of the band at 1400 cm^{-1} in the infrared spectrum of $\text{LiZn}(\text{CH}_3)_2\text{AlH}_4$ to the unit (V) appears to be justified.

The ^1H NMR resonances for the organozinc methyl groups in $\text{LiZn}(\text{CH}_3)_2\text{AlH}_4$ and $\text{LiZn}_2(\text{CH}_3)_4\text{AlH}_4$ are given in Table 2 and Figure 4. The organozinc methyl resonance shifts progressively upfield on proceeding from $(\text{CH}_3)_2\text{Zn}$ to $\text{LiZn}_2(\text{CH}_3)_4\text{H}$ to $\text{LiZn}(\text{CH}_3)_2\text{H}$. This behavior is consistent with the assignment of structures III and IV suggested for these compounds. One would have expected the methyl resonance to shift upfield from $(\text{CH}_3)_2\text{Zn}$ upon formation of the anionic hydride complex $\text{LiZn}(\text{CH}_3)_2\text{H}$. A similar shift upfield would also be expected for $\text{LiZn}_2(\text{CH}_3)_4\text{H}$; however, the shift would not be expected to be as great as that observed for $\text{LiZn}(\text{CH}_3)_2\text{H}$. The methyl resonances for $\text{LiZn}_2(\text{CH}_3)_4\text{AlH}_4$ are upfield from $(\text{CH}_3)_2\text{Zn}$ indicating the formation of an anionic hydride complex or complexes. These two signals are believed to be due to the methyl groups on II and VI which are in equilibrium as shown in Eq. 4. The S in Eq. 4 represents solvent and will be used this way throughout the remainder of this discussion.

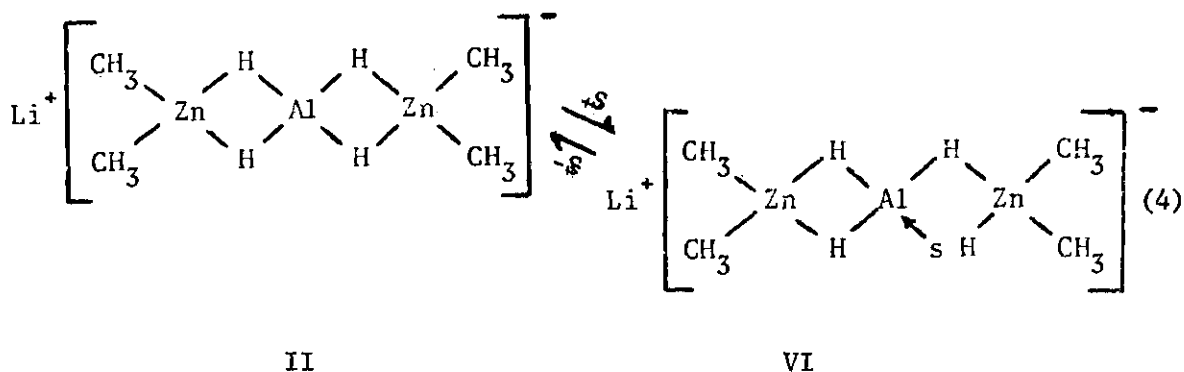


Table 2. Chemical Shifts for Methyl Groups in $(\text{CH}_3)_2\text{Zn}$, $\text{LiZn}(\text{CH}_3)_2\text{H}$, $\text{LiZn}_2(\text{CH}_3)_4\text{H}$, $\text{LiZn}(\text{CH}_3)_2\text{AlH}_4$, and $\text{LiZn}_2(\text{CH}_3)_4\text{AlH}_4$ in THF^a

Sample	Concentration (M)	Chemical Shifts ^b (τ)
$(\text{CH}_3)_2\text{Zn}$		10.79
$\text{LiZn}_2(\text{CH}_3)_4\text{H}$		10.90
$\text{LiZn}(\text{CH}_3)_2\text{H}$		10.97
$\text{LiZn}(\text{CH}_3)_2\text{AlH}_4$	0.10	10.95 (10.7), 10.98 (1.0), 11.02 (2.3)
$(\text{LiZn}(\text{CH}_3)_2\text{H} + \text{AlH}_3)$	0.18	10.96 (6.5), 10.98 (2.4), 11.02 (1.0)
$\text{LiZn}_2(\text{CH}_3)_4\text{AlH}_4$	0.12	10.96 (3.1), 11.02 (1.0)
$(\text{LiZn}_2(\text{CH}_3)_4\text{H} + \text{AlH}_3)$		

^aSpectra were recorded at probe temperature of 35°C . ^bRelative integration is given in parentheses. Typical error limits in the chemical shift measurements were ± 1 Hz or ± 0.02 τ .

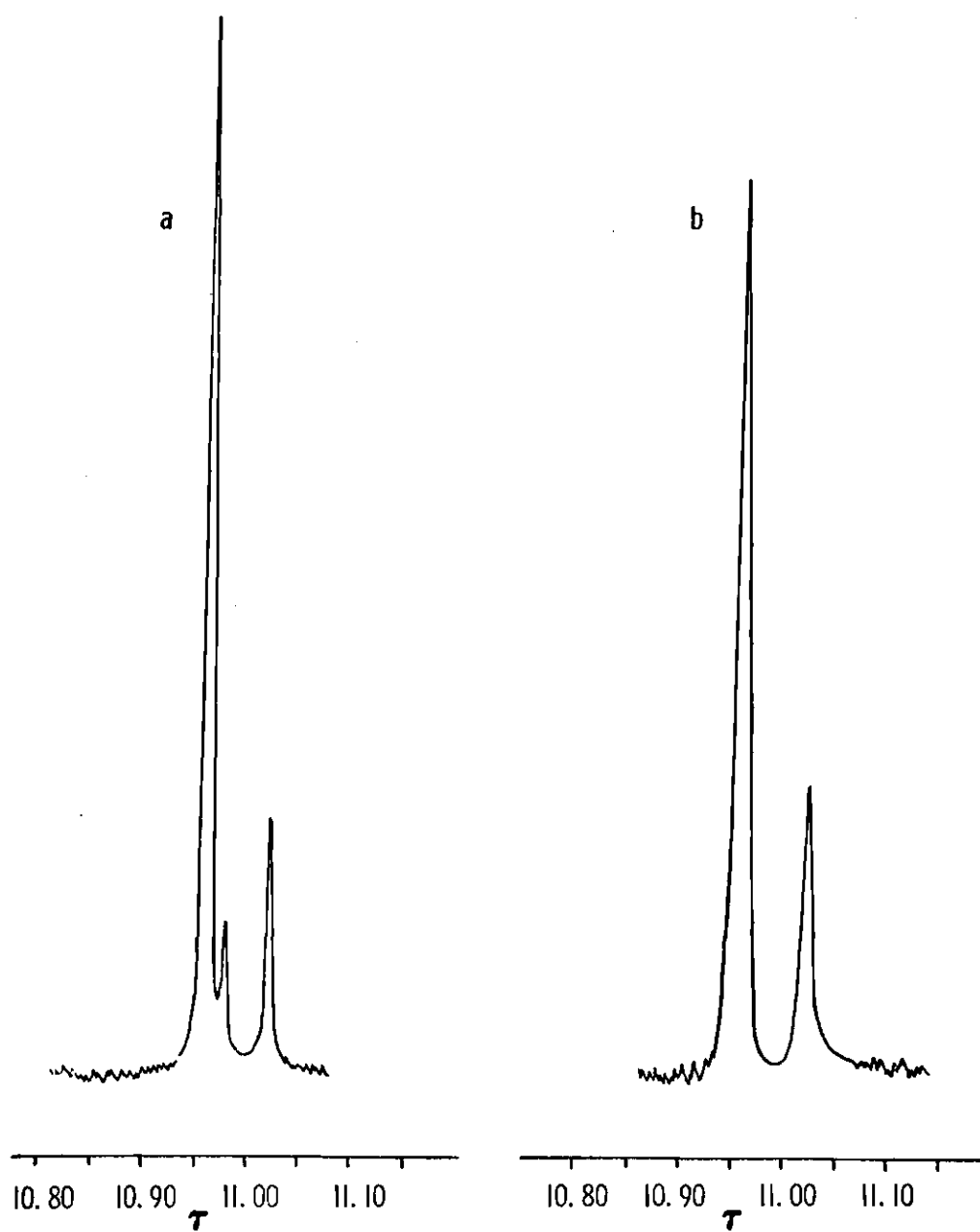
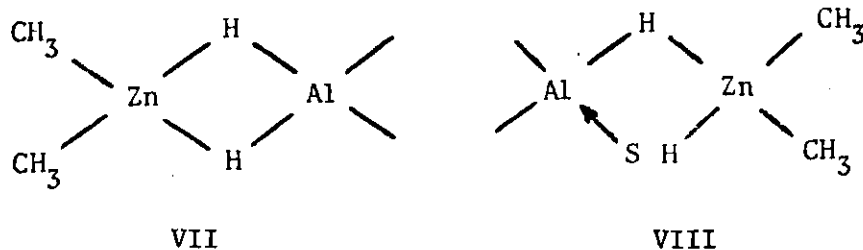
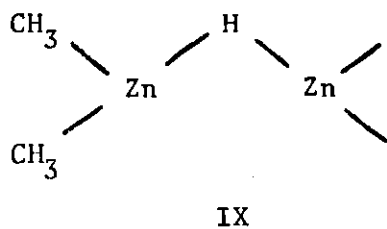


Figure 4. ^1H NMR Spectra in THF at 35° : (a) $\text{LiZn}(\text{CH}_3)_2\text{AlH}_4$,
(b) $\text{LiZn}_2(\text{CH}_3)_4\text{AlH}_4$

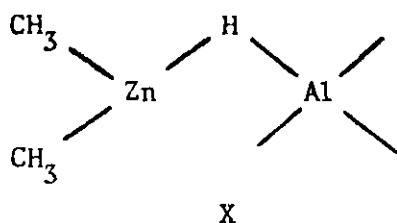
The low field resonances are assigned to the methyl groups in the structural unit VII whereas the high field resonance would be due to the methyl groups in VIII.



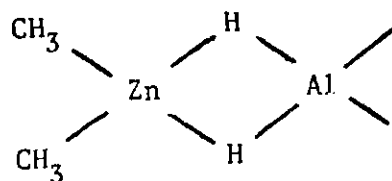
One can readily see that II and VI would give rise to just two NMR signals and fit the observed infrared and molecular association data. Also, based on the position of the methyl resonances for $(\text{CH}_3)_2\text{Zn}$, $\text{LiZn}_2(\text{CH}_3)_4\text{H}$, and $\text{LiZn}(\text{CH}_3)_2\text{H}$, the two signals for $\text{LiZn}_2(\text{CH}_3)_4\text{AlH}_4$ are about where one would predict for structures like II and VI. For example, on formation of the structural unit IX from $(\text{CH}_3)_2\text{Zn}$, the methyl resonance shifted 0.11 ppm upfield. Thus, one would expect a similar upfield shift on the



formation of the structural unit X from $(\text{CH}_3)_2\text{Zn}$. However, on formation



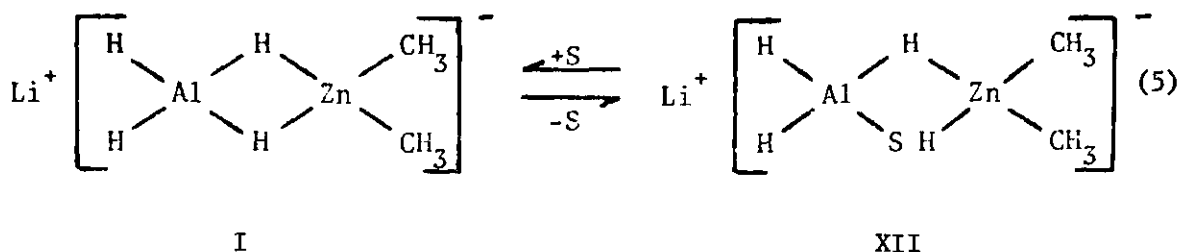
of the double hydrogen bridge structure XI from the above unit, one would



XI

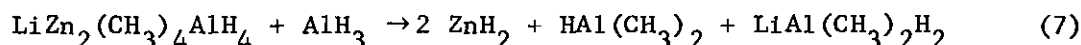
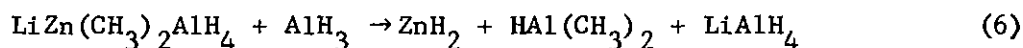
not expect to see another full 0.11 ppm upfield shift. The upfield shift should only be about 60% of this amount.¹³ So the position of the methyl resonance for the double hydrogen bridge unit should be about 0.17 ppm upfield from $(\text{CH}_3)_2\text{Zn}$. This is what one observes. Similarly, the position of the methyl resonance for the structural unit VIII should be about 0.22 ppm upfield from $(\text{CH}_3)_2\text{Zn}$. Again this is what one observes.

Three methyl resonances are observed for $\text{LiZn}(\text{CH}_3)_2\text{AlH}_4$. The low field and high field resonances are the same as those observed for $\text{LiZn}_2(\text{CH}_3)_4\text{AlH}_4$ and can be assigned, using the local environment hypothesis,¹⁴ to the methyl groups in structures I and XII, which are in equilibrium as shown in Eq. 5. The middle resonance which is 0.19 ppm upfield from $(\text{CH}_3)_2\text{Zn}$, is due to the dimer form of $\text{LiZn}(\text{CH}_3)_2\text{AlH}_4$.



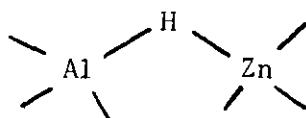
This assignment is consistent with the fact that the relative intensity of the center resonance increases as the solution becomes more concentrated. At lower temperatures (to -83°C) the same signals are observed for $\text{LiZn}(\text{CH}_3)_2\text{AlH}_4$ and $\text{LiZn}_2(\text{CH}_3)_4\text{AlH}_4$. Thus, at room temperature, the methyl group exchange between structures like I and XII is slow on the NMR time scale.

It was felt that the triple metal ate complexes $\text{LiZn}(\text{CH}_3)_2\text{AlH}_4$ and $\text{LiZn}_2(\text{CH}_3)_4\text{AlH}_4$ could be used as precursors in the synthesis of the triple metal hydride complexes LiZnAlH_6 and $\text{LiZn}_2\text{AlH}_8$. Along this line, the two ate complexes were reacted with both AlH_3 and LiAlH_4 . The reactions of $\text{LiZn}(\text{CH}_3)_2\text{AlH}_4$ and $\text{LiZn}_2(\text{CH}_3)_4\text{AlH}_4$ with AlH_3 produced ZnH_2 according to Eq. 6 and 7, while the addition of LiAlH_4 to each of these resulted in no reaction.



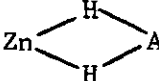
The addition of either LiAlH_4 to $(\text{CH}_3)_2\text{Zn}$ or $(\text{CH}_3)_2\text{Zn}$ to LiAlH_4 in a 1:1 molar ratio in THF yields a clear solution whose infrared spectrum corresponds closely to that of $\text{LiZn}(\text{CH}_3)_2\text{AlH}_4$ prepared from $\text{LiZn}(\text{CH}_3)_2\text{H}$ and AlH_3 . The only difference being the presence of a band at 1500 cm^{-1} in the infrared spectrum of the 1:1 LiAlH_4 and $(\text{CH}_3)_2\text{Zn}$ mixture. Likewise, the addition of either LiAlH_4 to $(\text{CH}_3)_2\text{Zn}$ in 1:2 ratio or $(\text{CH}_3)_2\text{Zn}$ to LiAlH_4 in 2:1 ratio in THF yields a clear solution whose infrared spectrum corresponds closely to that of $\text{LiZn}_2(\text{CH}_3)_4\text{AlH}_4$, again the

difference being the occurrence of a band at 1500 cm^{-1} . Also the addition of LiAlH_4 to $(\text{CH}_3)_2\text{Zn}$ in 2:3 ratio or $(\text{CH}_3)_2\text{Zn}$ to LiAlH_4 in 3:2 ratio in THF yields a clear solution whose infrared spectrum corresponds to a mixture of $\text{LiZn}(\text{CH}_3)_2\text{AlH}_4$ and $\text{LiZn}_2(\text{CH}_3)_4\text{AlH}_4$ except for the band at 1500 cm^{-1} . The infrared spectra of the LiAlH_4 - $(\text{CH}_3)_2\text{Zn}$ mixtures are recorded in Figures 5 and 6. The observed infrared bands are tabulated in Table 3 for a more convenient comparison with the reported bands for $\text{LiZn}(\text{CH}_3)_2\text{AlH}_4$ and $\text{LiZn}_2(\text{CH}_3)_4\text{AlH}_4$. As reported previously, the terminal Zn-H stretching band in $\text{LiZn}(\text{CH}_3)_2\text{H}$ occurs at 1450 cm^{-1} , whereas the bridging Zn-H-Zn stretching band in $\text{LiZn}_2(\text{CH}_3)_4\text{H}$ occurs at 1290 cm^{-1} . Formation of a bridging zinc-hydrogen bond compound to a terminal one results in a shifting of the asymmetric stretching band to a lower frequency by 160 cm^{-1} . Based on this, one would expect the terminal Al-H stretching band in $\text{LiZn}(\text{CH}_3)_2\text{AlH}_4$ to shift about 160 cm^{-1} to lower frequency on formation of an Al-H-Zn bridging bond. Since the terminal Al-H stretching band in $\text{LiZn}(\text{CH}_3)_2\text{AlH}_4$ occurs at 1660 cm^{-1} , one would expect an Al-H-Zn bridging hydride absorption in this compound to be at about 1500 cm^{-1} . This seems reasonable since the band at 1400 cm^{-1} in $\text{LiZn}(\text{CH}_3)_2\text{AlH}_4$ has been assigned to the double hydrogen bridged unit V and one would expect a single hydrogen bridging unit to absorb at somewhat higher frequency. In light of this reasoning, the band observed at 1500 cm^{-1} for solutions obtained by mixing LiAlH_4 and $(\text{CH}_3)_2\text{Zn}$ is assigned the structural unit, XIII.



XIII

Table 3. Infrared Spectra of $(\text{CH}_3)_2\text{Zn}$, LiAlH_4 , $\text{LiZn}(\text{CH}_3)_2\text{AlH}_4$, $\text{LiZn}_2(\text{CH}_3)_4\text{AlH}_4$, and the Products Obtained by Mixing LiAlH_4 and $(\text{CH}_3)_2\text{Zn}$ in THF^a

Observed IR Bands, cm^{-1} ^b							Approximate Assignment
$(\text{CH}_3)_2\text{Zn}$	LiAlH_4	$\text{LiZn}(\text{CH}_3)_2\text{AlH}_4^{\text{d}}$	$\text{LiZn}_2(\text{CH}_3)_4\text{AlH}_4^{\text{e}}$	1:1 $\text{LiAlH}_4 + (\text{CH}_3)_2\text{Zn}^{\text{f}}$	2:3 $\text{LiAlH}_4 + (\text{CH}_3)_2\text{Zn}^{\text{g}}$	1:2 $\text{LiAlH}_4 + (\text{CH}_3)_2\text{Zn}^{\text{h}}$	
550 s		475 s	479 s	472 s	475 s	475 s	Zn-C Stretch
674 vs		690 vs	700 vs	690 vs	697 vs	700 vs	CH_3 Rock
	760 m	720 sh,s 775 s		720 sh,s 775 s	720 sh,w 775 m		Al-H Deformation
840 m							Solvent O-C Stretch
1153 m		1118 m 1162 m	1140 m 1170 w	1118 m 1162 m	1130 sh,w 1164 w	1140 m 1170 w	CH_3 Deformation
		1400 br, ^c s	1400 br, ^c s	1400 br, ^c s	1400 br, ^c s	1400 br, ^c s	 Zn-Al Stretch
				1500 sh,s	1500 sh,s	1500 sh,s	Zn-H-Al Stretch
	1691 s	1660 br,vs		1660 br,vs	1660 br,vs		Terminal Al-H Stretch

^aAll spectra were run with THF as reference. Typical error in the measurements was $\pm 5 \text{ cm}^{-1}$.

^bAbbreviations: w, weak; m, medium; s, strong; sh, shoulder; v, very; br, broad. ^cThese bands were very broad. The frequency given is approximately the center of the band. ^dConcentration = 0.15 M;

^eConcentration = 0.10 M; ^fConcentration = 0.52 M; ^gConcentration = 0.47 M; ^hConcentration = 0.40 M.

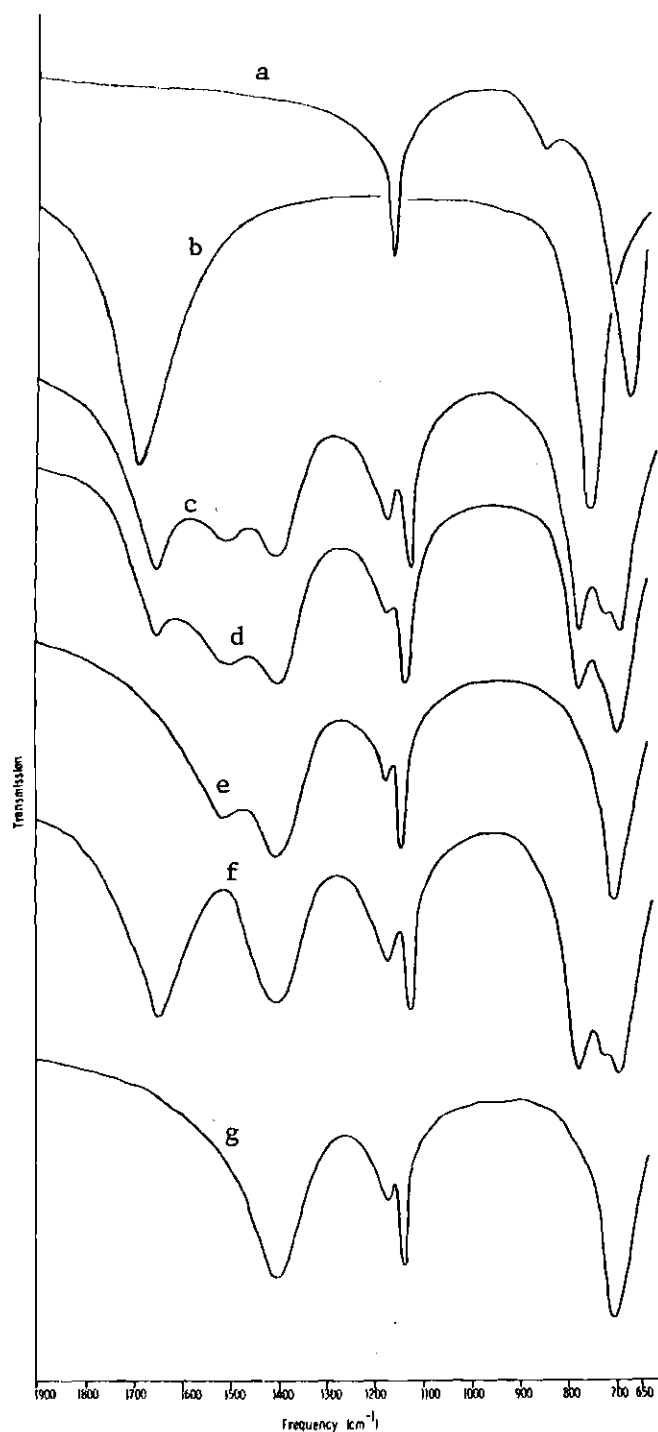


Figure 5. Infrared Spectra of Solutions Obtained by Adding LiAlH_4 to $(\text{CH}_3)_2\text{Zn}$ in THF: (a) $(\text{CH}_3)_2\text{Zn}$; (b) LiAlH_4 ; (c) 1:1 $\text{LiAlH}_4 + (\text{CH}_3)_2\text{Zn}$; (d) 2:3 $\text{LiAlH}_4 + (\text{CH}_3)_2\text{Zn}$; (e) 1:2 $\text{LiAlH}_4 + (\text{CH}_3)_2\text{Zn}$; (f) $\text{LiZn}(\text{CH}_3)_2\text{AlH}_4$; (g) $\text{LiZn}_2(\text{CH}_3)_4\text{AlH}_4$

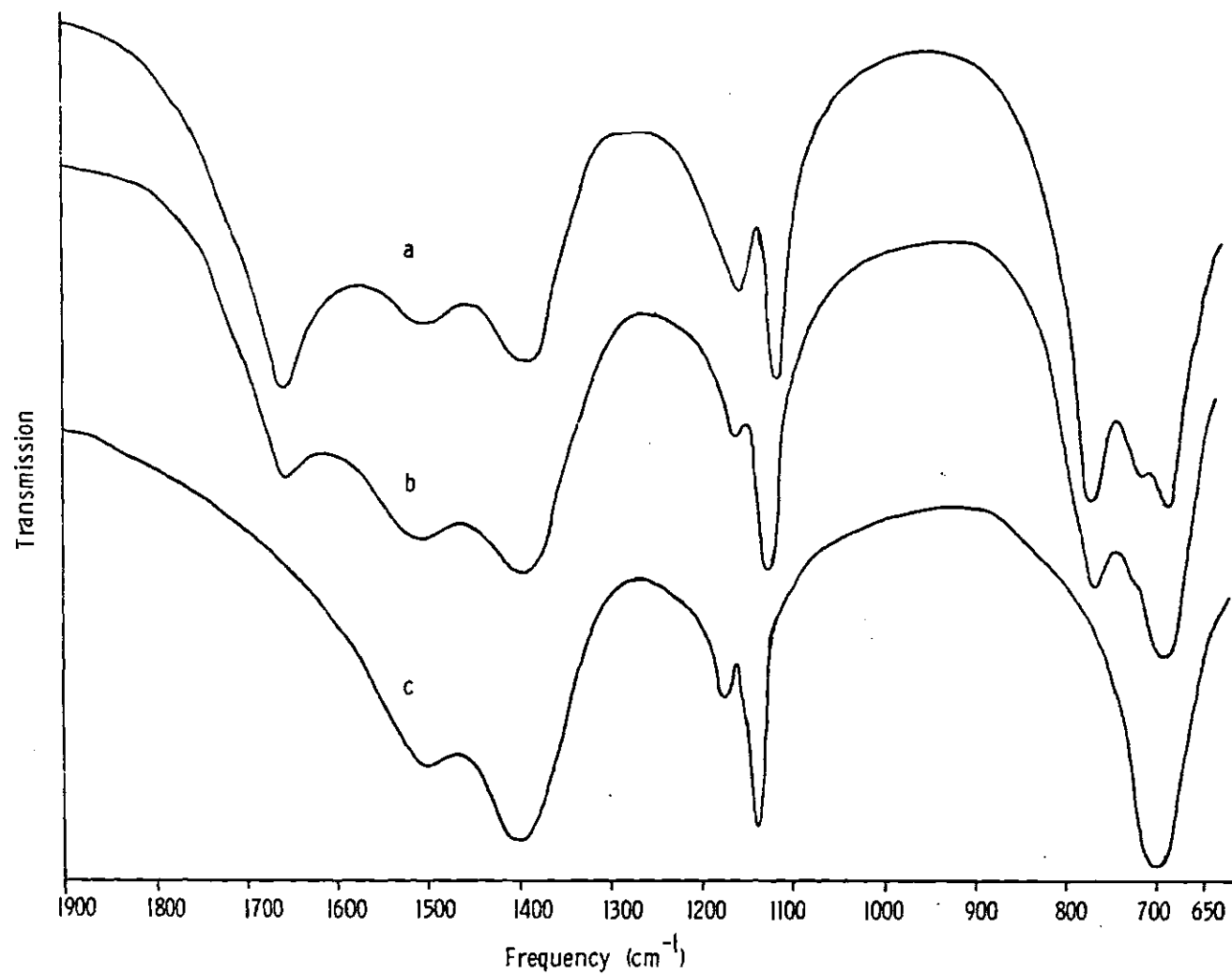
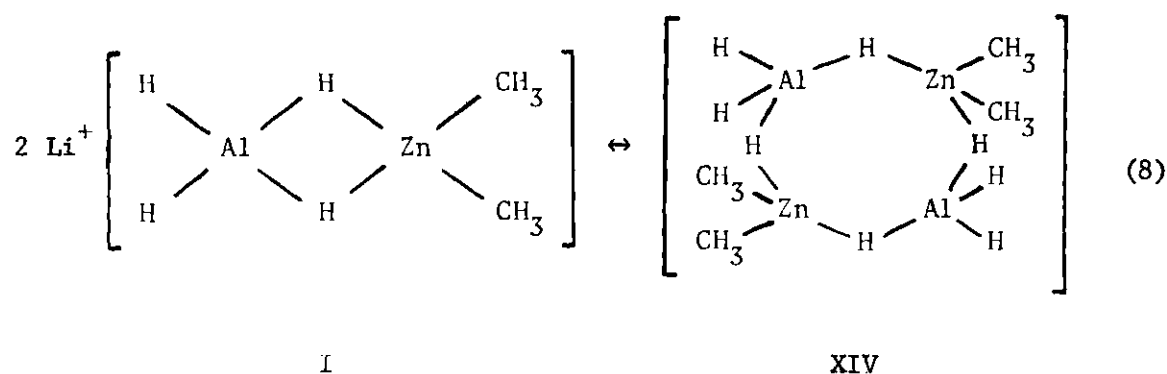


Figure 6. Infrared Spectra of Solutions Obtained by Adding (CH₃)₂Zn to LiAlH₄ in THF: (a) 1:1 (CH₃)₂Zn + LiAlH₄; (b) 2:3 (CH₃)₂Zn + LiAlH₄; (c) 1:2 (CH₃)₂Zn + LiAlH₄

In the solutions of $\text{LiZn}(\text{CH}_3)_2\text{AlH}_4$ and $\text{LiZn}_2(\text{CH}_3)_4\text{AlH}_4$ prepared by reacting AlH_3 with $\text{LiZn}(\text{CH}_3)_2\text{H}$ and $\text{LiZn}_2(\text{CH}_3)_4\text{H}$, the compounds were present in concentrations of 0.15 and 0.10 M when the infrared spectra were recorded. The solutions of $\text{LiZn}(\text{CH}_3)_2\text{AlH}_4$ and $\text{LiZn}_2(\text{CH}_3)_4\text{AlH}_4$ prepared in this study by mixing LiAlH_4 and $(\text{CH}_3)_2\text{Zn}$ had concentrations in the range 0.4-0.5 M when the infrared spectra were recorded. The observation of a band, due to a single hydrogen bridging unit, at higher concentrations, when it was not seen at lower concentration, leads one to conclude that this type of unit might be the result of higher associated species. In this connection, molecular association studies were carried out on solutions of $\text{LiZn}(\text{CH}_3)_2\text{AlH}_4$ and $\text{LiZn}_2(\text{CH}_3)_4\text{AlH}_4$ prepared by mixing LiAlH_4 with $(\text{CH}_3)_2\text{Zn}$. The resulting association values are shown in Figure 7 for $\text{LiZn}(\text{CH}_3)_2\text{AlH}_4$ and Figure 8 for $\text{LiZn}_2(\text{CH}_3)_4\text{AlH}_4$. The data in these figures show that, in the concentration range 0.4-0.5 M, significant association to a dimer unit is occurring. At concentrations near 0.10 M, little association beyond the monomer is observed. Therefore, an equilibrium of the type shown in Eq. 8 is indicated for $\text{LiZn}(\text{CH}_3)_2\text{AlH}_4$ in THF.



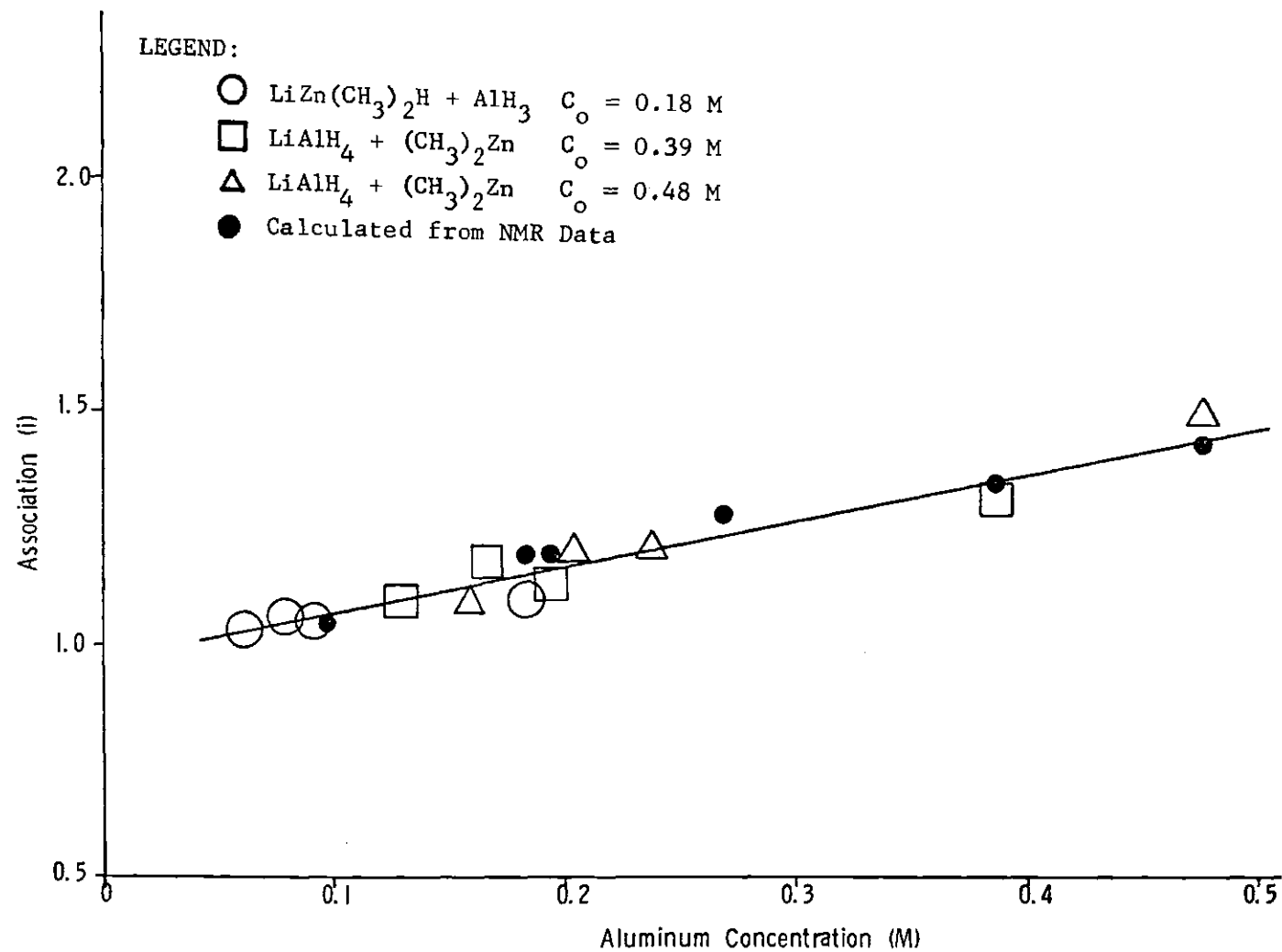


Figure 7. Molecular Association Values for $\text{LiZn}(\text{CH}_3)_2\text{AlH}_4$

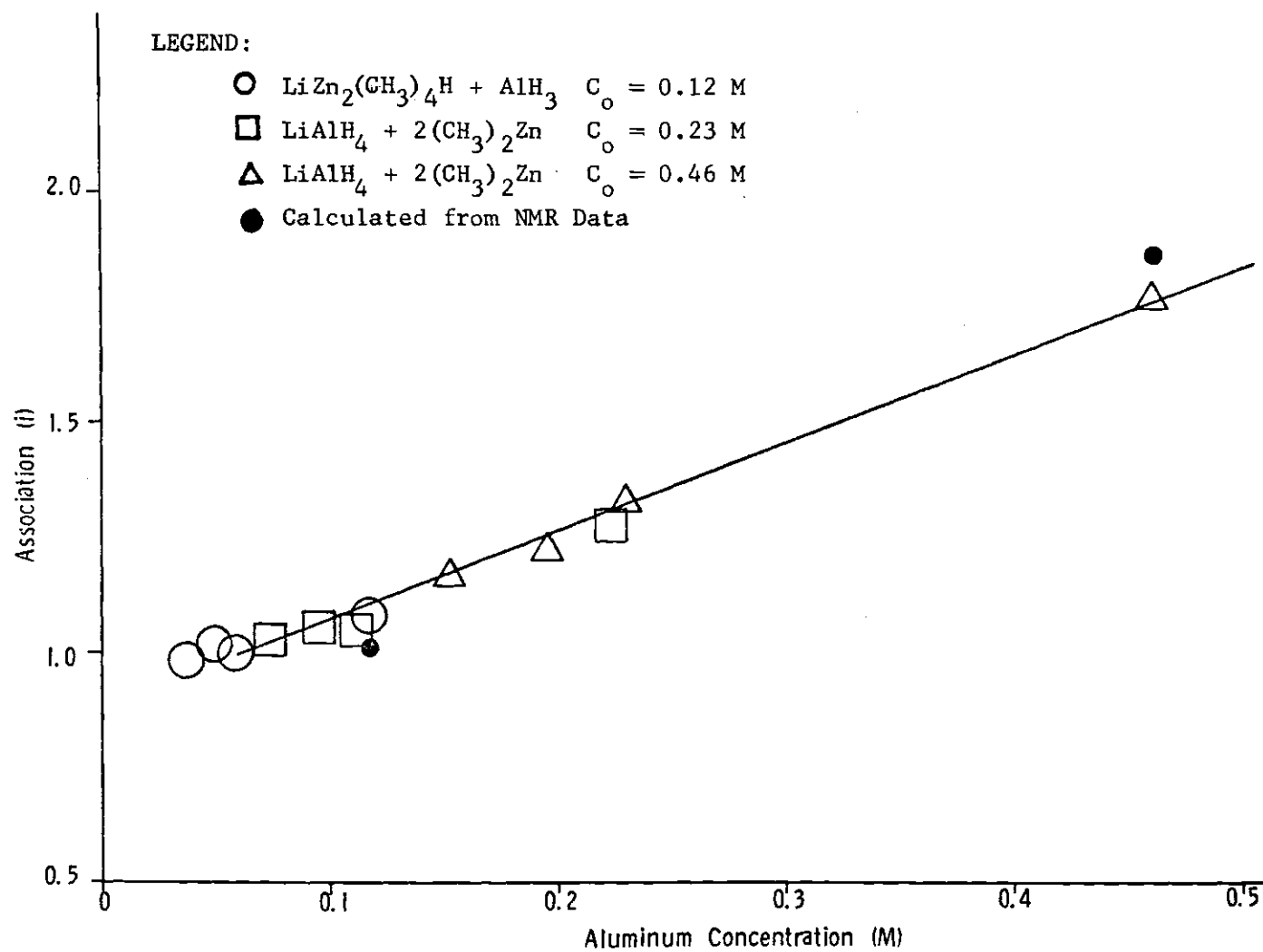
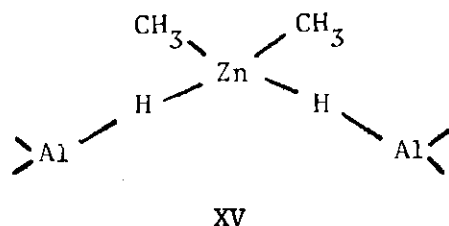


Figure 8. Molecular Association Values for $\text{LiZn}_2(\text{CH}_3)_4\text{AlH}_4$

A similar equilibrium could be written for $\text{LiZn}_2(\text{CH}_3)_4\text{AlH}_4$. Structure XIV, the dimer of $\text{LiZn}(\text{CH}_3)_2\text{AlH}_4$, does contain the single hydrogen bridged unit. It is easy for one to see how the observed infrared spectra could arise when two compounds with the structures of I and XIV are present.

The ^1H NMR chemical shifts observed for $\text{LiZn}(\text{CH}_3)_2\text{AlH}_4$ and $\text{LiZn}_2(\text{CH}_3)_4\text{AlH}_4$ (prepared from LiAlH_4 and $(\text{CH}_3)_2\text{Zn}$) are listed in Table 4. The chemical shifts are the same as those observed for $\text{LiZn}(\text{CH}_3)_2\text{AlH}_4$ prepared from AlH_3 and $\text{LiZn}(\text{CH}_3)_2\text{H}$. The resonances at 10.96τ and 11.02τ have been previously assigned to methyl groups in the structural units VII and VIII, respectively. The resonance at 10.98τ is seen to become more intense as the concentration of $\text{LiZn}(\text{CH}_3)_2\text{AlH}_4$ and $\text{LiZn}_2(\text{CH}_3)_4\text{AlH}_4$ is increased (Table 4 and Figure 9). This suggests that the resonance is due to the dimer of these compounds. The dimer structure, XIV, contains the structural unit XV which would provide a magnetic environment somewhat different from the two units above. Therefore, the resonance at



10.98τ is assigned to this unit. The NMR data suggest an equilibrium between structures which contain the three units shown above. Such an equilibrium is shown in Scheme I. The NMR integration data can be used to calculate the relative amounts of I, XII, XIV, and XVI and with these an apparent association can be calculated. Such association values are

Table 4. Chemical Shifts for $\text{LiZn}(\text{CH}_3)_2\text{AlH}_4$ and $\text{LiZn}_2(\text{CH}_3)_4\text{AlH}_4$ at Various Concentrations in THF^a

Sample	Concentration	Chemical Shifts ^b	Calculated Association
	(M)	(τ)	(i)
LiZn(CH ₃) ₂ AlH ₄	0.48	10.96 (1.9), 10.98 (1.8), 11.02 (1.0)	1.42
(LiAlH ₄ + (CH ₃) ₂ Zn)	0.39	10.96 (3.3), 10.98 (2.5), 11.01 (1.0)	1.32
	0.28	10.95 (3.4), 10.98 (2.0), 11.02 (1.0)	1.27
	0.19	10.96 (6.1), 10.98 (2.3), 11.03 (1.0)	1.18
LiZn(CH ₃) ₂ AlH ₄	0.18	10.96 (6.5), 10.98 (2.4), 11.02 (1.0)	1.18
(LiZn(CH ₃) ₂ H + AlH ₃)	0.10	10.95 (10.7), 10.98 (1.0), 11.02 (2.3)	1.04
LiZn ₂ (CH ₃) ₄ AlH ₄	0.46	10.96 (6.7), 10.98 (3.1), 11.01 (1.0)	1.86
(LiAlH ₄ + 2(CH ₃) ₂ Zn)			
LiZn ₂ (CH ₃) ₄ AlH ₄	0.12	10.96 (3.1), 11.02 (1.0)	1.00
(LiZn ₂ (CH ₃) ₄ H + AlH ₃)			

^aSpectra were recorded at 35°C. ^bRelative integration is given in parentheses. Typical error limits in the chemical shift measurements were ± 1 Hz or $\pm 0.02 \tau$.

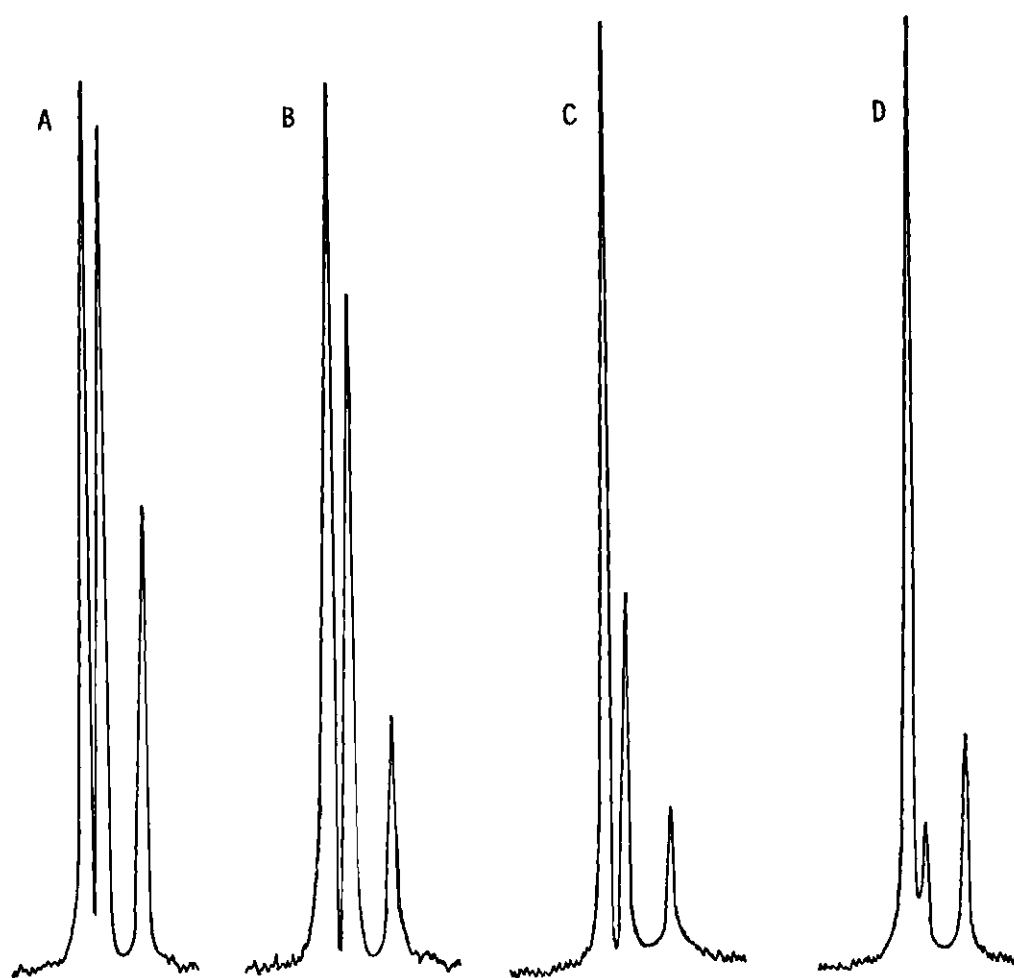
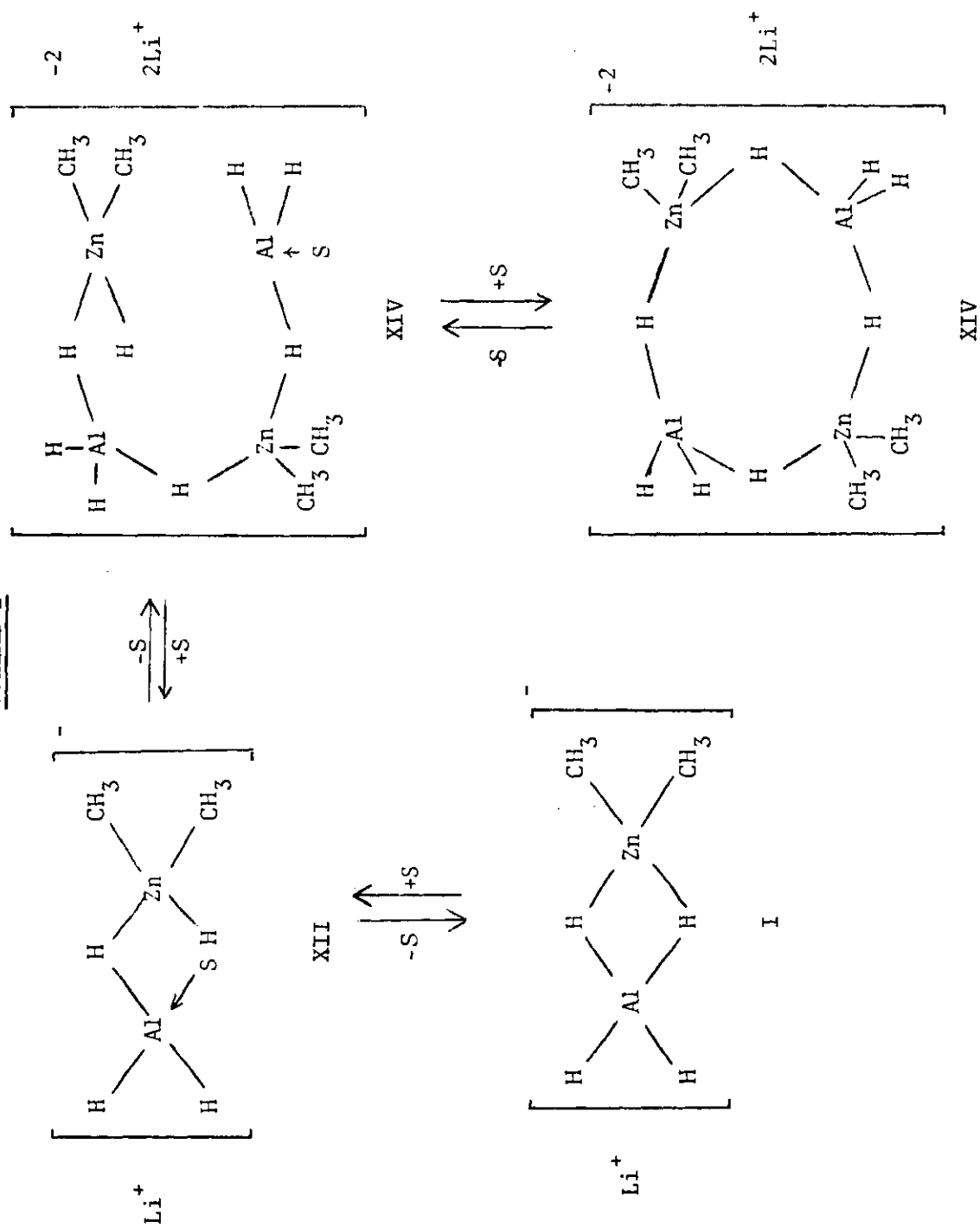


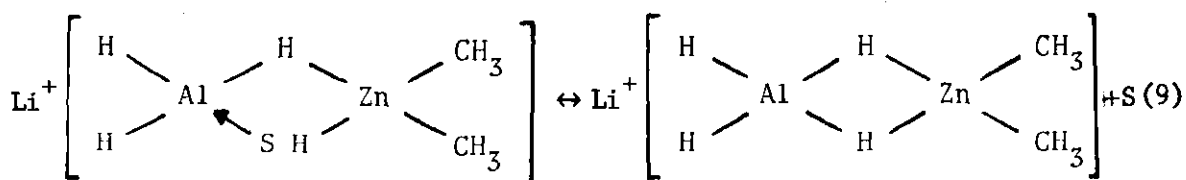
Figure 9. ^1H NMR Spectra of $\text{LiZn}(\text{CH}_3)_2\text{AlH}_4$ in THF at
Various Concentrations: (a) 0.48 M, (b) 0.39 M,
(c) 0.19 M, (d) 0.10 M

SCHEME I



shown in Table 4 and plotted in Figures 7 and 8. It is seen that the calculated association values based on Scheme I agree well with the experimentally determined values, thus indicating that Scheme I provides a very reasonable picture of the composition of $\text{LiZn}(\text{CH}_3)_2\text{AlH}_4$ in THF. The NMR data for $\text{LiZn}_2(\text{CH}_3)_4\text{AlH}_4$ suggest that a similar equilibrium can be written to describe its solution composition.

The chemical shifts recorded with variable temperature NMR for selected samples of $\text{LiZn}(\text{CH}_3)_2\text{AlH}_4$ and $\text{LiZn}_2(\text{CH}_3)_4\text{AlH}_4$ are shown in Table 5. The same three resonances are observed, but they move to higher field as the temperature is decreased due to solvent anisotropy.* Integration of these signals shows that, in the case of $\text{LiZn}(\text{CH}_3)_2\text{AlH}_4$, the equilibrium in Scheme I is shifted in favor of I as the temperature is decreased, i.e., the amounts of solvated structures XII and XVI decrease with decreasing temperature. Using the NMR integration data, equilibrium constants can be calculated for this process (Eq. 9).



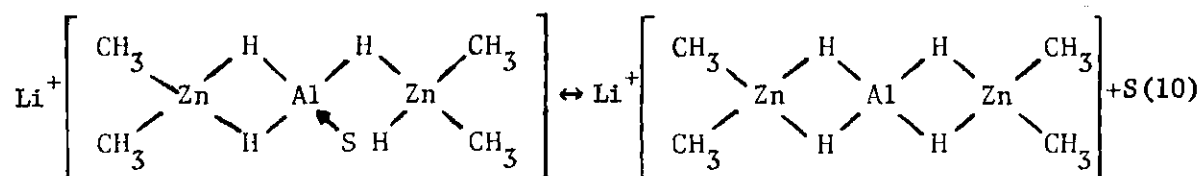
*The magnetic field experienced by a solute molecule will depend in part on the bulk magnetic susceptibility of the solution. The average orientation of molecules in the bulk solvent surrounding a solute molecule is temperature and concentration dependent and as this average orientation changes, so will the chemical shift. These effects are usually small compared to specific solvation effects but may amount to a tenth of a ppm in chemical shift or more in specific cases. Solvent anisotropy in connection with concentration changes was not observed here, since the concentration was never much greater than 0.5 M. In studies on Grignard reagents these effects were not observed until the concentration became 2.0 M.

Table 5. Chemical Shifts for $\text{LiZn}(\text{CH}_3)_2\text{AlH}_4$ and $\text{LiZn}_2(\text{CH}_3)_4\text{AlH}_4$ at Various Temperatures in THF

Sample	Concentration (M)	Temperature (°C)	Chemical Shifts ^a (τ)	Relative Integration
LiZn(CH ₃) ₂ AlH ₄ (LiAlH ₄ + (CH ₃) ₂ Zn)	0.39	35	10.96, 10.98, 11.01	3.3:2.5:1.0
		21	10.98, 11.00, 11.03	3.9:2.8:1.0
		4	10.99, 11.01, 11.03	4.8:2.9:1.0
		-19	10.99, 11.01, 11.04	5.6:3.1:1.0
		-36	11.00, 11.02, 11.07	6.1:3.4:1.0
		-51	11.01, 11.04, 11.11	6.8:3.5:1.0
		-63	11.02, 11.06, 11.14	7.6:3.7:1.0
		-81	11.02, 11.06, 11.17	8.6:3.8:1.0
LiZn ₂ (CH ₃) ₄ AlH ₄ (LiAlH ₄ + 2(CH ₃) ₂ Zn)	0.46	35	10.96, 10.98, 11.01	6.7:3.1:1.0
		-63	10.98, 10.99, 11.08	9.5:4.3:1.0
LiZn ₂ (CH ₃) ₄ AlH ₄	0.12	-35	10.96, 11.02	3.1:1.0
		-63	10.99, 11.11	5.0:1.0

^aTypical error limits in the chemical shift measurements were ± 1 Hz or ± 0.02 τ.

The equilibrium constants are given in Table 6 and plotted as $\ln K$ vs $1/T$ in Figure 10. Equilibrium constants for the similar process involving $\text{LiZn}_2(\text{CH}_3)_4\text{AlH}_4$ (Eq. 10) are given in Table 7 and plotted in Figure 10.



The enthalpy and entropy of the reaction as written in Eq. 9 are calculated to be -0.80 Kcal/mole and 0.61 eu. For Eq. 10, ΔH and ΔS are calculated to be -0.72 Kcal/mole and -2.02 eu. The enthalpy of reactions 9 and 10 would be expected to be about equal since an aluminum-solvent coordinate bond is broken and an Al-H-Zn bridge bond is formed in both. Of course the calculated enthalpies support our suggestions, since they

$$\Delta H_{\text{reaction}} = \Delta H_{\text{solvation}} + \Delta H_{\text{bond energy}}$$

are equal within the uncertainty that lies in this type of calculation. The negative enthalpy of reaction indicated that the Al-H-Zn bridge bond is stronger than the aluminum solvent bond. The entropy of reaction 9 is positive, which is expected since the partition function for two molecules translating independently should be greater than that for the vibration of the solvent coordinate bond. The magnitude of ΔS is, however, not as great as one would have expected (generally in the range of 10 eu^{13}) since formation of the double-hydrogen bridge restricts the degrees of freedom of the molecules. In Eq. 10, two double hydrogen bridge units are formed, which leads to a negative entropy of reaction.

Table 6. Equilibrium Constants at Various Temperatures for the Reaction
 $\text{LiZr}(\text{CH}_3)_2\text{AlH}_4 \cdot \text{S} = \text{LiZr}(\text{CH}_3)_2\text{AlH}_4 + \text{S}$ in Tetrahydrofuran

Temperature (°C)	K ^a	lnK	1/T (°K ⁻¹) x 10 ³
35	4.6	1.53	3.2
21	5.2	1.64	3.4
4	6.1	1.81	3.6
-19	7.0	1.95	3.9
-36	7.7	2.04	4.2
-51	8.5	2.14	4.5
-63	9.8	2.28	4.8
-81	10.3	2.33	5.2

^aAn exponential curve fit to the data yields $K = 1.4 e^{404/T}$ with a correlation factor of $R^2 = 0.96$. This equation gives the following thermodynamic parameters:

$$\begin{aligned}\Delta H &= -803 \text{ cal/mole} \\ \Delta S &= 0.61 \text{ eu}\end{aligned}$$

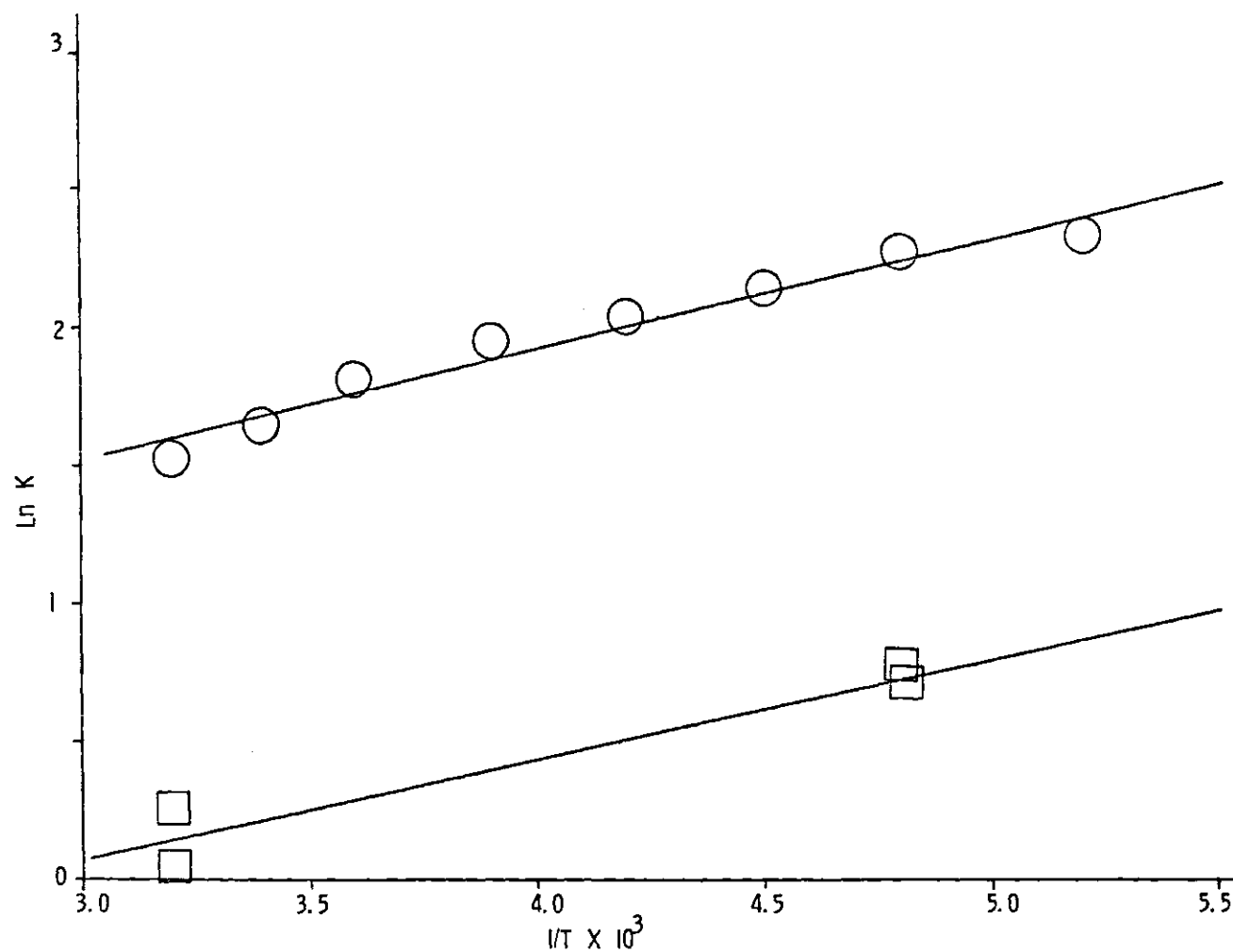


Figure 10. Plot of $\ln K$ vs $1/T$ for the Reactions: $\bigcirc \text{LiZn}(\text{CH}_3)_2\text{AlH}_4 \cdot \text{S} = \text{LiZn}(\text{CH}_3)_2\text{AlH}_4 + \text{S}$
 $\square \text{LiZn}_2(\text{CH}_3)_4\text{AlH}_4 \cdot \text{S} = \text{LiZn}_2(\text{CH}_3)_4\text{AlH}_4 + \text{S}$

Table 7. Equilibrium Constants at Various Temperatures for the Reaction
 $\text{LiZn}_2(\text{CH}_3)_4\text{AlH}_4 \cdot \text{S} = \text{LiZn}_2(\text{CH}_3)_4\text{AlH}_4 + \text{S}$ in Tetrahydrofuran

Temperature (°C)	K^a	$\ln K$	$1/T$ (°K ⁻¹) $\times 10^3$
35	1.0	0.04	3.2
35	1.3	0.25	3.2
-63	2.0	0.70	4.8
-63	2.1	0.76	4.8

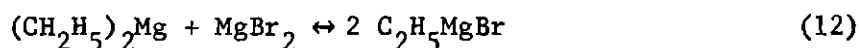
^aAn exponential curve fit to the data yields $K = 0.36 e^{364/T}$ with a correlation factor of $R^2 = 0.93$. This equation gives the following thermodynamic parameters:

$$\begin{aligned}\Delta H &= -724 \text{ cal/mole} \\ \Delta S &= -2.0 \text{ eu}\end{aligned}$$

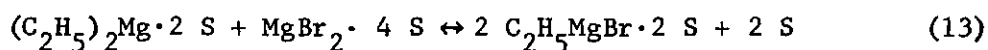
A simple representation of the basic solvation equilibrium is shown in Eq. 11. The forward reaction should be endothermic ($\Delta H > 0$) since a coordinate bond breaks and the entropy should be positive ($\Delta S > 0$).



Both reactions 9 and 10 violate this principle, so the solvation equilibrium cannot be as simple as that of Eq. 11. Indeed, the solvation equilibrium is complicated by simultaneous formation of a double hydrogen bridge. There is, however, a precedent for this type of behavior. The Schlenk equilibrium for C_2H_5MgBr (Eq. 12) is reported to have ΔH and ΔS values of 6.1 Kcal/mole and 23.7 eu in THF,¹⁷ whereas these values become -3.7 Kcal/mole and -0.3 eu in diethyl ether.¹⁸

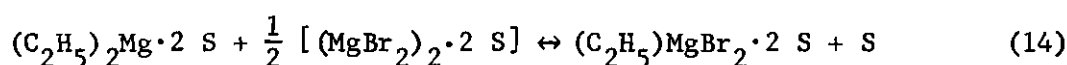


In THF, $(C_2H_5)_2Mg$, C_2H_5MgBr , and $MgBr_2$ are all monomeric.¹⁹ Typical organomagnesium halides have been shown to form disolvates in THF,²⁰ as do the diorganomagnesium compounds.²¹ The magnesium halides form tetrasolvates with THF.²² This leads one to revise Eq. 12 for the Schlenk equilibrium to Eq. 13 so that the solvation effects of THF can be included.¹³

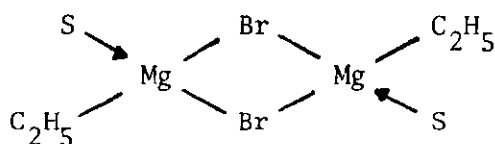
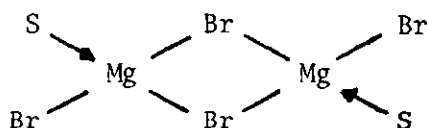


The signs of ΔH and ΔS for this reaction should follow the predictions

based on the solvation equilibrium in Eq. 11, since only monomeric species are present, i.e., no bridge bonds are being formed. The data, of course, are consistent with this suggestion. In diethyl ether, $(C_2H_5)_2Mg$ is monomeric while C_2H_5MgBr is essentially dimeric. Magnesium bromide is more highly associated than even a dimer.¹⁹ The Schlenk equilibrium in Eq. 8 should then be revised to Eq. 14, so solvation effects can be included.



(For simplicity, magnesium bromide is written as the dimer in this equation.) Diorganomagnesium compounds are known to form bis (diethyl etherates), whereas dimeric $MgBr_2$ and C_2H_5MgBr would have one solvent molecule per magnesium as shown by the structures below.



The reaction in Eq. 14 is similar to reactions 9 and 10 above in that coordinated solvent is displaced with the formation of a double halogen bridge. Both the ΔH and ΔS for this reaction are negative, not what one would predict based on the simple solvation equilibrium of Eq. 11, but indeed consistent with the thermodynamic parameters observed for reactions 9 and 10.

The concentration of the THF solutions of $LiZn(CH_3)_2AlH_4$ studied initially by infrared analysis were about 0.2 to 0.4 M. These solutions,

after preparation, remained clear for a few hours at room temperature, but then began to deposit a black solid. It was found that even after sitting one week not all of the zinc deposited from these solutions. Analysis of the black solid revealed that it contained Li:Zn:H:Al in a molar ratio of 1.06:2.00:3.20:0.05. An x-ray powder diffraction pattern of the solid contained lines due to LiZnH_3 and Zn metal only. It is suggested that LiZn_2H_5 precipitated from the solution of $\text{LiZn}(\text{CH}_3)_2\text{AlH}_4$ in THF and then decomposed rapidly to LiZnH_3 and ZnH_2 , with the ZnH_2 undergoing subsequent decomposition to Zn metal. (This point will be discussed in more detail later.) On the other hand, when a 0.2 M solution of $\text{LiZn}(\text{CH}_3)_2\text{AlH}_4$ was diluted 20-fold or greater with THF, a white precipitate of ZnH_2 formed within five minutes. Also, if LiAlH_4 is added to a dilute solution of $(\text{CH}_3)_2\text{Zn}$ in THF, i.e., about 0.01 M, a white precipitate of ZnH_2 begins to form within five minutes. The yields of ZnH_2 , however, are low, never being greater than 50%. The fact that LiZnH_3 is formed at concentrations greater than 0.1 M, but not at concentrations less than this, suggests that this hydride results from XIV, the dimer of $\text{LiZn}(\text{CH}_3)_2\text{AlH}_4$. The complex metal hydride only precipitates from solutions of $\text{LiZn}(\text{CH}_3)_2\text{AlH}_4$ where the association value is at least 1.10. Solutions of $\text{LiZn}(\text{CH}_3)_2\text{AlH}_4$, which contain for the most part only the monomeric form I, result in the precipitation of ZnH_2 only. The fact that ZnH_2 is formed by way of $\text{LiZn}(\text{CH}_3)_2\text{AlH}_4$ in THF is good evidence that $\text{LiZn}(\text{CH}_3)_2\text{AlH}_4$ is the intermediate involved in the alkyl-hydrogen exchange reaction between LiAlH_4 and $(\text{CH}_3)_2\text{Zn}$ to give ZnH_2 . It has been known for quite some time that the reaction of a dialkylzinc compound with LiAlH_4

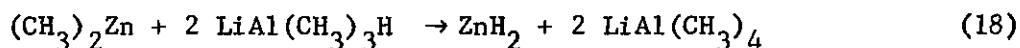
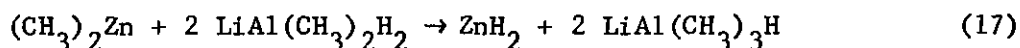
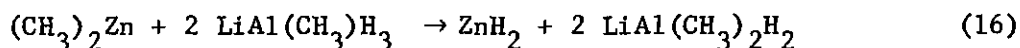
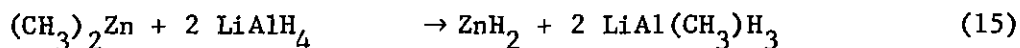
in diethyl ether produces ZnH_2 ¹⁶; however, no attempts have been made to determine the intermediates involved in the reaction. This work suggests that $\text{LiZn}(\text{CH}_3)_2\text{AlH}_4$ is an intermediate in this reaction. The fact that $\text{LiZn}(\text{CH}_3)_2\text{AlH}_4$ can be detected in the reaction mixture of LiAlH_4 with $(\text{CH}_3)_2\text{Zn}$ which produces ZnH_2 in THF is strong evidence to support the above statement.

Schlesinger and co-workers have reported that the most satisfactory method of preparing ZnH_2 involves the addition of one part $(\text{CH}_3)_2\text{Zn}$ to two parts LiAlH_4 in diethyl ether solution. They did not report the results that would be obtained if one were to vary the ratio of reactants or reverse the mode of addition. Because of some observations that we made in a previous study, we had reason to believe that the results of this reaction may be different if carried out under different conditions than those reported by Schlesinger and co-workers. We have now studied this reaction under a variety of conditions and the results are summarized in Table 8. The data indicate that the course of the reaction is greatly influenced by both the mode of addition and the ratio of reactants. These results are quite unusual, since previous studies in this laboratory have shown that the reactions of LiAlH_4 with $(\text{C}_2\text{H}_5)_2\text{Mg}$,²³ $(\text{CH}_3)_2\text{Mg}$,²⁴ and $(\text{C}_6\text{H}_5)_2\text{Mg}$ ²⁵ in diethyl ether are not sensitive to either of these parameters.

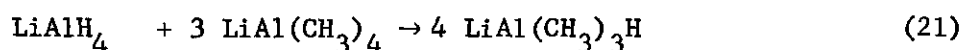
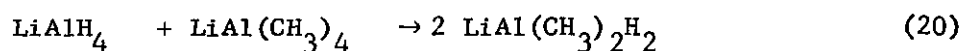
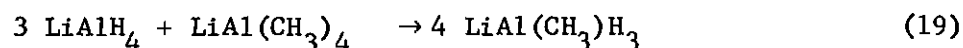
When $(\text{CH}_3)_2\text{Zn}$ was added to LiAlH_4 in four equal increments such the ratio of total zinc to aluminum was 0.5:1, 1:1, 1.5:1, and 2:1 after each of the four additions, the reaction proceeded in a stepwise fashion exchanging methyl groups on zinc for hydrogen on aluminum as shown in Eq. 15-18.

Table 8. Products Obtained from Various Reactions Between LiAlH_4 and $(\text{CH}_3)_2\text{Zn}$ in Diethyl Ether

Ratio $(\text{CH}_3)_2\text{Zn}/$ LiAlH_4	Analysis of Solid Li:Zn:H:Al	Components of Solid As Inferred from Powder Diffraction	Analysis of Solution Li:Al:CH ₃ :H:Zn	Components of Solution As Inferred from Infrared Spectra
Reactions Where $(\text{CH}_3)_2\text{Zn}$ Was Added to LiAlH_4 ^a				
0.5	0.02:1.00:2.04:0.03	ZnH_2	1.04:1.00:0.98:3.11:0.00	$\text{LiAl}(\text{CH}_3)\text{H}_3$
1.0	0.01:1.00:2.03:0.03	ZnH_2	1.01:1.00:2.01:1.99:0.02	$\text{LiAl}(\text{CH}_3)_2\text{H}_2$
1.5	0.01:1.00:2.08:0.02	ZnH_2	1.03:1.00:2.97:0.96:0.04	$\text{LiAl}(\text{CH}_3)_3\text{H}$
2.0	0.03:1.00:2.05:0.02	ZnH_2	1.04:1.00:3.98:0.00:0.03	$\text{LiAl}(\text{CH}_3)_4$
Reactions Where LiAlH_4 Was Added to $(\text{CH}_3)_2\text{Zn}$ ^a				
2.0	--	--	1.02:0.99:3.98:4.02:2.00	$\text{LiZn}(\text{CH}_3)_4\text{AlH}_4$
1.0	0.62:2.00:4.63:0.00	$\text{LiZnH}_3 + \text{ZnH}_2$	0.69:1.00:1.98:1.70:0.03	$(\text{CH}_3)_2\text{AlH} + \text{LiAl}(\text{CH}_3)_2\text{H}_2$
0.5	0.01:1.00:2.02:0.00	ZnH_2	1.01:1.00:1.03:3.04:0.00	$\text{LiAl}(\text{CH}_3)\text{H}_3$
^a Reactions were stirred for one hour before the products were separated.				



Support for these reactions proceeding as shown is provided by the infrared spectra of the supernatant solutions remaining after each incremental addition. These spectra (Figure 11) are identical to the infrared spectra of $\text{LiAl}(\text{CH}_3)\text{H}_3$, $\text{LiAl}(\text{CH}_3)_2\text{H}_2$, $\text{LiAl}(\text{CH}_3)_3\text{H}$, and $\text{LiAl}(\text{CH}_3)_4$ in diethyl ether solution prepared by allowing $\text{LiAl}(\text{CH}_3)_4$ to redistribute with LiAlH_4 according to the stoichiometry shown in Eq. 19-21. Lithium tetramethylaluminate was prepared by reacting CH_3Li with $(\text{CH}_3)_3\text{Al}$ in diethyl ether.²⁶



Further support for these reactions proceeding as shown is provided by the fact that the aluminum complexes $\text{LiAl}(\text{CH}_3)_2\text{H}_2$, $\text{LiAl}(\text{CH}_3)_3\text{H}$, and $\text{LiAl}(\text{CH}_3)_4$ were formed according to Eq. 16-18 when $(\text{CH}_3)_2\text{Zn}$ was added to authentic preformed samples of $\text{LiAl}(\text{CH}_3)\text{H}_3$, $\text{LiAl}(\text{CH}_3)_2\text{H}_2$, and $\text{LiAl}(\text{CH}_3)_3\text{H}$ in 1:2 ratio in diethyl ether.

When $(\text{CH}_3)_2\text{Zn}$ was added separately to LiAlH_4 in 0.5:1, 1:1, 1.5:1, and 2:1 molar ratios, the reactions proceeded according to Eq. 22-25.

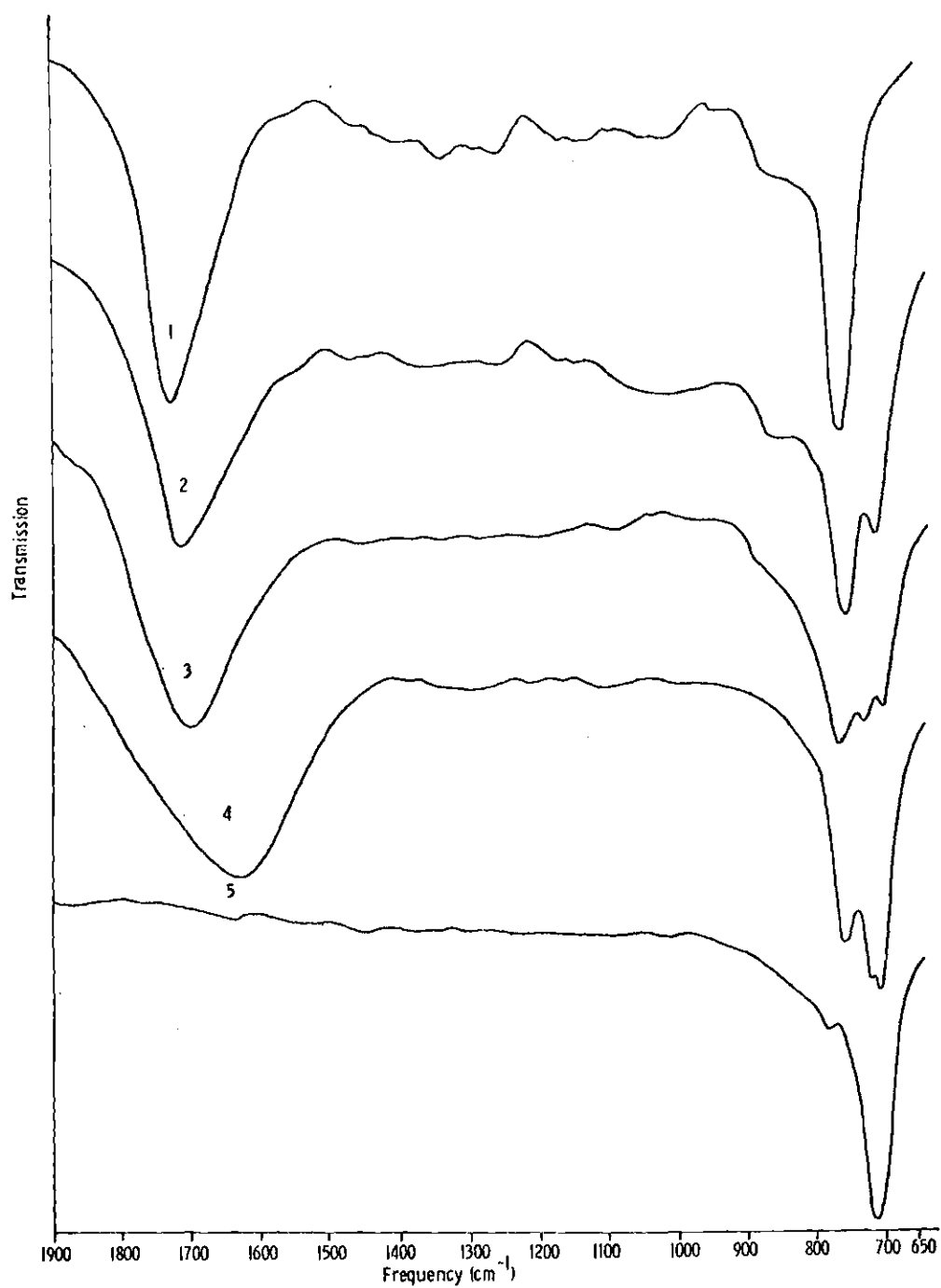
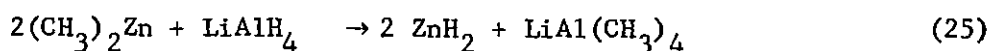
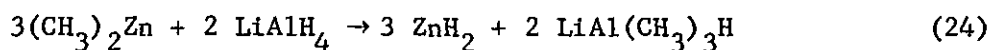
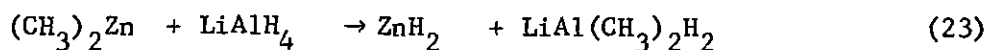
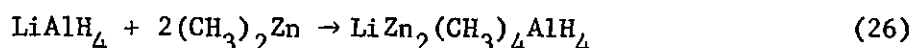


Figure 11. Infrared Spectra of Supernatant Solutions Obtained by Adding $(\text{CH}_3)_2\text{Zn}$ to LiAlH_4 in Diethyl Ether--Ratio $(\text{CH}_3)_2\text{Zn}:\text{LiAlH}_4$ (1) Pure LiAlH_4 , (2) 0.5:1.0, (3) 1.0:1.0, (4) 1.5:1.0, (5) 2.0:1.0



Support for these reactions is provided by data in Table 8. In each case, the solid isolated from these reactions was found to be ZnH_2 . Infrared spectra of the supernatant solutions showed the presence of the aluminum complexes listed in reactions 22-25.

The infrared spectra of the solutions that resulted when LiAlH_4 was added to $(\text{CH}_3)_2\text{Zn}$ in four increments, such that the ratio of total aluminum to zinc was 0.5:1, 0.75:1, 1:1, and 2:1, are shown in Figure 12. After the addition of each increment, the resulting mixture was stirred for five minutes before the infrared spectrum was recorded. Upon the addition of the first increment, a clear solution resulted. The infrared spectrum of the solution (bands at 1500 cm^{-1} sh,s; 1400 cm^{-1} br,s; 795 cm^{-1} w; and 705 cm^{-1} s) corresponded very closely to that of $\text{LiZn}_2(\text{CH}_3)_4\text{-AlH}_4$ in THF. Evidently, when one part LiAlH_4 is added to two parts $(\text{CH}_3)_2\text{Zn}$, the two reagents do not react to give ZnH_2 and $\text{LiAl}(\text{CH}_3)_4$ but instead form $\text{LiZn}_2(\text{CH}_3)_4\text{AlH}_4$ according to Eq. 26. Upon addition of the second increment, some solid began to precipitate.



The infrared spectrum of the solution (1700 cm^{-1} sh; 1640 cm^{-1} br,s;

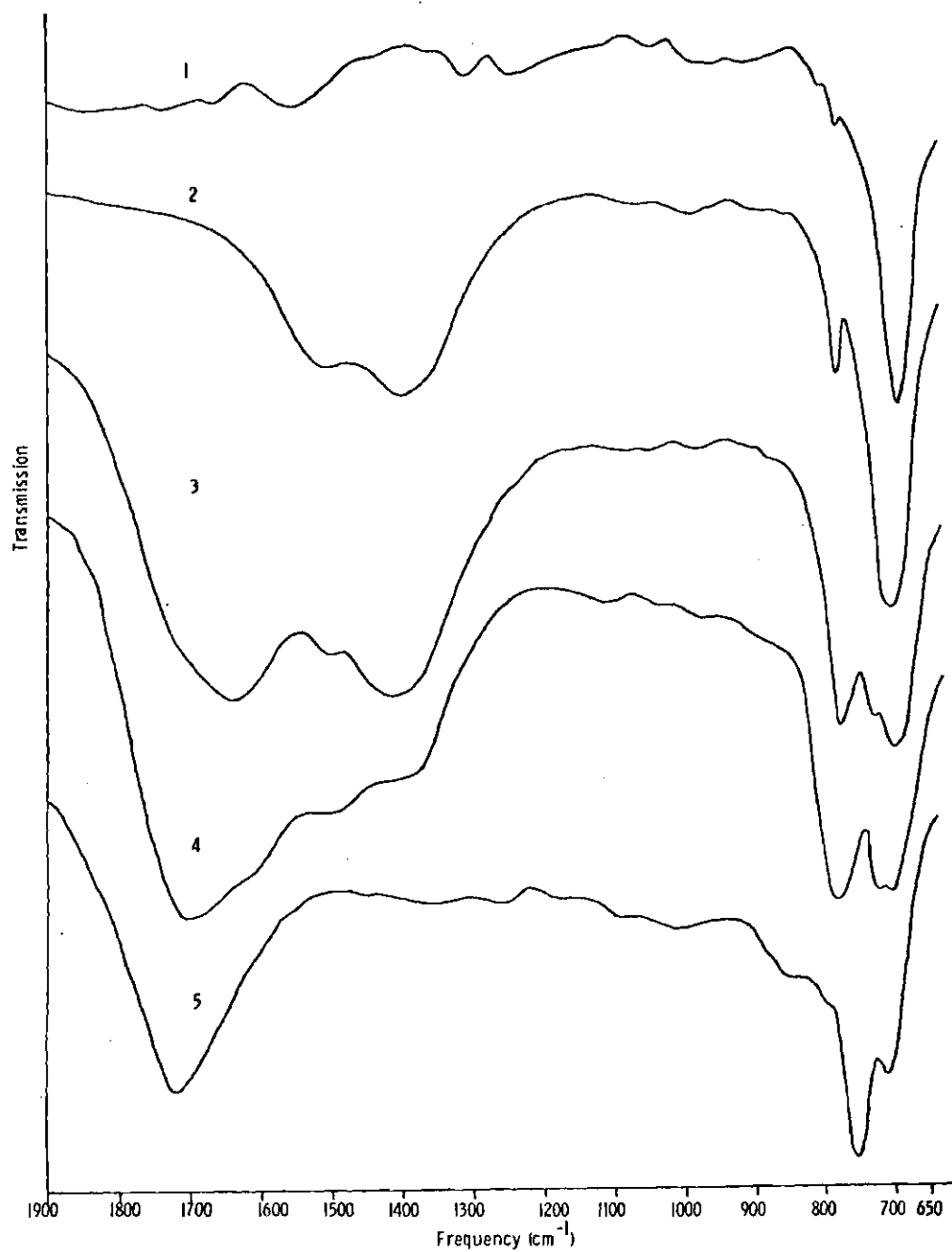
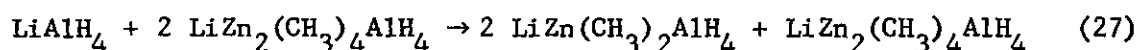
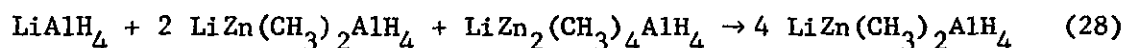


Figure 12. Infrared Spectra of Supernatant Solutions Obtained by Adding LiAlH_4 to $(\text{CH}_3)_2\text{Zn}$ in Diethyl Ether--Ratio $\text{LiAlH}_4:(\text{CH}_3)_2\text{Zn}$ (1) Pure $(\text{CH}_3)_2\text{Zn}$, (2) 0.5:1.0, (3) 0.75:1.0, (4) 1.0:1.0, (5) 2.0:1.0 -- Reaction Time of Five Minutes

1500 cm^{-1} sh,s; 1400 cm^{-1} br,s; 780 cm^{-1} s; 735 cm^{-1} sh,m; 700 cm^{-1} s) was characteristic of a mixture of $\text{LiAl}(\text{CH}_3)_2\text{H}_2$ ($\nu(\text{Al-H})$ 1700 cm^{-1}), $\text{LiZn}(\text{CH}_3)_2\text{AlH}_4$ (1660 cm^{-1} br,s; 1500 cm^{-1} sh,s; 1400 cm^{-1} br,s; 775 cm^{-1} s; 720 cm^{-1} sh,s in THF), and $\text{LiZn}_2(\text{CH}_3)_4\text{AlH}_4$ (1500 cm^{-1} sh,s; 1400 cm^{-1} br,s; 700 cm^{-1} s). The reaction which occurred upon addition of this increment is shown in Eq. 27. The precipitate and $\text{LiAl}(\text{CH}_3)_2\text{H}_2$ arise through the disproportionation of $\text{LiZn}(\text{CH}_3)_2\text{AlH}_4$.

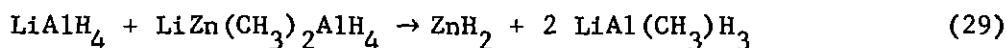


Equation 27 is supported by the fact that in THF $\text{LiZn}(\text{CH}_3)_2\text{AlH}_4$ decomposes to give $\text{LiAl}(\text{CH}_3)_2\text{H}_2$ as one of its products. Equation 27 shows that LiAlH_4 reacts with $\text{LiZn}_2(\text{CH}_3)_4\text{AlH}_4$ to produce two parts $\text{LiZn}(\text{CH}_3)_2\text{AlH}_4$; a reaction which is known to occur in THF. Upon addition of the third increment, more solid precipitated. The infrared spectrum of the solution (1700 cm^{-1} br,s; 1640 cm^{-1} sh; 1500 cm^{-1} sh; 1400 cm^{-1} sh,s; 780 cm^{-1} s; 720 cm^{-1} s) corresponded to a mixture of $\text{LiAl}(\text{CH}_3)_2\text{H}_2$ and $\text{LiZn}(\text{CH}_3)_2\text{AlH}_4$ (Eq. 28).

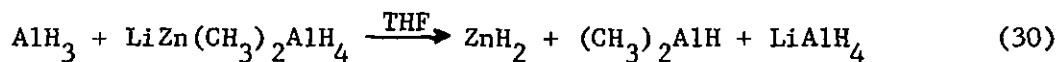


Again $\text{LiAl}(\text{CH}_3)_2\text{H}_2$ and the precipitate arise through disproportionation of $\text{LiZn}(\text{CH}_3)_2\text{AlH}_4$. Upon addition of the last increment copious quantities of solid precipitated. The infrared spectrum of the resulting super-

natant solution showed it to contain $\text{LiAl}(\text{CH}_3)_3\text{H}_3$ and the solid was found to be mostly ZnH_2 (Eq. 29).



It is known that in THF, AlH_3 reacts with $\text{LiZn}(\text{CH}_3)_2\text{AlH}_4$ to produce ZnH_2 according to Eq. 30. Therefore, it seems reasonable that a similar reaction would occur in diethyl ether between LiAlH_4 and $\text{LiZn}(\text{CH}_3)_2\text{AlH}_4$.



The infrared spectra of the solutions that result when LiAlH_4 is added separately to $(\text{CH}_3)_2\text{Zn}$ in molar ratios of 0.5:1, 1:1, and 2:1 ($\text{LiAlH}_4:(\text{CH}_3)_2\text{Zn}$) are shown in Figure 13. After the three additions were made, the resulting mixtures were stirred for one hour before the infrared spectra were recorded on the supernatant solutions. The data in Table 8 summarize the composition of the supernatant solutions and the solids that resulted from these reactions. The additions of LiAlH_4 to $(\text{CH}_3)_2\text{Zn}$ in 0.5:1 ratio again produced a solution which remained clear even after stirring for one hour. The infrared spectrum of the solution corresponded to $\text{LiZn}_2(\text{CH}_3)_4\text{AlH}_4$.

The addition of LiAlH_4 to $(\text{CH}_3)_2\text{Zn}$ in 1:1 ratio produced, after one hour of stirring, a solid which corresponded to 1:2.2 mixture of LiZnH_3 and ZnH_2 . The infrared spectrum of the supernatant solution (1760 cm^{-1} sh; 1700 cm^{-1} s; 780 cm^{-1} s; 725 cm^{-1} s; 700 cm^{-1} sh) corres-

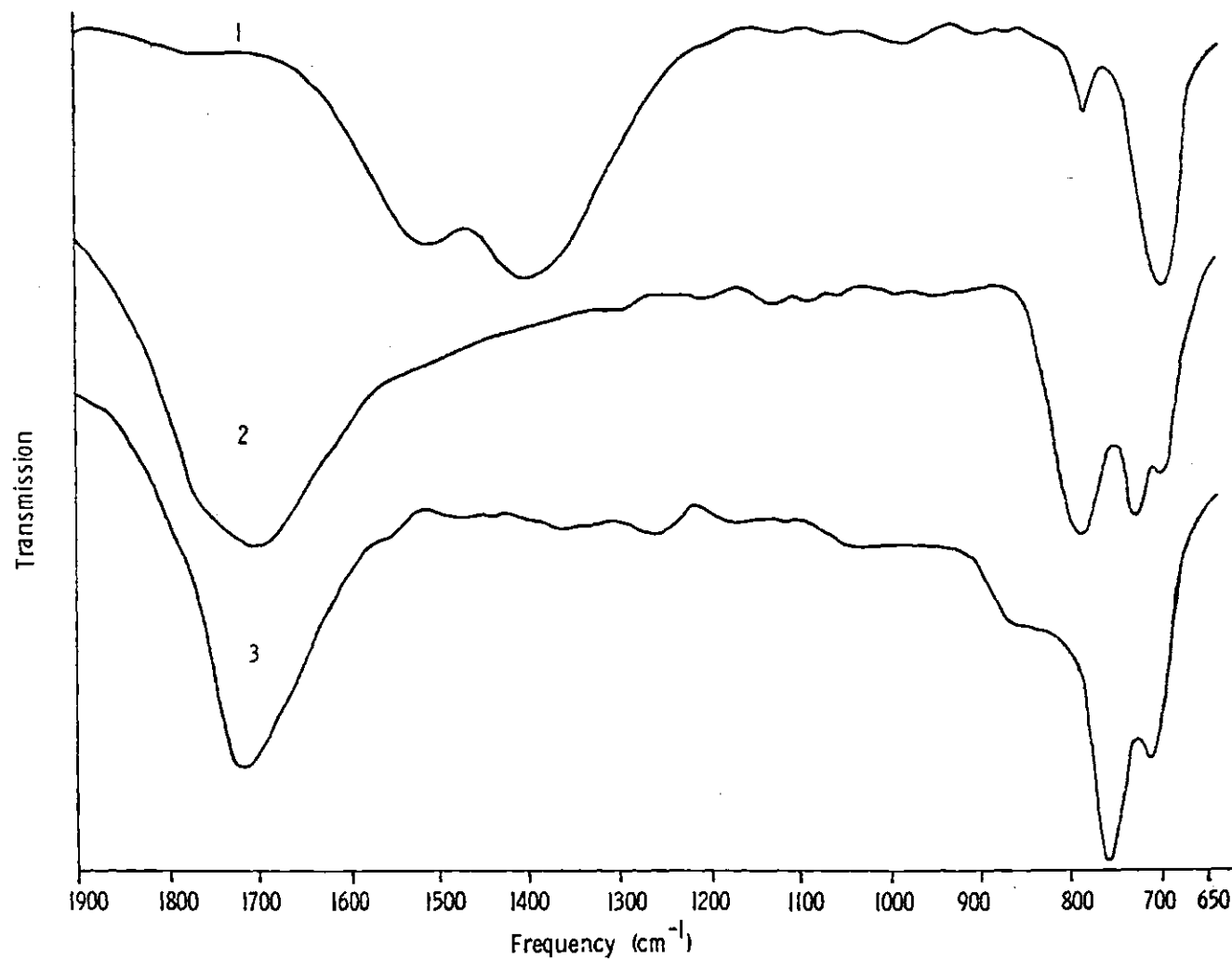
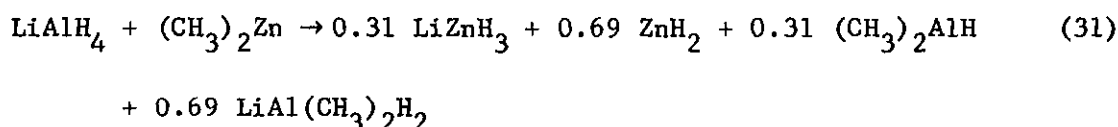
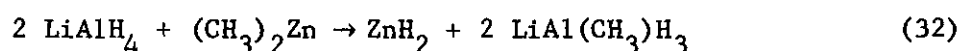


Figure 13. Infrared Spectra of Supernatant Solution Obtained by Adding LiAlH_4 to $(\text{CH}_3)_2\text{Zn}$ in Diethyl Ether--Ratio $\text{LiAlH}_4:(\text{CH}_3)_2\text{Zn}$ (1) 0.5:1.0, (2) 1.0:1.0, (3) 2.0:1.0 -- Reaction Time of One Hour

ponded to a mixture of $(\text{CH}_3)_2\text{AlH}$ ($\nu(\text{Al-H})$ 1760 cm^{-1}) and $\text{LiAl}(\text{CH}_3)_2\text{H}_2$. Analysis of the supernatant solution indicated that $(\text{CH}_3)_2\text{AlH}$ and $\text{LiAl}(\text{CH}_3)_2\text{H}_2$ were present in a 1:2.2 ratio; hence, Eq. 31.



The products arise through disproportionation of the initially formed $\text{LiZn}(\text{CH}_3)_2\text{AlH}_4$. This suggestion is reasonable since $\text{LiZn}(\text{CH}_3)_2\text{AlH}_4$ was observed spectroscopically after a reaction time of five minutes and, in addition, $\text{LiZn}(\text{CH}_3)_2\text{AlH}_4$ is known to decompose in THF giving a solid which contains LiZnH_3 and ZnH_2 . The addition of LiAlH_4 to $(\text{CH}_3)_2\text{Zn}$ in 2:1 ratio produced, after one hour of stirring, a solid which was found to be ZnH_2 . An infrared spectrum of the supernatant solution showed $\text{LiAl}(\text{CH}_3)_2\text{H}_3$ to be present. The reaction then proceeds as shown in Eq. 32.



It is very unusual to see only ZnH_2 formed in this reaction (Eq. 32), when the two previous reactions produced LiZnH_3 as well. The following explanation is presented for this behavior. The first equivalent of LiAlH_4 reacts with $(\text{CH}_3)_2\text{Zn}$ to form $\text{LiZn}(\text{CH}_3)_2\text{AlH}_4$, which can then decompose to give LiZnH_3 and ZnH_2 . But, before this happens, it is possible for the second equivalent of LiAlH_4 to react with $\text{LiZn}(\text{CH}_3)_2\text{AlH}_4$ to yield ZnH_2 and $\text{LiAl}(\text{CH}_3)_2\text{H}_3$. This explanation assumes that $\text{LiZn}(\text{CH}_3)_2\text{AlH}_4$ decom-

poses to LiZnH_3 and ZnH_2 at a rate much slower than it reacts with additional LiAlH_4 . This assumption is reasonable since, when LiAlH_4 was added incrementally to $(\text{CH}_3)_2\text{Zn}$ in 1:1 ratio, $\text{LiZn}(\text{CH}_3)_2\text{AlH}_4$ was observed spectroscopically after a reaction time of only five minutes and about 90% of the zinc was still in solution. The subsequent addition of an equivalent of LiAlH_4 to this solution caused an immediate precipitation of all the remaining zinc as ZnH_2 and the formation of $\text{LiAl}(\text{CH}_3)_2\text{H}_3$ in the solution.

The addition of LiAlH_4 to a 0.05 M solution of $(\text{CH}_3)_2\text{Zn}$ in 1:1 molar ratio produced, after one hour of stirring, a solid which was found to be ZnH_2 (no LiZnH_3 was present). The resulting supernatant solution was found to contain only $\text{LiAl}(\text{CH}_3)_2\text{H}_2$. Evidently $\text{LiZn}(\text{CH}_3)_2\text{AlH}_4$ is formed in this reaction also, but in the dilute solution (less than 0.10 M), it disproportionated to give only ZnH_2 . In the more concentrated solution, i.e., greater than 0.2 M, $\text{LiZn}(\text{CH}_3)_2\text{AlH}_4$ disproportionates to give mixtures of LiZnH_3 and ZnH_2 . This same behavior was observed in the reaction between LiAlH_4 and $(\text{CH}_3)_2\text{Zn}$ in THF. The disproportionation to ZnH_2 in dilute solution was shown to occur through the monomer form of $\text{LiZn}(\text{CH}_3)_2\text{AlH}_4$, whereas LiZnH_3 resulted from the dimer of $\text{LiZn}(\text{CH}_3)_2\text{AlH}_4$. This indicates that $\text{LiZn}(\text{CH}_3)_2\text{AlH}_4$ is capable of existing as an equilibrium between monomer and dimer forms in diethyl ether also.

There have been two recent studies where the synthesis of ZnH_2 has been reported.^{1,4} Earlier we reported that the addition of LiAlH_4 to a solution of $(\text{CH}_3)_2\text{Zn}$ in diethyl ether in a 1.5:1.0 ratio resulted in the precipitation of a solid which contained Zn and H in a ratio of 1.00:2.02. On the other hand, Shriver and co-workers, who did not report any

experimental details except to say that the procedure of Schlesinger¹⁶ was used, obtained a solid with Zn and H in a ratio of 1.00:2.26. The solid gave a positive flame test for Li, but the authors did not report the ratio of Li:Zn. The x-ray powder diffraction pattern of the solid did, however, contain lines due to LiZnH_3 ,³ showing that the solid was a mixture of LiZnH_3 and ZnH_2 . Therefore, it is likely that these workers added LiAlH_4 to $(\text{CH}_3)_2\text{Zn}$ in about a 1:1 ratio in diethyl ether. These two reports indicate a trend similar to what we have reported here. The addition of LiAlH_4 to $(\text{CH}_3)_2\text{Zn}$ in a ratio greater than 1:1 yields ZnH_2 , but addition at this ratio or less leads to mixtures of LiZnH_3 and ZnH_2 .

With the aid of our earlier results concerning the solution composition of $\text{LiZn}(\text{CH}_3)_2\text{AlH}_4$ and $\text{LiZn}_2(\text{CH}_3)_4\text{AlH}_4$, one can begin to rationalize the unusual results of the reaction of AlH_3 with $\text{NaZn}(\text{CH}_3)_2\text{H}$ and $\text{KZn}(\text{CH}_3)_2\text{H}$, that is, the formation of NaZn_2H_5 and KZn_2H_5 .

First, it is important to consider the structures of $\text{NaZn}(\text{CH}_3)_2\text{H}$ and $\text{KZn}(\text{CH}_3)_2\text{H}$ in THF.

The Zn-H stretching mode for $\text{NaZn}(\text{CH}_3)_2\text{H}$ (Figure 14) appears as a broad band extending from 1050 to 750 cm^{-1} with the center at 920 cm^{-1} . This unusually low Zn-H stretching frequency cannot be explained as being the result of solvent cleavage, since an analysis of the solution, just prior to obtaining the spectrum, showed that Na, Zn, CH_3 , and H were present in ratios of 1.03:1.00:1.96:0.91. Shriver and Kubas¹⁰ have reported that $\text{NaZn}(\text{CH}_3)_2\text{H}$ and $\text{NaZn}_2(\text{CH}_3)_4\text{H}$ are monomeric in THF. The asymmetric Zn-H stretching vibration for $\text{NaZn}_2(\text{CH}_3)_4\text{H}$ (Figure 15) appears as a broad band between 1400 and 1150 cm^{-1} with the peak maximum occurring

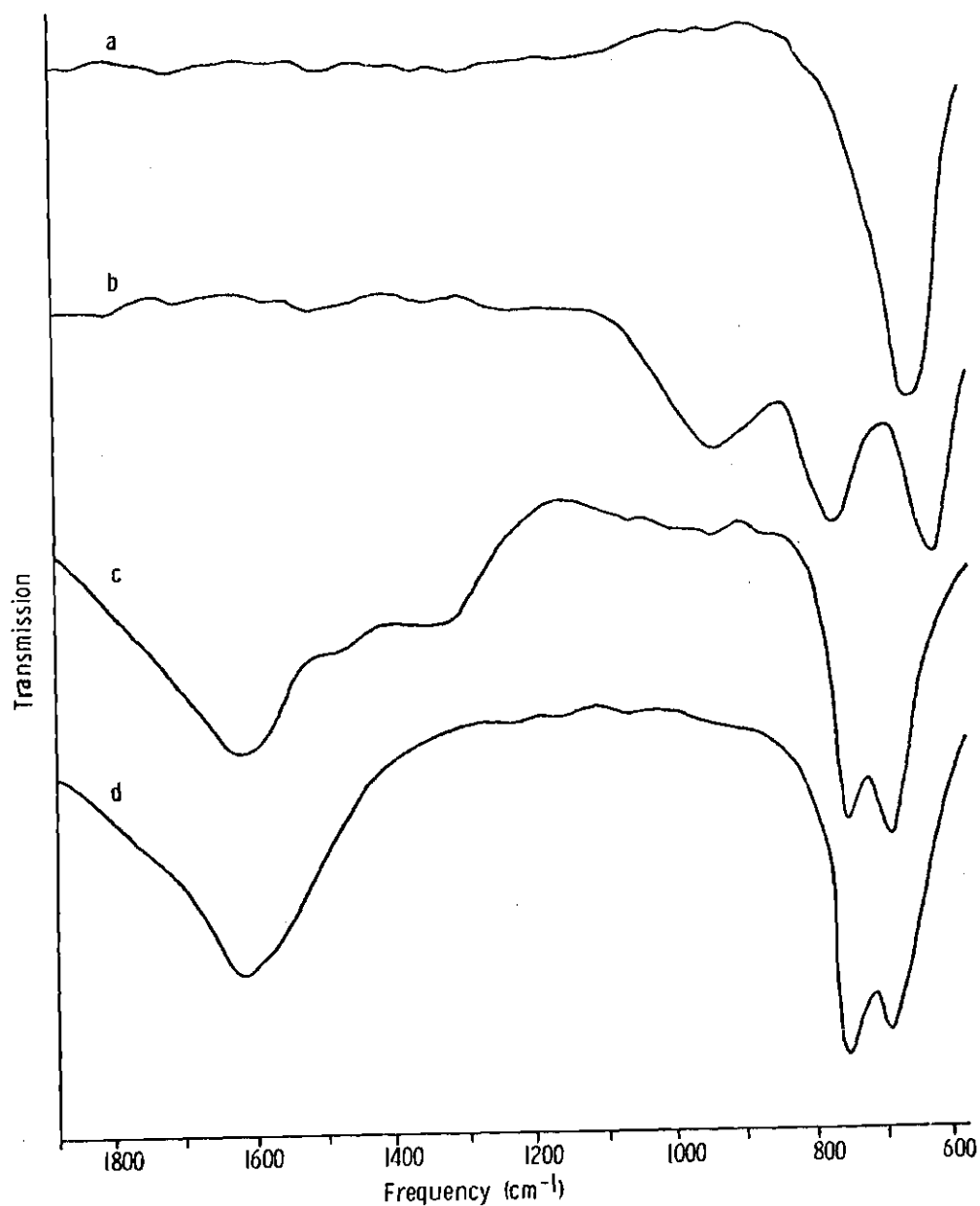


Figure 14. Infrared Spectra of $\text{NaZn}(\text{CH}_3)_2\text{H}$ and THF Soluble Products from Its Reaction with AlH_3 --(a) $(\text{CH}_3)_2\text{Zn}$ in THF, (b) $\text{NaZn}(\text{CH}_3)_2\text{H}$ in THF, (c) $\text{NaZn}(\text{CH}_3)_2\text{H} + \text{AlH}_3$ in THF after Five Minutes, (d) $\text{NaZn}(\text{CH}_3)_2\text{H} + \text{AlH}_3$ in THF after 24 Hours-- $\text{NaAl}_2(\text{CH}_3)_4\text{H}_3$

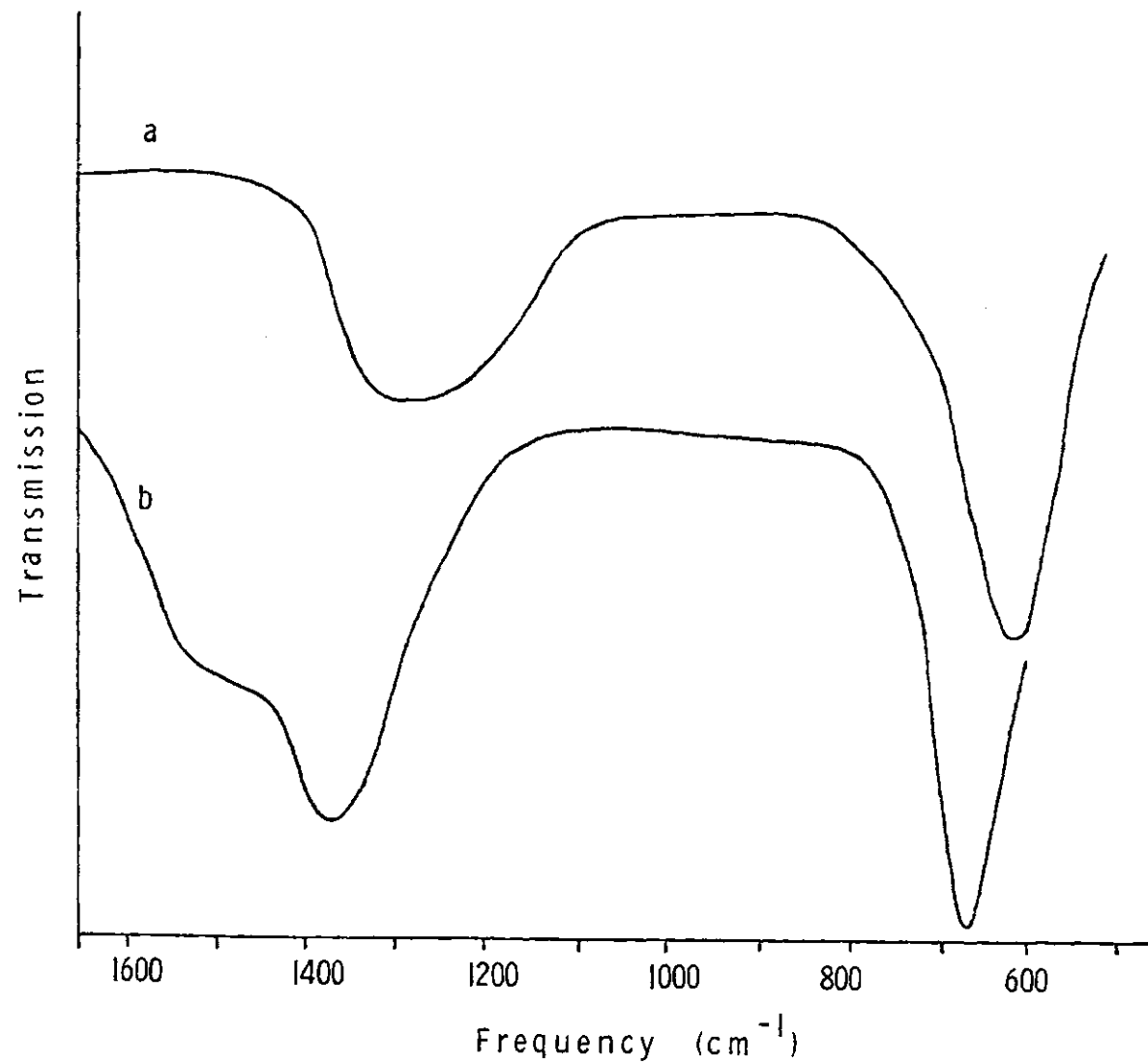
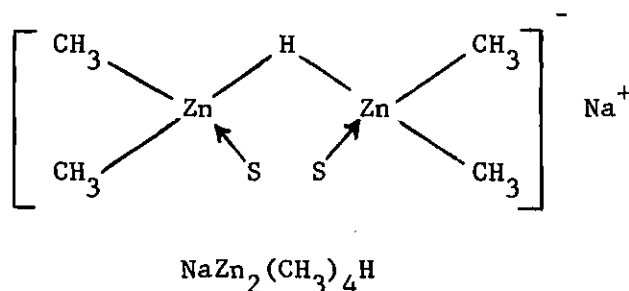


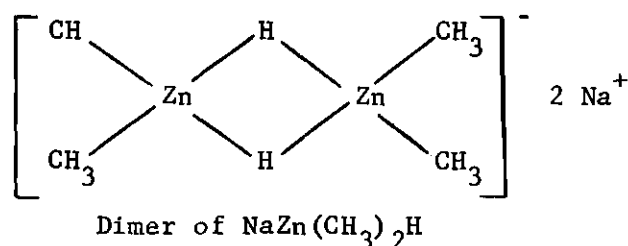
Figure 15. Infrared Spectra of (a) $\text{NaZn}_2(\text{CH}_3)_4\text{H}$ and (b) $\text{NaZn}_2(\text{CH}_3)_4\text{AlH}_4$

at 1260 cm^{-1} . This corresponds very closely to the Zn-H stretching vibration for $\text{LiZn}_2(\text{CH}_3)_4\text{H}$ at 1290 cm^{-1} , which indicates that the structures of the two compounds in THF should be similar. If $\text{NaZn}(\text{CH}_3)_2\text{H}$ is indeed monomeric in the solutions used in this study, then one would have expected to see a Zn-H stretching band for this compound somewhere in the region of $1400\text{--}1450\text{ cm}^{-1}$.



Since this was not observed, $\text{NaZn}(\text{CH}_3)_2\text{H}$ cannot have the same monomeric structure as $\text{LiZn}(\text{CH}_3)_2\text{H}$. However, the solutions of $\text{NaZn}(\text{CH}_3)_2\text{H}$ used in this work had concentrations in the range $0.8\text{--}1.0\text{ M}$ and therefore $\text{NaZn}(\text{CH}_3)_2\text{H}$ could be present as a dimer. Since Shriver and Kubas¹⁰ did not report the concentration range over which their association data apply, the possibility exists that their solutions were more dilute than ours. (Some of the results from this study do suggest that $\text{NaZn}(\text{CH}_3)_2\text{H}$ is monomeric at lower concentration.)

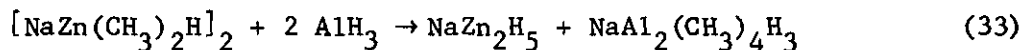
A dimer of $\text{NaZn}(\text{CH}_3)_2\text{H}$ would be expected to have the structure shown below where the two zinc atoms are tetrahedrally coordinated and connected by a double hydrogen bridge.



One would expect the asymmetric Zn-H stretching vibration for such a structure to be lower than the corresponding frequency for $\text{NaZn}_2(\text{CH}_3)_4\text{H}$ which has only one Zn-H-Zn bridge bond. This is what one observes. Therefore, it is not unreasonable that a 1.0 M solution of $\text{NaZn}(\text{CH}_3)_2\text{H}$ in THF exists as a dimer in solution. Shriver and Kubas²⁷ have also reported that the complex $\text{NaZn}(\text{C}_6\text{F}_5)_2\text{H}$ exists as a dimer with double hydrogen bridge bonds in diethyl ether. They report that the asymmetric Zn-H stretching vibration for the dimer appears as a strong broad band between 1300 and 1700 cm^{-1} . However, their spectra were recorded as nujol mulls of the completely desolvated solid and not as solutions in diethyl ether.

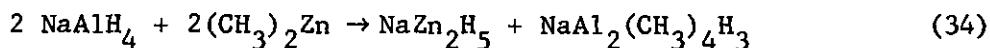
The infrared spectrum of an approximately 1.0 M solution of $\text{KZn}(\text{CH}_3)_2\text{H}$ in THF is shown later in Figure 19. It exactly matches the spectrum observed for $\text{NaZn}(\text{CH}_3)_2\text{H}$ in THF. Therefore, $\text{KZn}(\text{CH}_3)_2\text{H}$ is also believed to be a dimer in THF with a structure similar to that suggested for the $\text{NaZn}(\text{CH}_3)_2\text{H}$ dimer.

When a 0.9 M solution of $\text{NaZn}(\text{CH}_3)_2\text{H}$ in THF was allowed to react with an equimolar quantity of AlH_3 , an off white precipitate which was NaZn_2H_5 appeared immediately. After two hours all the zinc disappeared from the solution, indicating complete conversion to NaZn_2H_5 . The THF soluble product, $\text{NaAl}_2(\text{CH}_3)_4\text{H}_3$, remained in solution. The stoichiometry of the reaction is given by Eq. 33.

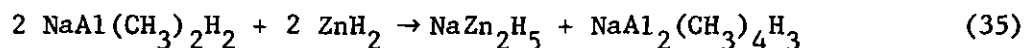


The reaction of NaAlH_4 with $(\text{CH}_3)_2\text{Zn}$ in 1:1 molar ratio also yielded

NaZn_2H_5 and $\text{NaAl}_2(\text{CH}_3)_4\text{H}_3$ according to Eq. 34.



In this case, however, a precipitate did not appear until a few minutes after the reactants had been mixed and in addition all the zinc disappeared from solution only after a period of one week. The reaction of $\text{NaAl}(\text{CH}_3)_2\text{H}_2$ with ZnH_2 in a 1:1 molar ratio yielded NaZn_2H_5 and $\text{NaAl}_2(\text{CH}_3)_4\text{H}_3$ according to Eq. 35.



In this case a clear solution remained for about 20 minutes before any solid began to form. After sitting for a period of one week, all the zinc finally disappeared from solution.

In each of these three cases the intermediate leading to the products could be observed by infrared spectroscopy. Figure 18 contains infrared spectra of the supernatant solution from the reaction of NaAlH_4 with $(\text{CH}_3)_2\text{Zn}$ in a 1:1 molar ratio after 5 minutes, 2.5 hours, 28 hours, 4 days, and 7 days. Only after seven days does the spectrum approach that of $\text{NaAl}_2(\text{CH}_3)_4\text{H}_3$. The remainder of the spectra which are of the intermediate leading to the product, are essentially identical; therefore, the spectrum of the reaction mixture after five minutes is representative and will be studied in detail. There is a very broad band in the metal-hydrogen stretching region extending from

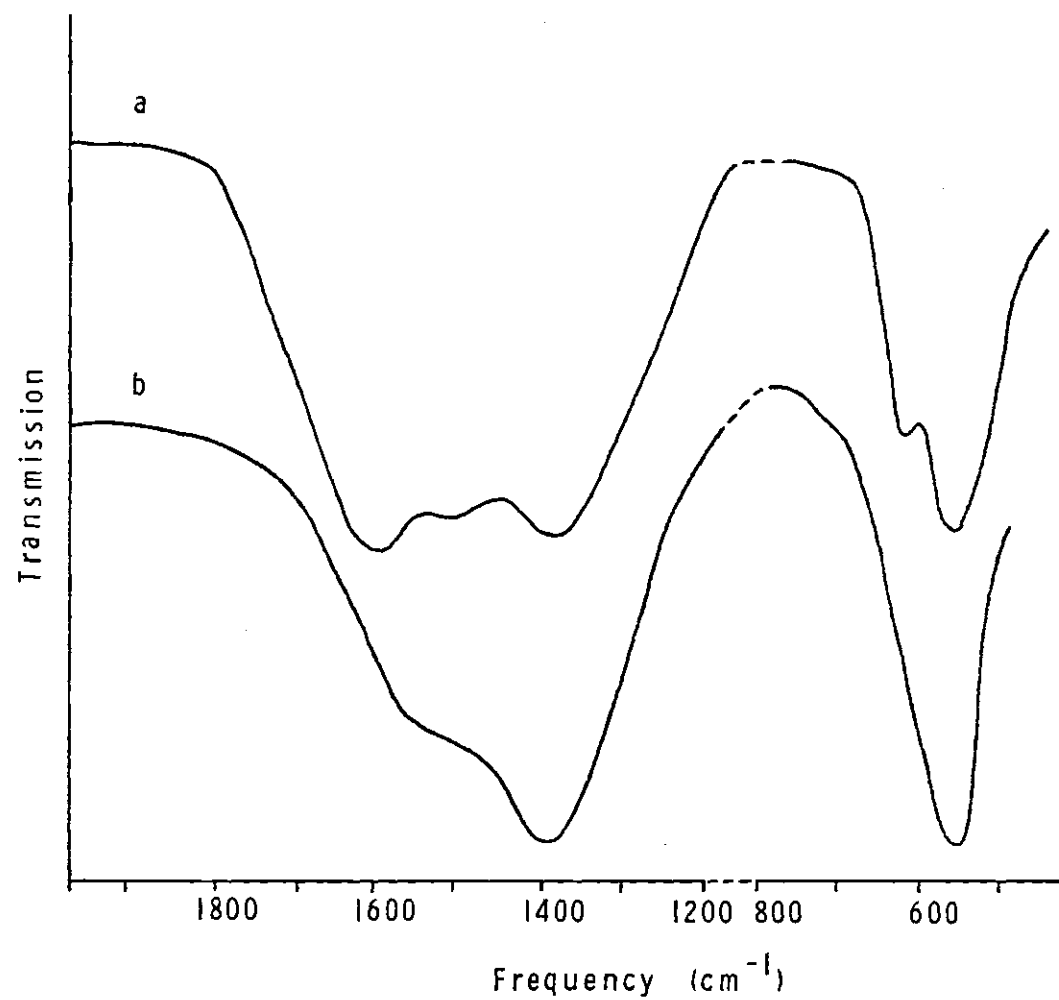


Figure 16. Infrared Spectra of Solutions Obtained When $(\text{CH}_3)_2\text{Zn}$ Was Added to NaAlH_4 in Tetrahydrofuran (a) NaAlH_4 to $(\text{CH}_3)_2\text{Zn}$, 1:1 (b) 1:2

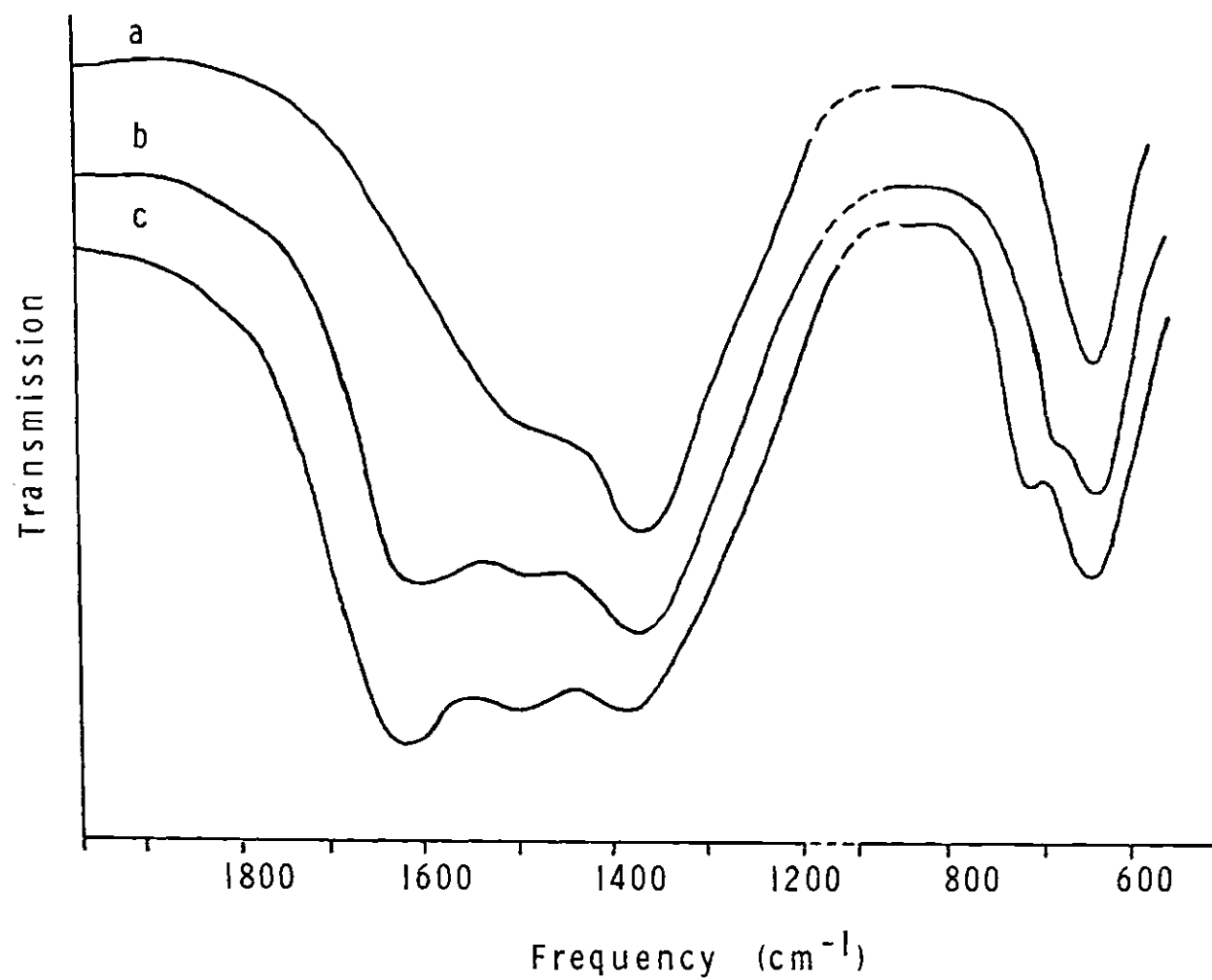


Figure 17. Infrared Spectra of Solutions Obtained by Adding NaAlH_4 to $(\text{CH}_3)_2\text{Zn}$ in Tetrahydrofuran - (a) 1:2 NaAlH_4 to $(\text{CH}_3)_2\text{Zn}$ (b) 2:3 NaAlH_4 to $(\text{CH}_3)_2\text{Zn}$, (c) 1:1 NaAlH_4 to $(\text{CH}_3)_2\text{Zn}$

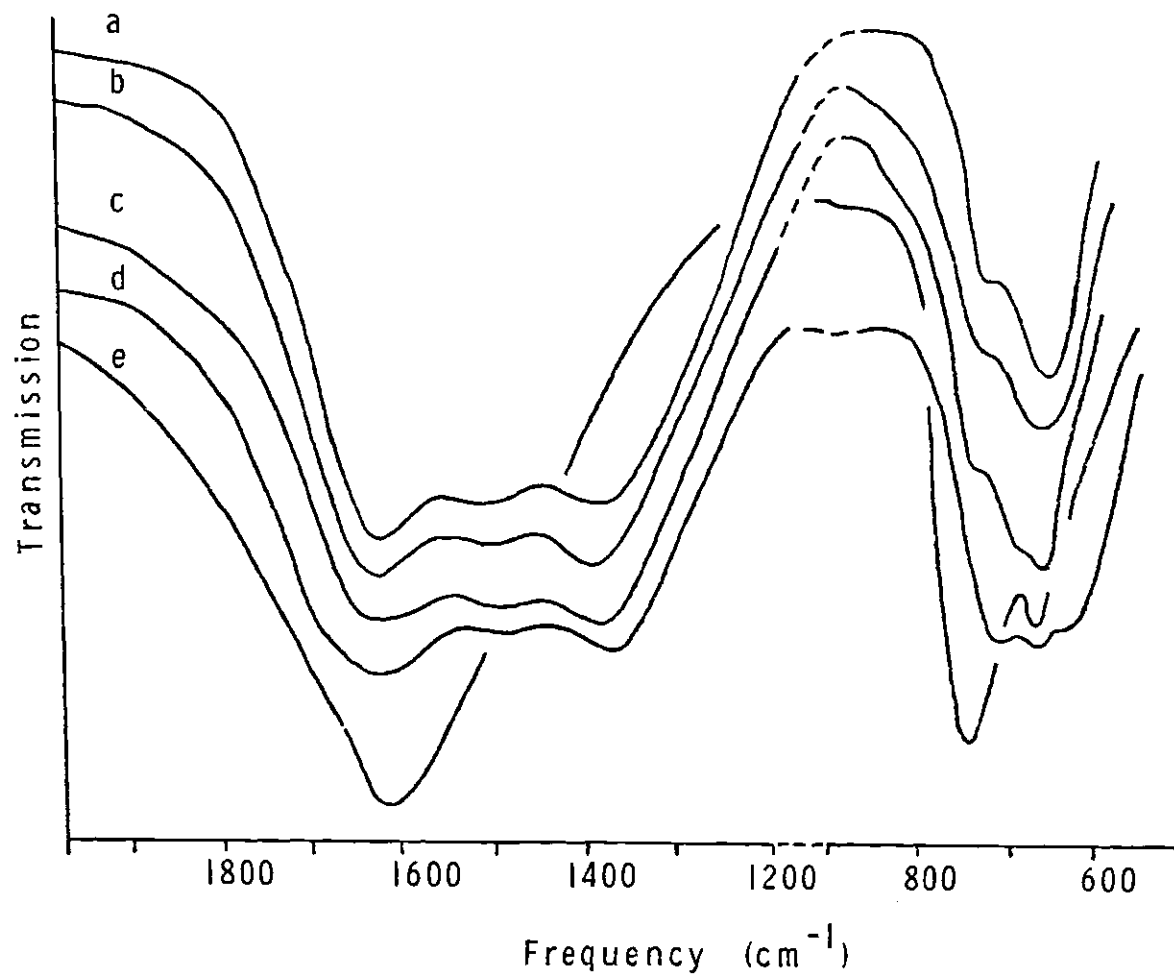


Figure 18. Infrared Spectra of Solutions Obtained by Adding NaAlH_4 to $(\text{CH}_3)_2\text{Zn}$ in Tetrahydrofuran: (a) 1:1 NaAlH_4 to $(\text{CH}_3)_2\text{Zn}$ after Five Minutes, (b) 1:1 NaAlH_4 to $(\text{CH}_3)_2\text{Zn}$ after 2.5 Hours, (c) 1:1 NaAlH_4 to $(\text{CH}_3)_2\text{Zn}$ after 28 Hours, (d) 1:1 NaAlH_4 to $(\text{CH}_3)_2\text{Zn}$ after Four Days, (e) 1:1 NaAlH_4 to $(\text{CH}_3)_2\text{Zn}$ after Seven Days

1800 to 1200 cm^{-1} . This spectrum is very similar to the one observed for $\text{LiZn}(\text{CH}_3)_2\text{AlH}_4$ prepared from LiAlH_4 and CH_3Zn except that in this case the terminal Al-H asymmetric stretching vibration occurs at 1615 cm^{-1} . The solution composition of $\text{LiZn}(\text{CH}_3)_2\text{AlH}_4$ which gave rise to such spectra was found to consist of an equilibrium between monomer and dimer forms of this compound. In view of the very close correspondence between the infrared spectra, the intermediate in the above reaction is probably $\text{NaZn}(\text{CH}_3)_2\text{AlH}_4$, which would have a solution composition similar to that of $\text{LiZn}(\text{CH}_3)_2\text{AlH}_4$ (see Scheme I).

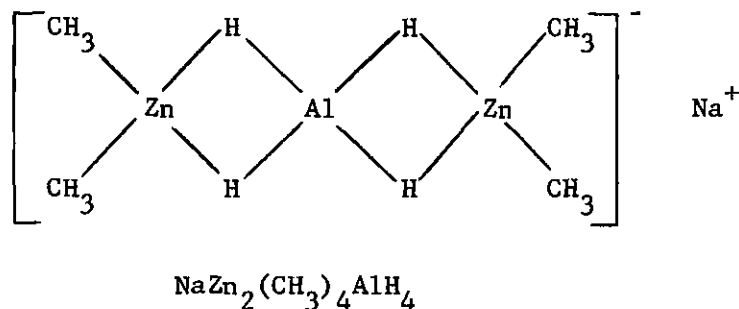
The intermediate involved in the formation of NaZn_2H_5 by the reaction of $\text{NaAl}(\text{CH}_3)_2\text{H}_2$ with ZnH_2 must also be $\text{NaZn}(\text{CH}_3)_2\text{AlH}_4$, since an infrared spectrum of the clear solution, which was initially formed, contained these same bands.

Earlier it was mentioned that solutions of $\text{LiZn}(\text{CH}_3)_2\text{AlH}_4$ decompose on standing to give a solid containing Li and Zn in a ratio of 1:2. However, the solutions were never observed to precipitate all of the zinc. Solutions of $\text{LiZn}(\text{CH}_3)_2\text{AlH}_4$ when diluted to about 0.01 M were found to precipitate ZnH_2 . Also the reactions of $\text{LiZn}(\text{CH}_3)_2\text{H}$ with AlH_3 or LiAlH_4 with $(\text{CH}_3)_2\text{Zn}$ in 1:1 ratio, when carried out in dilute solution, were found to precipitate ZnH_2 . Similar behavior occurs when either $\text{NaZn}(\text{CH}_3)_2\text{H}$ and AlH_3 or NaAlH_4 and $(\text{CH}_3)_2\text{Zn}$ are allowed to react in dilute solution. Both reactions produce ZnH_2 . However, when these same two reactions are carried out at concentrations greater than 0.2 M, NaZn_2H_5 was precipitated and not ZnH_2 . Earlier it was mentioned that $\text{NaZn}(\text{CH}_3)_2\text{H}$ appears to be dimeric at concentrations above 0.2 M but monomeric in more

dilute solutions. Solutions of $\text{LiZn}(\text{CH}_3)_2\text{H}$ appeared to be monomeric at all the concentrations employed in these studies. Based on these observations, it appears that monomeric $\text{MZn}(\text{CH}_3)_2\text{H}$ compounds react with alane to give $\text{MZn}(\text{CH}_3)_2\text{AlH}_4$ which can then undergo alkyl-hydrogen exchange to yield MZn_2H_5 or ZnH_2 depending on the concentration of the solution. In solutions above 0.2 M in concentration, $\text{MZn}(\text{CH}_3)_2\text{AlH}_4$ yields MZn_2H_5 . In more dilute solutions, it gives ZnH_2 . Reactions of MAlH_4 compounds with $(\text{CH}_3)_2\text{Zn}$ proceed in a similar way since they also produce the intermediate $\text{MZn}(\text{CH}_3)_2\text{AlH}_4$. It seems that the concentration of the intermediate is the factor which determines the products, either MZn_2H_5 or ZnH_2 , in these reactions. This leads one to conclude that a species similar to the dimer form of $\text{MZn}(\text{CH}_3)_2\text{AlH}_4$ would be the primary intermediate in the exchange reactions which lead to MZn_2H_5 . This statement is supported by the fact that association studies on solutions of $\text{LiZn}(\text{CH}_3)_2\text{AlH}_4$, when the concentration is greater than 0.2 M, indicate the presence of a considerable amount of a dimeric species. The primary intermediate in the exchange reactions which lead to ZnH_2 must be the monomeric form of $\text{MZn}(\text{CH}_3)_2\text{AlH}_4$ (I). This statement is supported by the fact that ZnH_2 is only precipitated from solution of $\text{LiZn}(\text{CH}_3)_2\text{AlH}_4$ where the association value is one.

The reaction of $\text{NaZn}_2(\text{CH}_3)_4\text{H}$ with alane behaves in a similar way to the reaction of $\text{LiZn}_2(\text{CH}_3)_4\text{H}$ with alane in that $\text{NaZn}_2(\text{CH}_3)_4\text{AlH}_4$ is formed. The infrared spectra of $\text{NaZn}_2(\text{CH}_3)_4\text{H}$ and $\text{NaZn}_2(\text{CH}_3)_4\text{AlH}_4$ are shown in Figure 15. The spectrum of $\text{NaZn}_2(\text{CH}_3)_4\text{AlH}_4$ is very similar to that of $\text{LiZn}_2(\text{CH}_3)_4\text{AlH}_4$. There is a very broad peak in the metal-hydrogen stretching region with a shoulder at 1480 and maximum at 1380 cm^{-1} . There

is no band in the terminal Al-H stretching or deformation region. The structure of $\text{NaZn}_2(\text{CH}_3)_4\text{AlH}_4$, therefore, must be similar to that of $\text{LiZn}_2(\text{CH}_3)_4\text{AlH}_4$.



The reactions of $\text{KZn}(\text{CH}_3)_2\text{H}$ with alane and KAlH_4 with $(\text{CH}_3)_2\text{Zn}$ in 1:1 molar ratio behave differently than the corresponding sodium system, although KZn_2H_5 is formed in both reactions. The difference is due to the fact that there is no concentration dependence by the reaction product and the rate of formation of KZn_2H_5 is much faster than in the sodium system. The reaction of KAlH_4 with $(\text{CH}_3)_2\text{Zn}$ in 1:1 molar ratio is complete within three hours regardless of the concentration of the starting materials and the reaction of $\text{KZn}(\text{CH}_3)_2\text{H}$ with alane is complete within five minutes. In view of this large rate increase and the non-concentration dependence of the product, the mechanism for the formation of KZn_2H_5 could be different from that presented for the sodium systems. One would expect $\text{KZn}(\text{CH}_3)_2\text{AlH}_4$ to be involved in the reaction of KAlH_4 with $(\text{CH}_3)_2\text{Zn}$; however, infrared spectral analysis of the reaction mixture in its intermediate stages failed to show the bands characteristic of the $[\text{Zn}(\text{CH}_3)_2\text{AlH}_4]^{-1}$ system. One such spectrum is shown in Figure 19. There is a broad band extending from $1500\text{--}1150\text{ cm}^{-1}$ in the metal-hydrogen stretching

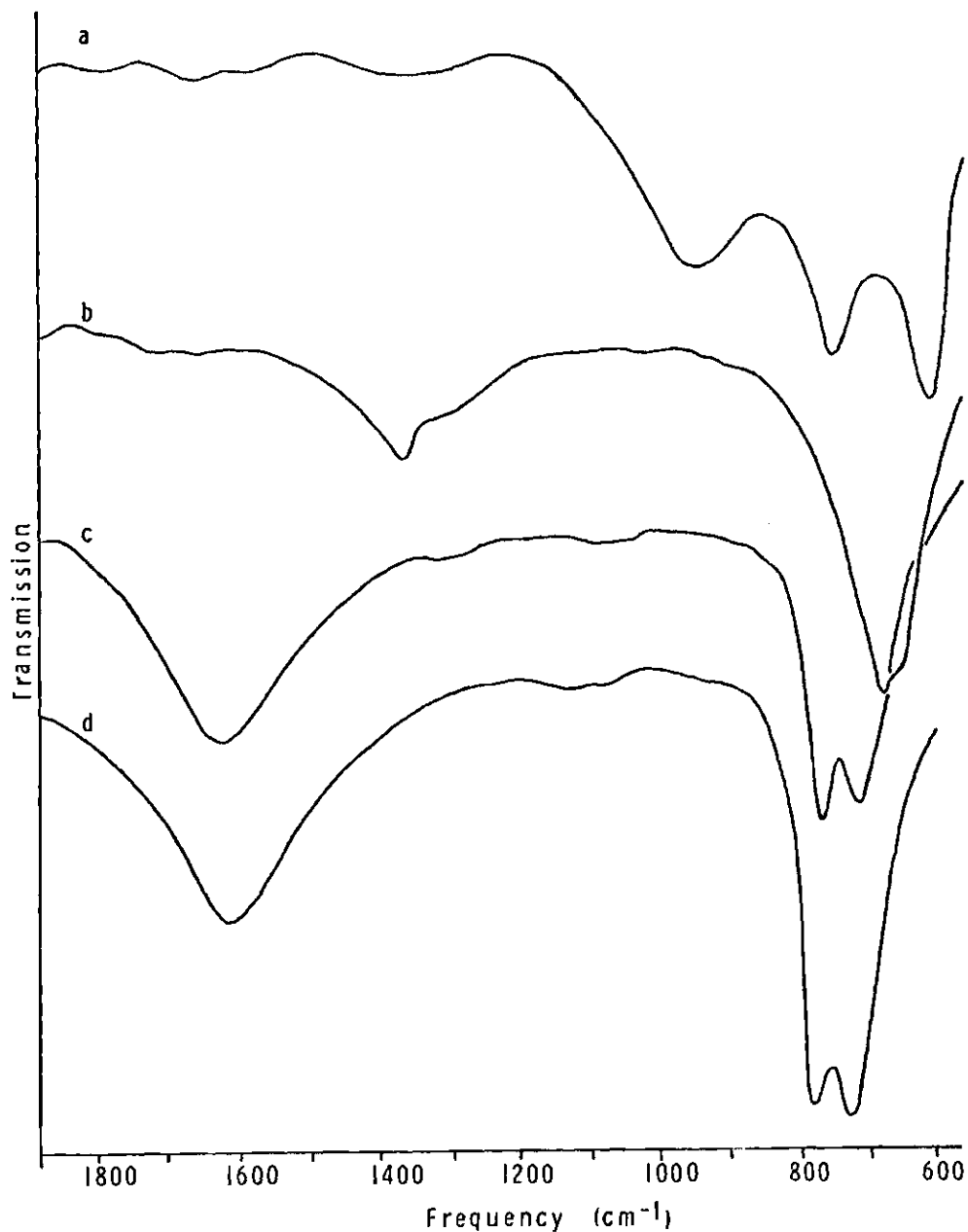


Figure 19. Infrared Spectra of $\text{KZn}(\text{CH}_3)_2\text{H}$, the Products from Its Reaction with AlH_3 , and the Products from the Reaction of KAlH_4 with $(\text{CH}_3)_2\text{Zn}$ in Tetrahydrofuran: (a) $\text{KZn}(\text{CH}_3)_2\text{H}$ in THF, (b) 1:1 $\text{KAlH}_4 + (\text{CH}_3)_2\text{Zn}$ after Three Minutes, (c) 1:1 $\text{KZn}(\text{CH}_3)_2\text{H}$ to AlH_3 after Three Hours, (d) 1:1 $\text{KAlH}_4 + (\text{CH}_3)_2\text{Zn}$ after Three Hours

region. This band has its maximum adsorption at 1380 cm^{-1} and has a shoulder at 1300 cm^{-1} . In the $700\text{--}600\text{ cm}^{-1}$ region there is a band at 675 cm^{-1} which has a shoulder at 650 cm^{-1} . Attempts to record infrared spectra of the intermediates involved in the reaction of $\text{KZn}(\text{CH}_3)_2\text{H}$ were unsuccessful. It may be that the mechanism of these reactions is similar to those given for the sodium system, but due to lack of evidence we cannot say definitely whether this is true.

The reaction of $\text{KZn}_2(\text{CH}_3)_4\text{H}$ with alane differs considerably from the reaction of $\text{LiZn}_2(\text{CH}_3)_4\text{H}$ and $\text{NaZn}_2(\text{CH}_3)_4\text{H}$ with alane. While the latter two reactions yield $\text{LiZn}_2(\text{CH}_3)_4\text{AlH}_4$ and $\text{NaZn}_2(\text{CH}_3)_4\text{AlH}_4$, $\text{KZn}_2(\text{CH}_3)_4\text{H}$ reacts with either one or two equivalents of alane to yield KZn_2H_5 and apparently not $\text{KZn}_2(\text{CH}_3)_4\text{AlH}_4$. More evidence along this line is provided by considering the reactions of $\text{LiZn}_2(\text{CH}_3)_4\text{H}$ and $\text{NaZn}_2(\text{CH}_3)_4\text{H}$ with AlH_3 in 1:2 ratio. Both these reactions produce ZnH_2 , presumably by the reaction of AlH_3 with the initially formed $\text{LiZn}_2(\text{CH}_3)_4\text{AlH}_4$ and $\text{NaZn}_2(\text{CH}_3)_4\text{AlH}_4$. Since $\text{KZn}_2(\text{CH}_3)_4\text{H}$ reacts with AlH_3 in 1:2 ratio to produce KZn_2H_5 , this indicates that $\text{KZn}_2(\text{CH}_3)_4\text{AlH}_4$ was not formed.

When KAlH_4 and $(\text{CH}_3)_2\text{Zn}$ are allowed to react in a 1:2 molar ratio, a clear solution results. The infrared spectrum of this solution, shown in Figure 20, is exactly like the infrared spectrum of $\text{LiZn}_2(\text{CH}_3)_4\text{AlH}_4$ and $\text{NaZn}_2(\text{CH}_3)_4\text{AlH}_4$. If this clear solution is allowed to stand, after about 10 minutes a white solid which is KZn_2H_5 begins to precipitate. But if immediately after the clear solution is formed an equivalent of alane is added, ZnH_2 is formed. In view of this evidence, one can conclude that $\text{KZn}_2(\text{CH}_3)_4\text{AlH}_4$ is formed by the reaction of KAlH_4 with $(\text{CH}_3)_2\text{Zn}$ in 1:2 molar ratio.

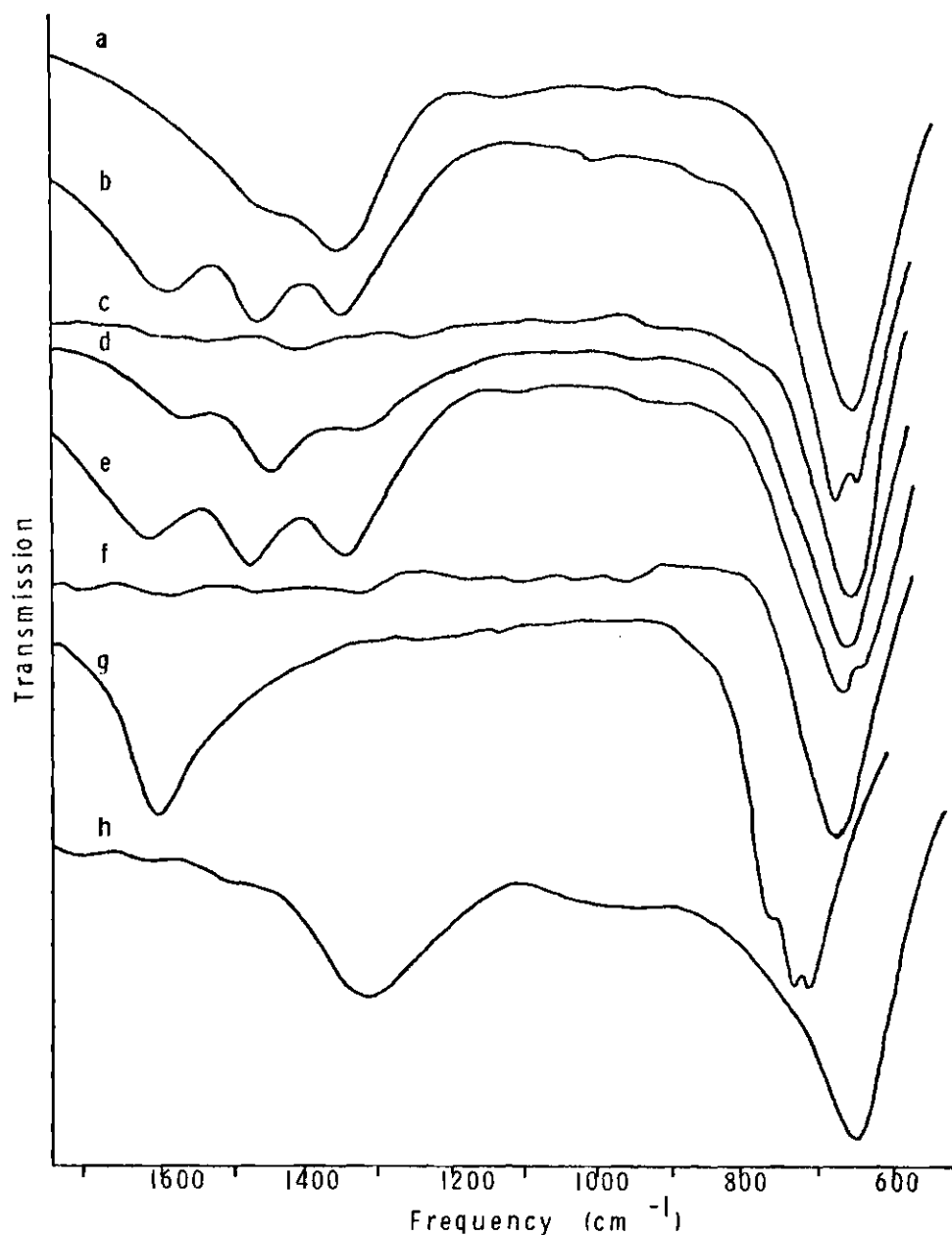
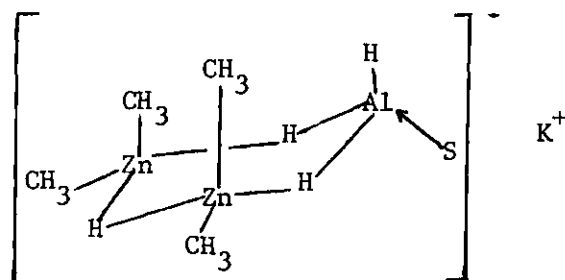


Figure 20. Infrared Spectra of $\text{KZn}_2(\text{CH}_3)_4\text{H}$, Products from the Reaction of KAlH_4 with $(\text{CH}_3)_2\text{Zn}$ in 1:2 Ratio, and Products from the Reaction of $\text{KZn}_2(\text{CH}_3)_4\text{H}$ with AlH_3 in Tetrahydrofuran: (a) 1:2 KAlH_4 to $(\text{CH}_3)_2\text{Zn}$ after Five Minutes, (b) 1:2 KAlH_4 to $(\text{CH}_3)_2\text{Zn}$ after 20 Minutes, (c) 1:2 KAlH_4 to $(\text{CH}_3)_2\text{Zn}$ after Four Hours, (d) 2:1 $\text{KZn}_2(\text{CH}_3)_4\text{H}$ to AlH_3 , (e) 1:1 $\text{KZn}_2(\text{CH}_3)_4\text{H}$ to AlH_3 after Five Minutes, (f) 1:1 $\text{KZn}_2(\text{CH}_3)_4\text{H}$ to AlH_3 after Four Hours, (g) 1:2 $\text{KZn}_2(\text{CH}_3)_4\text{H}$ to AlH_3 ($\text{Al}(\text{CH}_3)_2\text{H}$), and (h) $\text{KZn}_2(\text{CH}_3)_4\text{H}$

Now when alane is added to $\text{KZn}_2(\text{CH}_3)_4\text{H}$ in a 1:1 molar ratio, a white precipitate begins to form immediately. An infrared spectrum of the supernatant left after five minutes reaction time is shown in Figure 20. This spectrum is clearly not that of $\text{KZn}_2(\text{CH}_3)_4\text{AlH}_4$, but is assigned to the compound XVII.



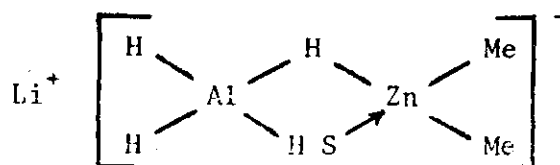
XVII

The infrared spectrum of XVII contains three bands in the metal-hydrogen stretching region, one at 1610, another at 1490, and the third at 1340 cm^{-1} . The band at 1610 cm^{-1} is assigned to the stretching modes of the terminal Al-H group in XVII. The band at 1490 cm^{-1} is assigned to the stretching modes of the bridging hydrogen between aluminum and zinc. The band at 1340 cm^{-1} is assigned to the stretching modes of the bridging hydrogen between the two zinc atoms. These assignments are reasonable based on our earlier results. The terminal Al-H stretch for $\text{NaZn}(\text{CH}_3)_2\text{AlH}_4$ was assigned to the Al-H-Zn bridging unit. The stretching vibrations for the Zn-H-Zn bonds in $\text{LiZn}_2(\text{CH}_3)_4\text{H}$ and $\text{NaZn}_2(\text{CH}_3)_4\text{H}$ occur at 1290 and 1260 cm^{-1} .

CHAPTER IV

CONCLUSIONS

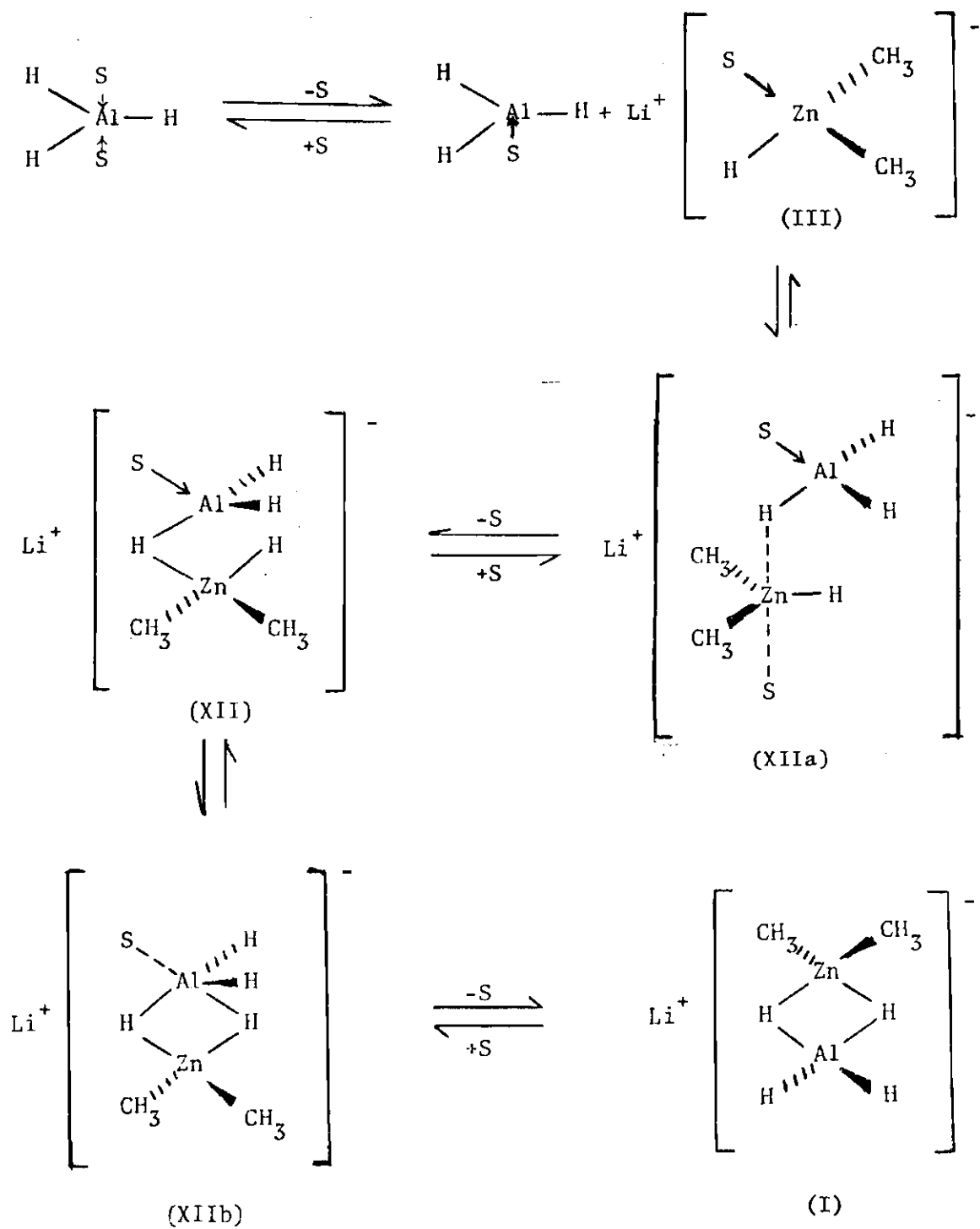
The structures I and XII can give some insight into the mechanism by which $\text{LiZn}(\text{CH}_3)_2\text{AlH}_4$ is formed in the reaction of $\text{LiZn}(\text{CH}_3)_2\text{H}$ with AlH_3 . Scheme II shows the steps which we believe take place in this reaction. First aluminum hydride reacts with $\text{LiZn}(\text{CH}_3)_2\text{H}$ in a nucleophilic solvent displacement reaction on zinc to yield the intermediate XII via transition state XIIIa. The result of this nucleophilic solvent displacement is the formation of a three-center Al-H-Zn bond. It would be unreasonable to assume that $\text{LiZn}(\text{CH}_3)_2\text{H}$ attacks AlH_3 via a nucleophilic solvent displacement reaction on aluminum since the coordination bonds between aluminum and solvent are stronger than those between zinc and solvent. In addition, such a reaction would yield, instead of XII, an intermediate such as XVIII and no evidence was found in the NMR for this species.



XVIII

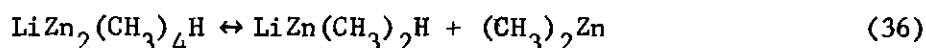
Aluminum hydride, which is known to be in four coordinate-five coordinate equilibrium in THF,¹⁵ would most likely react as the four coordinate species in order to minimize steric interactions in the transition state,

SCHEME II



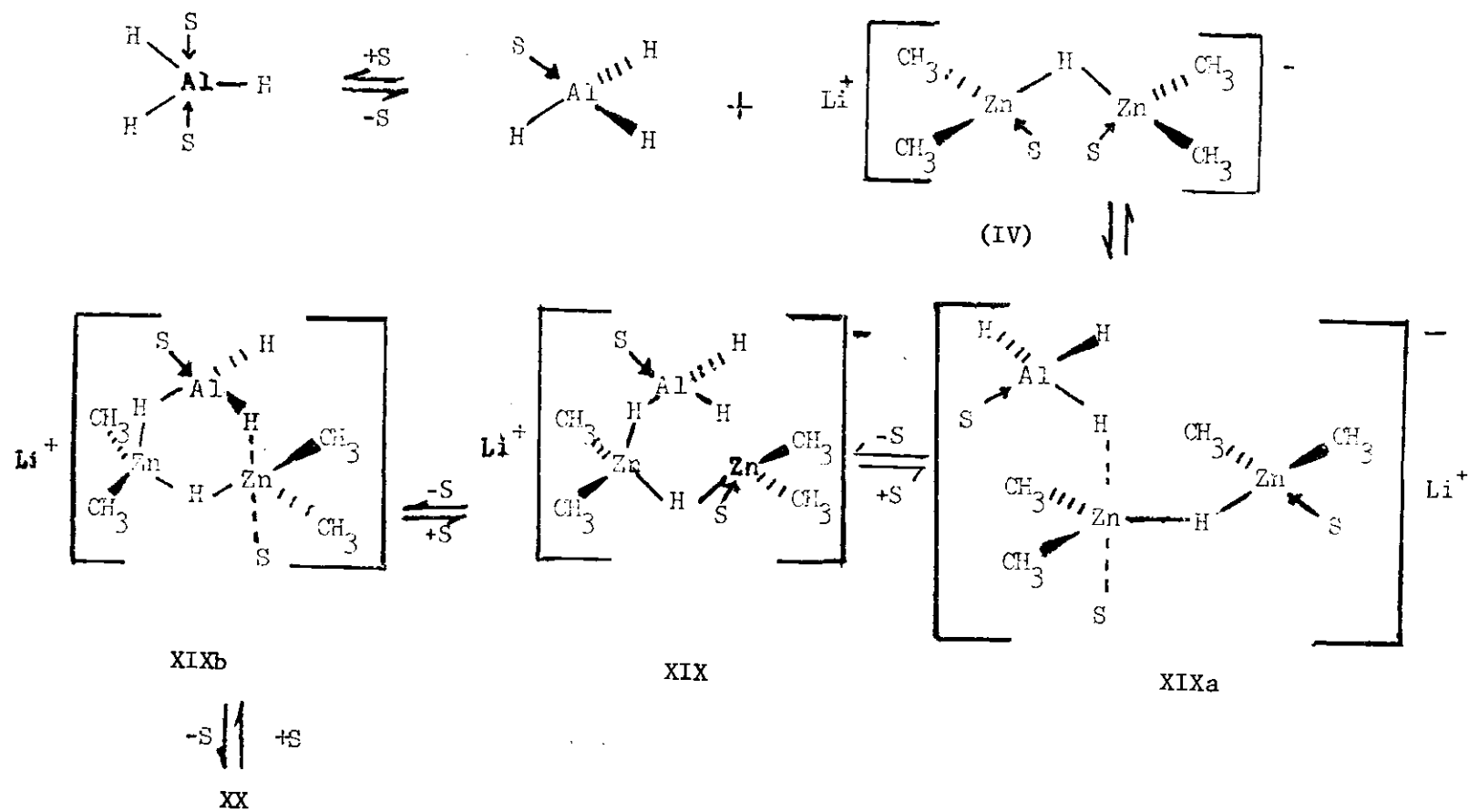
XIIa. The product I is formed when XII undergoes an intramolecular nucleophilic solvent displacement on aluminum via transition state XIIb. The strength of the aluminum-coordinated solvent bond is shown by the fact that XII is observed in the NMR. Failure to detect any of the starting materials indicates that the zinc-coordinated solvent bond is much weaker than the Al-H-Zn bridge bond. The fact that AlH_3 is monomeric in THF indicates that the aluminum-coordinated solvent bond is stronger than the Al-H-Al bridge bond in THF. However, in the solvent the Al-H-Zn bridge bond must be slightly stronger than the aluminum-solvent bond since the ratio of I:XII as shown by NMR is about six. All the steps shown in Scheme II are suggested to be reversible; however, the equilibrium must lie predominantly in the direction of XII and I.

The ^1H NMR of $\text{LiZn}_2(\text{CH}_3)_4\text{AlH}_4$ indicates the presence of both a solvated and an unsolvated monomer in THF solution, with the solvent coordinated to aluminum in the solvated form. A reasonable mechanism for the formation of these two compounds by the reaction of AlH_3 with $\text{LiZn}_2(\text{CH}_3)_4\text{H}$ is shown in Scheme III. Another, but equally reasonable mechanism which recognizes that $\text{LiZn}_2(\text{CH}_3)_4\text{H}$ is subject to equilibrium (Eq. 36) in THF,¹⁰ is shown in Scheme IV.

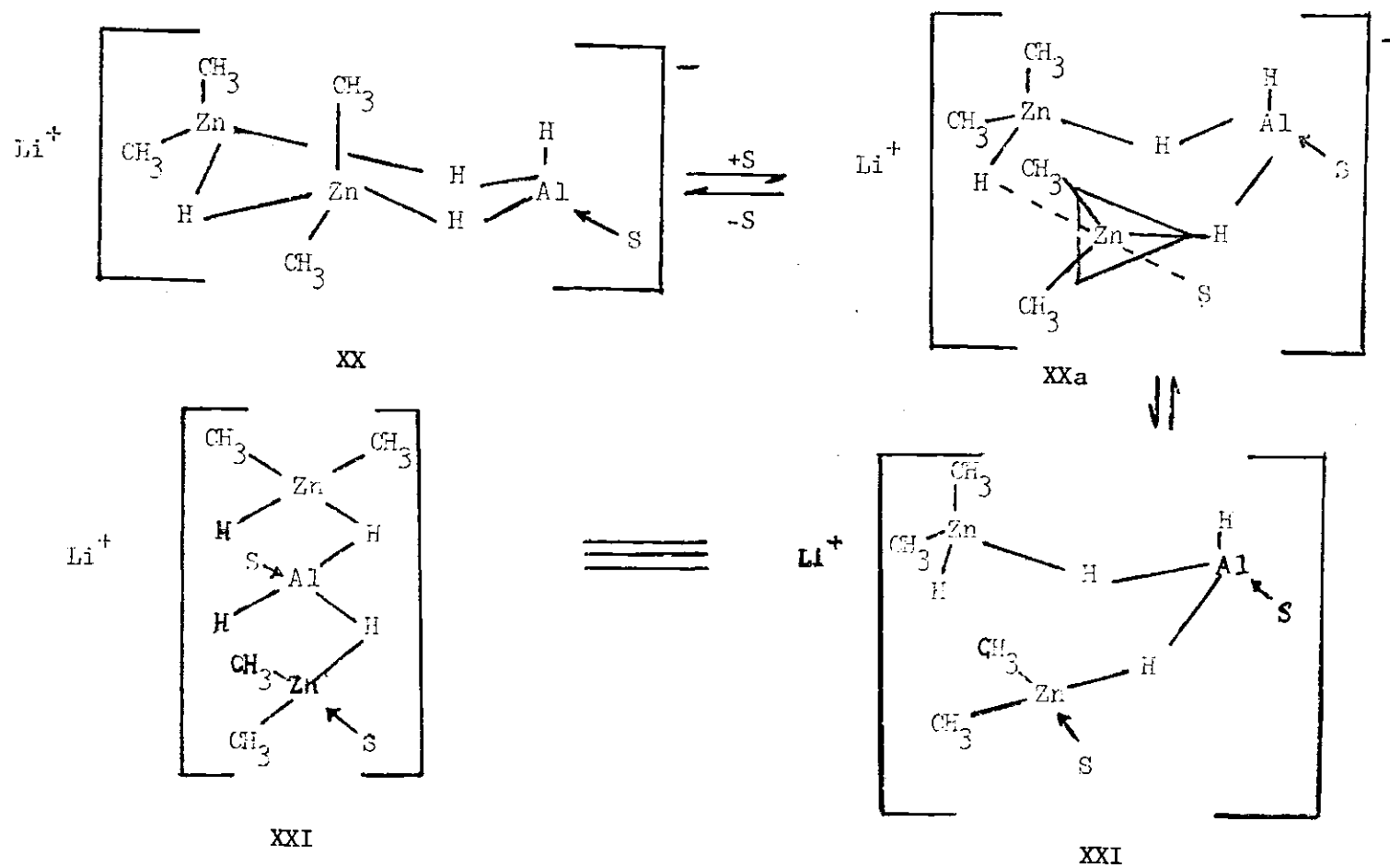


Of course, it could be argued that both schemes are operative. We, however, believe Scheme III to be the most reasonable in light of the observed chemistry. The reaction of AlH_3 with either $\text{LiZn}_2(\text{CH}_3)_4\text{AlH}_4$ or $\text{NaZn}_2(\text{CH}_3)_4\text{AlH}_4$ produces ZnH_2 , but the reaction of $\text{KZn}_2(\text{CH}_3)_4\text{H}$ with either

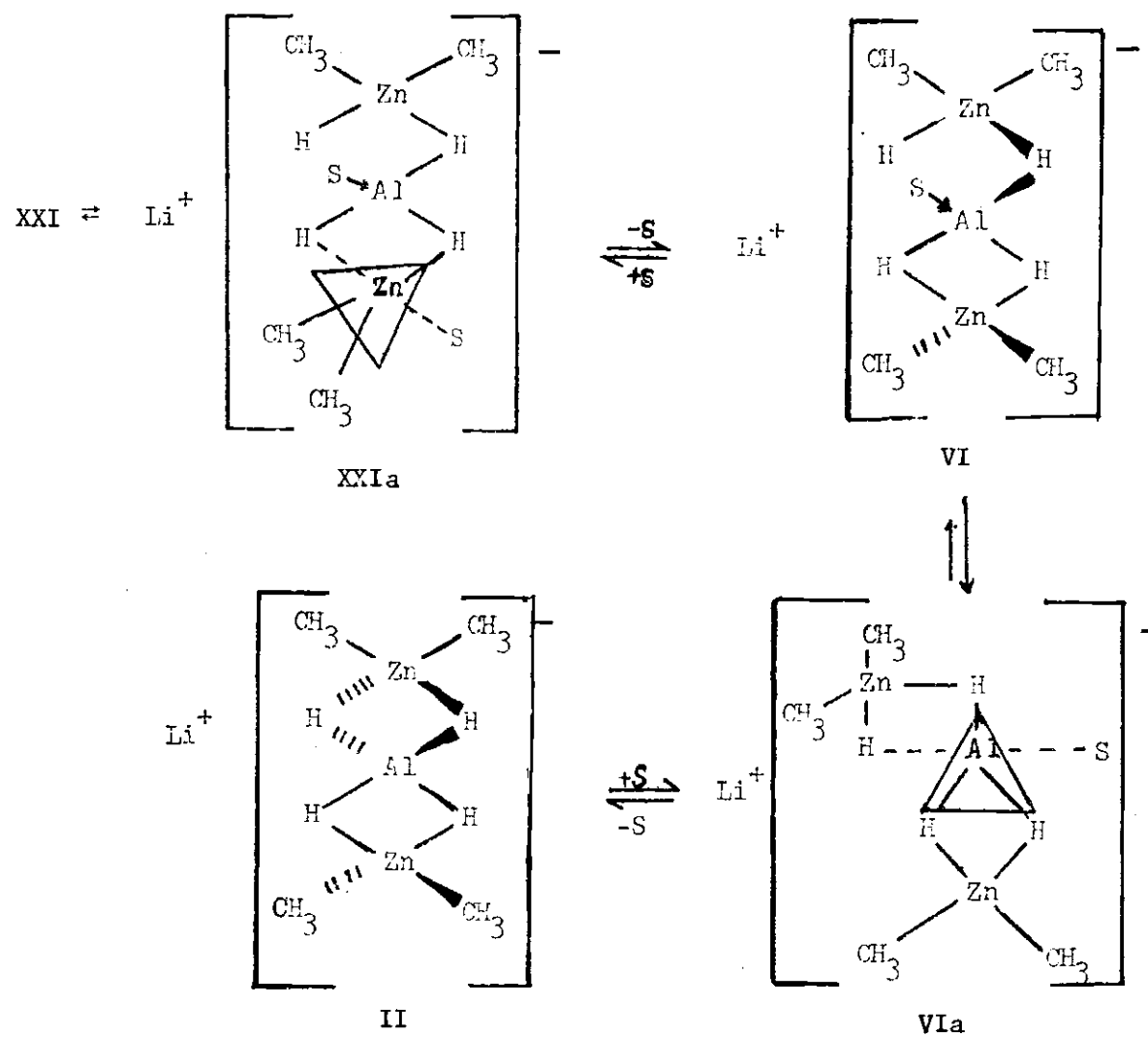
SCHEME III



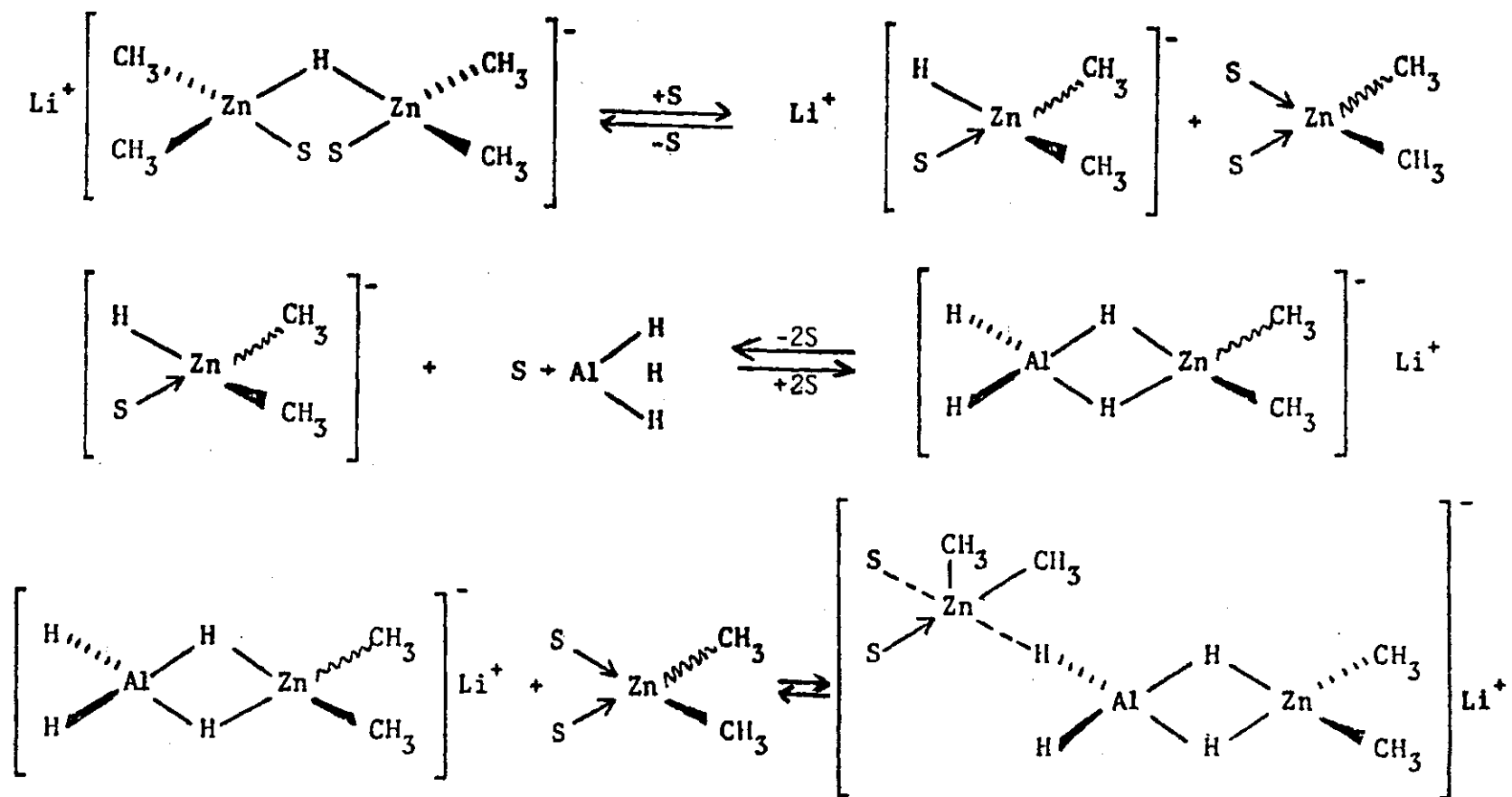
SCHEME III (Continued)



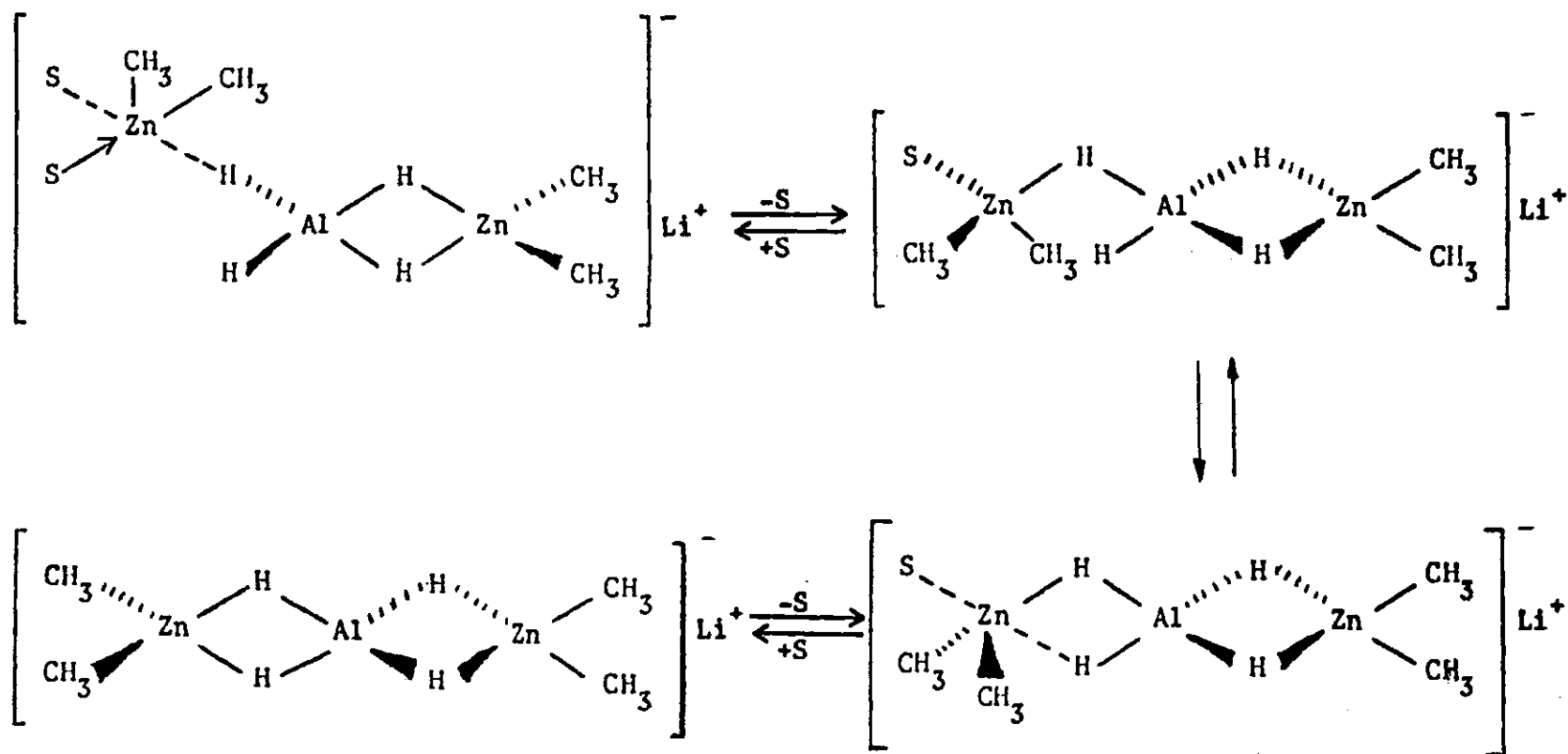
SCHEME III (Concluded)



SCHEME IV



SCHEME IV (Concluded)



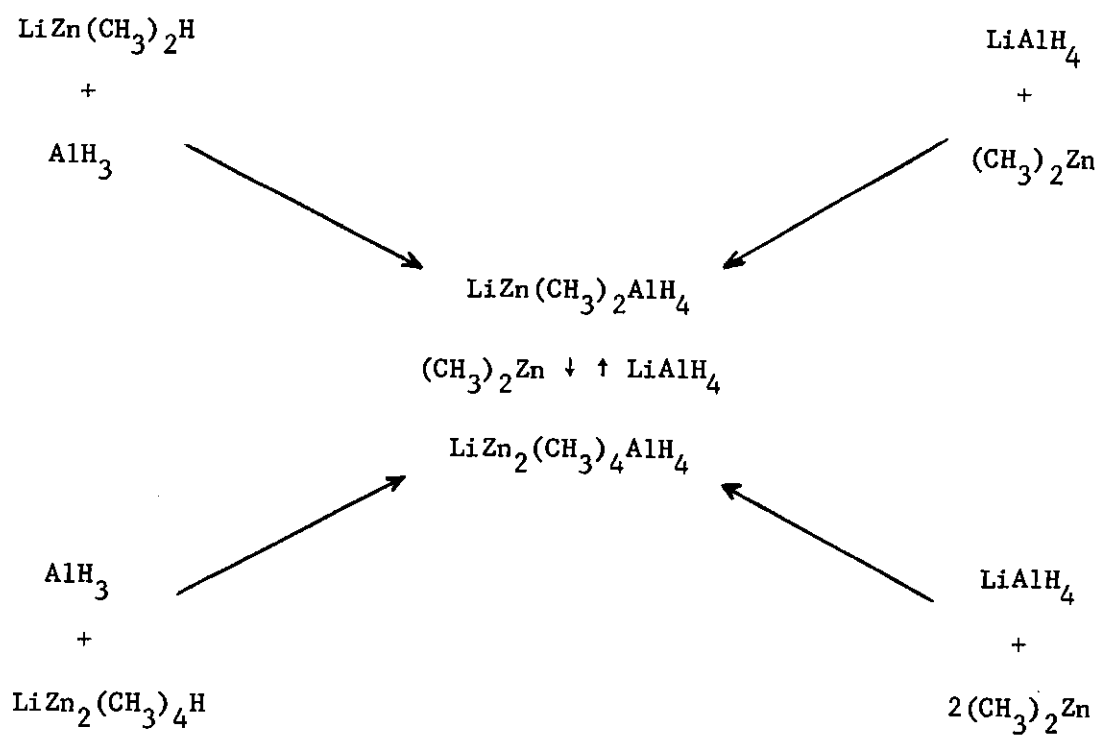
one or two equivalents of AlH_3 yields KZn_2H_5 . The only way that one can rationalize the formation of KZn_2H_5 is to assume that direct alkyl-hydrogen exchange has occurred between $\text{KZn}_2(\text{CH}_3)_4\text{H}$ and AlH_3 through an intermediate, such as XX, shown in Scheme III. Infrared spectra obtained upon reaction of AlH_3 with $\text{KZn}_2(\text{CH}_3)_4\text{H}$ do indicate the existence of an intermediate such as XX. In light of this, it seems reasonable to us that $\text{LiZn}_2(\text{CH}_3)_4\text{H}$ would also react with AlH_3 to give an intermediate like XX which would then undergo an intramolecular rearrangement to give VI and II. The critical step in this type of rearrangement would be a solvent aided breakage of the Zn-H-Zn bond in XX to give XXI through transition state XXa. If, when the cation is K, the Zn-H-Zn bridge bond in XX is too strong to be broken by a solvent attack on zinc, then XX would be observed and not VI or II. With the lifetime of XX increased, it could then undergo exchange with AlH_3 to give KZn_2H_5 . Our studies show that, in solutions where the alkali metal:zinc ratio is 1:2, the percent $\text{MZn}_2(\text{CH}_2)_3\text{H}_4$ present (see Eq. 36) is 60, 71, and 85 when the cation is Li, Na, and K, respectively. This certainly does indicate that the Zn-H-Zn bond in XVI would be stronger when the cation is K as compared to Li or Na.

In the mechanism shown in Scheme III, the first step involves the loss of solvent in five coordinate alane to form four coordinate alane, which then reacts with $\text{LiZn}_2(\text{CH}_3)_4\text{H}$ to give intermediate XIX via transition state XIXa. Intermediate XX is then formed via transition state XIXb. The Zn-H-Zn bridge bond in XX is then cleaved by reaction with solvent via transition state XXa to form intermediate XXI. Intermediate

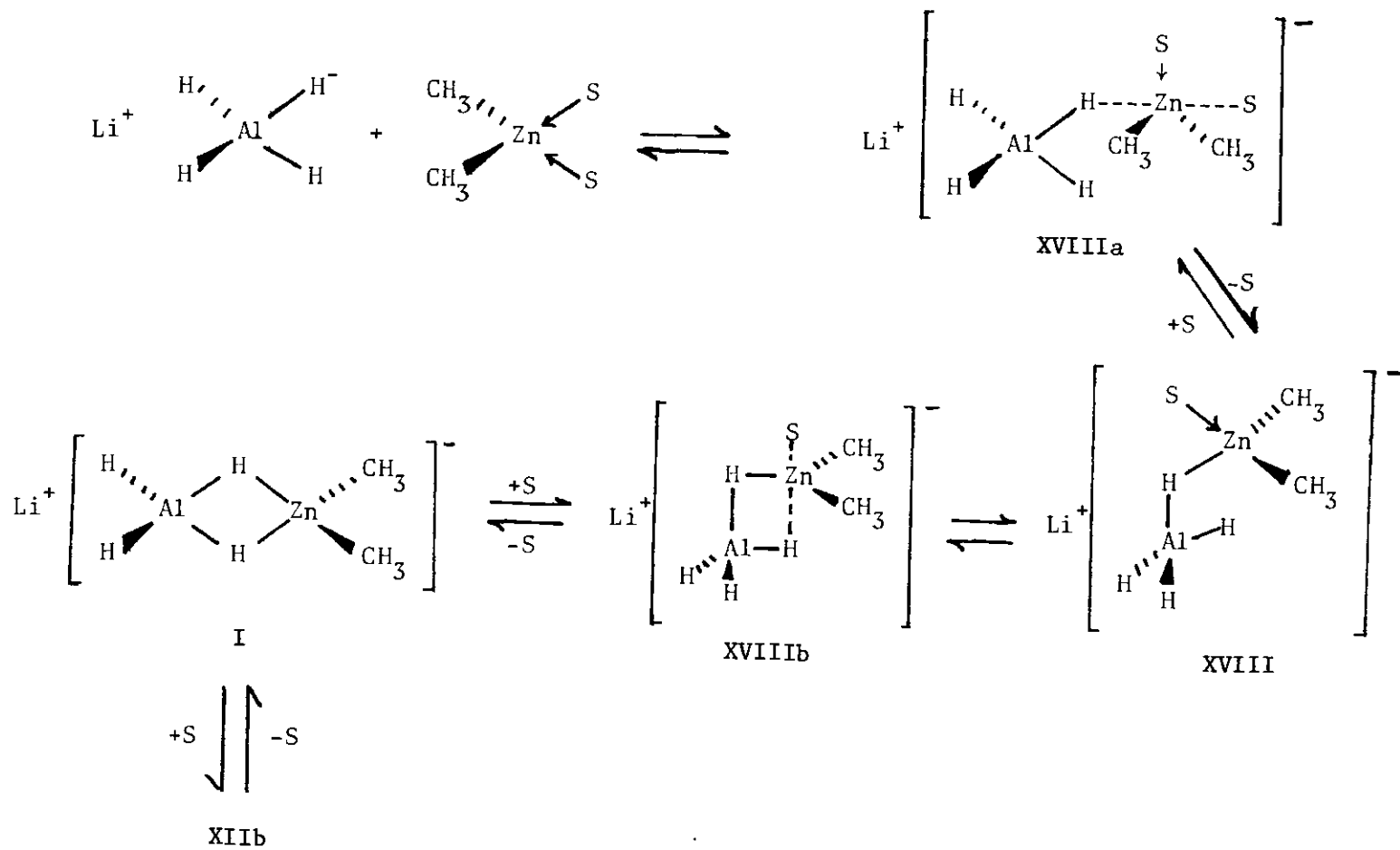
XXI then undergoes loss of solvent from zinc and aluminum via transition states XXIIa and VIa, respectively, to form the final products VI and II. Again, the equilibrium lies largely in favor of VI and II since they are the species observed spectroscopically.

Whether LiAlH_4 is added to $(\text{CH}_3)_2\text{Zn}$ or $(\text{CH}_3)_2\text{Zn}$ is added to LiAlH_4 makes no difference as far as the final products of the reaction are concerned. The infrared spectra observed when the ratio of $(\text{CH}_3)_2\text{Zn}$ to LiAlH_4 is 1:1, 3:2, or 2:1 are the same. As LiAlH_4 is added to $(\text{CH}_3)_2\text{Zn}$, there is a smooth conversion of the $(\text{CH}_3)_2\text{Zn}$ to $\text{LiZn}_2(\text{CH}_3)_4\text{AlH}_4$ and then to $\text{LiZn}(\text{CH}_3)_2\text{AlH}_4$. On the other hand, when $(\text{CH}_3)_2\text{Zn}$ is added to LiAlH_4 , there is a smooth conversion of the LiAlH_4 to $\text{LiZn}(\text{CH}_3)_2\text{AlH}_4$ and then to $\text{LiZn}_2(\text{CH}_3)_4\text{AlH}_4$. These reactions are shown in Scheme V. Thus, $\text{LiZn}_2(\text{CH}_3)_4\text{AlH}_4$ can be converted to $\text{LiZn}(\text{CH}_3)_2\text{AlH}_4$ by addition of LiAlH_4 , and $\text{LiZn}(\text{CH}_3)_2\text{AlH}_4$ can be converted to $\text{LiZn}_2(\text{CH}_3)_4\text{AlH}_4$ by addition of $(\text{CH}_3)_2\text{Zn}$. These interconversions indicate that there exists a mobile equilibrium between $\text{LiZn}(\text{CH}_3)_2\text{AlH}_4$ and $\text{LiZn}_2(\text{CH}_3)_4\text{AlH}_4$. This statement is supported by the fact that a 3:2 mixture of $(\text{CH}_3)_2\text{Zn}$ and LiAlH_4 gives rise to both $\text{LiZn}_2(\text{CH}_3)_4\text{AlH}_4$ and $\text{LiZn}(\text{CH}_3)_2\text{AlH}_4$.

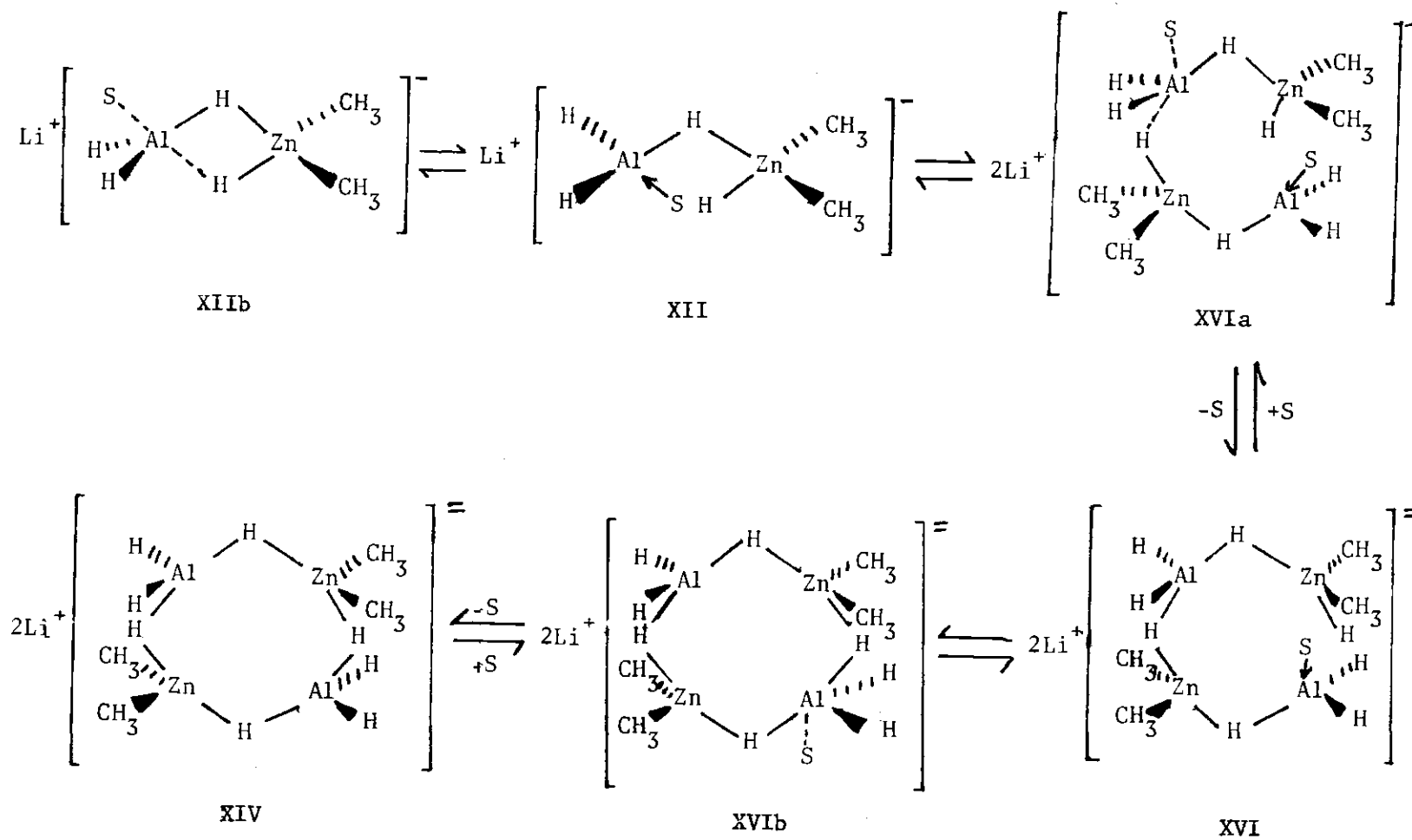
The mechanism for the formation of $\text{LiZn}(\text{CH}_3)_2\text{AlH}_4$ when $(\text{CH}_3)_2\text{Zn}$ and LiAlH_4 are allowed to react in THF can be visualized as occurring in the manner shown in Scheme VI. Lithium aluminum hydride (solvent separated ion pair²⁸) reacts with the THF solvate of dimethylzinc by nucleophilic attack of AlH_4^- on zinc displacing solvent to give XVIII by way of transition state XVIIIa. In this reaction one of the zinc-THF solvate bonds is broken with formation of a zinc-hydrogen bridge bond. The

SCHEME V

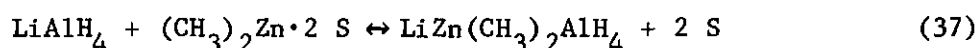
SCHEME VI



SCHEME VI (Concluded)



forward reaction should be exothermic ($\Delta H < 0$) and the entropy should be positive ($\Delta S > 0$), thus making the formation of XVIII from LiAlH_4 and $(\text{CH}_3)_2\text{Zn}$ very favorable. One would expect ΔH to be negative since a zinc-THF solvate bond, which should be weaker than an aluminum-THF solvate bond, is being replaced by a Zn-H-Al bridge bond. Our studies here have shown that Al-H-Zn bridge bonds are stronger than aluminum-THF solvate bonds. Intermediate XVIII then proceeds to form I via transition state XVIIIb by an intramolecular nucleophilic displacement of solvent on zinc. In the latter intramolecular reaction, the remaining zinc-THF solvate bond is broken with formation of a second zinc-hydrogen bridge bond. This reaction would also be expected to be very favorable for the same reasons just given. The equilibrium between I and XVIII would be expected to be shifted largely in favor of I. This is shown to be true experimentally since no signals for a compound such as XVIII are observed in the NMR. Moreover, the entire equilibrium represented by reaction 37 would be expected to be shifted entirely in favor of $\text{LiZn}(\text{CH}_3)_2\text{AlH}_4$,



again, for the reasons cited above. The forward reaction should be strongly exothermic and the entropy positive. This again is shown experimentally, since spectroscopic studies on $\text{LiZn}(\text{CH}_3)_2\text{AlH}_4$ failed to show any evidence to indicate the presence of LiAlH_4 or $(\text{CH}_3)_2\text{Zn}$. The solvate XII is then formed via transition state XIIb by a nucleophilic solvent attack on the aluminum in I. In this reaction, the Al-H-Zn bridge bonds

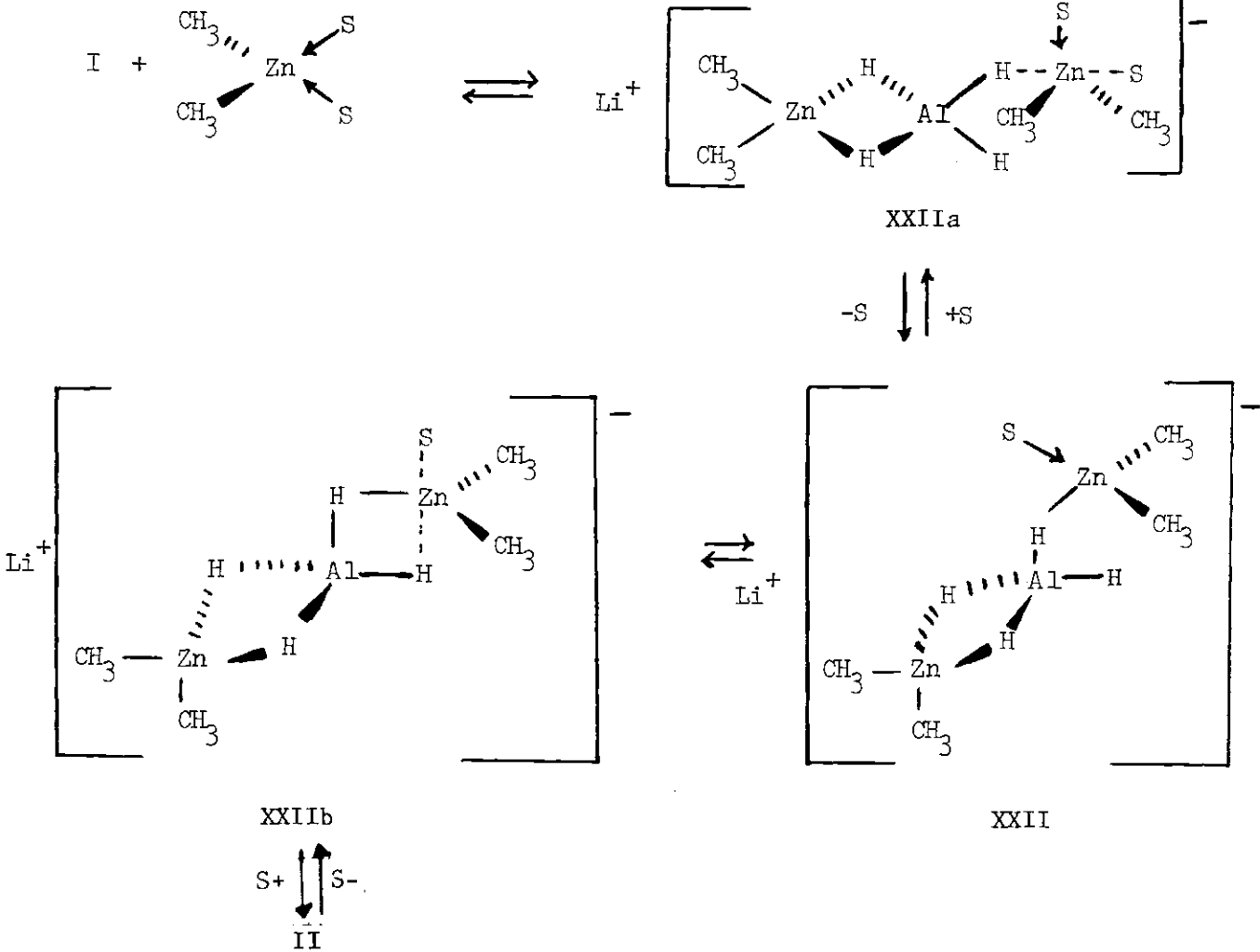
are broken with formation of an aluminum-THF solvate bond.* The equilibrium between I and XII which was discussed earlier, lies slightly in favor of I. If the concentration of the solution is such that dimers will be present, then the dimer forms XVI and XIV will be formed through transition states XVIa and XVIb, respectively. The equilibrium between XVI and XIV lies in favor of XIV. The amount of XIV relative to I depends upon both the concentration and temperature of the solution.

The mechanism for the formation of $\text{LiZn}_2(\text{CH}_3)_4\text{AlH}_4$ when LiAlH_4 and $(\text{CH}_3)_2\text{Zn}$ are allowed to react in THF can be visualized as occurring in the manner shown in Scheme VII. Lithium aluminum hydride reacts with the THF solvate of $(\text{CH}_3)_2\text{Zn}$ to give I by the mechanism shown in Scheme VI. Then I reacts with the THF solvate of $(\text{CH}_3)_2\text{Zn}$ to form XXII by way of transition state XXIIa. This reaction is similar to the reaction of LiAlH_4 with $(\text{CH}_3)_2\text{Zn}$ to form XVIII in Scheme VI. Nucleophilic displacement of a THF solvent molecule from the tetrahedral zinc (transition state XXIIb) then results in the formation of another zinc-hydrogen bridge bond and the formation of II. On the whole, this mechanism is very similar to that shown in Scheme VI. Then II reacts through VIa to give VI. For solutions where dimers are present, VI reacts through XXIIIa to give XXIII, which then gives XXIV through XXIIIb. The reactions of XII, XVI, and XIV with $(\text{CH}_3)_2\text{Zn}$ could also form VI, XXIII, and XXIV.

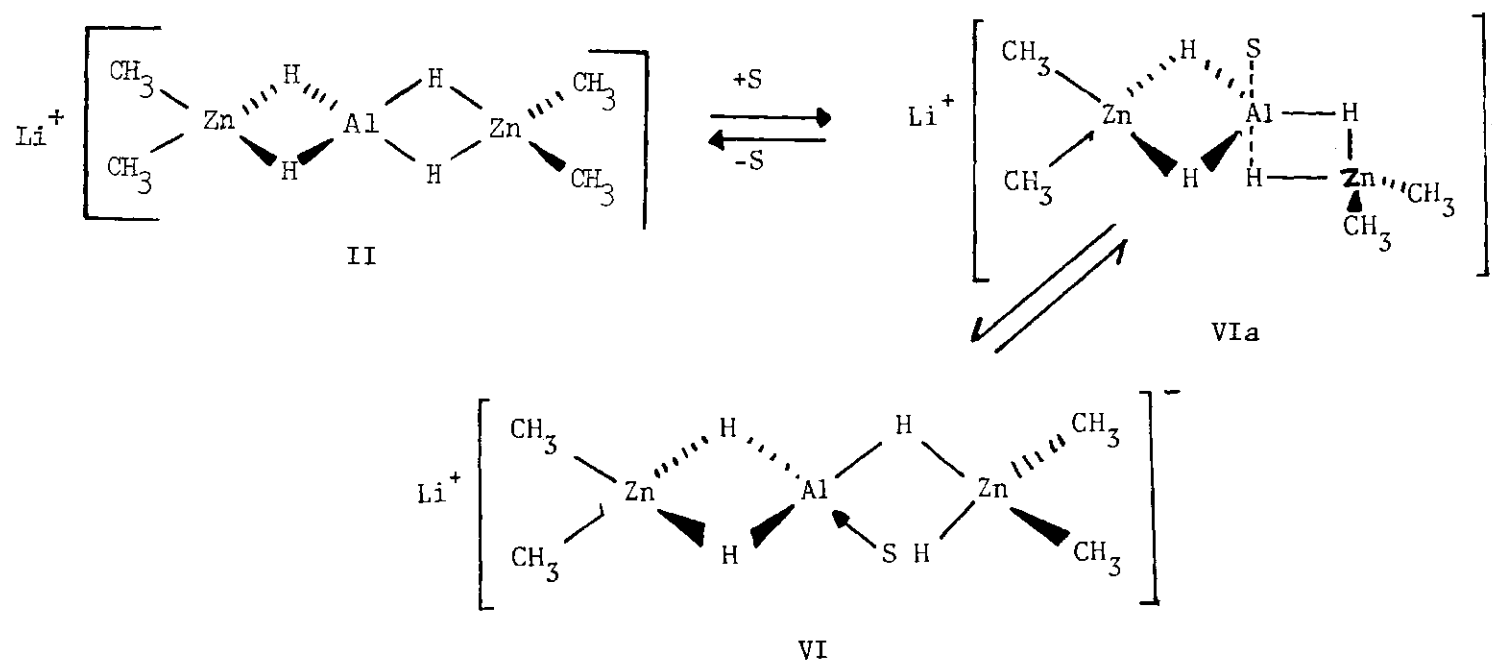
In both Scheme VI and Scheme VII, the transition states are pictured as involving five coordinate, trigonal bipyramidal zinc. This

* If the solutions of LiAlH_4 and $(\text{CH}_3)_2\text{Zn}$ are concentrated enough, mixing of the two reagents is frequently seen to cause the THF solvent to reflux.

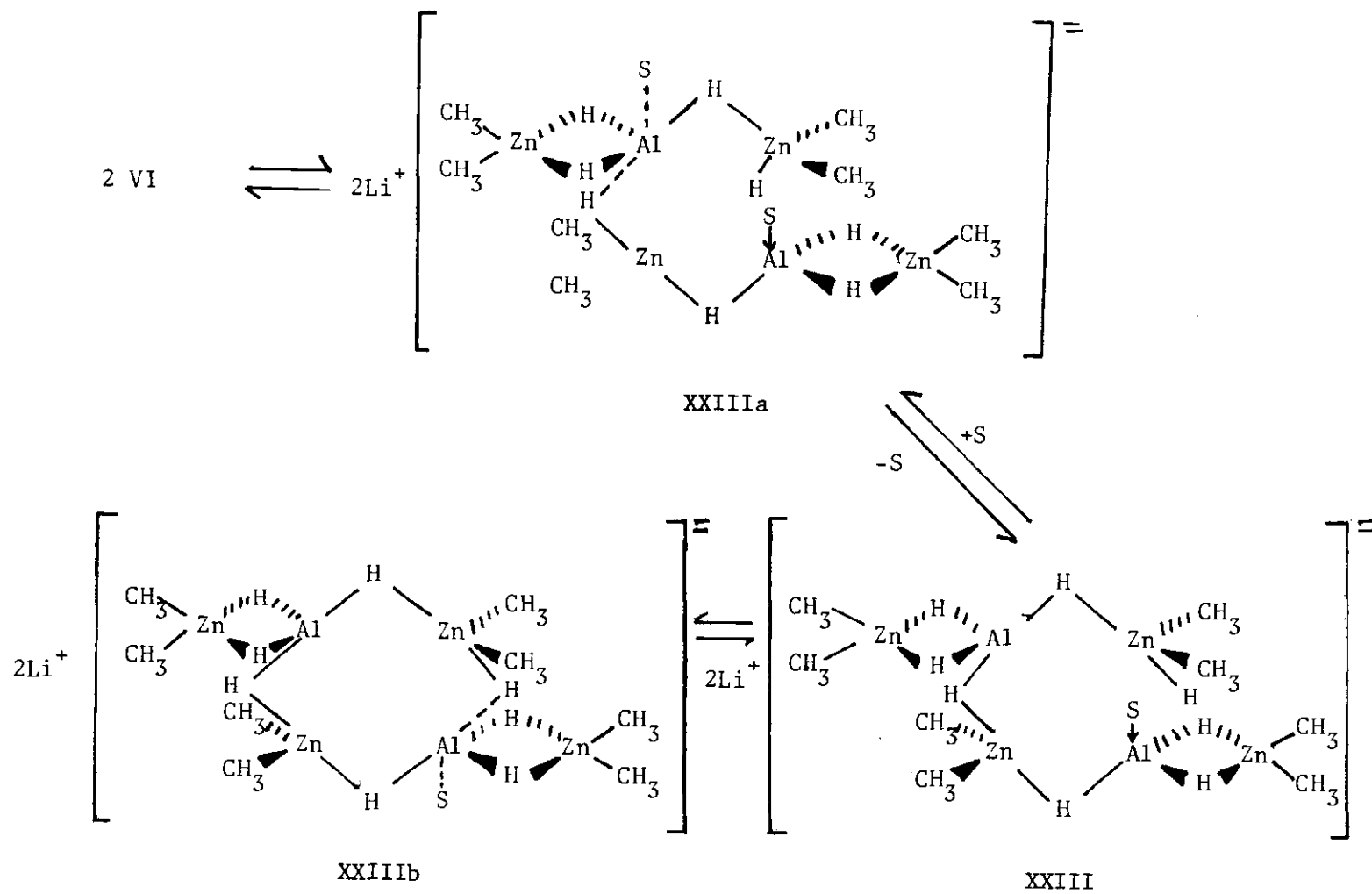
SCHEME VII



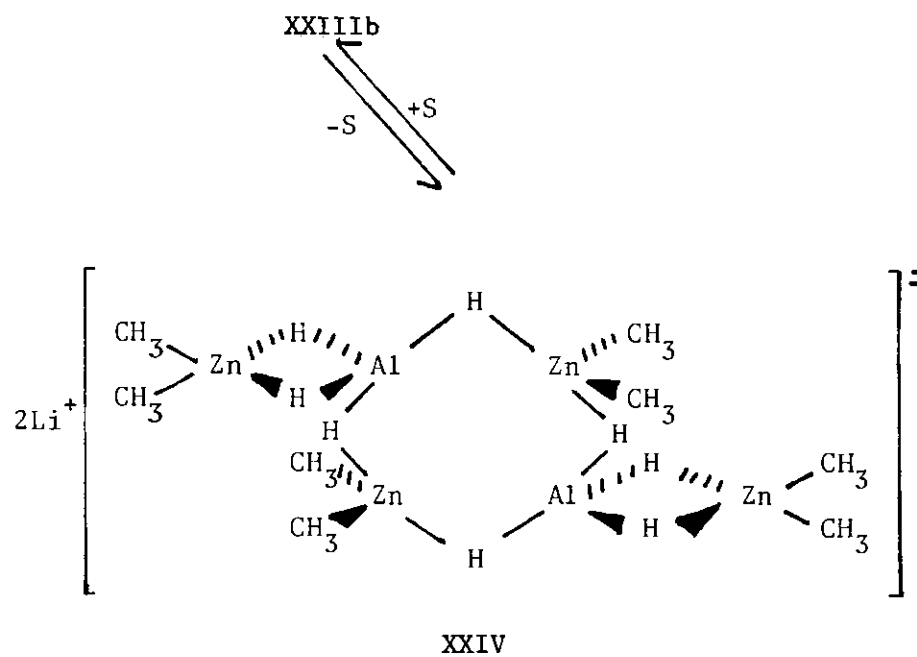
SCHEME VII (Continued)



SCHEME VII (Continued)

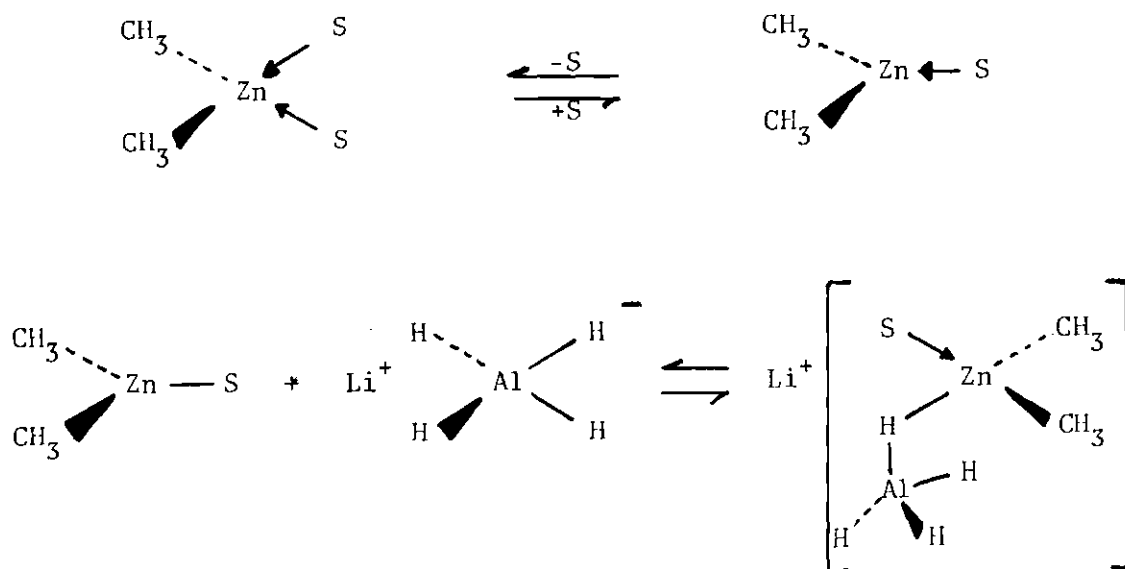


SCHEME VII (Concluded)



geometry assumes an S_N2 type displacement of solvent from zinc. Loss of solvent via an S_N1 type reaction was considered; however, this type of mechanism would necessarily imply the existence of three coordinate zinc as shown in Scheme VIII. Since four and five coordinate organo zinc species are much more common than three coordinate ones,²⁹ an S_N2 type nucleophilic displacement mechanism is favored.

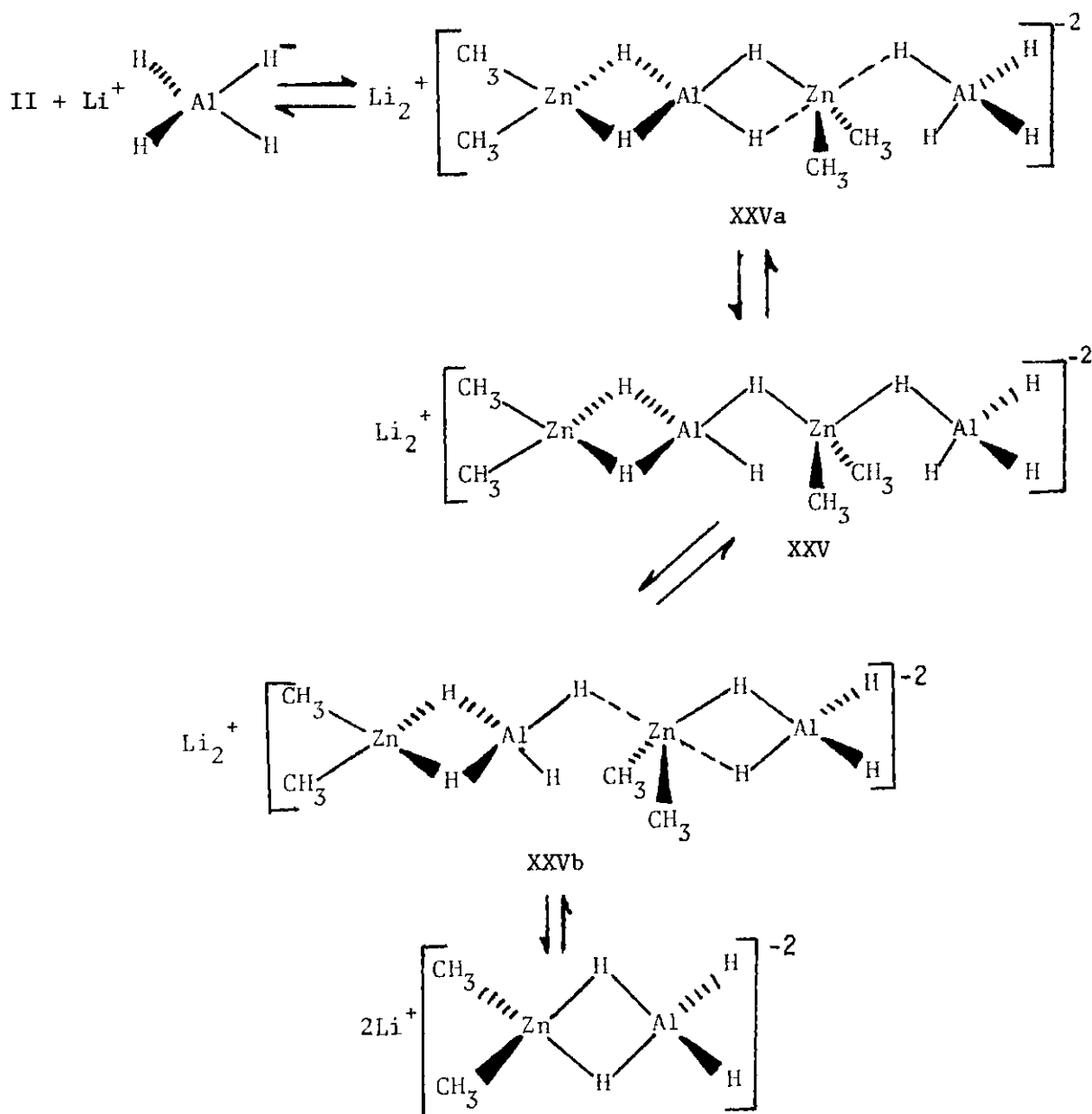
SCHEME VIII



The mechanism of conversion of $LiZn_2(CH_3)_4AlH_4$ to $LiZn(CH_3)_2AlH_4$ in THF by the addition of $LiAlH_4$ (see Scheme V) is pictured in Scheme IX. Lithium aluminum hydride reacts with $LiZn_2(CH_3)_4AlH_4$ to give XXV by way of transition state XXVa. One of the zinc-hydrogen bridge bonds in $LiZn_2(CH_3)_4AlH_4$ is broken by S_N2 attack of AlH_4 on one of the terminal zinc atoms and a new zinc-hydrogen bridge bond is formed between the terminal

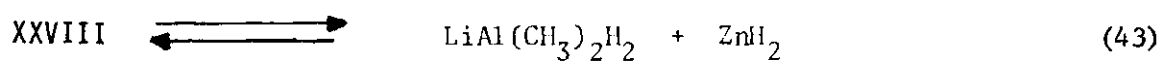
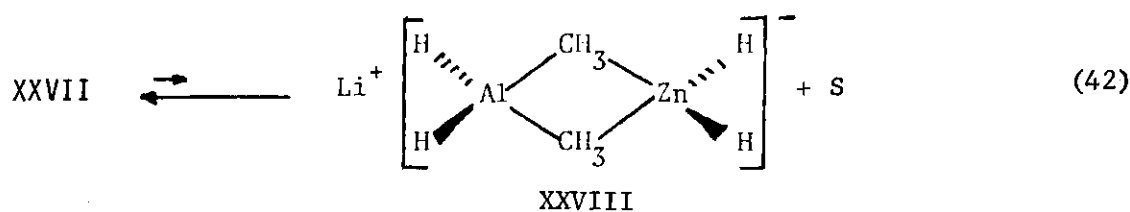
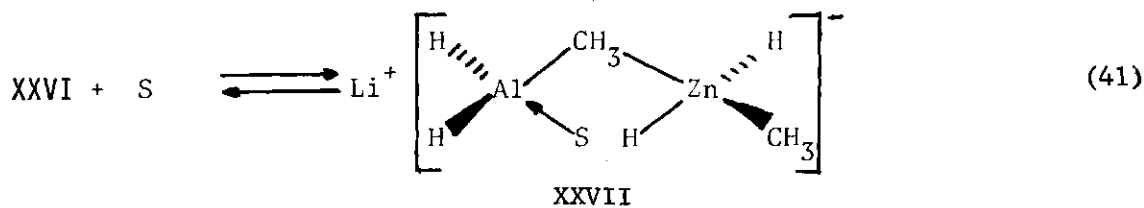
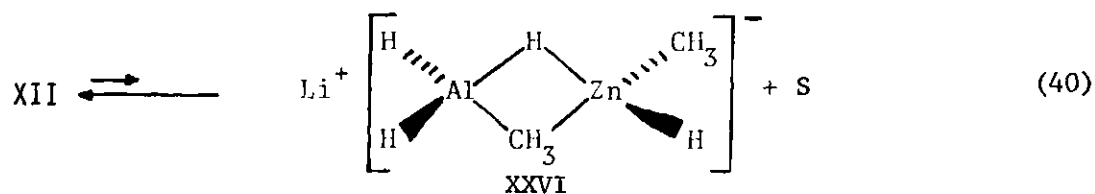
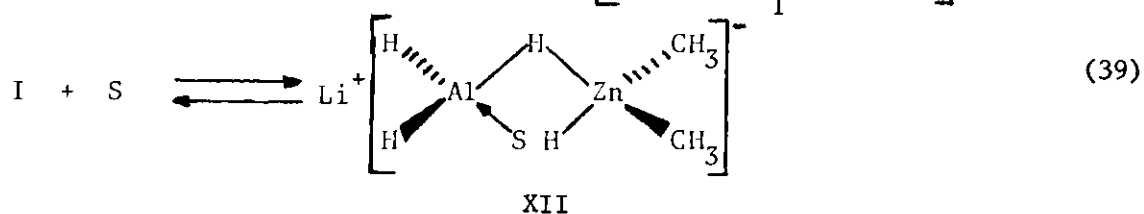
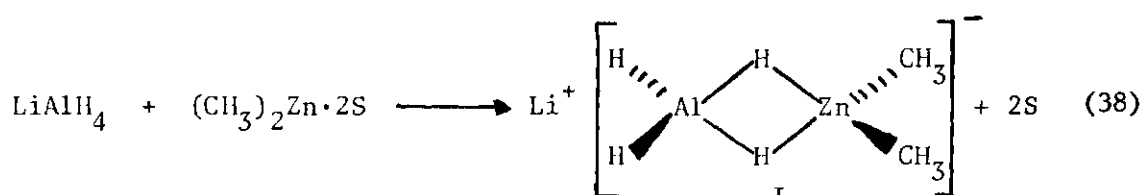
zinc and the incoming AlH_4^- group. Intermediate XXV then forms two molecules of $\text{LiZn}(\text{CH}_3)_2\text{AlH}_4$ by way of XXVb.

SCHEME IX



Concerning the reaction of LiAlH_4 with $(\text{CH}_3)_2\text{Zn}$ to produce ZnH_2 , the work reported here clearly establishes that $\text{LiZn}(\text{CH}_3)_2\text{AlH}_4$ is the primary intermediate involved in this reaction. Scheme X shows a reasonable mechanism for this reaction using the intermediates that have been detected by spectroscopic means in this study.

SCHEME X



The intermediates I and XII are formed rapidly from LiAlH_4 and $(\text{CH}_3)_2\text{Zn}$, since they were detected immediately after mixing the two reactants. The formation of the mixed bridge intermediate XXVI in reaction 40 is probably very slow and could very well be the rate limiting step. This reaction would be expected to be slow since an aluminum-THF solvate bond is being broken by the formation of a methyl bridge bond between zinc and aluminum. The methyl bridge bond would be expected to be weaker than the aluminum solvate bond.¹³ Formation of the double methyl bridged intermediate XXVIII in reaction 42 would be slow also, perhaps slower than reaction 40. Reaction 43 completes the sequence with XXVIII disproportionating to $\text{LiAl}(\text{CH}_3)_2\text{H}_2$ and ZnH_2 , which precipitates from solution. All the reactions, except 38 are actual equilibria which are never displaced entirely towards ZnH_2 . This is supported by the fact that, after standing one week, sufficient time for full equilibrium to be reached, the supernatant solution above ZnH_2 still contained about 50% of the original zinc.

It would be reasonable also to assume that the reaction between LiAlH_4 and $(\text{CH}_3)_2\text{Zn}$ in diethyl ether, which is known to produce ZnH_2 , proceeds through an intermediate such as $\text{LiZn}(\text{CH}_3)_2\text{AlH}_4$. This assumption is borne out in our study of the reaction between LiAlH_4 and $(\text{CH}_3)_2\text{Zn}$ in diethyl ether.

The results of this study allow us to say something about the mechanism by which LiAlH_4 and $(\text{CH}_3)_2\text{Zn}$ react to give ZnH_2 in diethyl ether. In THF when LiAlH_4 and $(\text{CH}_3)_2\text{Zn}$ were allowed to react (the mode of addition did not matter), $\text{LiZn}(\text{CH}_3)_2\text{AlH}_4$, $\text{LiZn}_2(\text{CH}_3)_4\text{AlH}_4$, or mixtures of the two were obtained depending on the ratio of reactants. On standing,

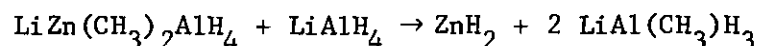
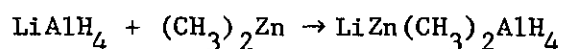
solutions of $\text{LiZn}(\text{CH}_3)_2\text{AlH}_4$ (where the concentrations were greater than 0.1 M) precipitated a mixture of LiZnH_3 and ZnH_2 . More dilute solutions of $\text{LiZn}(\text{CH}_3)_2\text{AlH}_4$ (concentrations in the range 0.04-0.01 M) precipitated ZnH_2 only. Molecular weight measurements, coupled with NMR and infrared spectral studies, showed that an equilibrium between the monomer and dimer units I and XIV (Eq. 8) existed in $\text{LiZn}(\text{CH}_3)_2\text{AlH}_4$ solutions at concentrations of 0.1 M. Predominantly the monomer is present in solutions where the concentration is in the range 0.04-0.01 M. It was proposed that LiZnH_3 arises from intramolecular exchange of the methyl groups on zinc for the hydrogens on aluminum in an intermediate like XIV, since LiZnH_3 is only precipitated from solutions where XIV is observed. Likewise, in dilute solutions where only I is observed, ZnH_2 is precipitated as a result of intramolecular exchange within I. It is easy to see how the proper mixed bridge intermediates could arise from I.

When LiAlH_4 is added to solutions of $(\text{CH}_3)_2\text{Zn}$ in diethyl ether such that LiAlH_4 is never in excess, the results indicate that the same phenomena are occurring. The addition of LiAlH_4 to $(\text{CH}_3)_2\text{Zn}$ in 1:1 ratio initially gives a solution of $\text{LiZn}(\text{CH}_3)_2\text{AlH}_4$. At concentrations greater than 0.1 M this solution precipitates a mixture of LiZnH_3 and ZnH_2 ; however, solutions less than 0.1 M precipitate ZnH_2 only. It is reasonable, therefore, to propose that in diethyl ether LiZnH_3 results from intramolecular exchange in an intermediate like XIV, whereas ZnH_2 results from intramolecular exchange in I.

When LiAlH_4 is added to $(\text{CH}_3)_2\text{Zn}$, such that LiAlH_4 is in excess, the mechanism of the reaction appears to be different. The solid product

from the reaction is always ZnH_2 . Since the addition of LiAlH_4 to a solution of $\text{LiZn}(\text{CH}_3)_2\text{AlH}_4$ results in the immediate precipitation of ZnH_2 , it seems reasonable that the above reaction would be proceeding by the mechanism shown in Scheme XI.

SCHEME XI



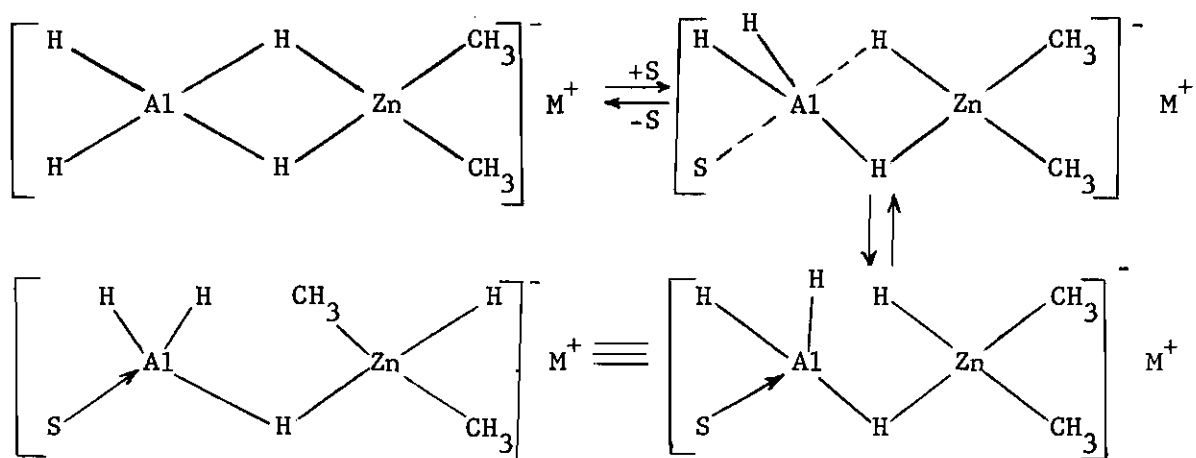
When $(\text{CH}_3)_2\text{Zn}$ is added to LiAlH_4 , the reaction proceeds in a similar manner. As the $(\text{CH}_3)_2\text{Zn}$ is added, LiAlH_4 is always in excess. This results in the initial formation of $\text{LiZn}(\text{CH}_3)_2\text{AlH}_4$ followed by a rapid reaction with LiAlH_4 to give ZnH_2 . As the addition of $(\text{CH}_3)_2\text{Zn}$ is continued, a point is reached where the ratio of total Al to Zn is two. At this point all the LiAlH_4 has reacted, all the zinc has precipitated as ZnH_2 and all the aluminum is present as $\text{LiAl}(\text{CH}_3)\text{H}_3$. Subsequent addition of more $(\text{CH}_3)_2\text{Zn}$ results in reaction between the $(\text{CH}_3)_2\text{Zn}$ and $\text{LiAl}(\text{CH}_3)\text{H}_3$ (which is in large excess now) to give ZnH_2 in a manner similar to that shown in Scheme XI except that now $\text{LiAl}(\text{CH}_3)_2\text{H}_2$ is formed. With continued $(\text{CH}_3)_2\text{Zn}$ addition the ratio of total Al to Zn soon becomes one. At this point all the $\text{LiAl}(\text{CH}_3)\text{H}_3$ has reacted, all the zinc has precipitated as ZnH_2 and all the aluminum is present as $\text{LiAl}(\text{CH}_3)_2\text{H}_2$. If the addition of $(\text{CH}_3)_2\text{Zn}$ is continued further, one sees reaction of $(\text{CH}_3)_2\text{Zn}$ with LiAl -

$(\text{CH}_3)_3\text{H}$ to give ZnH_2 . Throughout the entire course of the reaction when $(\text{CH}_3)_2\text{Zn}$ is added to LiAlH_4 (if the addition is done in a slow dropwise fashion), there will always be an aluminohydride species present in excess over $(\text{CH}_3)_2\text{Zn}$. This is then what always causes the precipitation of zinc hydride.

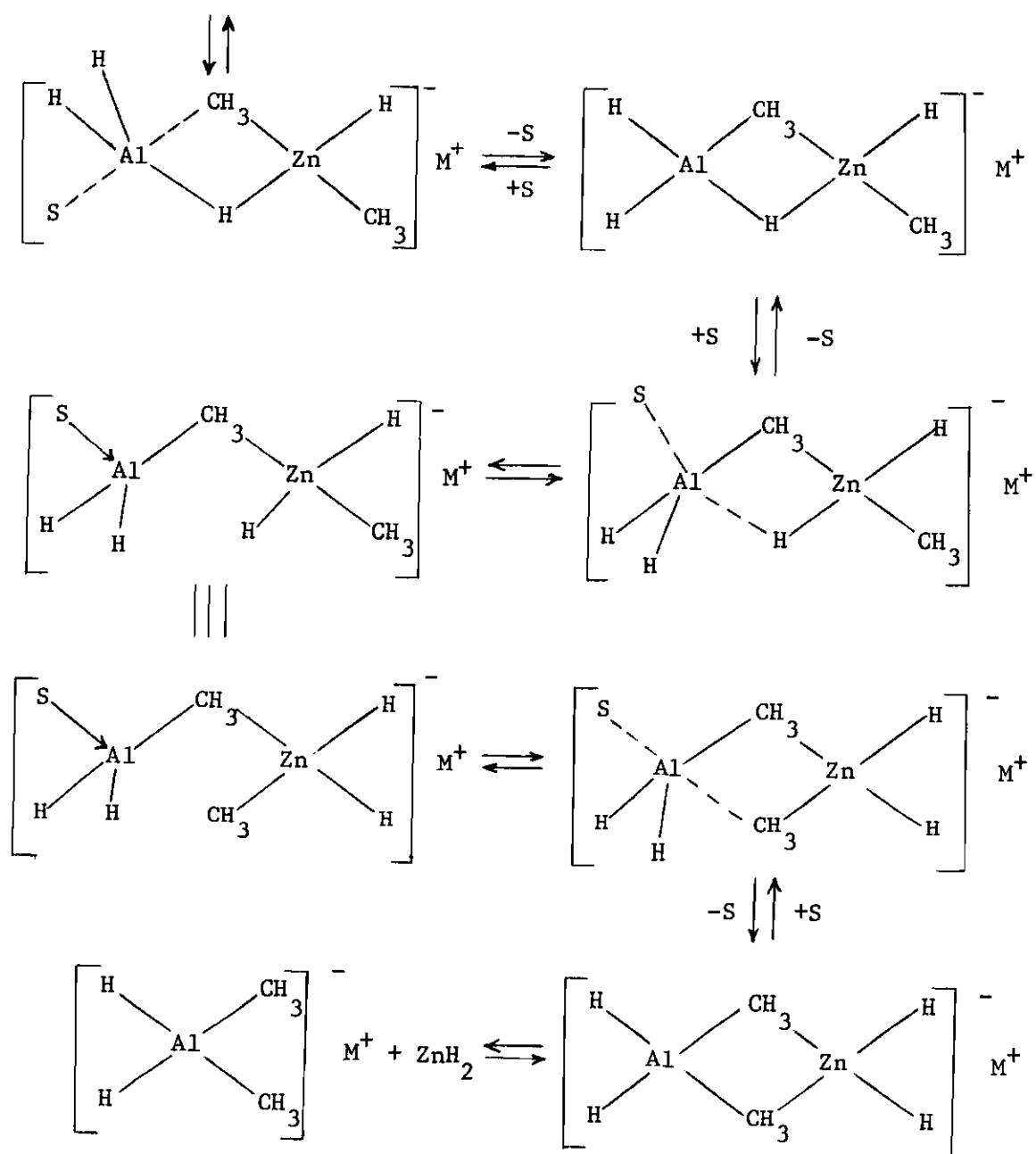
The results of this study have shown that, if one is to obtain relatively pure ZnH_2 by reacting LiAlH_4 and $(\text{CH}_3)_2\text{Zn}$ in diethyl ether, the reaction must be carried out by adding $(\text{CH}_3)_2\text{Zn}$ slowly to LiAlH_4 not allowing the ratio of total Al to total Zn to drop below two.

A reasonable mechanism by which $\text{MZn}(\text{CH}_3)_2\text{AlH}_4$ can undergo intramolecular exchange to produce ZnH_2 is shown in Scheme XII. This scheme of reactions is essentially identical to that given earlier for the reaction between LiAlH_4 and $(\text{CH}_3)_2\text{Zn}$ to produce ZnH_2 . The mechanism was discussed in some detail there. The rate limiting step in the scheme is thought to be formation of the mixed bridged intermediate XXIX, since formation of methyl bridge bond with simultaneous breakage of an aluminum-THF solvate bond should be unfavorable.

SCHEME XII

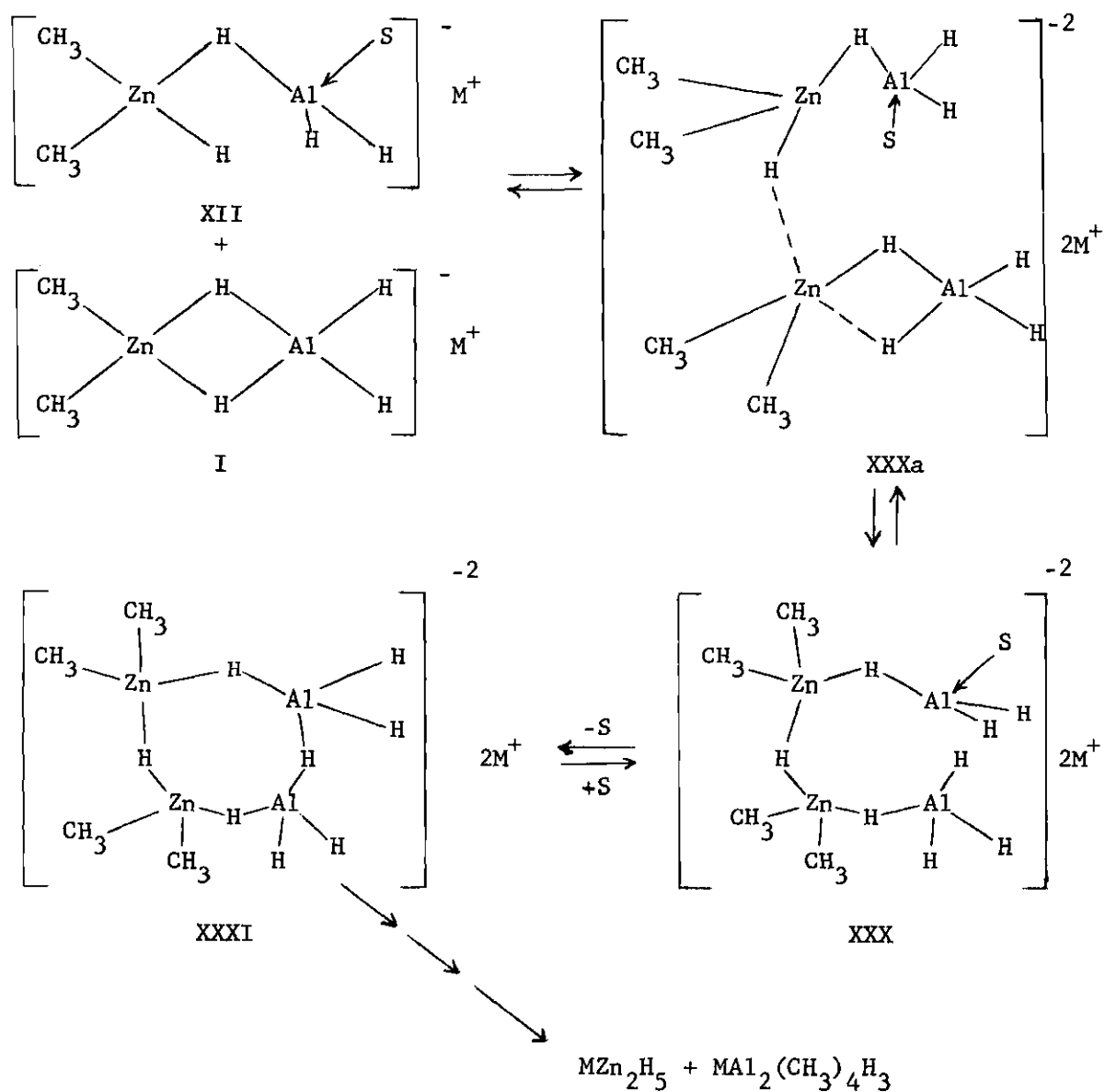


SCHEME XII (Concluded)



A reasonable mechanism by which $\text{MZn}(\text{CH}_3)_2\text{AlH}_4$ can undergo exchange to produce MZn_2H_5 is shown in Scheme XIII.

SCHEME XIII



Intermediate XXX results from the reaction of I with XII through transition state XXXa. In this reaction one of the Al-H-Zn bridge bonds in I is broken with subsequent formation of the Zn-H-Zn bridge bond in XXX. Intermediate XXX then undergoes an intramolecular displacement of the solvent on aluminum with simultaneous formation of an Al-H-Al bridge bond to give intermediate XXXI. It is easy for one to see how XXXI could undergo intramolecular methyl hydride exchange to produce MZn_2H_5 and $\text{MAl}_2(\text{CH}_3)_4\text{H}_3$.

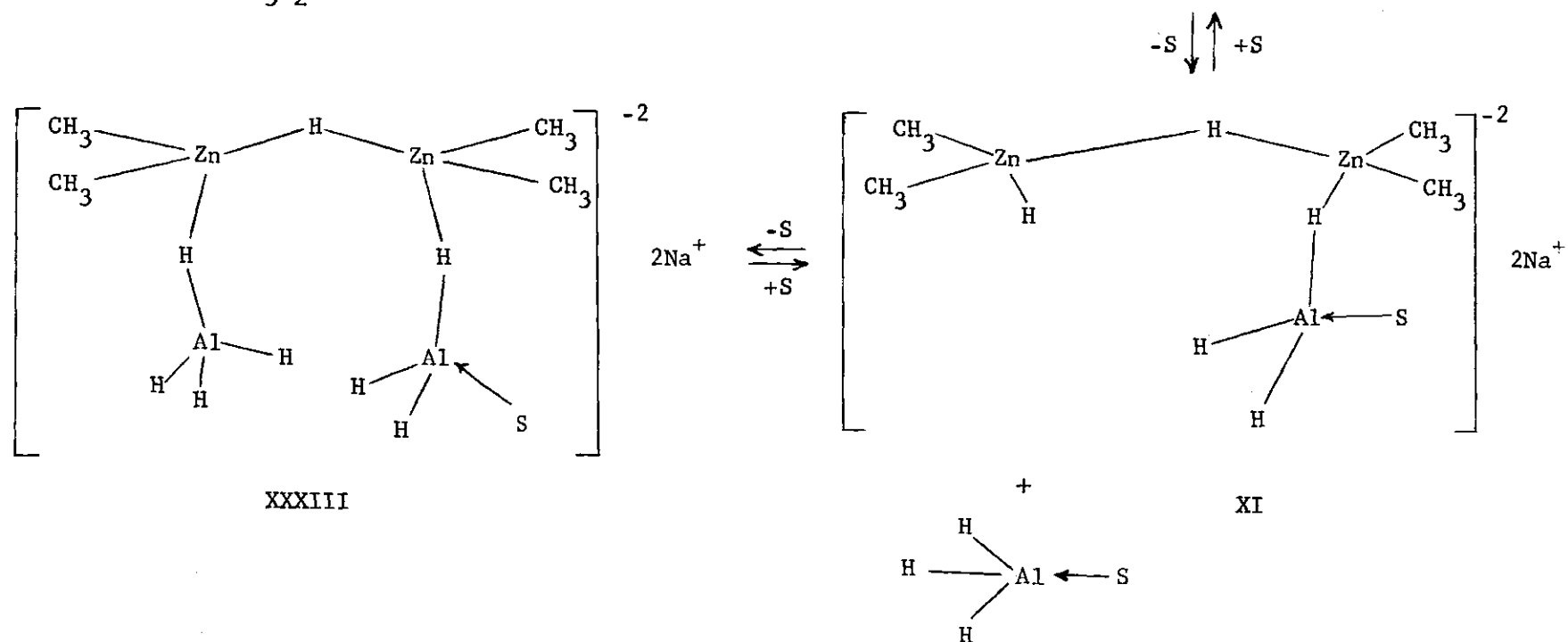
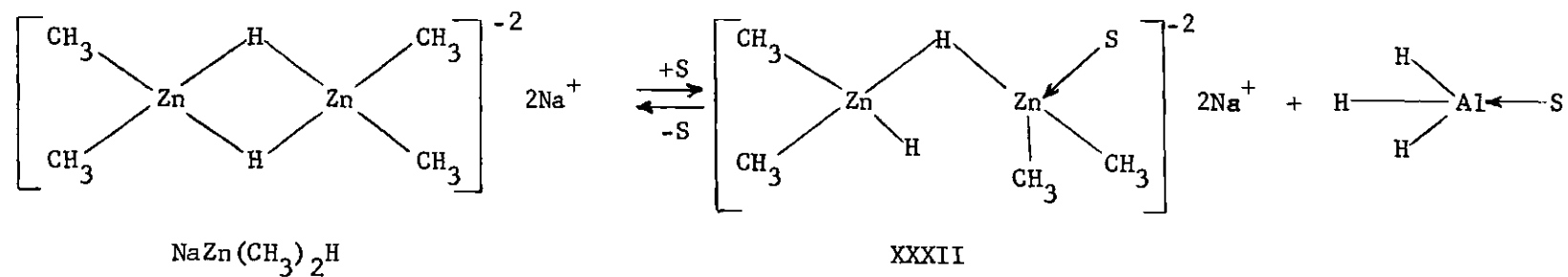
Figure 14 contains infrared spectra of the supernatant solution from the reaction of $\text{NaZn}(\text{CH}_3)_2\text{H}$ with AlH_3 after 5 minutes and 24 hours. The spectrum of the supernatant left after five minutes contained a broad band extending from 1550 to 1200 cm^{-1} with no well defined maximum. The rest of the spectrum corresponded to $\text{NaAl}_2(\text{CH}_3)_4\text{H}_3$ which was also formed. The broad band extending from 1550 to 1200 cm^{-1} could be due to $\text{NaZn}(\text{CH}_3)_2\text{AlH}_4$, but this seems unlikely due to the rate at which NaZn_2H_5 is formed in this reaction. If $\text{NaZn}(\text{CH}_3)_2\text{AlH}_4$ were the actual intermediate leading to NaZn_2H_5 , then one would have expected it to take about one week for all the zinc to disappear from solution, but instead it takes only a few hours. However, the intermediate must be similar to $\text{NaZn}(\text{CH}_3)_2\text{AlH}_4$, since the bands observed in the infrared are similar to those found for this compound. A likely candidate for this intermediate is XXXI, since it should give rise to an infrared spectrum similar to $\text{NaZn}(\text{CH}_3)_2\text{AlH}_4$. But in addition to this, XXXI is a necessary intermediate in any mechanistic scheme for the production of NaZn_2H_5 . A reasonable mechanism then for the reaction between $\text{NaZn}(\text{CH}_3)_2\text{H}$ and AlH_3 to give NaZn_2H_5 is

shown in Scheme XIV. The first step in this mechanism is solvent cleavage of one of the two bridging Zn-H-Zn bonds, then two molecules of alane can add rapidly to give intermediate XXXI. This intermediate then undergoes intramolecular alkyl-hydrogen exchange to yield NaZn_2H_5 .

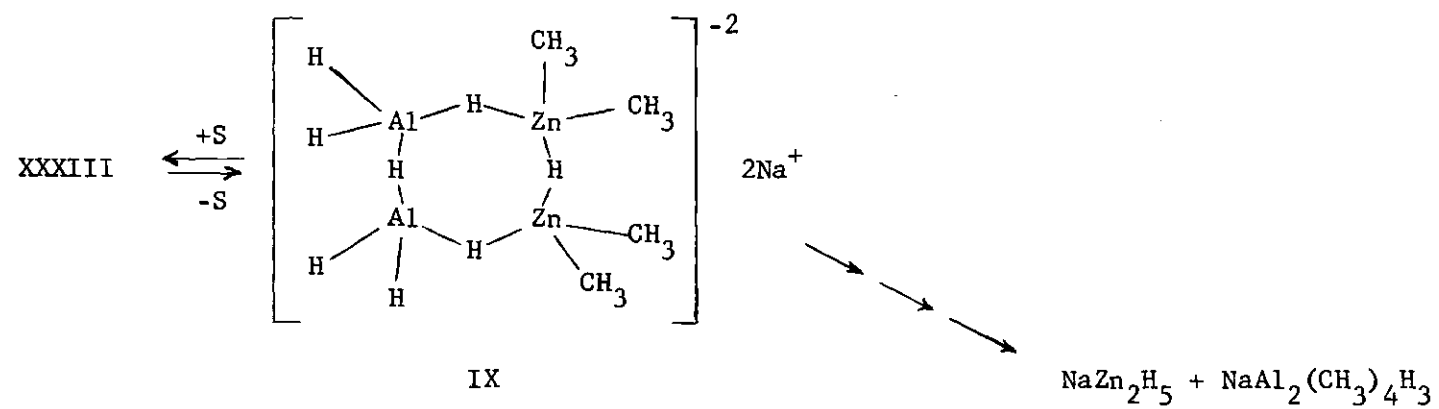
Earlier it was pointed out that the critical step in the formation of $\text{LiZn}_2(\text{CH}_3)_4\text{AlH}_4$ is the attack of a solvent molecule on an intermediate like XVII to cleave the Zn-H-Zn bridge bond. Evidently, in the reaction of $\text{KZn}_2(\text{CH}_3)_4\text{H}$ with alane, the Zn-H-Zn bridge bond in XVII is too strong to be cleaved by a solvent molecule and $\text{KZn}_2(\text{CH}_3)_4\text{AlH}_4$ is never formed. Instead of forming $\text{KZn}_2(\text{CH}_3)_4\text{AlH}_4$, XVII undergoes intramolecular exchange to yield KZn_2H_5 .

In Scheme III it was pointed out that a mobile equilibrium exists between $\text{LiZn}_2(\text{CH}_3)_4\text{AlH}_4$ and intermediates like XVII. When lithium or sodium is the cation, the equilibrium lies in the direction of $\text{MZn}_2(\text{CH}_3)_4\text{-AlH}_4$; however, when potassium is the cation, the equilibrium lies in the direction of XVII. Thus, when KAlH_4 and $(\text{CH}_3)_2\text{Zn}$ are allowed to react in a 1:2 molar ratio, the initial product is $\text{KZn}_2(\text{CH}_3)_4\text{AlH}_4$; however, it is converted to XVII after a few minutes. Intermediate XVII then undergoes intramolecular exchange to give KZn_2H_5 . Proof that both reactions proceed by way of the same intermediates is offered by the fact that an infrared spectrum of the supernatant solution (taken about 10 minutes after KZn_2H_5 began to precipitate) was exactly the same as the spectrum observed after five minutes in the reaction of $\text{KZn}_2(\text{CH}_3)_4\text{H}$ with alane in a 1:1 molar ratio. This spectrum is shown in Figure 20.

SCHEME XIV



SCHEME XIV (Concluded)



In this study we have tried to present reasonable mechanisms, based on the information gathered in this study, for the exchange reactions of the zinc ate complexes, $\text{MZn}(\text{CH}_3)_2\text{H}$ and $\text{MZn}_2(\text{CH}_3)_4\text{H}$ with alane. In these mechanisms we have tried to indicate the importance of the role of the solvent in exchange reactions of this type and have shown the dependence of the reaction between $(\text{CH}_3)_2\text{Zn}$ and MAlH_4 on solvent concentration.

LITERATURE CITED*

1. E. C. Ashby and R. G. Beach, Inorg. Chem., 10, 2486 (1971).
2. E. C. Ashby and John Watkins, J. Chem. Soc., Chem. Comm., 998 (1972).
3. E. C. Ashby and John J. Watkins, Inorg. Chem., 12, 2493 (1973).
4. This compound was first prepared by Shriver and co-workers. D. J. Shriver, G. J. Kubas, and J. A. Marshall, J. Amer. Chem. Soc., 93, 5067 (1971).
5. D. F. Shriver, "The Manipulation of Air Sensitive Compounds," McGraw-Hill, New York, N.Y., 1969.
6. E. C. Ashby and R. D. Schwartz, J. Chem. Ed., 51, 65 (1974).
7. F. W. Walker and E. C. Ashby, J. Chem. Ed., 45, 654 (1968).
8. C. R. Noller, Org. Syn., 12, 86 (1932).
9. H. C. Brown and H. M. Yoon, J. Amer. Chem. Soc., 88, 1464 (1966).
10. G. J. Kubas and D. F. Shriver, J. Amer. Chem. Soc., 92, 1949 (1970).
11. T. Mole and E. A. Jeffery, "Organoaluminum Compounds," Elsevier Publishing Co., Amsterdam, 1972.
12. D. F. Evans and I. Wharf, J. Chem. Soc., (A), 783 (1968).
13. G. E. Parris, Ph.D. Dissertation, Georgia Institute of Technology, 1974.
14. L. M. Seitz and T. L. Brown, J. Amer. Chem. Soc., 88, 4140 (1966).
15. R. Dautel and W. Zeil, Zeit. Elektrochem., 62, 1139 (1958).
16. G. D. Barbaras, C. Dillard, A. E. Finholt, J. Wartik, K. E. Wilzbach, and H. D. Schlesinger, J. Amer. Chem. Soc., 73, 4858 (1951).

* Journal title abbreviations used are listed in "List of Periodicals," Chemical Abstracts (1961).

17. M. B. Smith and W. E. Becker, Tetrahedron, 23, 4215 (1967).
18. M. B. Smith and W. E. Becker, Tetrahedron, 22, 3027 (1966).
19. F. W. Walker and E. C. Ashby, J. Amer. Chem. Soc., 91, 3845 (1969).
20. F. Schroder and H. Spandau, Naturwissen-Schaften, 53, 360 (1966).
21. G. E. Coates and J. A. Heslop, J. Chem. Soc., (A), 514 (1968).
22. M. C. Perucand and M. T. LeBihan, Acta. Cryst. Sec. B, 24, 1502 (1968).
23. E. C. Ashby and R. G. Beach, Inorg. Chem., 9, 2300 (1970).
24. E. C. Ashby and T. F. Korenowski, unpublished results.
25. E. C. Ashby and A. B. Goel, manuscript submitted for publication.
26. D. T. Hurd, J. Org. Chem., 13, 711 (1948).
27. G. J. Kubas and D. F. Shriver, Inorg. Chem., 9, 1951 (1970).
28. E. C. Ashby, Frank R. Dobbs, and Harry P. Hopkins, Jr., J. Amer. Chem. Soc., 95, 2823 (1973).
29. J. Boersma and J. G. Noltes, "Organozinc Coordination Chemistry," Elsevier Publishing Co., The Netherlands, 1968.

PART IV

The Composition of Lithium Methylcuprates in Etheral Solvents

CHAPTER I

INTRODUCTION

Lithium dialkylcuprates have proven to be very versatile reagents in organic synthesis.¹ Several recent reports, however, have been concerned with unusual reactivity of reagents prepared by mixing lithium dialkyl- or diaryl-cuprates with the corresponding organolithium compounds. For example, the reagent having the stoichiometry $\text{LiCuPh}_2 \cdot \text{PhLi}$ appears to be more reactive than LiCuPh_2 in metal-halogen exchange reactions and coupling with aryl bromides.² Also it has been recently found that a 3:2 mixture of $\text{LiCu}(\text{CH}_3)_2$ and CH_3Li is more stereoselective toward 4-tert-butylcyclohexanone than either $\text{LiCu}(\text{CH}_3)_2$ or CH_3Li .³ In addition, mixtures of $\text{LiCu}(\text{CH}_3)_2$ and CH_3Li have been found to react with diaryl ketones as if a reducing agent more powerful than either $\text{LiCu}(\text{CH}_3)_2$ or CH_3Li is present.⁴ These reports suggest that lithium diorganocuprates and organolithium compounds are capable of reacting to form complexes of the type $\text{Li}_2\text{Cu}(\text{CH}_3)_3$ and $\text{Li}_3\text{Cu}(\text{CH}_3)_4$. However, previous ^1H and natural abundance ^{13}C NMR studies on the system $\text{CH}_3\text{Li}-\text{LiCu}(\text{CH}_3)_2$ in diethyl ether at -60° failed to detect the existence of any complexes.^{4,5,13} In view of the intense interest in this area and the obvious possibility of the existence of other cuprates in addition to $\text{LiCu}(\text{CH}_3)_2$, we decided to study the ^1H NMR of the $\text{CH}_3\text{Li}-\text{CH}_3\text{Cu}$ mixture further.

Dimethyl ether was chosen as the initial solvent for this study

since methyl group exchange rates should be significantly slower in dimethyl ether (due to its greater basicity) than conventional ether solvents (e.g., diethyl ether). In addition, considerably lower solution temperatures can be reached with dimethyl ether (-136° vs -100°) than with most other ethers. After the studies in dimethyl ether, the cuprates were studied in tetrahydrofuran and then finally in diethyl ether. It was our hope that the results obtained in the more basic solvents, dimethyl ether and THF, could be used to help explain the system in diethyl ether. In addition, various ligands were added to cuprates in diethyl ether in an effort to clarify the situation in that solvent.

CHAPTER II

EXPERIMENTAL

Apparatus

Reactions were performed under nitrogen at the bench using Schlenk tube techniques.⁶ Other manipulations were carried out in a glove box equipped with a recirculating system using manganese oxide columns to remove oxygen and dry ice-acetone to remove solvent vapors.⁷ Proton NMR spectra were obtained at 60 MHz using a Varian A-60 NMR spectrometer and the ¹³C NMR spectra were determined at 25 MHz with a JEOL Fourier transform spectrometer, Model PFT-100. All chemical shift values are expressed in values (ppm) relative to (CH₃)₄Si. Calibrated syringes equipped with stainless steel needles were used for transfer of reagents. Deliveries could be reproduced to better than 0.5%.

Analytical

Active CH₃ group analysis was carried out by hydrolyzing samples with hydrochloric acid on a standard vacuum line and collecting the evolved methane with a Toepler pump.⁶ Lithium was determined by flame photometry. Iodide was determined by the Volhard procedure. Copper was determined by electrolytic deposition on a Pt electrode. The product analysis for the isomeric alcohols resulting from methylation of 4-tert-butylcyclohexanone has been previously described.¹⁴ Glpc analyses were performed using 6-ft matched columns of 10% FFAP on 80-100 mesh

Diatoport S. The identity of the peaks was determined by comparison of the hydrolyzed products formed on reaction of 4-tert-butylcyclohexanone with methyllithium and methylmagnesium bromide.¹⁹ Under the conditions of rate 55 ml/min, injection temperature 200°, and detector temperature 310°, the retention times for tetradecane, cis alcohol, ketone, and trans alcohol are 12, 28, 31, and 36 minutes at a column temperature of 80°. The two alcohols are known to have the same response ratio.²⁰ The response factors for the ketone and tetradecane were the same as those for the alcohols. In no case was the presence of 1-methylene-4-tert-butylcyclohexane (from the dehydration of the alcohols) detected.¹⁹ The amount of the recovered ketone was calculated from the area ratio of ketone to internal standard before and after the reaction.

Materials

Tetrahydrofuran (Fisher Certified Reagent Grade) was distilled under nitrogen over NaAlH_4 and diethyl ether (Fisher Reagent) over LiAlH_4 prior to use. Dimethyl ether was stored in a dry ice-acetone bath over LiAlH_4 and vapor transferred (by means of a vacuum line) just prior to use. Lithium metal was obtained as a 30% dispersion in petrolatum from Alfa-Ventron. Dimethylmercury, obtained from Org-Met, was found to be pure and therefore used without any further purification. Methyllithium in THF, Me_2O , and Et_2O was prepared halide free by the reaction of $(\text{CH}_3)_2\text{Hg}$ with excess lithium metal. All solutions of methyllithium were stored at - 78° until ready to use. Analysis of the methyllithium solutions gave $\text{CH}_3:\text{Li}$ ratios of essentially 1:1. The Me_2O and THF solutions were used within a week of preparation. Analysis prior to use indicated

that ether cleavage did not occur during one week storage in a dry ice-acetone bath. Cuprous iodide (Fisher Reagent) was purified by precipitating from an aqueous KI-CuI solution.⁸ The precipitated solid was washed with distilled water, ethanol, and diethyl ether, then dried at room temperature under reduced pressure. Cuprous chloride was prepared by the reaction of copper (II) chloride dihydrate (Baker Purified) with sodium sulfite.⁹ The resulting precipitated solid was washed with an aqueous solution of SO₂, glacial acetic acid, ethanol, and diethyl ether, then dried at room temperature under reduced pressure. Tri-n-butylphosphine (98%) was obtained from Aldrich Chemical Co. and used without further purification. Solutions of tetrakis [chloro (tri-n-butylphosphine) copper (I)] in diethyl ether were prepared by adding tri-n-butylphosphine to a slurry of CuCl in 1:1 ratio. The resulting mixture was stirred overnight, then filtered the next day to remove traces of residual material that remained. An analysis of the resulting solution indicated that Cu and Cl were present in a 1.00:1.03 ratio. Frinton Laboratories 4-tert-butylcyclohexanone was sublimed under nitrogen prior to use and found by glpc to be 99.9% pure. Solutions of 4-tert-butylcyclohexanone were prepared by weighing out a known amount of ketone in a calibrated volumetric flask and diluting to the mark with either Et₂O or THF. Lithium bromide, LiI, and LiClO₄ were made anhydrous by fusing under vacuum. Solutions of LiBr, LiI, and LiClO₄ were prepared by stirring the anhydrous solids in either Et₂O or THF. Solution concentrations were determined by analyzing for Li and halide in the case of LiBr and LiI and just Li for LiClO₄.

Procedure

Preparation of Cuprates

Diethyl Ether Solvent. Solutions of the cuprates were prepared free of contaminants for NMR and molecular weight experiments. Cuprous iodide was allowed to react with methyllithium in 1:1 ratio in a dry ice-acetone bath to produce methylcopper as a yellow solid slurry. The yellow solid was prepared free of LiI by centrifuging, decanting, and washing with several portions of dry diethyl ether. These manipulations were carried out under nitrogen at dry ice-acetone temperature. The resulting methylcopper was slurried with dry ether and used in this way as a reagent. A typical analysis of the slurry showed Li, Cu, CH₃, and I present in molar ratios of 0.02:1.00:0.97:0.01. The slurry was stored in a dry ice-acetone bath.

Methyllithium was then allowed to react with samples of the methylcopper slurry in ratios of 0.50, 0.75, 1.00, 2.00, 3.00, and 4.00 (CH₃Li/CH₃Cu) at dry ice-acetone temperature. For running NMR spectra samples of the resulting solutions were transferred at dry ice-acetone temperature to NMR tubes with rubber septum caps by means of a cannula. These solutions were also analyzed for Li, Cu, and CH₃. (See Table 3 for some representative data.)

Solutions of Li₂Cu₃(CH₃)₅, LiCu(CH₃)₂, and Li₂Cu(CH₃)₃ used in the molecular weight measurements, were prepared in a similar way.

Tetrahydrofuran Solvent. Solutions of cuprates in this solvent were prepared in the same way as described above for diethyl ether. In addition the same cuprates were prepared in the presence of LiI by adding

CH_3Li to CuI in the proper ratios.

Dimethyl Ether Solvent. Since LiI was found to be mostly insoluble in dimethyl ether, solutions of cuprates in this solvent were prepared by adding methyllithium directly to CuI in 1.50, 1.75, 2.00, 3.00, and 4.00 ratios of $\text{CH}_3\text{Li}:\text{CuI}$ at dry ice-acetone temperature. For running NMR spectra, samples of the supernatant solutions were transferred at dry ice-acetone temperature by means of a cannula to NMR tubes with rubber septum caps. The supernatant solutions were also analyzed for Li , Cu , and CH_3 . (See Table 2 for some representative data.) Typically, the amount of LiI remaining in these solutions was equivalent to about 15% of the copper present. It is felt, however, that the presence of this halide did not influence the NMR spectra. This statement is based on the fact that the NMR in THF were unchanged by the presence of halide and were essentially the same as the spectra observed in dimethyl ether.

Diethyl Ether Solvent With $\text{P}(\text{n-Bu})_3$ Present. The cuprates in this system were prepared by reacting methyllithium with $[\text{CuCl}.\text{P}(\text{n-Bu})_3]_4$ in ratios of 1.50, 1.75, 2.00, 3.00, 4.00, and 5.00 $\text{CH}_3\text{Li}:\text{CuCl}$ in diethyl ether at room temperature. The resulting mixtures were stirred at this temperature for about two hours in order to assure complete precipitation of LiCl . They were then cooled to dry ice-acetone temperature and the LiCl allowed to settle. The supernatant solutions were analyzed and prepared for running NMR spectra in the way described above. (See Table 4 for representative data).

General Reactions with 4-tert-Butylcyclohexanone

A 10 ml Erlenmeyer flask with a Teflon coated magnetic stirring

bar was dried in an oven and allowed to cool under nitrogen flush, then sealed with a rubber septum and connected by means of a needle to a nitrogen filled manifold equipped with a mineral oil filled bubbler. The organometallic reagent (ca. 1-0.5 mmoles) was syringed into the flask, then the calculated amount of ketone (in THF or Et₂O solvent with internal standard, n-C₁₂H₂₆ or n-C₁₄H₃₀) was added to the stirred reagent at dry ice-acetone temperature. After three hours the reaction was quenched by H₂O slowly and dried by MgSO₄. The yield of products was determined by glpc. In the reactions of cuprates with this ketone, n-C₁₂H₂₆ was used as the internal standard to calculate the reaction yield.

Molecular Weight Measurements

The solutions of LiCu₂(CH₃)₃, LiCu(CH₃)₂, and Li₂Cu(CH₃)₃, used in the molecular weight measurements, were prepared as above except the LiCl by-product was removed in order to obtain pure solutions.

The ebullioscopic technique reported earlier¹⁰ was used for determining molecular weights of the cuprates in this study. The concentration of solute molecules is given approximately by Eq. 1 where ρ is the density of the solvent

$$C = \frac{1000 \rho}{M_1 \left(1 + \frac{1000 K_B}{M_1 \Delta T_B} \right)} \quad (1)$$

in gm/cc, M_1 is the molecular weight of the solvent, K_B is the molal boiling point elevation constant, and ΔT_B is the boiling point elevation

in °C. The concentration of solute molecules C is in units of molarity. Equation 1 was derived from Eq. 2 reported earlier¹⁰

$$i = \frac{W_2 M_1}{W_1 M_2} \left[\frac{1}{e^{\frac{\Delta T_B M_1}{1000 K_B}} - 1} \right] \quad (2)$$

where i is the molecular association. In this study the molecular association was determined by taking the ratio of the solution concentration (as determined by analysis) to the apparent solution concentration given by Eq. 1. The results of these molecular weight measurements are given in Figures 4-6. Molecular weight measurements in diethyl ether were carried out at 740.0 mm Hg pressure of N_2 ($K_B = 2.06$). In THF the measurements were made at 240.0 mm Hg pressure of N_2 ($K_B = 1.79$).

Interpretation of Exchange Mechanisms for NMR Data

Information regarding the kinetics of exchange processes can be extracted for NMR data in various ways.¹¹ In this study use has been made of the method which utilizes measurement of line half-intensity widths in the slow-exchange region. The system under investigation here, $CH_3Li-LiCu(CH_3)_2$, is particularly suitable for NMR analysis of rates because the individual components of the two site system can each be examined throughout the entire temperature range of interest. Thus, the line half-intensity widths in the absence of exchange are known.

It is sometimes possible to test an exchange mechanism by evaluating the dependences of the individual τ_A and τ_B values, the mean lifetimes for a stay on A and B sites, on concentration, or on a ratio of two concentrations. For this purpose, it is best to examine the

individual line widths at a temperature corresponding to slow exchange. Under these conditions, the mean lifetime at site i , τ_i , is related to the line width at half-intensity, $\Delta 1/2$, by Eq. 3

$$\frac{1}{\tau_i} = \pi \left(\Delta \frac{1}{2} - \Delta^o \frac{1}{2} \right) \quad (3)$$

where $\Delta^o \frac{1}{2}$ is the measured half-intensity width for the i^{th} component in the absence of exchange.

Measurement of $1/\tau_i$ for a single sample at a series of temperatures in the temperature region below coalescence can also be employed to determine the activation energy for the exchange process.

For testing exchange mechanisms, the mean lifetimes for stay of methyl groups on CH_3Li and $\text{LiCu}(\text{CH}_3)_2$ were evaluated at -51° . This temperature is in the slow exchange region as is indicated by the typical spectra shown in Figure 7. At this temperature, $\text{LiCu}(\text{CH}_3)_2$ half-width ranged from 2.3-10.3 Hz depending on the $\text{CH}_3\text{Li}/\text{LiCu}(\text{CH}_3)_2$ ratio. In the absence of exchange the half-widths varied from 1.4-1.7 Hz. The half-widths corresponding to the methyllithium signal varied from 6.2-5.1 Hz.

The probe temperature was calibrated externally with methanol.

CHAPTER III

RESULTS AND DISCUSSION

Signals due to $\text{Li}_2\text{Cu}(\text{CH}_3)_3$, $\text{LiCu}(\text{CH}_3)_2$, and $\text{LiCu}_2(\text{CH}_3)_3$ can be observed in the ^1H NMR spectra of the system $\text{CH}_3\text{Li}-\text{CH}_3\text{Cu}$ at -136° in dimethyl ether solvent. The spectra are shown in Figure 1 for molar ratios of $\text{CH}_3\text{Li}:\text{CH}_3\text{Cu}$ ranging from 0.51 to 1.97. The chemical shifts observed upfield from TMS are listed in Table 1 at various temperatures for selected $\text{CH}_3\text{Li}:\text{CH}_3\text{Cu}$ ratios. When the ratio of $\text{CH}_3\text{Li}:\text{CH}_3\text{Cu}$ was less than one, three signals were observed (-0.22δ , -1.17δ , and 1.38δ). The signal at -1.38δ (due to $\text{LiCu}(\text{CH}_3)_2$) became more intense as the $\text{CH}_3\text{Li}:\text{CH}_3\text{Cu}$ ratio was increased from 0.53 to 1.02 and was the only signal observed at the latter ratio. The signals at -0.22δ and -1.17δ always integrated in the ratio 1:2 and were due to $\text{LiCu}_2(\text{CH}_3)_3$, since these signals were the only ones observed at a $\text{CH}_3\text{Li}:\text{CH}_3\text{Cu}$ ratio of 0.51. When the ratio of $\text{CH}_3\text{Li}:\text{CH}_3\text{Cu}$ was greater than one, four signals were observed (-1.25δ , -1.38δ , -1.49δ , and 2.03δ). The signal at -2.03δ was due to CH_3Li and the signal at -1.38δ was due to $\text{LiCu}(\text{CH}_3)_2$. The signals at -1.25δ and -1.49δ always integrated in a 1:2 ratio and were due to $\text{Li}_2\text{Cu}(\text{CH}_3)_3$. The presence of $\text{Li}_2\text{Cu}(\text{CH}_3)_3$ was indicated by the fact that equilibrium constants calculated at -136° for the reaction^{*} described by Eq. 4 at various $\text{CH}_3\text{Li}/\text{CH}_3\text{Cu}$ ratios,

^{*}The reactants are written with the degree of association that has been found for them by molecular weight measurements. Methyl lithium has been found to be a tetramer in both diethylether and THF.¹² Lithium dimethylcuprate has been found to be dimeric in diethyl ether.¹³ The results of this work show that $\text{LiCu}(\text{CH}_3)_2$ is dimeric in THF; and, in

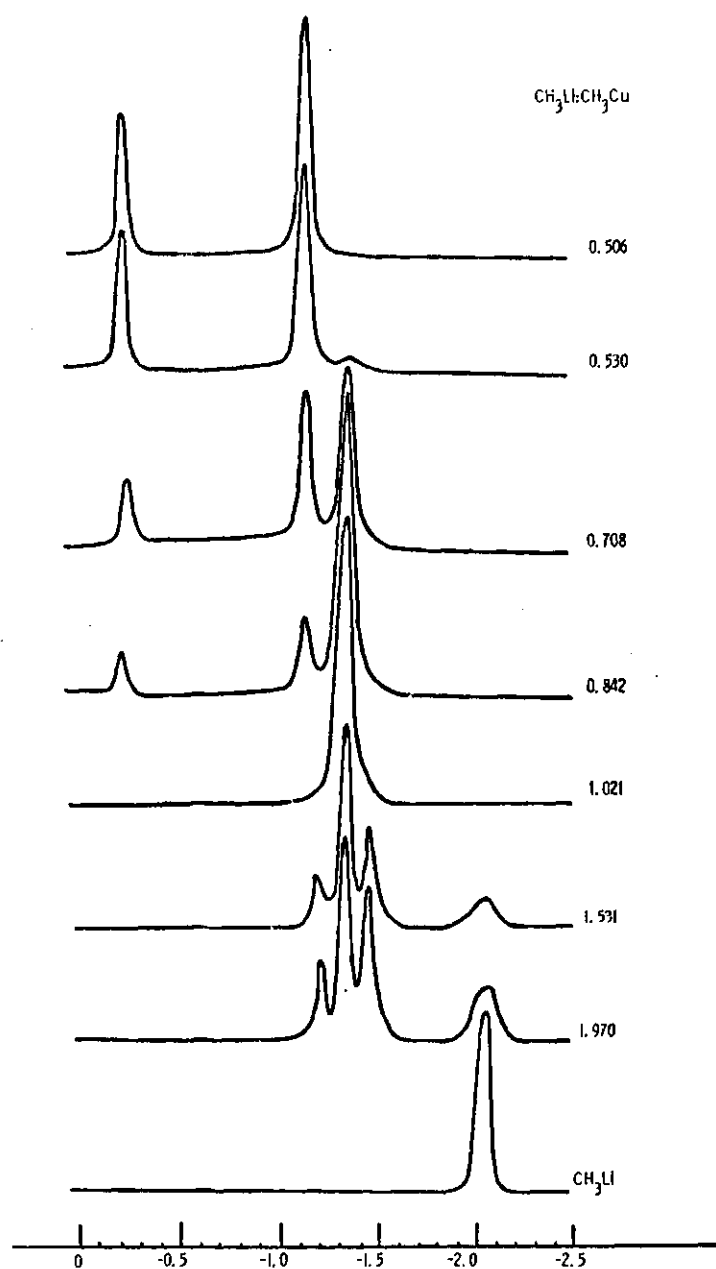
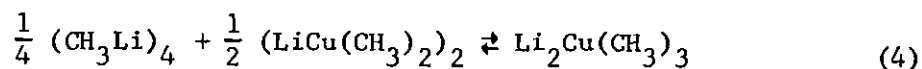


Figure 1. 60 MHz ^1H NMR at -136° in Dimethyl Ether for Solutions of $\text{CH}_3\text{Li}-\text{CH}_3\text{Cu}$

Table 1. Chemical Shifts for the System $\text{CH}_3\text{Li}-\text{CH}_3\text{Cu}$ in Dimethyl Ether

Approximate Ratio $\text{CH}_3\text{Li}/\text{CH}_3\text{Cu}$	Temperature ^b (°C)	$\delta^{a,b}$ (PPM)	Analysis of the Solution Li : Cu : CH_3
2	- 84	1.38, 2.03	1.97:1.00:3.01
	-102	1.37, 2.03	
	-119	1.38, 2.03	
	-136	1.25, 1.38, 1.49, 2.03	
1	- 67	1.38	1.02:1.00:1.91
	- 84	1.37	
	-102	1.39	
	-112	1.38	
	-132	1.38	
	-140	1.39 1.38	
0.75	- 31	1.13	0.71:1.00:1.68
	- 48	1.22	
	- 66	1.28	
	- 84	0.22, 1.17, 1.38	
	-102	0.22, 1.18, 1.38	
	-119	0.23, 1.17, 1.39	
	-136	0.22, 1.17, 1.38	
0.50	- 66	1.10	0.51:1.00:1.47
	- 84	0.22, 1.17	
	-102	0.24, 1.18	
	-119	0.22, 1.17	
	-136	0.33, 1.18	

^aPPM upfield from TMS.^bTypical errors in the chemical shift and temperature were ± 0.02 ppm and $\pm 5^\circ$.



were essentially the same. For example, the equilibrium constant at -136° at a $\text{CH}_3\text{Li}/\text{CH}_3\text{Cu}$ ratio of 1.53 was 0.36. At a ratio of 1.97 at the same temperature, the equilibrium constant was again 0.36. In addition to this evidence, when equilibrium constants were calculated at several different temperatures and plotted as $\ln K$ vs $1/T$, a straight line was obtained (see Figure 3 and later discussion). If any equilibrium mixture other than CH_3Li , $\text{LiCu}(\text{CH}_3)_2$, and $\text{Li}_2\text{Cu}(\text{CH}_3)_3$ is assumed, the calculated equilibrium constants do not have the consistency as those above. This leads us to conclude that the signals at -1.25δ and -1.49δ must be due to $\text{Li}_2\text{Cu}(\text{CH}_3)_3$. Increasing the $\text{CH}_3\text{Li}:\text{CH}_3\text{Cu}$ ratio above two did not result in the appearance of any new signals.

One could explain the signals observed in dimethyl ether as resulting from the presence of LiI . The ^1H NMR spectra in THF at -98° , however, were very similar to those observed in dimethyl ether, indicating the presence of the same three ate complexes. These same signals were observed both with and without the presence of LiI . Therefore, the presence of LiI in both dimethyl ether and THF has no influence on complexes formed between CH_3Li and $\text{LiCu}(\text{CH}_3)_2$.

The chemical shifts observed upfield from TMS in tetrahydrofuran solvent at various temperatures are given in Table 2. When the ratio of $\text{CH}_3\text{Li}:\text{CH}_3\text{Cu}$ was 0.51, two signals, which always integrated in a ratio of 1:2, were observed at -0.24δ and -1.24δ . These signals correspond very addition, that $\text{Li}_2\text{Cu}(\text{CH}_3)_3$ is monomeric in THF. Since dimethyl ether is similar in many respects to THF, one would expect CH_3Li , $\text{LiCu}(\text{CH}_3)_2$, and $\text{Li}_2\text{Cu}(\text{CH}_3)_3$ to have the same association in dimethyl ether as in THF.

Table 2. Chemical Shifts for the System $\text{CH}_3\text{Li}-\text{CH}_3\text{Cu}$ in Tetrahydrofuran

Approximate Ratio $\text{CH}_3\text{Li}/\text{CH}_3\text{Cu}$	Temperature ^b (°C)	$\delta^{a,b}$ (PPM)	Analysis of the Solution Li : Cu : CH_3
4	4	1.36, 1.98	4.07:1.00:4.47
	-19	1.43, 2.01	
	-37	1.45, 2.01	
	-51	1.50, 2.01	
	-67	1.50, 1.99	
	-98	1.37, 1.50, 1.63, 2.01	
3	-51	1.49, 1.99	2.89:1.00:3.62
	-67	1.50, 1.98	
	-83	1.50, 2.02	
	-98	1.37, 1.50, 1.62, 2.02	
1	-67	1.50	1.02:1.00:2.12
	-83	1.49	
	-98	1.50	
0.75	-37	1.22	0.75:1.00:1.55
	-51	1.23 (br)	
	-67	1.28 (sh), 1.45	
	-83	0.25, 1.24, 1.50	
	-98	0.24, 1.25, 1.51	
0.50	4	0.97	0.51:1.00:1.52
	-19	0.98	
	-37	0.97 (br)	
	-51	1.02 (sh), 1.13	
	-67	0.25, 1.22	
	-83	0.25, 1.24	
	-98	0.24, 1.24	

^aPPM upfield from TMS. ^bTypical errors in the chemical shift and temperature were ± 0.02 ppm and $\pm 5^\circ$.

closely to those observed for $\text{LiCu}_2(\text{CH}_3)_3$ in dimethyl ether and are assigned to that compound. At $\text{CH}_3\text{Li}:\text{CH}_3\text{Cu}$ ratios intermediate between 0.5 and 1.0, three signals were observed at -0.24δ , -1.24δ , and -1.50δ . The signal at -1.50δ (due to $\text{LiCu}(\text{CH}_3)_2$) became more intense as the $\text{CH}_3\text{Li}:\text{CH}_3\text{Cu}$ ratio was increased from 0.51 to 1.02 and was the only signal observed at the latter ratio. When the ratio of $\text{CH}_3\text{Li}:\text{CH}_3\text{Cu}$ was greater than one, four signals were observed at -1.37δ , -1.50δ , -1.63δ , and -2.01δ . The signal at -2.01δ was due to CH_3Li . The signals at -1.37δ and -1.63δ , which always integrated in a 1:2 ratio, were due to $\text{Li}_2\text{Cu}(\text{CH}_3)_3$, since they were very similar to the signals observed for $\text{Li}_2\text{Cu}(\text{CH}_3)_3$ in dimethyl ether. This point was established, however, by calculating equilibrium constants from the integration data for several equilibrium mixtures. The system, CH_3Li , $\text{LiCu}(\text{CH}_3)_2$, $\text{Li}_2\text{Cu}(\text{CH}_3)_3$ (Eq. 4), yielded the most consistent equilibrium constants; therefore, the signals at -1.37δ and -1.63δ are attributed to $\text{Li}_2\text{Cu}(\text{CH}_3)_3$.

The chemical shifts observed upfield from TMS in diethyl ether at various temperatures and selected ratios of $\text{CH}_3\text{Li}:\text{CH}_3\text{Cu}$ are given in Table 3. In this solvent the direct observation of signals due to any complexes other than $\text{LiCu}(\text{CH}_3)_2$ was not possible. However, indirect evidence can be presented for the existence of the complexes $\text{Li}_2\text{Cu}_3(\text{CH}_3)_5$ and $\text{Li}_2\text{Cu}(\text{CH}_3)_3$. The addition of CH_3Li to a slurry of CH_3Cu in diethyl ether yielded a clear solution when the ratio of $\text{CH}_3\text{Li}:\text{CH}_3\text{Cu}$ reached 0.67. In both dimethyl ether and THF, this happened when the ratio was 0.50. Since $\text{LiCu}_2(\text{CH}_3)_3$ was observed in both of these solvents, the above observation indicated that $\text{Li}_2\text{Cu}_3(\text{CH}_3)_5$ was formed in diethyl

Table 3. Chemical Shifts for the System $\text{CH}_3\text{Li}-\text{CH}_3\text{Cu}$ in Diethyl Ether

Approximate Ratio $\text{CH}_3\text{Li}/\text{CH}_3\text{Cu}$	Temperature ^b (°C)	δ ^{a,b} (PPM)	Analysis of the Solution Li : Cu : CH_3
3	- 51	1.09, 1.95	2.80:1.00:3.88
	- 67	1.13, 2.01	
	- 83	1.09, 1.98	
	- 98	1.09, 1.98	
1	- 83	1.09	1.02:1.00:1.96
	- 98	1.10	
0.75	- 67	0.95	2.18:3.00:5.09
	- 83	0.99	
	- 98	1.03	
0.50	- 67	0.93	2.24:3.00:4.97
	- 83	0.99	
	- 98	0.94 (sh), 1.01	
	-106	0.88 (sh), 1.08	

^a PPM upfield from TMS

^b Typical errors in the chemical shift and temperature were ± 0.02 ppm and $\pm 5^\circ$.

ether. The addition of CH_3Li to a slurry of CH_3Cu in diethyl ether such that the ratio was 1:2 did not result in a clear solution. An analysis of the supernatant solution resulting from this mixture shows that Li, Cu, and CH_3 were present in a ratio of 2:3:5 (see Table 3). This again indicates that 2:3 is the lowest ratio of Li/Cu that can be obtained in a cuprate complex.

The integration of NMR spectra recorded on diethyl ether solutions where the ratio of $\text{CH}_3\text{Li}:\text{CH}_3\text{Cu}$ was greater than one always showed less area under the CH_3Li signal than would have been expected based on an analysis of the solution. This type of behavior is consistent with the formation of a complex between CH_3Li and $\text{LiCu}(\text{CH}_3)_2$. Using the integration data, equilibrium constants were calculated for several mixtures which contained CH_3Li , $\text{LiCu}(\text{CH}_3)_2$, and complexes between these two reagents. The equilibrium shown in Equation 4 yielded the most consistent set of equilibrium constants. This result indicated that the complex between CH_3Li and $\text{LiCu}(\text{CH}_3)_2$ was $\text{Li}_2\text{Cu}(\text{CH}_3)_3$.

The chemical shifts observed upfield from TMS in diethyl ether when the ligand $\text{P}(\text{n-Bu})_3$ is present are given in Table 4. For this system, signals due to $\text{LiCu}(\text{CH}_3)_2$ and $\text{Li}_2\text{Cu}(\text{CH}_3)_3$ were observed directly. However indirect evidence can be presented for the existence of the complex $\text{LiCu}_2(\text{CH}_3)_3$. The addition of CH_3Li to a solution of $\text{CuCl}\cdot\text{P}(\text{n-Bu})_3$ yielded slurries of CH_3Cu until the ratio of $\text{CH}_3\text{Li}:\text{CuCl}$ reached 1.50. At that point all the CH_3Cu dissolved and only a slurry of LiCl remained. This result indicated that the complex $\text{LiCu}_2(\text{CH}_3)_3$ was formed. Evidently, the presence of $\text{P}(\text{n-Bu})_3$ favors the formation of $\text{LiCu}_2(\text{CH}_3)_3$.

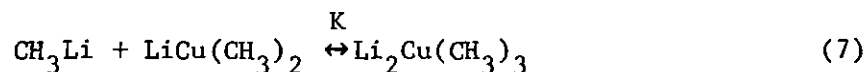
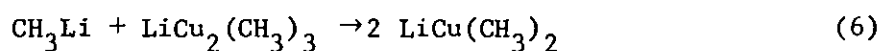
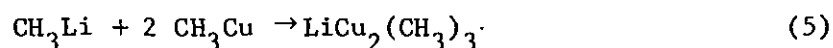
Table 4. Chemical Shifts for the System $\text{CH}_3\text{Li}-\text{CH}_3\text{Cu}\cdot\text{P}(\text{n-Bu})_3$ in Diethyl Ether

Approximate Ratio $\text{CH}_3\text{Li}/\text{CH}_3\text{Cu}$	Temperature ^b (°C)	$\delta^{a,b}$ (PPM)	Analysis of the Solution Li : Cu : CH_3
4	- 51	1.13, 1.97	4.06:1.00:4.87
	- 67	1.10, 1.23, 1.98	
	- 83	1.10, 1.25, 1.96	
	- 98	1.09, 1.24, 1.98	
2	- 36	1.11, 1.97	2.04:1.00:2.86
	- 51	1.12, 1.97	
	- 67	1.10, 1.25, 1.98	
	- 83	1.11, 1.24, 1.99	
	- 98	1.10, 1.24, 1.98	
1	- 67	1.11	1.02:1.00:1.91
	- 83	1.09	
	- 98	1.10	
0.75	- 51	0.85	1.97:3.00:4.87
	- 67	0.85	
	- 83	0.85	
	- 98	0.85	
0.50	- 51	0.69	0.98:2.00:2.86
	- 67	0.68	
	- 83	0.69	
	- 98	0.68	
	-106	0.69	

^aPPM upfield from TMS. ^bTypical errors in the chemical shift and temperature were ± 0.02 ppm and $\pm 5^\circ$.

over $\text{Li}_2\text{Cu}_3(\text{CH}_3)_5$ in diethyl ether. When the ratio of $\text{CH}_3\text{Li}:\text{CuCl}$ was greater than two, three signals were observed at -1.10δ , -1.24δ , and -1.97δ . The signals at -1.10δ and -1.97δ were due to $\text{LiCu}(\text{CH}_3)_2$ and CH_3Li . The signal at -1.24δ was due to $\text{Li}_2\text{Cu}(\text{CH}_3)_3$. This point was established in the same way as was done in the three previous cases.

The cuprate complexes that exist in the three solvents studied here are listed in Table 5. In dimethyl ether and THF, the NMR data suggest that the reactions as shown in Eq. 5-7 are taking place.



Reactions 5 and 6 proceed essentially to completion, whereas reaction 7 is an equilibrium between CH_3Li , $\text{LiCu}(\text{CH}_3)_2$, and $\text{Li}_2\text{Cu}(\text{CH}_3)_3$. In diethyl ether alone, the reactions are shown in Eq. 8-10. Reactions 8 and 9 proceed essentially to completion whereas reaction 10 is an equilibrium.

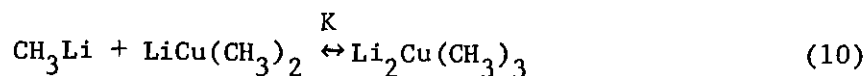
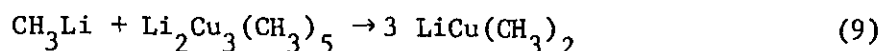
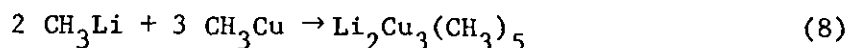


Table 5. Cuprate Complexes That Exist in Various Ether Solvents

Dimethyl Ether	Tetrahydrofuran	Diethyl Ether	
		Without $P(n\text{-Bu})_3$	With $P(n\text{-Bu})_3$
$\text{LiCu}_2(\text{CH}_3)_3$	$\text{LiCu}_2(\text{CH}_3)_3$	$\text{Li}_2\text{Cu}_3(\text{CH}_3)_5$	$\text{LiCu}_2(\text{CH}_3)_3$
$\text{LiCu}(\text{CH}_3)_2$	$\text{LiCu}(\text{CH}_3)_2$	$\text{LiCu}(\text{CH}_3)_2$	$\text{LiCu}(\text{CH}_3)_2$
$\text{Li}_2\text{Cu}(\text{CH}_3)_3$	$\text{Li}_2\text{Cu}(\text{CH}_3)_3$	$\text{Li}_2\text{Cu}(\text{CH}_3)_3$	$\text{Li}_2\text{Cu}(\text{CH}_3)_3$

All four systems yield $\text{Li}_2\text{Cu}(\text{CH}_3)_3$ when the ratio $\text{CH}_3\text{Li}:\text{CH}_3\text{Cu}$ is greater than one; and they all yield $\text{LiCu}(\text{CH}_3)_2$ when the ratio is one. When the ratio is less than one, all of the systems except diethyl ether without $\text{P}(\text{n-Bu})_3$ yield $\text{LiCu}_2(\text{CH}_3)_3$.

Using the NMR integration data for the above systems, equilibrium constants can be calculated for reaction 4. The equilibrium constants at various temperatures for these systems are listed in Table 6. Plots of $\ln K$ as a function of $1/T$ for these systems are shown in Figures 2 and 3. It can be seen that these plots give rise to straight lines, from which the thermodynamic parameters ΔH and ΔS can be calculated (Table 6). It is readily seen that both ΔH and ΔS decrease from positive to negative values as the solvent is changed from diethyl ether to dimethyl ether to THF. This order of solvents also reflects increasing basicity. So it is seen, then, that ΔH and ΔS decrease as the basicity of the solvent is increased as would be expected from increased specific solvation.

Ebullioscopic molecular weight measurements have been carried out on the systems $\text{CH}_3\text{Li}-\text{CH}_3\text{Cu}$ in THF, $\text{CH}_3\text{Li}-\text{CH}_3\text{Cu}$ in diethyl ether, and $\text{CH}_3\text{Li}-\text{CH}_3\text{Cu}\cdot\text{P}(\text{n-Bu})_3$ in diethyl ether. The results of these studies are shown in Figures 4-6. For $\text{LiCu}(\text{CH}_3)_2$ in THF, the association values varied from 1.81-1.91 over a concentration range of 0.071-0.142 M. These results indicate that $\text{LiCu}(\text{CH}_3)_2$ is dimeric in THF. For $\text{LiCu}_2(\text{CH}_3)_3$ the association values varied from 1.83-2.11 over a concentration range of 0.065-0.094 M, indicating that $\text{LiCu}_2(\text{CH}_3)_3$ is also dimeric in THF. In order to determine the association of $\text{Li}_2\text{Cu}(\text{CH}_3)_3$, an approximately 3:1 mixture of CH_3Li and CH_3Cu was prepared. This mixture of CH_3Li and CH_3Cu

Table 6. Equilibrium Constants and Thermodynamic Parameters for
the Reaction $\frac{1}{4}(\text{CH}_3\text{Li})_4 + \frac{1}{2}(\text{LiCu}(\text{CH}_3)_2)_2 \xrightleftharpoons{K} \text{Li}_2\text{Cu}(\text{CH}_3)_3$

System	Temperature ^c	K	ΔH° ^a	ΔS° ^b
$\text{CH}_3\text{Li}-\text{CH}_3\text{Cu}$ (Et_2O)	- 38	2.2	5.9	27
	- 51	0.76		
	- 67	0.32		
	- 83	0.19		
	- 98	0.02		
$\text{CH}_3\text{Li}-\text{CH}_3\text{Cu} \cdot \text{P}(\text{n-Bu})_3$ (Et_2O)	- 51	1.8	3.3	16
	- 67	0.77		
	- 83	0.53		
	- 98	0.22		
	-106	0.12		
$\text{CH}_3\text{Li}-\text{CH}_3\text{Cu}$ (THF)	- 5	0.12	- 1.2	- 8.6
	- 19	0.13		
	- 36	0.17		
	- 51	0.22		
	67	0.19		
	- 83	0.27		
	- 98	0.42		
$\text{CH}_3\text{Li}-\text{CH}_3\text{Cu}$ (Me_2O)	- 84	0.27	- 0.25	- 3.9
	-102	0.30		
	-119	0.30		
	-136	0.36		

^aKcal/mole

^bCal/^oK-mole

^cTypical error limit was $\pm 5^\circ$.

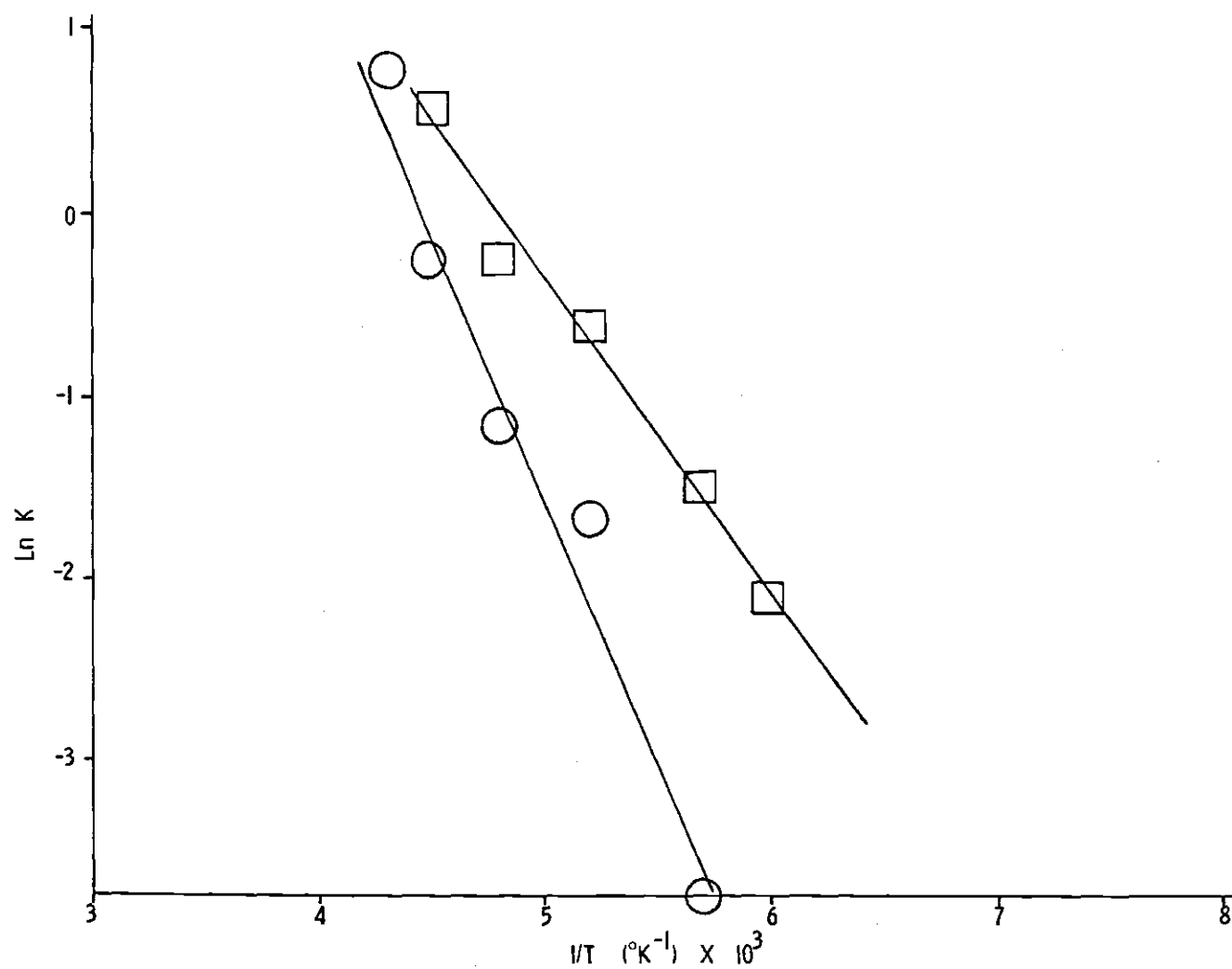


Figure 2. Plot of $\ln K$ versus $1/T$ for the Reaction $1/4(\text{CH}_3\text{Li})_4 + 1/2(\text{LiCu}(\text{CH}_3)_2)_2 \leftrightarrow \text{Li}_2\text{Cu}(\text{CH}_3)_3$ in the Systems: \bigcirc $\text{CH}_3\text{Li}-\text{CH}_3\text{Cu}$ in Diethyl Ether, \square $\text{CH}_3\text{Li}-\text{CH}_3\text{Cu} \cdot \text{P}(\text{n-Bu})_3$ in Diethyl Ether

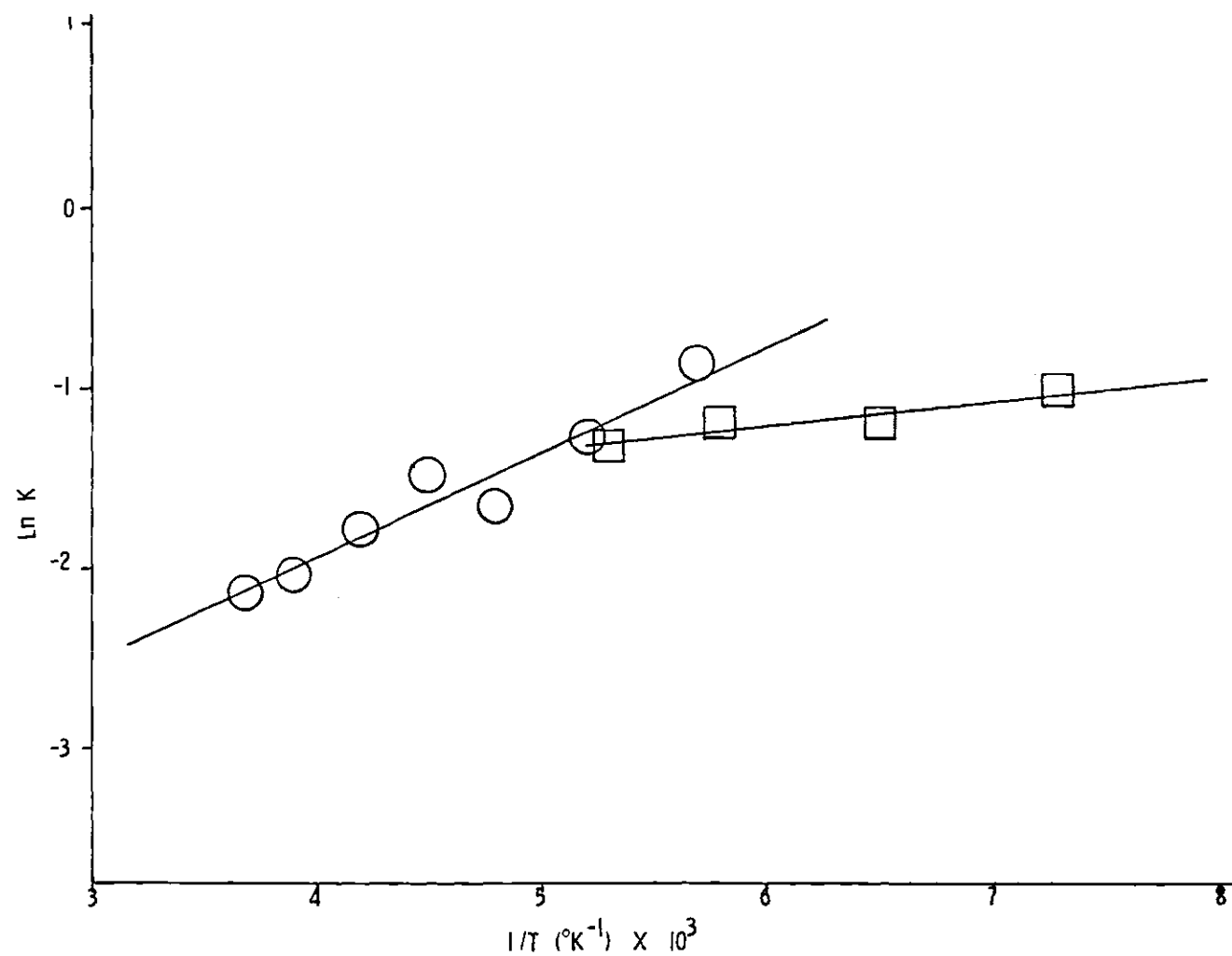


Figure 3. Plot of $\ln K$ versus $1/T$ for the Reaction $1/4(\text{CH}_3\text{Li})_4 + 1/2(\text{LiCu}(\text{CH}_3)_2)_2 \leftrightarrow \text{Li}_2\text{Cu}(\text{CH}_3)_3$ in the Systems: \bigcirc $\text{CH}_3\text{Li}-\text{CH}_3\text{Cu}$ in THF, \square $\text{CH}_3\text{Li}-\text{CH}_3\text{Cu}$ in Dimethyl Ether

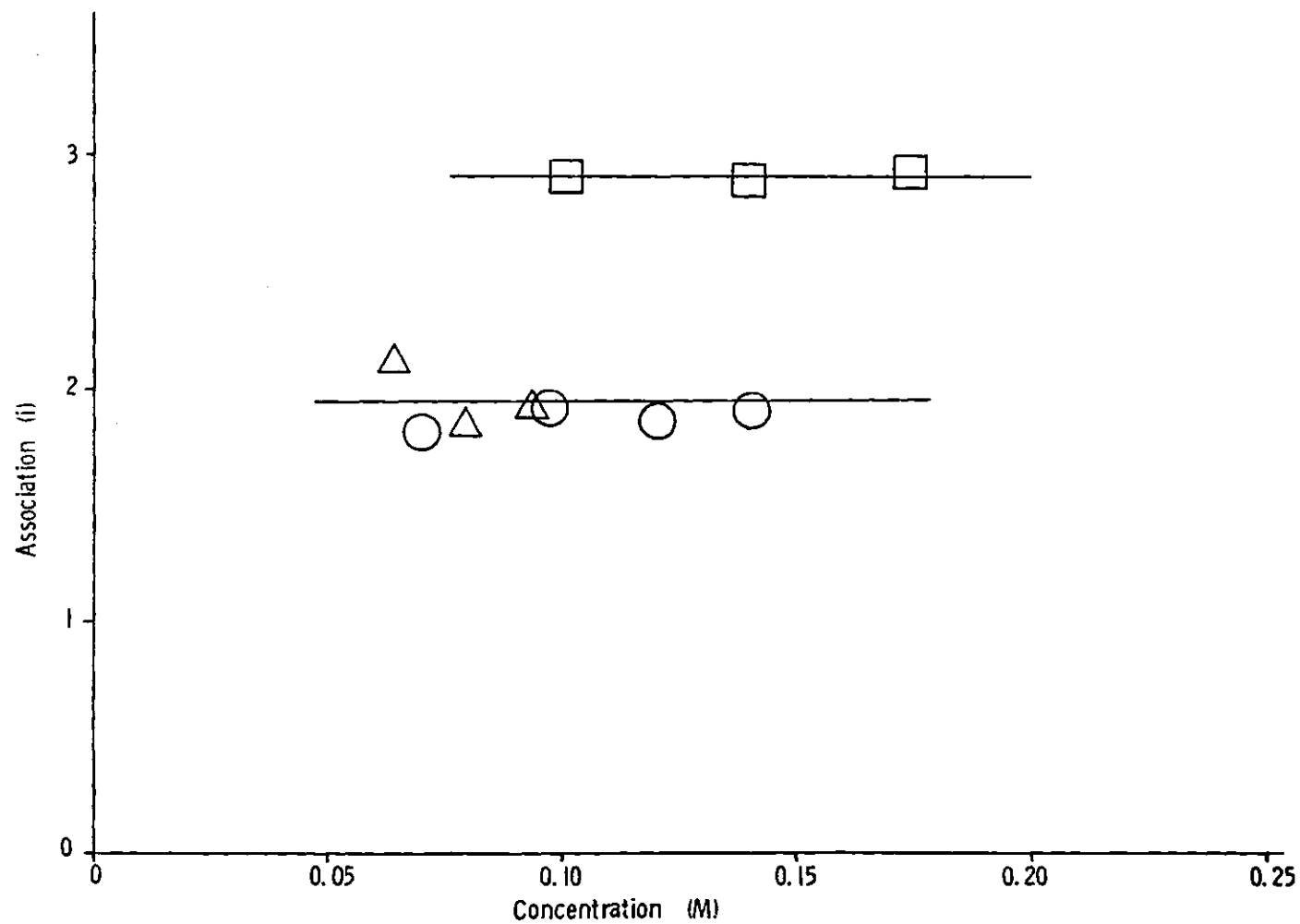


Figure 4. Molecular Association Data for the System $\text{CH}_3\text{Li}-\text{CH}_3\text{Cu}$ in THF -- Ratio $\text{CH}_3\text{Li}/\text{CH}_3\text{Cu}$: \square 2.89, \circ 1.02, \triangle 0.52

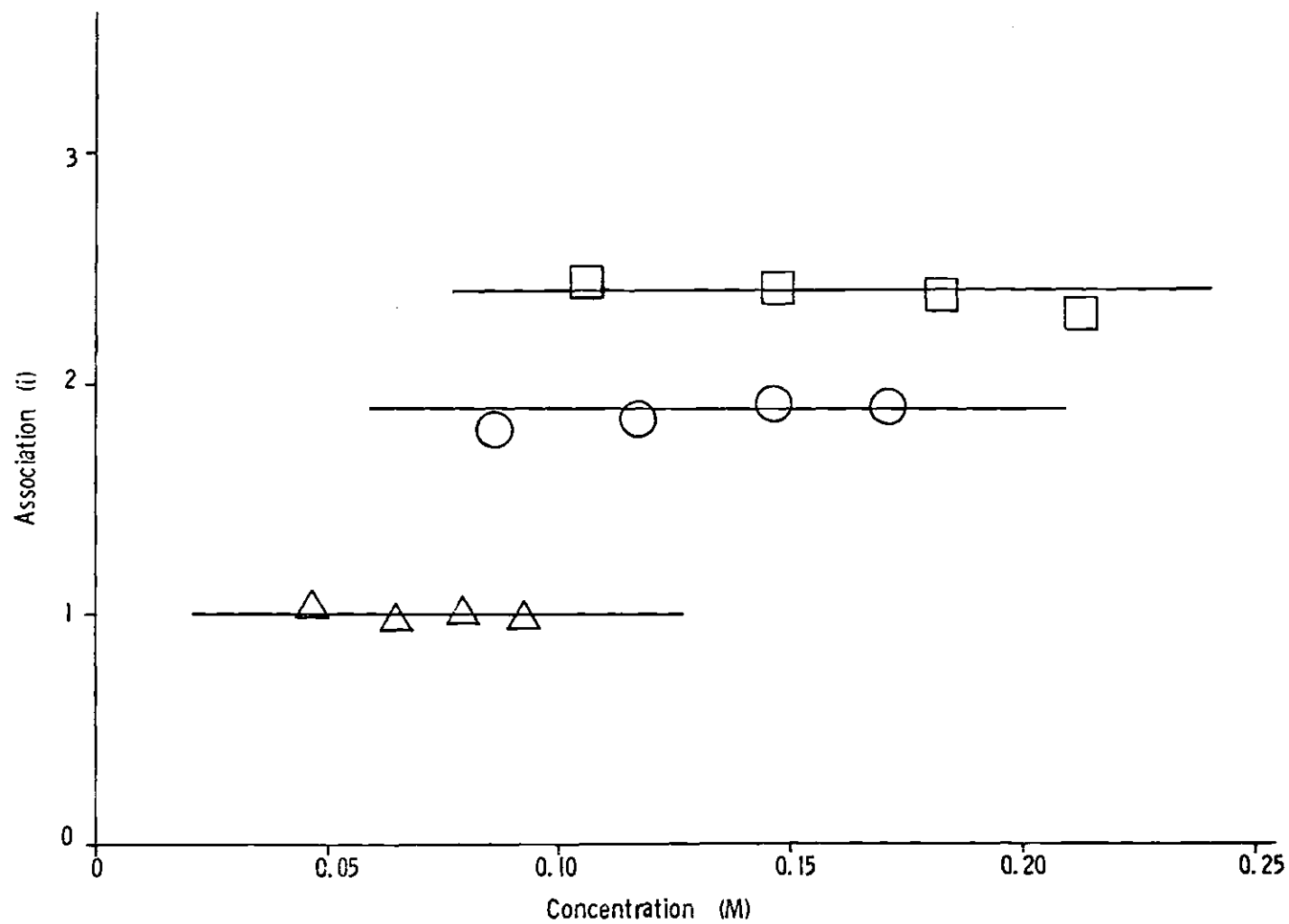


Figure 5. Molecular Association Data for the System $\text{CH}_3\text{Li}-\text{CH}_3\text{Cu}$ in Diethyl Ether --
Ratio $\text{CH}_3\text{Li}/\text{CH}_3\text{Cu}$: □ 2.91, ○ 1.04, △ 0.68

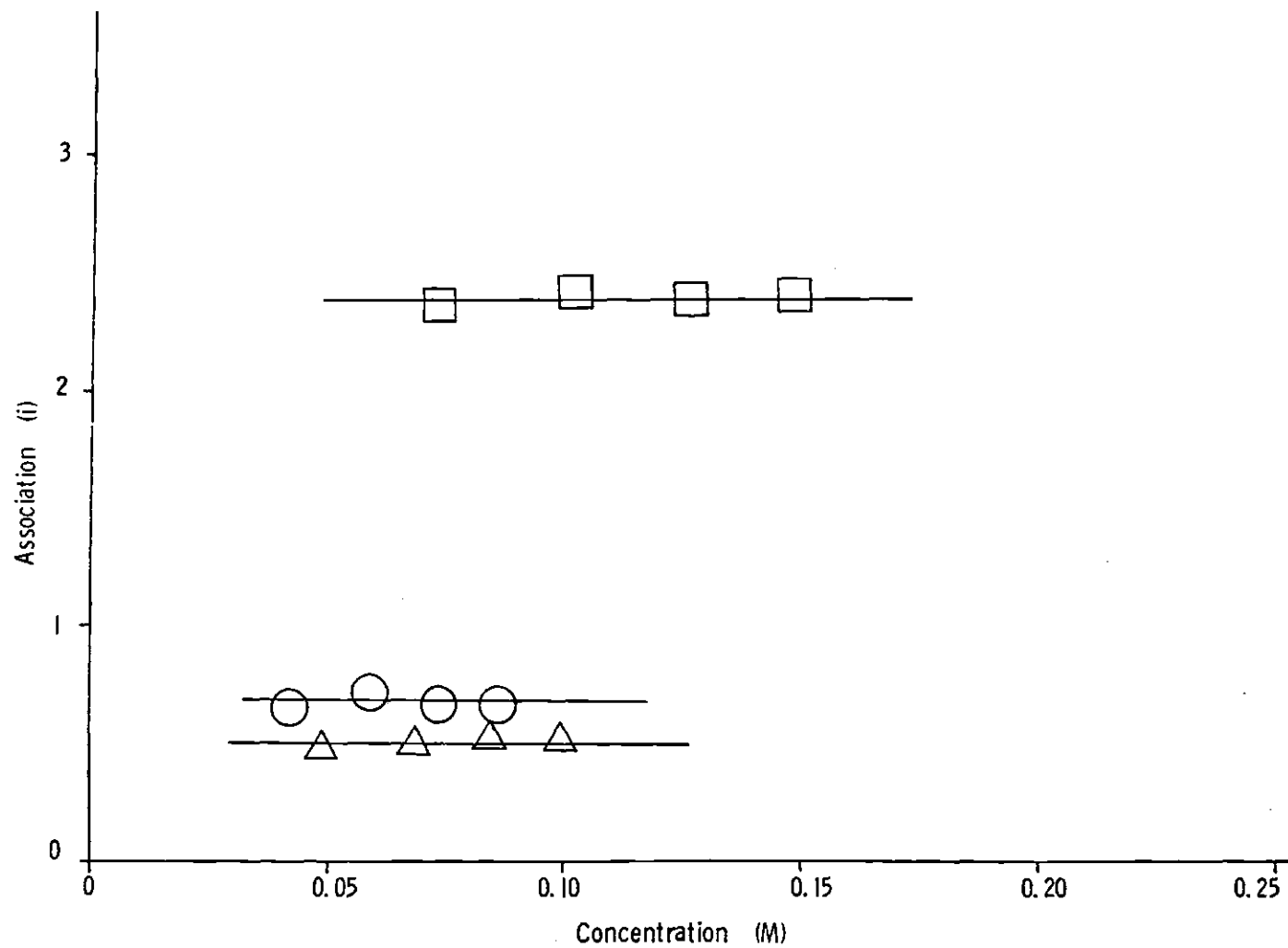


Figure 6. Molecular Association Data for the System $\text{CH}_3\text{Li}-\text{CH}_3\text{Cu}\cdot\text{P}(\text{n-Bu})_3$ in Diethyl Ether -- Ratio $\text{CH}_3\text{Li}/\text{CH}_3\text{Cu}$: □ 2.93, ○ 1.02, △ 0.52

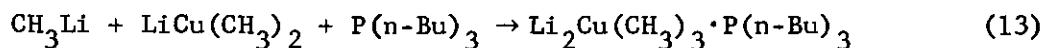
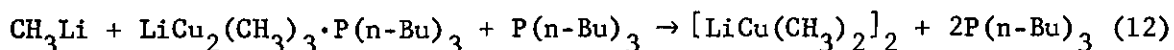
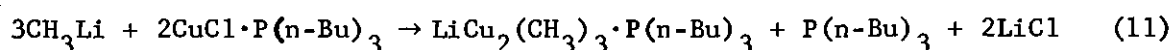
yielded association values which varied from 2.85-2.90 over the concentration range 0.102-0.175 M (concentration of lithium). Using the equilibrium data from Table 6, the amounts of CH_3Li , $\text{LiCu}(\text{CH}_3)_2$, and $\text{Li}_2\text{Cu}(\text{CH}_3)_3$ present in the mixture can be calculated. With these data, two association values were calculated--one assuming that $\text{Li}_2\text{Cu}(\text{CH}_3)_3$ was a monomer, the other assuming it was a dimer. The calculated association value, assuming $\text{Li}_2\text{Cu}(\text{CH}_3)_3$ as a monomer, was 2.84. Assuming $\text{Li}_2\text{Cu}(\text{CH}_3)_3$ as a dimer, this becomes 3.12. The data are more consistent with $\text{Li}_2\text{Cu}(\text{CH}_3)_3$ as a monomer.

For $\text{LiCu}(\text{CH}_3)_2$ in diethyl ether, the association values varied from 1.78-1.90 over a concentration range of 0.086-0.172 M, indicating that $\text{LiCu}(\text{CH}_3)_2$ is dimeric in this solvent. For $\text{Li}_2\text{Cu}_3(\text{CH}_3)_5$ the association values varied from 1.04-0.96 over a concentration range of 0.047-0.093 M, indicating that $\text{Li}_2\text{Cu}_3(\text{CH}_3)_5$ is monomeric. A 3:1 mixture of CH_3Li and CH_3Cu gave association values which varied from 2.44-2.29 over the concentration range 0.107-0.214 M (concentration of lithium). Again, by using the equilibrium data in Table 6, it is possible to calculate the amounts of CH_3Li , $\text{LiCu}(\text{CH}_3)_2$, and $\text{Li}_2\text{Cu}(\text{CH}_3)_3$ present. With these data two association values were calculated--again one for monomer and one for dimer $\text{Li}_2\text{Cu}(\text{CH}_3)_3$. The calculated association value based on monomer was 2.37. Based on dimer the association was 4.00. The assignment of $\text{Li}_2\text{Cu}(\text{CH}_3)_3$ as a monomer is more consistent with the data.

Solutions of $\text{LiCu}(\text{CH}_3)_2$ prepared by reacting CH_3Li with $\text{CuCl}\cdot\text{P}(\text{n-Bu})_3$ in diethyl ether gave association values varying from 0.63-0.71 over the concentration range 0.043-0.087 M. If it is assumed that a mixture of dimeric $\text{LiCu}(\text{CH}_3)_2$ and free uncoordinated $\text{P}(\text{n-Bu})_3$ is present,

then an association value of 0.67 can be calculated. This value agrees very well with the data. Solutions of $\text{LiCu}_2(\text{CH}_3)_3$ gave association values varying from 0.49-0.53 over the concentration range 0.050-0.099 M. A mixture of monomeric $\text{LiCu}_2(\text{CH}_3)_3$ with an equivalent of $\text{P}(\text{n-Bu})_3$ coordinated and another equivalent of $\text{P}(\text{n-Bu})_3$ uncoordinated gives a calculated association value of 0.50, which agrees very well with the observed values. A solution prepared by reacting CH_3Li with $\text{CuCl}\cdot\text{P}(\text{n-Bu})_3$ in 4:1 ratio gave association values varying from 2.35-2.42 over the concentration range 0.075-0.149 (concentration of lithium). If it is assumed that $\text{Li}_2\text{Cu}(\text{CH}_3)_3$ is present as a monomer with the $\text{P}(\text{n-Bu})_3$ coordinated to it, then, with the aid of the equilibrium data in Table 6, an association value of 2.38 can be calculated. This agrees very well with the experimentally determined values.

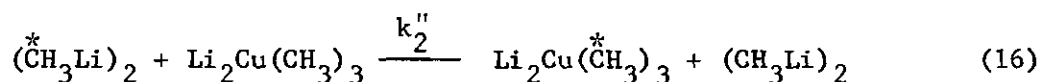
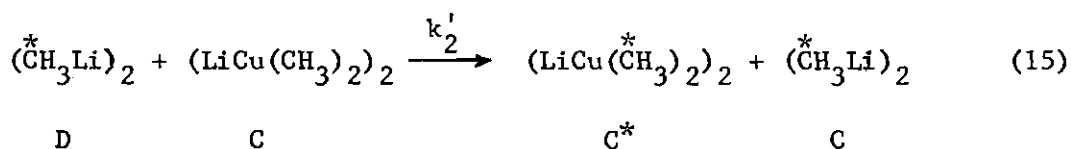
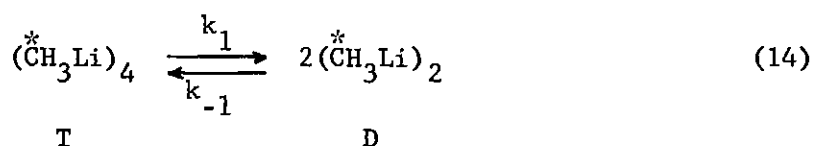
In diethyl ether, when $\text{P}(\text{n-Bu})_3$ is present, the NMR and molecular association data suggest that the reactions represented by Eq. 11-13 occur.



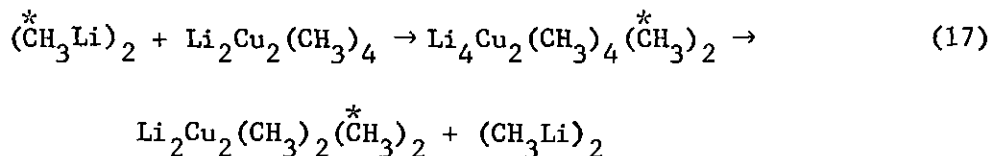
Solutions containing $\text{LiCu}(\text{CH}_3)_2$ and CH_3Li in diethyl ether exhibit rapid ^1H exchange at room temperature. On lowering the temperature the

slow-exchange limit is reached before -50° . Some representative spectra are shown in Figure 7. The results for this system can be explained in terms of the mechanism shown in Scheme I.

SCHEME I



It is not possible to determine directly whether both 15 and 16 are operative. It seems reasonable, however, that k''_2 should be smaller than k'_2 , since a concerted exchange process (Eq. 17) can be visualized for 15, but not for 16. This result means that $k'_2 \gg k''_2$, an assumption that will be employed in deriving the kinetic expressions to follow.



The fact that peaks due to both $\text{LiCu}(\text{CH}_3)_2$ and $\text{Li}_2\text{Cu}(\text{CH}_3)_3$ do not separate indicates that there is a rapid, concurrent exchange of methyl groups between the two complexes.

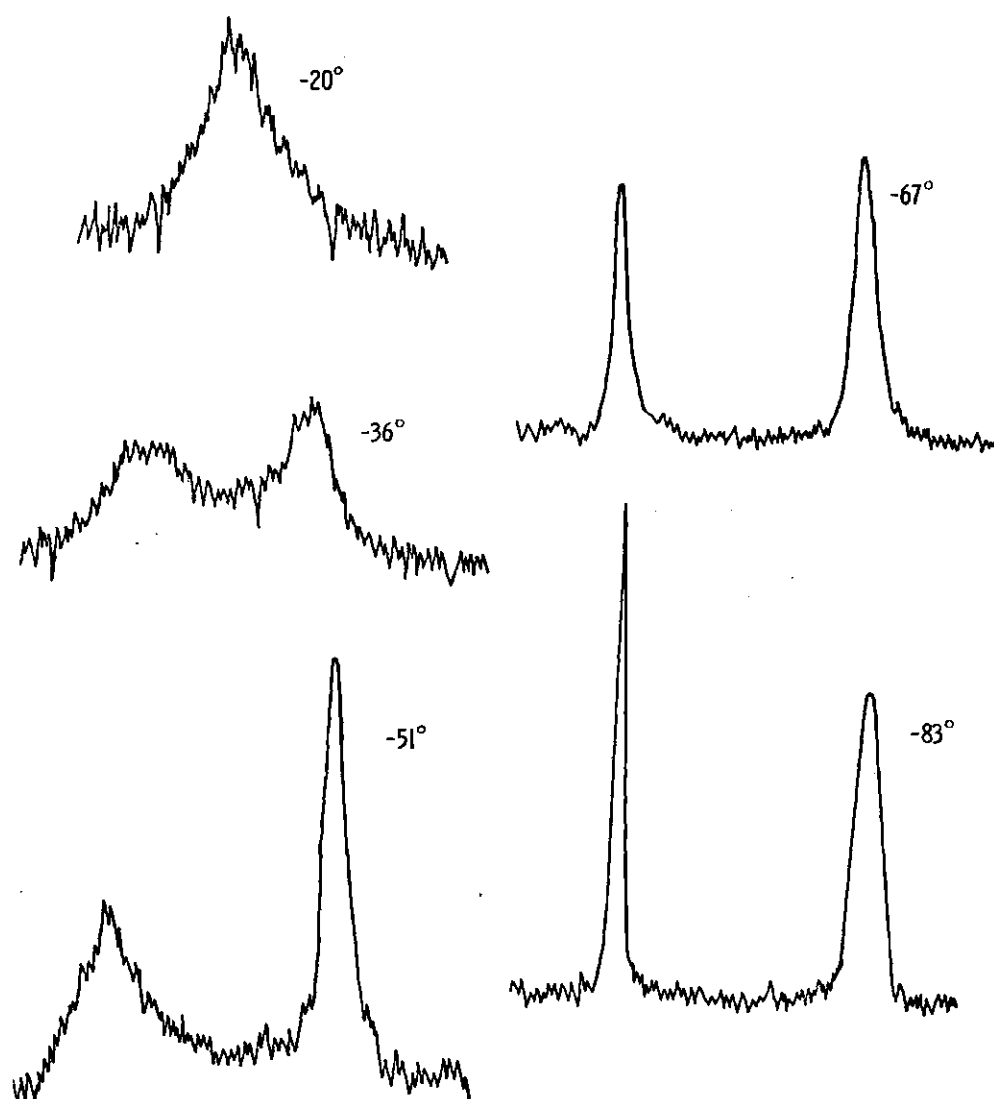


Figure 7. Representative ^1H Spectra of the $\text{CH}_3\text{Li-LiCu}(\text{CH}_3)_2$ System in Diethyl Ether

Adopting a steady-state assumption for (D), the following equations are applicable to ^1H exchange.

$$\frac{d(D)}{dt} = 2 k_1(T) - 2 k_{-1}(D)^2 - k_2(C)(D) = 0$$

$$(D) = \frac{2 k_1(T)}{2 k_{-1}(D) + k_2(C)}$$

$$\frac{d(C^*)}{dt} = k_2(C)(D) = \frac{2 k_1 k_2(T)(C)}{2 k_{-1}(D) + k_2(C)}$$

$$\text{If } 2 k_{-1}(D) \ll k_2(C),$$

$$\frac{d(C^*)}{dt} = 2 k_1(T)$$

$$1/\tau_c = \frac{1}{4} \frac{1}{(C)} \frac{d(C^*)}{dt} = \frac{1}{2} k_1 T/C \quad (18)$$

$$1/\tau_T = \frac{1}{4} \frac{1}{(T)} \frac{d(C^*)}{dt} = \frac{1}{2} k_1 \quad (19)$$

This mechanism, in which dissociation of methyllithium tetramer is rate determining, requires that the methyllithium line width should be independent of concentration and the increase in cuprate complex line width due to exchange should vary linearly with tetramer/cuprate complex ratio.

A number of samples with varying $[(\text{CH}_3\text{Li})_4]/[(\text{LiCu}(\text{CH}_3)_2)_2]$ ratios was examined at a single temperature in the slow-exchange region. Samples with $(\text{CH}_3\text{Li})_4/(\text{LiCu}(\text{CH}_3)_2)_2$ ratios from 0.250 to 1.000 were studied at

-51°, a temperature at which the slow-exchange approximation is reasonable. According to Eq. 18 and 19, $1/\tau_T$ should be invariant to the ratio, whereas $1/\tau_C$ should increase linearly with increasing ratio while having a slope of $1/2 k_1$. The experimental data for $1/\tau_C$ and $1/\tau_T$ are given in Table 7 for solutions in diethyl ether, both with and without $P(n-Bu)_3$. For solutions containing $P(n-Bu)_3$, $1/\tau_C$ is plotted as a function of the ratio T/C in Figure 8. The line which best accommodates the data passes through the origin and has a slope of 15. A very good fit to Eq. 18 is obtained. Consideration of the data in Table 7 shows that $1/\tau_T$ is independent of the ratio T/C with an average value of 13. This value matches the slope of the line in Figure 8 remarkably well, as Eq. 18 and 19 predict. These data then confirm that the mechanism of exchange between CH_3Li and $LiCu(CH_3)_2$ is rate limited by dissociation of the methyllithium tetramer.

For diethyl ether solutions, without $P(n-Bu)_3$, the line which best fits the data, when $1/\tau_C$ is plotted as a function of T/C, and passes through the origin has a slope of 22. As the data in Table 7 show, $1/\tau_T$ is again reasonably independent of the ratio T/C and has an average value of 12. These values are in reasonable agreement with those obtained on solutions containing $P(n-Bu)_3$ in view of the experimental difficulties encountered when trying to obtain accurate and reproducible low temperature 1H line shape data.

An attempt was made at obtaining activation parameters for the exchange between CH_3Li and $LiCu(CH_3)_2$ by studying samples with a constant ratio of $CH_3Li/LiCu(CH_3)_2$ over a wide temperature range. The data obtained, however, were not sufficiently accurate to make the type of

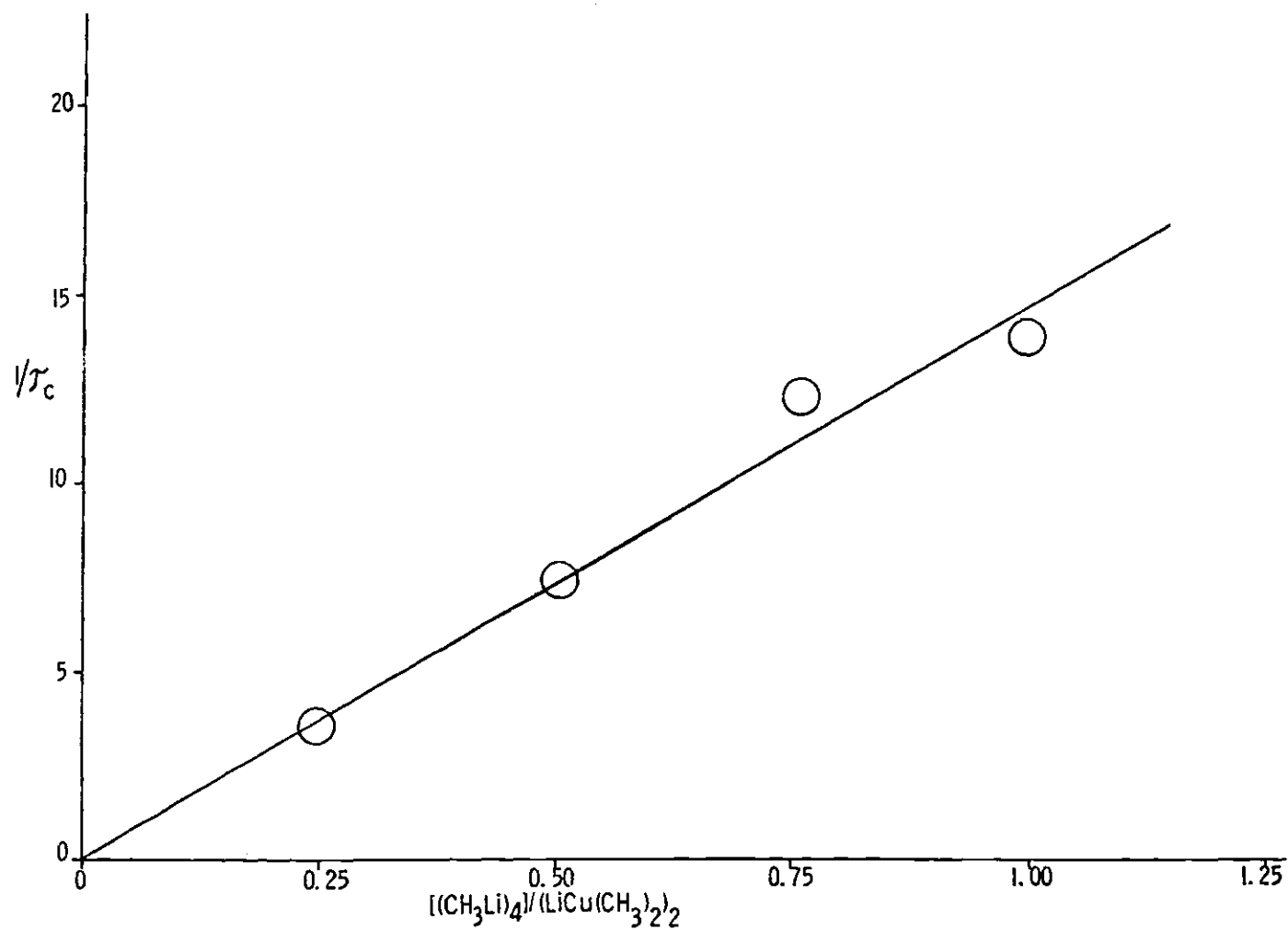


Figure 8. $1/\tau_c$ for the ^1H Spectra of the System $\text{CH}_3\text{Li}-\text{CH}_3\text{Cu}\cdot\text{P}(\text{n-Bu})_3$ in Diethyl Ether at -51° as a Function of $[(\text{CH}_3\text{Li})_4]/[(\text{LiCu}(\text{CH}_3)_2)_2]$

Table 7. Concentration Dependences of the Reciprocal Mean Exchange Times for ^1H Exchange in the $\text{CH}_3\text{Li}-\text{LiCu}(\text{CH}_3)_2$ System at -51° in Diethyl Ether

$[(\text{CH}_3\text{Li})_4]/[(\text{LiCu}(\text{CH}_3)_2)_2]^a$	$1/\tau (\text{CH}_3\text{Li})_4^a$	$1/\tau (\text{LiCu}(\text{CH}_3)_2)_2^a$
<u>With $\text{P}(\text{n-Bu})_3$</u>		
0.250	15	4
0.508	14	7
0.765	11	12
1.003	12	14
<u>Without $\text{P}(\text{n-Bu})_3$</u>		
0.362	14	9
0.767	12	17
0.799	11	16

^aTypical error limits on the concentration ratios and mean lifetimes were ± 0.005 and ± 3 .

analysis necessary possible.

Recently, it was reported that a mixture of CH_3Li and $\text{LiCu}(\text{CH}_3)_2$ provides unusually high stereoselectivity (94% equatorial attack) in the methylation of 4-tert-butylcyclohexanone compared to reaction of CH_3Li or $\text{LiCu}(\text{CH}_3)_2$ alone.³ It was suggested that "a bulky, highly reactive cuprate having the stoichiometry $\text{Li}_2\text{Cu}(\text{CH}_3)_3$ or $\text{Li}_3\text{Cu}(\text{CH}_3)_4$ " was formed when CH_3Li and $\text{LiCu}(\text{CH}_3)_2$ are allowed to react and that reaction of these cuprates with the ketone would explain the observed results. Evidence has been found which suggests that the observed stereoselectivity arises by the reaction of CH_3Li with a ketone complex of $\text{LiCu}(\text{CH}_3)_2$ and that similar stereoselectivity toward 4-tert-butylcyclohexanone can be obtained by the reaction of CH_3Li in the presence of other lithium salts, e.g., LiClO_4 .

The CH_3Li - $\text{LiCu}(\text{CH}_3)_2$ mixture used to methylate 4-tert-butylcyclohexanone was prepared by reacting CH_3Li with CuI in an 8:3 molar ratio in diethyl ether solvent. In such a mixture at least three species are present: $\text{LiCu}(\text{CH}_3)_2$, CH_3Li , and LiI . The reaction of any one of these compounds with 4-tert-butylcyclohexanone fails to produce the unusual stereochemistry reported above. One can suggest four possible explanations for this stereoselectivity: (1) CH_3Li reacts with $\text{LiCu}(\text{CH}_3)_2$ to form a complex which then reacts with the ketone.³ (2) CH_3Li reacts with LiI to form a complex (a reaction known to produce $\text{Li}_4(\text{CH}_3)_3\text{I}$)¹⁵ which then reacts with the ketone. (3) $\text{LiCu}(\text{CH}_3)_2$ and LiI react to form a complex which then reacts with the ketone. (4) One of the species in solution reacts with the ketone to form a complex followed by reaction of the

complexed carbonyl compound with CH_3Li .

Low temperature ^1H NMR evidence for the existence of $\text{Li}_2\text{Cu}(\text{CH}_3)_3$ in a mixture of CH_3Li and $\text{LiCu}(\text{CH}_3)_2$ in dimethyl ether, tetrahydrofuran, and diethyl ether solvents was discussed earlier. No evidence was found to indicate the presence of any higher order complexes, such as $\text{Li}_3\text{Cu}(\text{CH}_3)_4$. The reaction $\text{CH}_3\text{Li}-\text{LiCu}(\text{CH}_3)_2$ with 4-tert-butylcyclohexanone in THF did not yield any increased stereoselectivity when compared to CH_3Li alone (Table 8). Since we have determined that $\text{Li}_2\text{Cu}(\text{CH}_3)_3$ exists in both ether and THF and is monomeric in both solvents, it is doubtful that $\text{Li}_2\text{Cu}(\text{CH}_3)_3$ would react with 4-tert-butylcyclohexanone in diethyl ether to give unusual stereoselectivity while in THF no trace of unusual stereoselectivity is observed. Therefore, one is led to question that the observed stereoselectivity in diethyl ether is due to the reaction of $\text{Li}_2\text{Cu}(\text{CH}_3)_3$ with the ketone.*

*The hypothesis that $\text{Li}_2\text{Cu}(\text{CH}_3)_3$, when present in a mixture of CH_3Li and $\text{LiCu}(\text{CH}_3)_2$ in diethyl ether, is a "bulky, highly reactive cuprate"³ is questionable. Molecular weight measurements indicate that $\text{Li}_2\text{Cu}(\text{CH}_3)_3$ is monomeric in diethyl ether and THF, whereas CH_3Li is tetrameric¹² and $\text{LiCu}(\text{CH}_3)_2$ is dimeric.¹³ As a monomer, $\text{Li}_2\text{Cu}(\text{CH}_3)_3$ should not be considered more bulky than a tetrameric molecule such as CH_3Li . Reactions of $\text{Li}_2\text{Cu}(\text{CH}_3)_3$, $\text{LiCu}(\text{CH}_3)_2$, and $\text{LiCu}_2(\text{CH}_3)_3$ in both diethyl ether and THF with selected enones⁸ indicate that $\text{Li}_2\text{Cu}(\text{CH}_3)_3$ is only slightly more reactive than $\text{LiCu}(\text{CH}_3)_2$ toward conjugate addition. In view of this, it is doubtful that $\text{Li}_2\text{Cu}(\text{CH}_3)_3$ could be called highly reactive when compared with reagents like CH_3Li and $\text{LiCu}(\text{CH}_3)_2$. However, qualitative rate measurements indicate that in diethyl ether $\text{CH}_3\text{Li}-\text{LiI}$ mixture and a halide free $\text{CH}_3\text{Li}-\text{LiCu}(\text{CH}_3)_2$ mixture methylate 4-tert-butylcyclohexanone at least 1000-fold faster than CH_3Li alone. Therefore, while it is doubtful that $\text{Li}_2\text{Cu}(\text{CH}_3)_3$ is the source, the high stereoselectivity observed in this reaction is accompanied by a rapid reaction rate.

Table 8. Reactions of Organometallic Reagents with
4-tert-Butylcyclohexanone in Ether Solvents
at -78°

Reagent	% Yield of Axial Alcohol ^a	
	Ether	THF
CH_3Li	69	55 ^b
$2 \text{ CH}_3\text{Li} + \text{LiCu}(\text{CH}_3)_2$	92	65
$2 \text{ CH}_3\text{Li} + \text{LiCu}(\text{CH}_3)_2$ (halide free)	93	65
$\text{CH}_3\text{Li} + \text{LiBr}$	87	65
$\text{CH}_3\text{Li} + \text{LiI}$	87	65
$\text{CH}_3\text{Li} + \text{LiClO}_4$	92	67

^aBalance of yield was the equatorial alcohol, unless otherwise noted. Typical error in the yields was $\pm 2\%$.

^bRatio of axial/equatorial alcohols was 65/35. There was a 14% recovery of ketone.

The stereochemical improvement in the $\text{CH}_3\text{Li-LiCu}(\text{CH}_3)_2$ reagent in diethyl ether cannot be explained by assuming that a complex between CH_3Li and LiI (formed in the reaction of CH_3Li with CuI) is reacting with the ketone. A mixture of CH_3Li and LiI or LiBr (Table 8), while giving some improvement in stereoselectivity, does not give the selectivity observed with the $\text{CH}_3\text{Li-LiCu}(\text{CH}_3)_2$ mixture. Also a mixture of CH_3Li and LiI or LiBr in THF (Table 8) gives no improvement in stereoselectivity over CH_3Li alone. It is known that CH_3Li forms complexes with both LiI^{16} and LiBr^{17} in THF. Likewise, the stereochemical improvement cannot be explained by assuming that a complex between either $\text{LiCu}(\text{CH}_3)_2$ or $\text{Li}_2\text{Cu}(\text{CH}_3)_3$ and LiI is reacting with the ketone, since a halide free mixture of CH_3Li and $\text{LiCu}(\text{CH}_3)_2$ (Table 8) gives the same high stereoselectivity.

The only possibility remaining is that CH_3Li reacts with a complex between one of the components of the mixture and the ketone. This would explain the results in THF, since the ketone would not be expected to compete effectively with THF solvent molecules for coordination sites. This suggestion also explains the unusual rate enhancement in diethyl ether since the concentration of ketone complexed to $\text{LiCu}(\text{CH}_3)_2$, LiI , etc. would be considerably higher than in THF and certainly the complexed carbonyl compound would be much more reactive than uncomplexed.

In order to test this possibility, a system which would be composed of CH_3Li and a lithium salt, was chosen where there would be little chance for complex formation between CH_3Li and the lithium salt but a good chance for complex formation between the lithium salt and the ketone. Such a system would be CH_3Li and LiClO_4 , since LiClO_4 is known to complex the

carbonyl group of ketones.¹⁸ Low temperature ^1H and ^{13}C NMR of $\text{CH}_3\text{Li-LiClO}_4$ mixtures show only signals for pure CH_3Li indicating the absence of any complex formation. ^{13}C NMR of 4-tert-butylcyclohexanone mixtures with LiBr , LiI , $\text{LiCu}(\text{CH}_3)_2$, and LiClO_4 in diethyl ether show a downfield shift for the carbonyl carbon of about 10 ppm, indicating the presence of a complex. In THF, only a small downfield shift was observed with LiClO_4 indicating the presence of very little complexed ketone. The reaction of the $\text{CH}_3\text{Li-LiClO}_4$ mixture with 4-tert-butylcyclohexanone in diethyl ether (Table 8) shows the same stereochemical improvement as was obtained with $\text{CH}_3\text{Li-LiCu}(\text{CH}_3)_2$. In THF this reaction (Table 8) showed no improvement in stereoselectivity over that obtained with CH_3Li alone.

CHAPTER IV

CONCLUSIONS

The results shown in Table 8 indicate that $\text{CH}_3\text{Li-LiBr}$, $\text{CH}_3\text{Li-LiI}$, $\text{CH}_3\text{Li-LiClO}_4$, and $\text{CH}_3\text{Li-LiCu}(\text{CH}_3)_2$ mixtures react with 4-tert-butylcyclohexanone in diethyl ether to give higher stereoselectivity in the product methyl carbinols than were obtained with CH_3Li alone. The results suggest that the methylation reaction is proceeding by attack of CH_3Li on a ketone complex. In the particular case where a $\text{CH}_3\text{Li-LiCu}(\text{CH}_3)_2$ mixture is allowed to react with 4-tert-butylcyclohexanone, the results suggest that the methylation is proceeding by CH_3Li attack on a complex between $\text{LiCu}(\text{CH}_3)_2$ and the ketone.

LITERATURE CITED*

1. For recent reviews of organocopper chemistry, see G. H. Posner, Org. React., 19, 1 (1972); G. Posner, Org. React., 22, 253 (1975); J. Normant, Synthesis, 63 (1972); A. E. Jukes, Adv. Organomet Chem., 12, 215 (1975); H. O. House, Accs. Chem. Res., 9, 59 (1976).
2. H. O. House, D. G. Koepsel, and W. J. Campbell, J. Org. Chem., 37, 1003 (1972).
3. T. L. Macdonald and W. C. Still, J. Amer. Chem. Soc., 97, 5280 (1975).
4. H. O. House and C. Y. Chu, J. Org. Chem., 41, 3083 (1976).
5. H. O. House, W. L. Respess, and G. M. Whitesides, J. Org. Chem., 31, 3128 (1966).
6. D. F. Shriver, "The Manipulation of Air-Sensitive Compounds," McGraw-Hill, New York, New York, 1969.
7. E. C. Ashby and R. D. Schwartz, J. Chem. Ed., 51, 65 (1974).
8. G. B. Kauffman and L. A. Teter, Inorg. Syn., 7, 9 (1963).
9. R. N. Keller and H. D. Wycoff, Inorg. Syn., 2, 1 (1964).
10. F. W. Walker and E. C. Ashby, J. Chem. Ed., 45, 654 (1968).
11. C. S. Johnston, Jr., Advan. Magnetic Resonance, 1, 33 (1965).
12. P. West and R. Waack, J. Amer. Chem. Soc., 89, 4395 (1967).
13. R. G. Pearson and C. D. Gregory, J. Amer. Chem. Soc., 98, 4098 (1976).
14. E. C. Ashby, Simon H. Yu, and Paul V. Roling, J. Org. Chem., 37, 1918 (1972).
15. D. P. Novak and T. L. Brown, J. Am. Chem. Soc., 94, 3793 (1972).

* Journal title abbreviations used are listed in "List of Periodicals," Chemical Abstracts (1961).

16. L. D. McKeever, R. Waack, M. A. Doran, and E. D. Baker, J. Am. Chem. Soc., **91**, 1057 (1969).
17. R. Waack, M. A. Doran, and E. B. Baker, Chem. Comm., 1291 (1967).
18. A. E. Pullin and J. E. Poolock, Trans. Faraday Soc., **54**, 11 (1958).
19. R. R. Jones, E. J. Goller, and W. J. Kauffman, J. Org. Chem., **34**, 3566 (1969).
20. J. J. Uebel and H. W. Goodwin, J. Org. Chem., **33**, 3317 (1968).

VITA

John Joseph Watkins was born on August 23, 1947 in Wilmington, North Carolina and subsequently attended public school in Wilmington, Winston Salem, North Carolina, and Decatur, Georgia. He graduated from Avondale High School in June 1965 and attended the Georgia Institute of Technology in Atlanta from 1965 to 1970.

In November 1968, he married Alice C. Griner of Summerville, South Carolina and in January 1970 she gave birth to their first child, Lisa Elaine Watkins.

He received a B.S. degree in Chemistry as a Co-op in June 1970. In September 1970, he began graduate studies at the Georgia Institute of Technology in Atlanta, Georgia under Dr. E. C. Ashby in the area of organometallic chemistry.

In September 1973, he left graduate school at Georgia Tech to take the position as Development Engineer in the Kraft Research and Development Department of the St. Regis Paper Company in Pensacola, Florida. In December 1973 he received a M.S. degree in Chemical Engineering from the Georgia Institute of Technology. In July 1975, their second child, Karen Renee Watkins, was born.

In October 1975, he obtained leave of absence from the St. Regis Paper Company and resumed his graduate studies with Dr. Ashby at Georgia Tech. He was holding the position of Senior Development Engineer at the time of his return.

In January 1977, their third child, Susan Marie Watkins, was born.

After completion of his degree at Georgia Tech, Mr. Watkins will return to the St. Regis Paper Company at Pensacola and take the position of Senior Staff Engineer.